

Copyright

by

Jiajia Cai

2011

**The Dissertation Committee for Jiajia Cai Certifies that this is the approved version  
of the following dissertation:**

**Synthesis and Characterization Studies of Novel Macrocyclic  
Compounds with CH and NH Donor Groups**

**Committee:**

---

Jonathan L. Sessler, Supervisor

---

C. Grant Willson

---

Michael J. Krische

---

Alan H. Cowley

---

Walter L. Fast

---

Eric V. Anslyn

---

Christine E. Schmidt

**Synthesis and Characterization Studies of Novel Macrocyclic  
Compounds with CH and NH Donor Groups**

**by**

**Jiajia Cai, B.S.**

**Dissertation**

Presented to the Faculty of the Graduate School of  
The University of Texas at Austin  
in Partial Fulfillment  
of the Requirements  
for the Degree of

**Doctor of Philosophy**

**The University of Texas at Austin  
December 2011**

## **Dedication**

This dissertation is dedicated

To my parents

## Acknowledgements

First of all, I want to thank my supervisor Prof. Sessler for giving me the opportunity to work as a member in his research group as well as his mentorship. I still remember that six years ago I wrote a long and enthusiastic letter to Prof. Sessler because of his fame in the supramolecular chemistry area, when I was applying the graduate school. I rejected several other offers, waited until the very end and finally got this offer. In the past five and half years, Prof. Sessler gave me a lot of freedom to explore the research areas that I was interested in. I am very grateful for his encouragement and inspiration during my graduate school. This created an idea environment for me to be mature, both professionally and personally. The most important thing I learned after these years in graduate school are the value of independence and courageousness, which have provided me with the confidence to solve challenging problems that I have never met before.

I also want to thank my parents, to whom this dissertation is dedicated. My parents do not have a background in chemistry, but they value the importance of education and gave me the best education they could afford. Furthermore, they gave me strong support and encouragement to come to the United States to pursue a PhD degree after I finished my bachelor degree in China. During the past five and half years, I had very few chances to go back to China to visit them. Instead, they put their work aside and came to the United States to visit me several times. I will never forget their love and support.

Throughout my graduate research, I have had the privilege to work with some remarkable individuals, both in terms of scientific prowess and on the human level. I

would like to start by thanking all the past and present members of the Sessler group, a truly eclectic but wonderful assortment of people. (For fear of leaving someone out, I'm not going to list everyone's name here.)

In particular, I would like to thank Dr. Han-yuan Gong for his friendship and guidance in my first two years' graduate school life, when I was still struggling in the scientific jungle. I will definitely miss our lunch and dinner time. I would like to thank Dr. Dustin Gross for his help and advice to my second year candidacy exam. I am particularly grateful for our scientific discussions at that time. I wish him good luck in finding a faculty job.

I have had the great opportunity to work with great collaborators. I am grateful to Dr. Benjamin Hay and Dr. Neil Young for helping us with theoretical calculations, Dr. Xiaoping Yang for crystal refinements and Dr. Vince Lynch for teaching me X-ray diffraction techniques. I would also thank Prof. Christopher Bielawski for his kindness and suggestions regarding the carbene chemistry project, and Dr. Kuppuswamy Arumugam for working together on that project. Finally, I would thank my labmates, Dr. Jonathan Arambula and Mr. Eric Silver, for helping me to edit my papers.

# **Synthesis and Characterization Studies of Novel Macrocyclic Compounds with CH and NH Donor Groups**

Jiajia Cai, Ph.D.

The University of Texas at Austin, 2011

Supervisor: Jonathan L. Sessler

The dissertation focuses on the recent discovery in supramolecular chemistry of novel macrocyclic compounds with NH and CH donor groups. Chapter 1 provides a brief overview of the anions under study, supramolecular chemistry, the relevant other anion receptors, as well as previous findings involving the use of CH donor groups as functional building blocks. Chapter 2, as the major focus of this dissertation, describes a pyrrolyl-based triazolophane, incorporating CH and NH donor groups, which acts as a receptor for the pyrophosphate anion in chloroform solution. It shows selectivity for this trianion, followed by  $\text{HSO}_4^- > \text{H}_2\text{PO}_4^- > \text{Cl}^- > \text{Br}^-$  (all as the corresponding tetrabutylammonium salts), with NH–anion interactions being more important than CH–anion interactions. In the solid state, the receptor binds the pyrophosphate anion in a clip-like slot *via* NH and CH hydrogen bonds. Chapter 3 describes a pyrrole-based triazolium–phane which has been prepared through “click” chemistry in moderate yield. It displays a high selectivity for tetrahedral oxyanions relative to various test monoanions and trigonal planar anions in mixed polar organic–aqueous solvent media. It was also found that the binding affinity and selectivity of the macrocycle to the anions are solvent dependent. Several crystal structures were solved. They confirm that the cationic

macrocycle ring binds pyrophosphate and phosphate anions in the solid state. Finally, chapter 4 describes a novel 1,3,4-substituted 1,2,3-triazolium salt found to function as an effective precursor for the synthesis of structurally characterized cationic silver(I) and ruthenium(II) carbene complexes of overall 1:2 ligand-to-metal stoichiometry. The Ag(I) complex crystallized in the form of an eight silver atom containing cluster, whereas the Ru(II) complex proved to be a discrete species and was found to be capable of initiating the ring-opening metathesis polymerization of norbornene upon activation with (trimethylsilyl)diazomethane.



## Table of Contents

List of Tables .....	xi
List of Figures .....	xii
Chapter 1: Introduction .....	1
1.1 Anions under consideration in this work .....	1
1.2 Supramolecular Chemistry .....	4
1.2.1 Hydrogen Bonding .....	5
1.3 Synthetic Anion Receptors .....	6
1.4 Neutral C–H···Anion Hydrogen Bonds .....	7
1.5 Cationic (C–H) <sup>+</sup> ···Anion Hydrogen Bonds .....	11
1.5.1 Imidazoliums .....	11
1.5.2 Triazoliums .....	13
1.6 References .....	15
Chapter 2: A Pyrrolyl-Based Triazolophane: A Macrocyclic Receptor with CH and NH Donor Groups that Exhibits a Preference for Pyrophosphate Anions... 18	
2.1 Introduction .....	18
2.2 Results and Discussion .....	19
2.3 Conclusions .....	24
2.4 Experimental Section .....	25
2.4.1 General Procedures .....	25
2.4.2 Synthetic Experimental .....	25
2.4.3 Conformation Analysis for the Macrocycle in CDCl <sub>3</sub> .....	27
2.4.4 Details of Fitting UV-Vis Binding Curves .....	29
2.4.5 NMR Spectroscopic-based Anion Recognition Study .....	35
2.4.6 Details of High Resolution ESI Mass Spectrometric Study .....	41
2.4.7 Details of Electronic Structure Calculations .....	42
2.4.8 Crystallographic Data .....	49
2.5 References .....	54

Chapter 3: A Pyrrole-based Triazolium-phane with NH and Cationic CH Donor Groups as a Receptor for Tetrahedral Oxyanions that Functions in Polar Media	57
3.1 Introduction.....	57
3.2 Results and Discussions.....	59
3.3 Conclusions.....	73
3.4 Experimental Section.....	74
3.4.1 General Procedures.....	74
3.4.2 Synthetic Experimental.....	74
3.4.3 Details of Fitting the UV-Vis Binding Curves.....	75
3.4.4 NMR Spectroscopic-based Anion Recognition Study .....	95
3.4.5 Details of Electronic Structure Calculations .....	107
3.4.6 Crystallographic Data .....	109
3.5 References.....	115
Chapter 4: Structurally Characterized Cationic Silver(I) and Ruthenium(II) Carbene Complexes of 1,2,3-Triazol-5-ylidenes .....	119
4.1 Introduction.....	119
4.2 Results and Discussion.....	121
4.3 Conclusions.....	127
4.4 Experimental Section.....	128
4.4.1 General Procedures.....	128
4.4.2 Synthetic Experimental.....	129
4.4.3 Ring Opening Metathesis Polymer .....	132
4.4.4 NMR Spectroscopic-based Kinetic Studies.....	134
4.4.5 Crystallographic Data.....	135
4.5 References.....	138
References .....	141

## List of Tables

Table 1.1:	A comparison of the radii (r) and hydration energies ( $\Delta G_{\text{hyd}}$ ) of selected isoelectronic anions and cations.....	2
Table 2.1:	Chemical shift changes for selected signals of <b>2.1</b> seen in the presence of 10 equiv. of TBA <sub>3</sub> HP <sub>2</sub> O <sub>7</sub> , TBAH <sub>2</sub> PO <sub>4</sub> , TBAHSO <sub>4</sub> , TBACl and TBABr. The changes are relative to what is seen for pure <b>2.1</b> .....	35
Table 2.2:	ESI High Resolution Mass Spectra Study for Complexes.....	41
Table 2.3:	X-ray crystallographic data comparison of macrocycle <b>2.1</b> ·4CH <sub>3</sub> OH·H <sub>2</sub> O and complex <b>2.1</b> ·TBA <sub>3</sub> HP <sub>2</sub> O <sub>7</sub> ·3H <sub>2</sub> O.....	51
Table 3.1:	Binding Affinities of Several Different Anions to Receptor <b>3.1</b> <sup>4+</sup> ·4BF <sub>4</sub> <sup>-</sup> in Three Different Solvent Systems Were Investigated Using UV-Vis Titrations at 300 K.....	64
Table 3.2:	Influence of solvent on calculated $\Delta G$ values (kcal/mol) for the formation of hydrogen-bonded complexes between Cl <sup>-</sup> and representative simple donors (Figure 3.3).....	67
Table 3.3:	Anion binding constants ( $K_a$ ; M <sup>-1</sup> ) for the interaction of anion receptor [ <b>3.1</b> <sup>4+</sup> ·4BF <sub>4</sub> <sup>-</sup> ] with different anions in CH <sub>3</sub> CN at 300 K.....	84
Table 3.4:	Anion binding constants ( $K_a$ ; M <sup>-1</sup> ) for the interaction of anion receptor [ <b>3.1</b> <sup>4+</sup> ·4BF <sub>4</sub> <sup>-</sup> ] with different anions in CH <sub>3</sub> OH at 300 K.....	90
Table 3.5:	Anion binding constants ( $K_a$ ; M <sup>-1</sup> ) for the interaction of anion receptor [ <b>3.1</b> <sup>4+</sup> ·4BF <sub>4</sub> <sup>-</sup> ] with different anions in acetone-H <sub>2</sub> O (2 : 3) at 300 K. The solution was buffered at pH 7.2 with HEPES buffer (5.00 × 10 <sup>-3</sup> M). <sup>a</sup> n.d. = not able to determine.....	95
Table 3.6:	X-ray crystallographic data comparison of macrocycle <b>3.1</b> <sup>4+</sup> ·4BF <sub>4</sub> <sup>-</sup> ·CH <sub>3</sub> OH·3H <sub>2</sub> O, complex <b>3.1</b> <sup>4+</sup> ·HP <sub>2</sub> O <sub>7</sub> <sup>3-</sup> ·BF <sub>4</sub> <sup>-</sup> , and complex 2( <b>3.1</b> <sup>4+</sup> )·2H <sub>2</sub> PO <sub>4</sub> <sup>-</sup> ·6BF <sub>4</sub> <sup>-</sup> .....	110
Table 4.1:	X-ray crystallographic data comparison of compound <b>4.2</b> ·DMF, complex <b>4.3</b> and complex <b>4.4</b> ·3CHCl <sub>3</sub> .....	137

## List of Figures

Figure 1.1:	Representative anions, classified by size and shape.....	3
Figure 1.2:	Canonical Watson-Crick base-pairing modes.....	4
Figure 1.3:	Hydrogen bond donors found in Nature and used in supramolecular chemistry.....	7
Figure 1.4:	Structures of various types of receptors containing imidazolium moieties.....	12
Figure 1.5:	Structures of various types of receptors containing 1,2,3-triazolium moieties.....	14
Figure 2.1:	Chemical structure of the [3 <sub>4</sub> ]triazolophane reported by Flood .....	19
Figure 2.2:	(a) Top and (b) side views of the single crystal X-ray structure of <b>2.1</b> ·4CH <sub>3</sub> OH·H <sub>2</sub> O. All solvent molecules have been omitted for clarity.....	21
Figure 2.3:	<sup>1</sup> H NMR spectra (aromatic region) of <b>2.1</b> recorded upon titration with increasing quantities of (TBA) <sub>3</sub> HP <sub>2</sub> O <sub>7</sub> ; CDCl <sub>3</sub> , 300 K.....	23
Figure 2.4:	(a) Top and (b) side views of a single-crystal X-ray diffraction structure of <b>2.1</b> ·TBA <sub>3</sub> HP <sub>2</sub> O <sub>7</sub> ·3H <sub>2</sub> O in which the pyrophosphate anion is in a space filling representation. Solvent molecules and TBA cations have been omitted for clarity.....	24
Figure 2.5:	<sup>1</sup> H NMR spectrum of <b>2.1</b> recorded in CDCl <sub>3</sub> at 300 K. Note: The peak at 1.89 ppm is ascribed to H <sub>2</sub> O.....	27
Figure 2.6:	(a) Full view and (b), (c) expanded views of the 2D NOESY NMR spectrum of <b>2.1</b> recorded in CDCl <sub>3</sub> at 300 K.....	28
Figure 2.7:	Limiting conformations for the fragments present in <b>2.1</b> that were used to interpret the NOESY NMR spectra. Note that the conformers shown as c and c <sup>1</sup> are symmetry related.....	29
Figure 2.8:	Variable temperature <sup>1</sup> H NMR spectrum of macrocycle <b>2.1</b> in CDCl <sub>3</sub> ...	29

- Figure 2.9: (a) UV-vis spectra of **2.1** ( $1.00 \times 10^{-5}$  M) in chloroform with increasing quantities of pyrophosphate (as  $((n\text{-Bu})_4\text{N})_3\text{HP}_2\text{O}_7$ ) ( $0 \sim 3.0 \times 10^{-5}$  M). (b) Job plot for the interaction between host **2.1** and  $((n\text{-Bu})_4\text{N})_3\text{HP}_2\text{O}_7$  in chloroform with  $[\text{host} + \text{guest}] = 1.00 \times 10^{-5}$  M. A maximum value at 0.5 is seen; this is consistent with a 1:1 (host: guest) binding stoichiometry.....31
- Figure 2.10: (a) UV-vis spectra of **2.1** ( $1.00 \times 10^{-5}$  M) in chloroform with increasing quantities of  $(n\text{-Bu})_4\text{NH}_2\text{PO}_4$  ( $0 \sim 5.0 \times 10^{-5}$  M). (b) Job plot for the interaction between host **2.1** and  $(n\text{-Bu})_4\text{NH}_2\text{PO}_4$  in chloroform with  $[\text{host} + \text{guest}] = 5.00 \times 10^{-5}$  M. A maximum value at 0.5 is seen; this is consistent with a 1:1 (host: guest) binding stoichiometry.....32
- Figure 2.11: (a) UV-vis spectra of **2.1** ( $1.00 \times 10^{-5}$  M) in chloroform with increasing quantities of  $(n\text{-Bu})_4\text{NH}\text{SO}_4$  ( $0 \sim 3.0 \times 10^{-5}$  M). (b) Job plot for the interaction between host **2.1** and  $(n\text{-Bu})_4\text{NH}\text{SO}_4$  in chloroform with  $[\text{host} + \text{guest}] = 5.00 \times 10^{-5}$  M. A maximum value at 0.5 is seen; this is consistent with a 1:1 (host : guest) binding stoichiometry.....32
- Figure 2.12: (a) UV-vis spectra of **2.1** ( $1.00 \times 10^{-5}$  M) in chloroform with increasing quantities of  $(n\text{-Bu})_4\text{NCl}$  ( $0 \sim 8.0 \times 10^{-4}$  M). (b) UV-vis spectra of **2.1** ( $1.00 \times 10^{-5}$  M) in chloroform with increasing quantities of  $(n\text{-Bu})_4\text{NBr}$  ( $0 \sim 1.25 \times 10^{-3}$  M).....33
- Figure 2.13: (a) Variations in the absorbance at 340 nm (▪) of a solution of receptor **2.1** ( $1.00 \times 10^{-5}$  M) in  $\text{CHCl}_3$  as a function of  $(\text{TBA})_3\text{HP}_2\text{O}_7$  concentration ( $0 \sim 3.0 \times 10^{-5}$  M) at 300 K. (b) Variations in the absorbance (▪) at 340 nm of a solution of receptor **2.1** ( $1.00 \times 10^{-5}$  M) in  $\text{CHCl}_3$  as a function of  $\text{TBAH}_2\text{PO}_4$  concentration ( $0 \sim 5.0 \times 10^{-5}$  M) at 300 K. (c) Variations in the absorbance (▪) at 340 nm of a solution of receptor **2.1** ( $1.00 \times 10^{-5}$  M) in  $\text{CHCl}_3$  as a function of  $\text{TBAHSO}_4$  concentration ( $0 \sim 3.0 \times 10^{-5}$  M) at 300 K. (d) Variations in the absorbance (▪) at 300 nm of a solution of receptor **2.1** ( $1.00 \times 10^{-5}$  M) in  $\text{CHCl}_3$  as a function of  $\text{TBA}\text{Cl}$  concentration ( $0 \sim 8.0 \times 10^{-4}$  M) at 300 K. (e) Variations in the absorbance (▪) at 330 nm of a solution of receptor **2.1** ( $1.00 \times 10^{-5}$  M) in  $\text{CHCl}_3$  as a function of  $\text{TBA}\text{Br}$  concentration ( $0 \sim 1.25 \times 10^{-3}$  M) at 300 K.....34
- Figure 2.14:  $^1\text{H}$  NMR spectrum of macrocycle **2.1** and 0.5, 1.0, 2.0, 5.0, 10.0 equiv. of  $(\text{TBA})_3\text{HP}_2\text{O}_7$  recorded in  $\text{CDCl}_3$  at 300 K.....36
- Figure 2.15:  $^1\text{H}$  NMR spectrum of macrocycle **2.1** and 0.5, 1.0, 2.0, 5.0, 10.0 equiv. of  $\text{TBAH}_2\text{PO}_4$  recorded in  $\text{CDCl}_3$  at 300 K. (Peak “g” is as ascribed to the  $\text{H}_2\text{PO}_4^-$  anion.).....37

- Figure 2.16:  $^1\text{H}$  NMR spectrum of macrocycle **2.1** and 0.5, 1.0, 2.0, 5.0, 10.0 equiv. of  $\text{TBAHSO}_4$  recorded in  $\text{CDCl}_3$  at 300 K.....38
- Figure 2.17:  $^1\text{H}$  NMR spectrum of macrocycle **2.1** and 0.5, 1.0, 2.0, 5.0, 10.0 equiv. of  $\text{TBACl}$  recorded in  $\text{CDCl}_3$  at 300 K.....39
- Figure 2.18:  $^1\text{H}$  NMR spectrum of macrocycle **2.1** and 0.5, 1.0, 2.0, 5.0, 10.0 equiv. of  $\text{TBABr}$  recorded in  $\text{CDCl}_3$  at 300 K.....40
- Figure 2.19: ESI high resolution mass spectrum of samples containing, respectively, 1 molar equiv. of  $(\text{TBA})_3\text{HP}_2\text{O}_7$  (a),  $\text{TBAH}_2\text{PO}_4$  (b),  $\text{TBAHSO}_4$  (c),  $\text{TBACl}$  (d),  $\text{TBABr}$  (e) and host **2.1**.....42
- Figure 2.20: Views of the single crystal X-ray structure of **2.1** $\cdot 4\text{CH}_3\text{OH}\cdot\text{H}_2\text{O}$ . All solvent molecules have been omitted for clarity and the thermal ellipsoids have been drawn at the 25% probability level. Symmetry operator  $(-x, 1-y, -z)$  generates equivalent atoms marked with "A". **a**, Top view and **b**, side view showing the near planar conformation of **2.1**. Selected distances [ $\text{\AA}$ ]:  $a = 2.558$ ,  $b = 2.744$ ,  $c = 2.601$ ,  $d = 3.056$ . This leads us to suggest that intramolecular H-bonding interactions on the exterior of the ring help stabilize the observed planar conformation in the solid state; .....52
- Figure 2.21: Views of the single crystal X-ray structure of **2.1** $\cdot\text{TBA}_3\text{HP}_2\text{O}_7\cdot 3\text{H}_2\text{O}$ . All solvent molecules and TBA cations have been omitted for clarity and thermal ellipsoids drawn at the 25% probability level. **a**, Top view and **b**, **c** side view showing that the pyrophosphate anion is in a space filling representation. Selected distances [ $\text{\AA}$ ]:  $a = 1.905$ ,  $b = 2.324$ ,  $c = 3.870$ . This confirms that pyrrole NH and triazole CH protons are involved in hydrogen bond interactions with pyrophosphate guest;.....53
- Figure 3.1: (a) Top and (b) side views of the single crystal X-ray structure of **3.1** $^{4+}\cdot 4\text{BF}_4^-\cdot\text{CH}_3\text{OH}\cdot 3\text{H}_2\text{O}$ . All solvent molecules have been omitted for clarity.....61

- Figure 3.2: Variations in absorbance (▪) at 380 nm of a solution of receptor **3.1**<sup>4+</sup>•4BF<sub>4</sub><sup>-</sup> ( $5.00 \times 10^{-5}$  M) in acetone–H<sub>2</sub>O (2:3) (PH = 7.2 in HEPES buffer) as a function of the concentration in TBAHSO<sub>4</sub> ( $0\text{--}6.0 \times 10^{-5}$  M) (a), TBA<sub>3</sub>HP<sub>2</sub>O<sub>7</sub> ( $0\text{--}8.0 \times 10^{-5}$  M) (b) and TBAH<sub>2</sub>PO<sub>4</sub> ( $0\text{--}2.5 \times 10^{-4}$  M) (c) at 300K. The Job-plot for the complexation between **3.1**<sup>4+</sup>•4BF<sub>4</sub><sup>-</sup> and TBAHSO<sub>4</sub> (d), (TBA)<sub>3</sub>HP<sub>2</sub>O<sub>7</sub> (e) and TBAH<sub>2</sub>PO<sub>4</sub> (f) in acetone–H<sub>2</sub>O (2:3) (PH = 7.2 in HEPES buffer) at 300K. [host] + [guest] =  $5.00 \times 10^{-5}$  M. A maximum value at 0.5 is observed; this is consistent with a 1:1 (host : guest) binding stoichiometry.....65
- Figure 3.3: Representative complexes that provide examples of the hydrogen bonding interactions present in the macrocycles.....67
- Figure 3.4: <sup>1</sup>H NMR spectra (aromatic region) of receptor [**3.1**<sup>4+</sup>•4BF<sub>4</sub><sup>-</sup>] (4 mM) recorded upon titration with TBA<sub>3</sub>HP<sub>2</sub>O<sub>7</sub>; CD<sub>3</sub>OD, 300 K.....69
- Figure 3.5: (a) Top and (b) side views of a single-crystal X-ray diffraction structure of **3.1**<sup>4+</sup>•HP<sub>2</sub>O<sub>7</sub><sup>3-</sup>•BF<sub>4</sub><sup>-</sup> in which the pyrophosphate anion is in a space filling representation and the tetrafluoroborate anion resides outside of the ring.....70
- Figure 3.6: (a) A single-crystal X-ray diffraction structure of 2(**3.1**<sup>4+</sup>)•2H<sub>2</sub>PO<sub>4</sub><sup>-</sup>•6BF<sub>4</sub><sup>-</sup>. This structure contains two parts. The first is composed of **3.1**<sup>4+</sup>•2H<sub>2</sub>PO<sub>4</sub><sup>-</sup>•2BF<sub>4</sub><sup>-</sup> and the second is composed of the free receptor **3.1**<sup>4+</sup>•4BF<sub>4</sub><sup>-</sup>. (b) Top and (c) side views of a single-crystal X-ray diffraction structure of **3.1**<sup>4+</sup>•2H<sub>2</sub>PO<sub>4</sub><sup>-</sup>•2BF<sub>4</sub><sup>-</sup> with two phosphate anions located in the center of the ring, which is part of the structure of 2(**3.1**<sup>4+</sup>)•2H<sub>2</sub>PO<sub>4</sub><sup>-</sup>•6BF<sub>4</sub><sup>-</sup>. (d) Top and (e) side views of a single-crystal X-ray diffraction structure of **3.1**<sup>4+</sup>•4BF<sub>4</sub><sup>-</sup>, which is part of the structure of 2(**3.1**<sup>4+</sup>)•2H<sub>2</sub>PO<sub>4</sub><sup>-</sup>•6BF<sub>4</sub><sup>-</sup>.....72
- Figure 3.7: (a) UV-Vis spectra of [**3.1**<sup>4+</sup>•4BF<sub>4</sub><sup>-</sup>] ( $1.00 \times 10^{-5}$  M) in CH<sub>3</sub>CN with increasing quantities of (n-Bu)<sub>4</sub>NHSO<sub>4</sub> ( $0 \sim 2.0 \times 10^{-5}$  M). (b) The job plot corresponding to the complexation between host and (n-Bu)<sub>4</sub>NHSO<sub>4</sub> in CH<sub>3</sub>CN. [host + guest] =  $1.00 \times 10^{-5}$  M. A maximum value at 0.5 is seen; this is consistent with a 1:1 (host : guest) binding stoichiometry.....78
- Figure 3.8: (a) UV-Vis spectra of [**3.1**<sup>4+</sup>•4BF<sub>4</sub><sup>-</sup>] ( $1.00 \times 10^{-5}$  M) in CH<sub>3</sub>CN with increasing quantities of ((n-Bu)<sub>4</sub>N)<sub>3</sub>HP<sub>2</sub>O<sub>7</sub> ( $0 \sim 4.0 \times 10^{-5}$  M). (b) The job plot corresponding to the complexation between host and ((n-Bu)<sub>4</sub>N)<sub>3</sub>HP<sub>2</sub>O<sub>7</sub> in CH<sub>3</sub>CN. [host + guest] =  $1.00 \times 10^{-5}$  M. A maximum value at 0.5 is seen; this is consistent with a 1:1 (host : guest) binding stoichiometry.....79

Figure 3.9: (a) UV-Vis spectra of  $[\mathbf{3.1}^{4+} \cdot 4\text{BF}_4^-]$  ( $1.00 \times 10^{-5}$  M) in  $\text{CH}_3\text{CN}$  with increasing quantities of  $(\text{n-Bu})_4\text{NH}_2\text{PO}_4$  ( $0 \sim 1.7 \times 10^{-4}$  M). (b) The job plot corresponding to the complexation between host and  $(\text{n-Bu})_4\text{NH}_2\text{PO}_4$  in  $\text{CH}_3\text{CN}$ .  $[\text{host} + \text{guest}] = 1.00 \times 10^{-5}$  M. A maximum value at 0.33 is seen; this is consistent with a 1:2 (host : guest) binding stoichiometry.....79

Figure 3.10: (a) UV-Vis spectra of  $[\mathbf{3.1}^{4+} \cdot 4\text{BF}_4^-]$  ( $1.00 \times 10^{-5}$  M) in  $\text{CH}_3\text{CN}$  with increasing quantities of  $(\text{n-Bu})_4\text{NOAc}$  ( $0 \sim 3.0 \times 10^{-5}$  M). (b) The job plot corresponding to the complexation between host and  $(\text{n-Bu})_4\text{NOAc}$  in  $\text{CH}_3\text{CN}$ .  $[\text{host} + \text{guest}] = 1.00 \times 10^{-5}$  M. A maximum value at 0.50 is seen; this is consistent with a 1:1 (host : guest) binding stoichiometry. ....80

Figure 3.11: (a) UV-Vis spectra of  $[\mathbf{3.1}^{4+} \cdot 4\text{BF}_4^-]$  ( $1.00 \times 10^{-5}$  M) in  $\text{CH}_3\text{CN}$  with increasing quantities of  $(\text{n-Bu})_4\text{NCl}$  ( $0 \sim 5.0 \times 10^{-5}$  M). (b) The job plot corresponding to the complexation between host and  $(\text{n-Bu})_4\text{NCl}$  in  $\text{CH}_3\text{CN}$ .  $[\text{host} + \text{guest}] = 1.00 \times 10^{-5}$  M. A maximum value at 0.50 is seen; this is consistent with a 1:1 (host : guest) binding stoichiometry.....80

Figure 3.12: (a) UV-Vis spectra of  $[\mathbf{3.1}^{4+} \cdot 4\text{BF}_4^-]$  ( $1.00 \times 10^{-5}$  M) in  $\text{CH}_3\text{CN}$  with increasing quantities of  $(\text{n-Bu})_4\text{NBr}$  ( $0 \sim 1.5 \times 10^{-4}$  M). (b) The job plot corresponding to the complexation between host and  $(\text{n-Bu})_4\text{NBr}$  in  $\text{CH}_3\text{CN}$ .  $[\text{host} + \text{guest}] = 1.00 \times 10^{-5}$  M. A maximum value at 0.50 is seen; this is consistent with a 1:1 (host : guest) binding stoichiometry.....81

Figure 3.13: (a) UV-Vis spectra of  $[\mathbf{3.1}^{4+} \cdot 4\text{BF}_4^-]$  ( $1.00 \times 10^{-5}$  M) in  $\text{CH}_3\text{CN}$  with increasing quantities of  $(\text{n-Bu})_4\text{NNO}_3$  ( $0 \sim 5.0 \times 10^{-5}$  M). (b) The job plot corresponding to the complexation between host and  $(\text{n-Bu})_4\text{NNO}_3$  in  $\text{CH}_3\text{CN}$ .  $[\text{host} + \text{guest}] = 1.00 \times 10^{-5}$  M. A maximum value at 0.5 is seen; this is consistent with a 1:1 (host : guest) binding stoichiometry.....81



Figure 3.14: (a) Variations in the absorbance at 380 nm (▪) of a solution of receptor  $[3.1^{4+} \cdot 4BF_4^-]$  ( $1.00 \times 10^{-5}$  M) in  $CH_3CN$  as a function of  $TBAHSO_4$  concentration ( $0 \sim 2.0 \times 10^{-5}$  M) at 300 K. (b) Variations in the absorbance (▪) at 266 nm of a solution of receptor  $[3.1^{4+} \cdot 4BF_4^-]$  ( $1.00 \times 10^{-5}$  M) in  $CH_3CN$  as a function of  $TBA_3HP_2O_7$  concentration ( $0 \sim 4.0 \times 10^{-5}$  M) at 300 K. (c) Variations in the absorbance (▪) at 290 nm of a solution of receptor  $[3.1^{4+} \cdot 4BF_4^-]$  ( $1.00 \times 10^{-5}$  M) in  $CH_3CN$  as a function of  $TBAH_2PO_4$  concentration ( $0 \sim 5.0 \times 10^{-5}$  M) at 300 K. (d) Variations in the absorbance (▪) at 310 nm of a solution of receptor  $[3.1^{4+} \cdot 4BF_4^-]$  ( $1.00 \times 10^{-5}$  M) in  $CH_3CN$  as a function of  $TBAOAc$  concentration ( $0 \sim 3.0 \times 10^{-5}$  M) at 300 K. (e) Variations in the absorbance (▪) at 290 nm of a solution of receptor  $[3.1^{4+} \cdot 4BF_4^-]$  ( $1.00 \times 10^{-5}$  M) in  $CH_3CN$  as a function of  $TBACl$  concentration ( $0 \sim 6.0 \times 10^{-5}$  M) at 300 K. (f) Variations in the absorbance (▪) at 350 nm of a solution of receptor  $[3.1^{4+} \cdot 4BF_4^-]$  ( $1.00 \times 10^{-5}$  M) in  $CH_3CN$  as a function of  $TBABr$  concentration ( $0 \sim 6.0 \times 10^{-5}$  M) at 300 K. (g) Variations in the absorbance (▪) at 350 nm of a solution of receptor  $[3.1^{4+} \cdot 4BF_4^-]$  ( $1.00 \times 10^{-5}$  M) in  $CH_3CN$  as a function of  $TBANO_3$  concentration ( $0 \sim 5.0 \times 10^{-5}$  M) at 300 K.....82

Figure 3.15: (a) UV-Vis spectra of  $[3.1^{4+} \cdot 4BF_4^-]$  ( $1.00 \times 10^{-5}$  M) in  $CH_3OH$  with increasing quantities of  $(n-Bu)_4NHSO_4$  ( $0 \sim 3.0 \times 10^{-5}$  M). (b) The job plot corresponding to the complexation between host and  $(n-Bu)_4NHSO_4$  in  $CH_3OH$ .  $[host + guest] = 1.00 \times 10^{-5}$  M. A maximum value at 0.5 is seen; this is consistent with a 1:1 (host : guest) binding stoichiometry.....85

Figure 3.16: (a) UV-Vis spectra of  $[3.1^{4+} \cdot 4BF_4^-]$  ( $1.00 \times 10^{-5}$  M) in  $CH_3OH$  with increasing quantities of  $((n-Bu)_4N)_3HP_2O_7$  ( $0 \sim 2.0 \times 10^{-5}$  M). (b) The job plot corresponding to the complexation between host and  $((n-Bu)_4N)_3HP_2O_7$  in  $CH_3OH$ .  $[host + guest] = 1.00 \times 10^{-5}$  M. A maximum value at 0.5 is seen; this is consistent with a 1:1 (host : guest) binding stoichiometry.....85

Figure 3.17: (a) UV-Vis spectra of  $[3.1^{4+} \cdot 4BF_4^-]$  ( $1.00 \times 10^{-5}$  M) in  $CH_3OH$  with increasing quantities of  $(n-Bu)_4NH_2PO_4$  ( $0 \sim 4.0 \times 10^{-5}$  M). (b) The job plot corresponding to the complexation between host and  $(n-Bu)_4NH_2PO_4$  in  $CH_3OH$ .  $[host + guest] = 1.00 \times 10^{-5}$  M. A maximum value at 0.50 is seen; this is consistent with a 1:1 (host : guest) binding stoichiometry.....86

Figure 3.18: (a) UV-Vis spectra of  $[3.1^{4+} \cdot 4BF_4^-]$  ( $1.00 \times 10^{-5}$  M) in  $CH_3OH$  with increasing quantities of  $(n-Bu)_4NOAc$  ( $0 \sim 2.0 \times 10^{-3}$  M). (b) UV-Vis spectra of  $[3.1^{4+} \cdot 4BF_4^-]$  ( $1.00 \times 10^{-5}$  M) in  $CH_3OH$  with increasing quantities of  $(n-Bu)_4NNO_3$  ( $0 \sim 9.0 \times 10^{-4}$  M).....86

Figure 3.19: (a) UV-Vis spectra of  $[3.1^{4+} \cdot 4BF_4^-]$  ( $1.00 \times 10^{-5}$  M) in  $CH_3OH$  with increasing quantities of  $(n-Bu)_4NCl$  ( $0 \sim 2.5 \times 10^{-3}$  M). (b) UV-Vis spectra of  $[3.1^{4+} \cdot 4BF_4^-]$  ( $1.00 \times 10^{-5}$  M) in  $CH_3OH$  with increasing  $(n-Bu)_4NBr$  ( $0 \sim 1.5 \times 10^{-3}$  M).....87

Figure 3.20: (a) Variations in the absorbance at 305 nm ( $\blacksquare$ ) of a solution of receptor  $[3.1^{4+} \cdot 4BF_4^-]$  ( $1.00 \times 10^{-5}$  M) in  $CH_3OH$  as a function of  $TBAHSO_4$  concentration ( $0 \sim 3.0 \times 10^{-5}$  M) at 300 K. (b) Variations in the absorbance ( $\blacksquare$ ) at 310 nm of a solution of receptor  $[3.1^{4+} \cdot 4BF_4^-]$  ( $1.00 \times 10^{-5}$  M) in  $CH_3OH$  as a function of  $TBA_3HP_2O_7$  concentration ( $0 \sim 2.0 \times 10^{-5}$  M) at 300 K. (c) Variations in the absorbance ( $\blacksquare$ ) at 337 nm of a solution of receptor  $[3.1^{4+} \cdot 4BF_4^-]$  ( $1.00 \times 10^{-5}$  M) in  $CH_3OH$  as a function of  $TBAH_2PO_4$  concentration ( $0 \sim 4.0 \times 10^{-5}$  M) at 300 K. (d) Variations in the absorbance ( $\blacksquare$ ) at 305 nm of a solution of receptor  $[3.1^{4+} \cdot 4BF_4^-]$  ( $1.00 \times 10^{-5}$  M) in  $CH_3OH$  as a function of  $TBAOAc$  concentration ( $0 \sim 2.0 \times 10^{-3}$  M) at 300 K. (e) Variations in the absorbance ( $\blacksquare$ ) at 310 nm of a solution of receptor  $[3.1^{4+} \cdot 4BF_4^-]$  ( $1.00 \times 10^{-5}$  M) in  $CH_3OH$  as a function of  $TBACl$  concentration ( $0 \sim 2.5 \times 10^{-3}$  M) at 300 K. (f) Variations in the absorbance ( $\blacksquare$ ) at 308 nm of a solution of receptor  $[3.1^{4+} \cdot 4BF_4^-]$  ( $1.00 \times 10^{-5}$  M) in  $CH_3OH$  as a function of  $TBABr$  concentration ( $0 \sim 1.2 \times 10^{-3}$  M) at 300 K. (g) Variations in the absorbance ( $\blacksquare$ ) at 310 nm of a solution of receptor  $[3.1^{4+} \cdot 4BF_4^-]$  ( $1.00 \times 10^{-5}$  M) in  $CH_3OH$  as a function of  $TBANO_3$  concentration ( $0 \sim 5.0 \times 10^{-4}$  M) at 300 K.....88

Figure 3.21: (a) UV-Vis spectra of  $[3.1^{4+} \cdot 4BF_4^-]$  ( $5.00 \times 10^{-5}$  M) in acetone- $H_2O$  (2 : 3) with increasing quantities of  $(n-Bu)_4NH_4SO_4$  ( $0 \sim 6.0 \times 10^{-5}$  M). The solution was buffered at pH 7.2 with HEPES buffer ( $5.00 \times 10^{-3}$  M). (b) The job plot corresponding to the complexation between host and  $(n-Bu)_4NH_4SO_4$  in acetone- $H_2O$  (2 : 3). The solution was buffered at pH 7.2 with HEPES buffer ( $5.00 \times 10^{-3}$  M). [host + guest] =  $5.00 \times 10^{-5}$  M. A maximum value at 0.5 is seen; this is consistent with a 1:1 (host : guest) binding stoichiometry.....91

Figure 3.22: (a) UV-Vis spectra of  $[3.1^{4+} \cdot 4BF_4^-]$  ( $5.00 \times 10^{-5}$  M) in acetone- $H_2O$  (2 : 3) with increasing quantities of  $((n-Bu)_4N)_3HP_2O_7$  ( $0 \sim 8.0 \times 10^{-5}$  M). The solution was buffered at pH 7.2 with HEPES buffer ( $5.00 \times 10^{-3}$  M). (b) The job plot corresponding to the complexation between host and  $((n-Bu)_4N)_3HP_2O_7$  in acetone- $H_2O$  (2 : 3). The solution was buffered at pH 7.2 with HEPES buffer ( $5.00 \times 10^{-3}$  M). [host + guest] =  $5.00 \times 10^{-5}$  M. A maximum value at 0.5 is seen; this is consistent with a 1:1 (host : guest) binding stoichiometry.....92

- Figure 3.23: (a) UV-Vis spectra of  $[3.1^{4+} \cdot 4BF_4^-]$  ( $5.00 \times 10^{-5}$  M) in acetone–H<sub>2</sub>O (2 : 3) with increasing quantities of (n-Bu)<sub>4</sub>NH<sub>2</sub>PO<sub>4</sub> ( $0 \sim 2.5 \times 10^{-4}$  M). The solution was buffered at pH 7.2 with HEPES buffer ( $5.00 \times 10^{-3}$  M). (b) The job plot corresponding to the complexation between host and (n-Bu)<sub>4</sub>NH<sub>2</sub>PO<sub>4</sub> in acetone–H<sub>2</sub>O (2 : 3). The solution was buffered at pH 7.2 with HEPES buffer ( $5.00 \times 10^{-3}$  M). [host + guest] =  $5.00 \times 10^{-5}$  M. A maximum value at 0.50 is seen; this is consistent with a 1:1 (host : guest) binding stoichiometry.....93
- Figure 3.24: (a) Variations in the absorbance at 380 nm (▪) of a solution of receptor  $[3.1^{4+} \cdot 4BF_4^-]$  ( $5.00 \times 10^{-5}$  M) in acetone–H<sub>2</sub>O (2 : 3) as a function of TBAHSO<sub>4</sub> concentration ( $0 \sim 6.0 \times 10^{-5}$  M) at 300 K. The solution was buffered at pH 7.2 with HEPES buffer ( $5.00 \times 10^{-3}$  M). (b) Variations in the absorbance (▪) at 380 nm of a solution of receptor  $[3.1^{4+} \cdot 4BF_4^-]$  ( $5.00 \times 10^{-5}$  M) in acetone–H<sub>2</sub>O (2 : 3) as a function of TBA<sub>3</sub>HP<sub>2</sub>O<sub>7</sub> concentration ( $0 \sim 8.0 \times 10^{-5}$  M) at 300 K. The solution was buffered at pH 7.2 with HEPES buffer ( $5.00 \times 10^{-3}$  M). (c) Variations in the absorbance (▪) at 380 nm of a solution of receptor  $[3.1^{4+} \cdot 4BF_4^-]$  ( $5.00 \times 10^{-5}$  M) in acetone–H<sub>2</sub>O (2 : 3) as a function of TBAH<sub>2</sub>PO<sub>4</sub> concentration ( $0 \sim 2.5 \times 10^{-4}$  M) at 300 K. The solution was buffered at pH 7.2 with HEPES buffer ( $5.00 \times 10^{-3}$  M).....94
- Figure 3.25: <sup>1</sup>H NMR spectrum of anion receptor  $[3.1^{4+} \cdot 4BF_4^-]$  and 0.25, 0.50, 0.75, 1.0, 1.5, 2.0, 2.5, 3.0, 4.0, 5.0 equiv. TBA<sub>3</sub>HP<sub>2</sub>O<sub>7</sub> recorded in CD<sub>3</sub>OD at 300 K.....96
- Figure 3.26: <sup>1</sup>H NMR spectrum of anion receptor  $[3.1^{4+} \cdot 4BF_4^-]$  and 0.25, 0.50, 0.75, 1.0, 1.5, 2.0, 2.5, 3.0, 4.0, 5.0 equiv. TBAHSO<sub>4</sub> recorded in CD<sub>3</sub>OD at 300 K.....97
- Figure 3.27: <sup>1</sup>H NMR spectrum of anion receptor  $[3.1^{4+} \cdot 4BF_4^-]$  and 0.25, 0.50, 0.75, 1.0, 1.5, 2.0, 2.5, 3.0, 4.0, 5.0 equiv. TBAH<sub>2</sub>PO<sub>4</sub> recorded in CD<sub>3</sub>OD at 300 K.....98
- Figure 3.28: <sup>1</sup>H NMR spectrum of anion receptor  $[3.1^{4+} \cdot 4BF_4^-]$  and 1.0, 2.0, 3.0, 4.0, 6.0, 8.0, 10.0 equiv. TBACl recorded in CD<sub>3</sub>OD at 300 K.....99
- Figure 3.29: <sup>1</sup>H NMR spectrum of anion receptor  $[3.1^{4+} \cdot 4BF_4^-]$  and 1.0, 2.0, 3.0, 4.0, 5.0, 6.0, 7.0, 8.0, 10.0 equiv. TBABr recorded in CD<sub>3</sub>OD at 300 K.....100
- Figure 3.30: <sup>1</sup>H NMR spectrum of anion receptor  $[3.1^{4+} \cdot 4BF_4^-]$  and 1.0, 2.0, 3.0, 4.0, 5.0, 6.0, 7.0, 8.0, 9.0, 10.0 equiv. TBAOAc recorded in CD<sub>3</sub>OD at 300 K.....101

- Figure 3.31:  $^1\text{H}$  NMR spectrum of anion receptor  $\mathbf{3.1}^{4+}\cdot 4\text{BF}_4^-$  and 1.0, 2.0, 3.0, 4.0, 5.0, 6.0, 7.0, 8.0, 9.0, 10.0 equiv.  $\text{TBA}\text{NO}_3$  recorded in  $\text{CD}_3\text{OD}$  at 300 K.....102
- Figure 3.32: Full view of the 2D COSY NMR spectrum of  $\mathbf{3.1}^{4+}\cdot 4\text{BF}_4^-$  recorded in  $\text{CD}_3\text{OD}$  at 300 K. (The peak at 2.74 ppm and 2.91 ppm belong to the DMF solvent).....103
- Figure 3.33: Full view of the 2D NOESY NMR spectrum of  $\mathbf{3.1}^{4+}\cdot 4\text{BF}_4^-$  recorded in  $\text{CD}_3\text{OD}$  at 300 K. (The peak at 2.74 ppm and 2.91 ppm belong to the DMF solvent).....104
- Figure 3.34: Full view of the 2D COSY NMR spectrum of  $\mathbf{3.1}^{4+}\cdot 4\text{BF}_4^-$  containing two equivalent  $\text{TBA}_3\text{HP}_2\text{O}_7$  recorded in  $\text{CD}_3\text{OD}$  at 300 K. (The peak at 2.74 ppm and 2.91 ppm belong to the DMF solvent).....105
- Figure 3.35: Full view of the 2D NOESY NMR spectrum of  $\mathbf{3.1}^{4+}\cdot 4\text{BF}_4^-$  adding two equivalent  $\text{TBA}_3\text{HP}_2\text{O}_7$  recorded in  $\text{CD}_3\text{OD}$  at 300 K. (The peak at 2.74 ppm and 2.91 ppm belong to the DMF solvent).....106
- Figure 3.36: N-H $\cdots$ F and C-H $\cdots$ F hydrogen bonded interactions seen in the single crystal structure of  $\mathbf{3.1}^{4+}\cdot 4\text{BF}_4^- \cdot \text{CH}_3\text{OH} \cdot 3\text{H}_2\text{O}$ : C(8)-H $\cdots$ F(5): 2.399 Å, C-H-F 128.9°; C(20)-H $\cdots$ F(7): 2.230 Å, C-H-F 148.1°; N(8)-H $\cdots$ F(7): 1.983 Å, N-H-F 165.1°.....112
- Figure 3.37: N-H $\cdots$ O and C-H $\cdots$ O hydrogen bonded interactions seen in the single crystal structure of  $\mathbf{3.1}^{4+} \cdot \text{HP}_2\text{O}_7^{3-} \cdot \text{BF}_4^-$ : N(4)-H $\cdots$ O(5): 1.896 Å, N-H-O 170.5°; N(5)-H $\cdots$ O(7): 1.924 Å, N-H-O 168.5°; N(12)-H $\cdots$ O(2): 1.802 Å, N-H-O 163.9°; N(13)-H $\cdots$ O(3): 1.981 Å, N-H-O 166.6°; C(50)-H $\cdots$ O(3): 1.969 Å, C-H-O 156.6°; C(53)-H $\cdots$ O(3): 3.337 Å, C-H-O 143.5°; C(8)-H $\cdots$ O(5): 2.245 Å, C-H-O 147.5°; C(23)-H $\cdots$ O(7): 2.123 Å, C-H-O 150.6°; C(26)-H $\cdots$ O(7): 3.388 Å, C-H-O 154.4°; C(35)-H $\cdots$ O(2): 2.013 Å, C-H-O 145.3°.....113
- Figure 3.38: N-H $\cdots$ O and C-H $\cdots$ O hydrogen bonded interactions seen in the single crystal structure of  $2(\mathbf{3.1}^{4+}) \cdot 2\text{H}_2\text{PO}_4^- \cdot 6\text{BF}_4^-$ : N(4)-H $\cdots$ O(4): 2.246 Å, N-H-O 136.7°; N(5)-H $\cdots$ O(4): 2.485 Å, N-H-O 123.1°; N(12)-H $\cdots$ O(8): 1.982 Å, N-H-O 157.9°; N(13)-H $\cdots$ O(8): 2.004 Å, N-H-O 159.6°; C(8)-H $\cdots$ O(6): 2.661 Å, C-H-O 145.9°; C(52)-H $\cdots$ O(6): 2.341 Å, C-H-O 154.7°; C(37)-H $\cdots$ O(7): 2.411 Å, C-H-O 159.2°; C(32)-H $\cdots$ O(7): 2.598 Å, C-H-O 143.6°.....114

- Figure 4.1: Single-crystal X-ray structure of **4.2**. All solvent molecules have been omitted for clarity. The dihedral angle between the two triazolium rings is 53.4°. The dihedral angles between the triazolium and pyrrole rings are 9.1° (Plane<sub>N5</sub>/Plane<sub>N8</sub>) and 5.4° (Plane<sub>N2</sub>/Plane<sub>N1</sub>).....123
- Figure 4.2: Single-crystal X-ray structure of **4.3**. All solvent molecules have been omitted for clarity. Short intermolecular  $\pi$ - $\pi$  distances (X1A...X1B: 3.543 Å, X1C...X1D: 3.387 Å, and X1E...X1F: 3.576 Å) and C-H... $\pi$  interactions (C(68)-H... $\pi$ : 2.484 Å, C-H- $\pi$ : 164.6° and C(44)-H... $\pi$ : 2.894 Å and C-H- $\pi$ : 111.2°) are seen in this octa-Ag(I) complex.....124
- Figure 4.3: Single-crystal X-ray structure of **4.4**. All solvent molecules have been omitted for clarity. The dihedral angle between two triazolylidene rings is 50.9°. The dihedral angles between the triazolylidene and pyrrole rings are 3.0° (Plane<sub>N5</sub>/Plane<sub>N8</sub>) and 4.1° (Plane<sub>N2</sub>/Plane<sub>N1</sub>). Selected bond lengths and angles: Ru(1)-C(6) = 2.025(6) Å, Ru(1)-N(1) = 2.096(6) Å, Ru(1)-Cl(1) = 2.432(2) Å, Ru(1)-C(centroid) = 1.708 Å; C(6)-Ru(1)-N(1) = 76.3(2)°, C(6)-Ru(1)-Cl(1) = 85.21(18)°, N(1)-Ru(1)-Cl(1) = 87.74(16)°.....125
- Figure 4.4: <sup>1</sup>H NMR spectrum of **4.4** recorded in DMSO-*d*<sub>6</sub> at 300 K.....126
- Figure 4.5: Norbornene conversion as a function of time with two different catalyst systems.....127
- Figure 4.6: <sup>1</sup>H NMR spectrum of **4.3** recorded in DMSO-*d*<sub>6</sub> at 300 K.....131
- Figure 4.7: (a) Full view and (b) expanded view of the 2D COSY NMR spectrum of **4.4** recorded in DMSO-*d*<sub>6</sub> at 300 K.....132
- Figure 4.8: Gel permeation chromatography of polynorbornene **4.5**. Its number average molar mass (M<sub>n</sub>) is 46364 Daltons. Its weight average molar mass (M<sub>w</sub>) is 70240 Daltons.....133
- Figure 4.9: Gel permeation chromatography of polynorbornene **4.6**. Its number average molar mass (M<sub>n</sub>) is 29279 Daltons. Its weight average molar mass (M<sub>w</sub>) is 31496 Daltons.....134

## Chapter 1: Introduction

### 1.1 ANIONS

Anions are ubiquitous in the natural world. They have significant importance in chemistry, biology and environment, comprising the electron rich half of all ionic compounds. Their study has gained a tremendous attention in the last half century due to widespread deleterious effects. Sulfate is prominent as a toxic, troublesome species which causes acid rain.<sup>1</sup> Nitrate is the most abundant chemical contaminant in the world's ground water, because of its agricultural fertilizer runoff.<sup>2</sup> Nitrates and nitrites are used as widespread preservatives in meat, and are precursors in the formation of N-nitroso compounds (NOC), a class of genotoxic compounds, most of which are animal carcinogens.<sup>3</sup> The increasing amount of phosphate in rivers coming from factories and fertilizers present a problem, which leads to the eutrophication of waterways and the production of toxic algal blooms.<sup>4</sup> Pertechnetate, a radioactive product of nuclear fuel reprocessing, constitutes a major pollution hazard.<sup>4</sup>

Anions are critical to the maintenance of life and also play important roles in a range of biological processes. Indeed, the recognition, transport, or transformation of anions is involved at some level in almost every conceivable biochemical operation. ATP and other high-energy anionic phosphate derivatives are at the center of power processes as diverse and important as biosynthesis, molecular transport, and muscle contraction.<sup>1</sup> Pyrophosphate is the product of ATP hydrolysis under cellular conditions and is involved in DNA replication catalyzed by DNA polymerase.<sup>5</sup> The detection of pyrophosphate is thus being explored as a real time DNA sequencing method, a line of investigation that has implications in cancer research.<sup>6</sup> Its analogue, inorganic phosphate, has physiological relevance in biological energy storage and signal transduction. It is also a structural component in teeth and bones.<sup>7</sup>

Compared to cations, the design of anion receptors is particularly. There are a number of reasons for this. (1) Anions are larger than the equivalent isoelectronic cations, resulting in a lower charge to radius ratios.<sup>8</sup> The more diffuse nature of anions was the consequence that electrostatic binding interactions for anions are less effective than for the corresponding isoelectronic cations (Table 1.1). (2) Most anions are pH sensitive, many become protonated at low pH and lose their negative charge. Thus, receptors need to function within the pH window of their targeted anion. (3) Anions have a wide range of geometries (Figure 1.1).<sup>1</sup> Therefore, a better design of receptors is required to select for a particular anionic guest than is true for most simple cations. (4) Anions can be well-solvated in the polar protic solvents and they have large hydration energies (Table 1.1),<sup>9</sup> which make anions difficult to extract out of aqueous environments.

**Table 1.1:** A comparison of the radii ( $r$ ) and hydration energies ( $\Delta G_{\text{hyd}}$ ) of selected isoelectronic anions and cations<sup>9</sup>

Anion	$r$ (Å)	$\Delta G_{\text{hyd}}$ (kJ/mol)	Cation	$r$ (Å)	$\Delta G_{\text{hyd}}$ (kJ/mol)
F <sup>-</sup>	1.19	-465	Na <sup>+</sup>	1.16	-365
Cl <sup>-</sup>	1.67	-340	K <sup>+</sup>	1.52	-295
Br <sup>-</sup>	1.82	-315	Rb <sup>+</sup>	1.66	-275
I <sup>-</sup>	2.06	-275	Cs <sup>+</sup>	1.81	-250

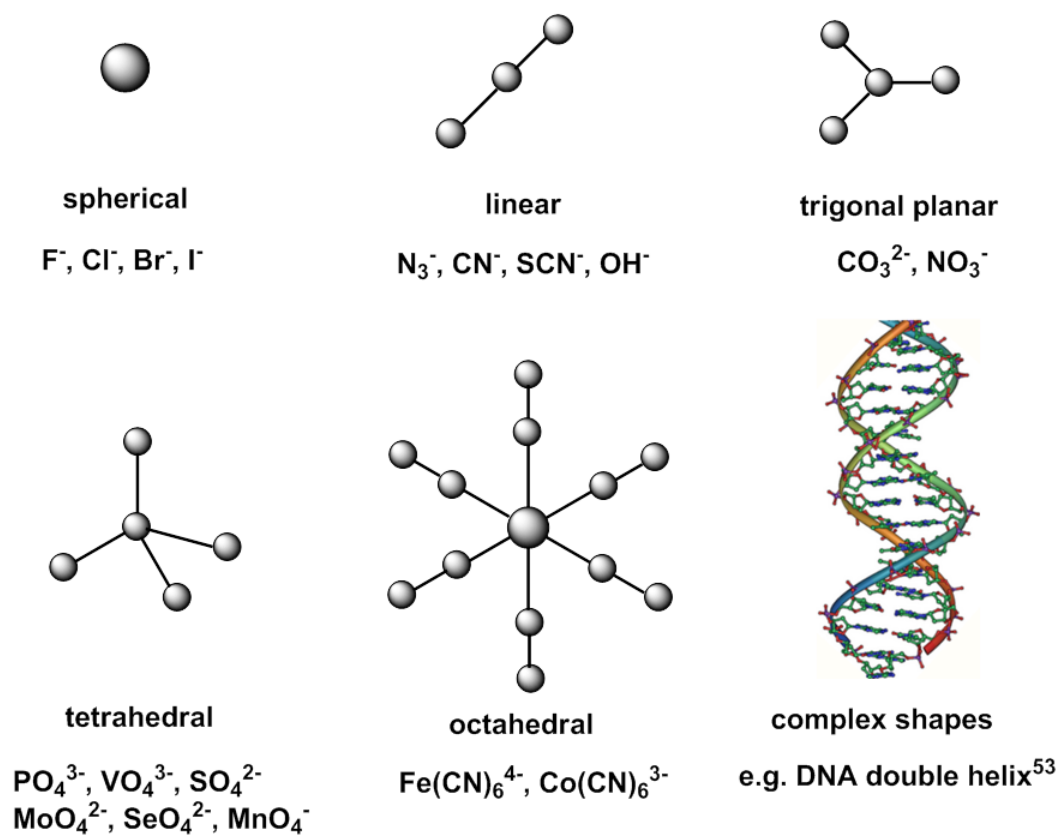


**Figure 1.1:** Representative anions, classified by shapes and sizes.



## 1.2 SUPRAMOLECULAR CHEMISTRY

Supramolecular chemistry is a highly interdisciplinary field of science covering the chemical, physical, and biological features of chemical species of greater complexity than simple molecules.<sup>10</sup> This relatively young area has extended into organic chemistry and the synthetic procedures for molecular construction. It also touches on coordination chemistry and metal ion-ligand complexes. It is relevant to physical chemistry and the experimental and theoretical studies of interactions. It can provide insights into biochemistry and biological processes that relate to substrate binding and recognition. Finally, supramolecular chemistry is extending its reach into materials science and the mechanical properties of solids.

In the broadest terms, supramolecular chemistry involves the study of noncovalent intermolecular interactions, which are generally weak and reversible in nature.<sup>11</sup> These interactions involve *inter alia* hydrogen bonding, electrostatic effects, hydrophobic forces, van der Waals forces,  $\pi$ - $\pi$  interactions, cation- $\pi$  or anion- $\pi$  interactions, and metal-ligand interactions. Of these forces, hydrogen bonding interactions are probably the most important. One of the most recognizable supramolecular systems is DNA, where self-complementary Watson-Crick hydrogen bonding interactions dictate specific base-pairing modes (Figure 1.2).

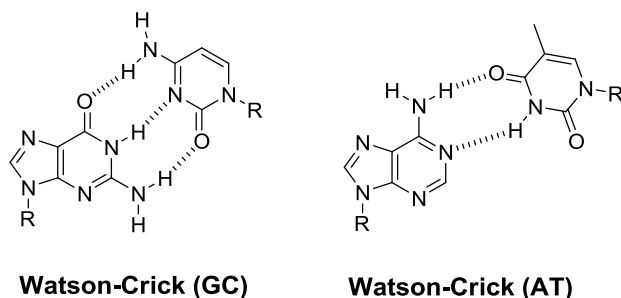
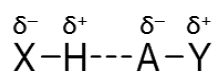


**Figure 1.2:** Canonical Watson-Crick base-pairing modes.

### 1.2.1 Hydrogen Bonding

Hydrogen bond is a weak electrostatic chemical bond which forms between covalently bonded hydrogen atoms and a strongly electronegative atom with a lone pair of electrons. A hydrogen bond is therefore the attractive force that arises between the donor covalent pair X-H in which a hydrogen atom H is bound to a more electronegative atom X i.e. O or N, and other non-covalently bound nearest neighbor electronegative acceptor atoms A.



A can be variety of species. Most common are N and O in biology; A can also be a negatively charged anion or even a  $\pi$ -electron containing species. Moreover, C-H hydrogen bonds have also been observed which will be discussed in detail in this dissertation. Hydrogen bonding interactions can be classified in terms of their energy.<sup>12</sup> The strongest interactions (15-40 kcal/mol) have significant covalent character between both electronegative atoms and the shared H, and typically involve  $\text{O}-\text{H} \cdots \text{A}^-$  and  $\text{N}-\text{H} \cdots \text{N}^+$  contacts. Medium range hydrogen bonding interactions (4-15 kcal/mol) are dominated by electrostatics, and often involve  $\text{X}-\text{H} \cdots \text{O}$  and  $\text{X}-\text{H} \cdots \text{N}$  contacts. Finally, at the low end of the energetic range ( $0.5 < 4$  kcal/mol) are weakly electrostatic and dispersion-repulsion driven, such as hydrogen bonds of the  $\text{X}-\text{H} \cdots \pi$  type. The distance for X-H and  $\text{A} \cdots \text{H}$  also depend on the strength of the hydrogen bond. The distance from donor to acceptor can range from 2.2-4.0 Å. The location of the hydrogen atom depends on the electronegativity of the competing species.

Hydrogen bonds have been exploited in supramolecular chemistry where kinetics, reversibility, and orientation are critical. This utility reflects their non-covalent nature and their directionality. Of importance to this dissertation are the hydrogen bonds of the N-H

$\cdots A^-$ ,  $C-H\cdots A^-$ , and  $(C-H)^+\cdots A^-$  types, which are likely from pyrrole, triazole and triazolium donor subunits, respectively, with  $A^-$  being the anion of interest.

### 1.3 SYNTHETIC ANION RECEPTOR

One of the goals of supramolecular chemistry is to understand the interactions between guest anions and host supramolecules. This context, a big challenge is to sequester, transfer, and sense selectively anionic species. The inherent interest in these phenomena as well as the potential practical benefits of supramolecular anion recognition chemistry, help explain why synthetic anion receptor chemistry has emerged as one of the fastest growing areas in supramolecular chemistry in recent years.<sup>1,13-17</sup>

Anion receptors can be classified into different forms. Many lewis acids and proton donor motifs fall into the neutral category; Transition metals, protonated nitrogen and heterocyclic species provide cationic charges. Anion receptors include neutral amides, thioamides, sulfonamides, ureas, thioureas, phenols, pyrroles, carbazoles, and indoles, as well as charged species, such as ammoniums, guanidiniums, pyridiniums, imidazoliums, and triazoliums (Figure 1.3). A combination of these motifs is used in many systems.

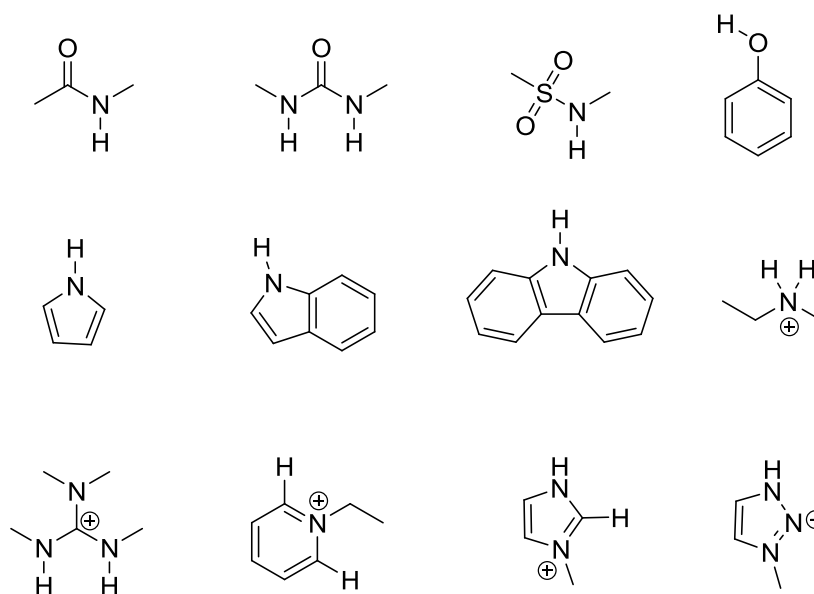


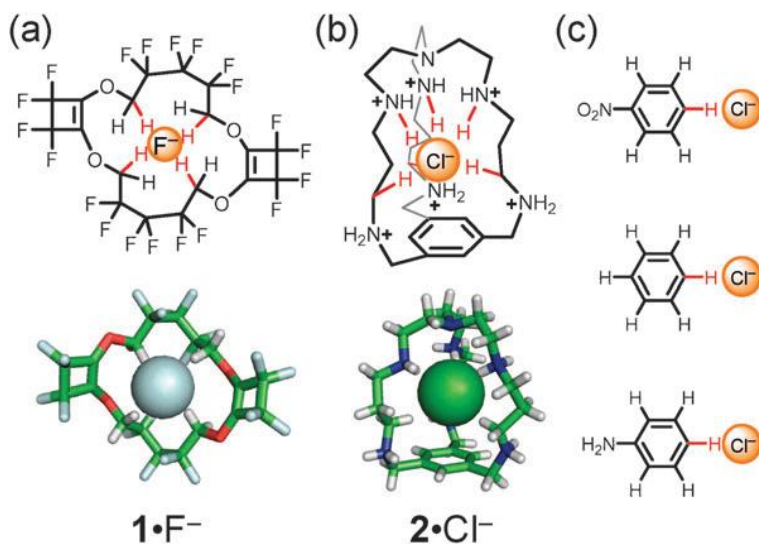
**Figure 1.3:** Hydrogen bond donors found in nature and used in supramolecular chemistry.

#### 1.4 NEUTRAL C-H...ANION HYDROGEN BONDS

The use of non-covalent interactions involving C-H hydrogen bond donors<sup>12</sup> took longer to gain acceptance for anion recognition than more traditional N-H and O-H donors. However, it is interesting to note that the possibility<sup>18</sup> of a CH hydrogen bond was first described in 1935, at the same time as traditional ones.<sup>19</sup> However, they were mentioned only occasionally in the literature until a systematic study involving the crystal structures of purines and pyrimidines was carried out in the 1960s.<sup>20</sup> Further investigations of them faltered momentarily after strong comments against the possibility of C-H based hydrogen bonds. Until a landmark analysis of crystallographic evidence for CH hydrogen bonds,<sup>21</sup> investigations culminated in a comprehensive and authoritative text about CH hydrogen bond donors which are entitled as “the weak hydrogen bond”.<sup>12</sup>

The book focuses on C-H $\cdots$ O interactions, while the discussions there are applicable to other hydrogen-bond acceptors, such as anions.

The awareness and use of neutral C-H hydrogen bonding in anion supramolecular chemistry started with observations of close C-H $\cdots$ anion contacts in crystal structures. The first discovery of note for neutral systems involved fluoride anion receptors<sup>22</sup> (*e.g.*, **1**, Scheme 1.1a) where aliphatic –CH<sub>2</sub>– groups are polarized by highly electronegative oxygen and fluorine atoms. In the second example, aliphatic –CH<sub>2</sub>– groups were implicated as stabilizing secondary interactions in macrobicyclic receptors (**2**, Scheme 1.1b).<sup>23</sup> At the same time, computational investigations played a large role in emphasizing the strength<sup>24,25</sup> and tunability<sup>26</sup> of aromatic (Scheme 1.1c) and aliphatic C-H $\cdots$ anion hydrogen bonds arising from neutral functional groups.



**Scheme 1.1:** Early discoveries of C-H $\cdots$ anion interactions in (a) macrocyclic and (b) macrobicyclic receptors, and, (c) recent theoretical works, helped to stimulate experimental studies of anion binding.<sup>51</sup>

In 2008, a number of studies aimed involving neutral C-H $\cdots$ anion interactions were published.<sup>27-34</sup> The first of these reports investigated the gas-phase binding of various anions using a cavitand-based receptor (**3**, Scheme 1.2).<sup>27</sup> In this case, the involved in CH-anion hydrogen bonds were methylene units activated by adjacent electronegative oxygen atoms. The second receptor involved the use of a strapped calix[4]pyrrole (**4**, Scheme 1.2)<sup>31</sup> and electron deficient receptors (**5**, Scheme 1.2)<sup>32</sup> to promote aromatic and aliphatic C-H $\cdots$ anion interactions. Here, evidence of interaction was inferred from enhancement in the anion affinity or from the shifts in the C-H proton resonances seen upon binding. At the same time, computational studies were carried out to interpret those experimental data. A third development involved the discovery of anion binding promoted by the 1,2,3-triazole unit in both macrocyclic receptors (**6-9**, Scheme 1.2)<sup>28,33</sup> and foldamer-based receptors (**10-13**, Scheme 1.2).<sup>28-30</sup> The investigations of the triazole-based anion recognition arose in independent laboratories. This highlights the confluence of new synthesis and ideas that were opened up with the advent of “Click Chemistry”.



## 1.5 CATIONIC (C-H)<sup>+</sup> ··· ANION HYDROGEN BONDS

Most positively charged anion receptors have ammonium, protonated pyrrole or guanidinium groups as binding sites and interact with targeted anions *via* (N-H)<sup>+</sup> ··· A<sup>-</sup> hydrogen bonds and electrostatic interactions.<sup>14,35</sup> In recent years, relatively new cationic subunits for anion recognition have been introduced, namely the 1,3-disubstituted imidazolium motif and 1,4-disubstituted 1,2,3-triazolium motif. Receptors based on the imidazolium and triazolium cations stabilize the corresponding anion complexes *via* a combination of electrostatic interactions and (C-H)<sup>+</sup> ··· A<sup>-</sup> hydrogen bonds. Imidazolium and triazolium-based receptors offer a significant advantage, namely the possibility of pH-independent binding, compared to systems based on cationic NH hydrogen bond donors.

### 1.5.1 Imidazoliums

Imidazolium group can stabilize a strong interaction with anions through (C-H)<sup>+</sup> ··· A<sup>-</sup> type ionic hydrogen bonds due to charge-charge electrostatic interactions. The presence of these interactions was inferred from the crystal structures of imidazolium based ionic liquids<sup>36(a),(b)</sup> and calix[4]pyrroles complexing with imidazolium salts.<sup>36(c)</sup> In 1994, Welton and co-workers provided evidence that receptor **1** can interact with halide anions in solution as inferred from multinuclear NMR spectroscopic measurement (Figure 1.4).<sup>37</sup> It was found that the series of complexes **1**-X (X = Cl<sup>-</sup>, Br<sup>-</sup>, and I<sup>-</sup>) displayed distinct CH resonances in their respective <sup>1</sup>H and <sup>13</sup>C NMR spectra as recorded in CDCl<sub>3</sub>. The greatest differences observed are the signals for the C(2)H group located between the two imidazolium nitrogen atoms. Subsequently, Sato and coworkers reported a benzene-based tripodal imidazolium receptor for anion recognition (**2**, Figure 1.4).<sup>38</sup>



Later on, various types of receptors containing imidazolium moieties were reported, such as imidazolium cyclophanes (**3**, Figure 1.4),<sup>39</sup> calix-imidazoliums (**4**, Figure 1.4),<sup>40</sup> imidazolium anthracenes (**5**, Figure 1.4),<sup>41</sup> imidazolium calix[4]arenes (**6**, Figure 1.4),<sup>42</sup> imidazolium cavitands (**7**, Figure 1.4)<sup>43</sup> and imidazolium polythiophenes (**8**, Figure 1.4).<sup>44</sup> All these receptors utilized the imidazolium moieties as the binding sites for anions. However, the different hosts in question provided different binding properties with anions, presumably as the result of the various binding pockets stabilized by framework in question.

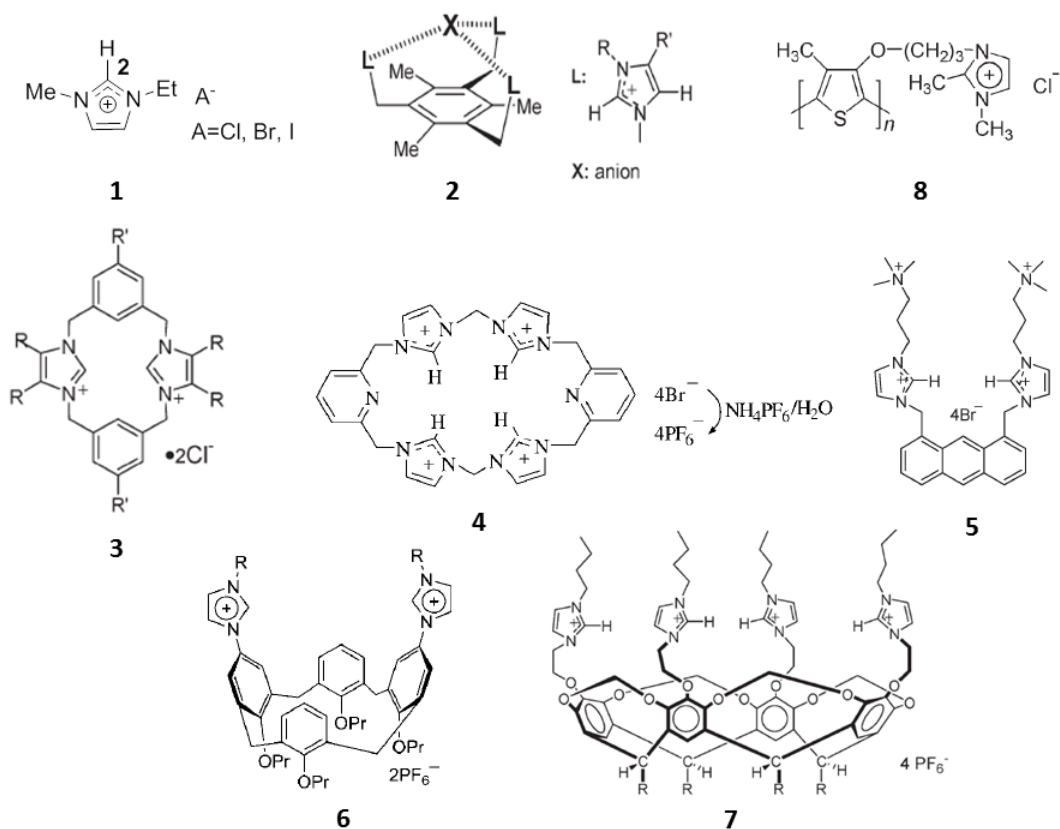


**Figure 1.4:** Structures of various types of receptors containing imidazolium moieties.<sup>52</sup>

### 1.5.2 1,2,3-Triazoliums

The copper(I)–catalyzed azide alkyne 1,3–dipolar cycloaddition (CuAAC)—one of the prime examples of the concept of highly efficient and modular reactions named “click” chemistry<sup>45</sup>—has been applied in the area of biological, materials, and medicinal chemistry.<sup>46</sup> In 2008, Albrecht and co-workers first reported the synthesis of 1,2,3-triazolylidenes as highly modular precursors for a new class of carbenes and their coordination chemistry with a variety of transition metals (Pd, Ru, Rh, and Ir).<sup>47</sup> Besides their participation in transition-metal coordination chemistry, the unique properties of the 1,4-disubstituted 1,2,3-triazolium ring have attracted attention in the area of anion recognition as a result of the ability of this subunit to stabilize triazolium (C-H)<sup>+</sup>···anion hydrogen bonds. Nevertheless, even today there are very few reports involving the use of positively charged triazolium motifs for anion recognition. In 2008, Pandey and co-workers reported a set of cyclic and acyclic bile acid-based 1,2,3-triazolium receptors that displayed a remarkable ability to recognize anions through (C-H)<sup>+</sup>···anion hydrogen bond interactions (**1**, Figure 1.5).<sup>48</sup> In 2009, Beer and co-workers reported the first examples wherein the 1,2,3-triazolium group was exploited for the anion templated formation of pseudorotaxane and rotaxane assemblies (**2**, Figure 1.5).<sup>49</sup> These systems are of interest because they exhibit rare selectivity for bromide over chloride. Later on, Schubert and co-workers designed mono- and bis-tridentate ligands employing the triazolium motif and showed that the systems in question could complex sulfate ions *via* a combination of hydrogen bonding and electrostatic interactions (**3**, Figure 1.5).<sup>50</sup>

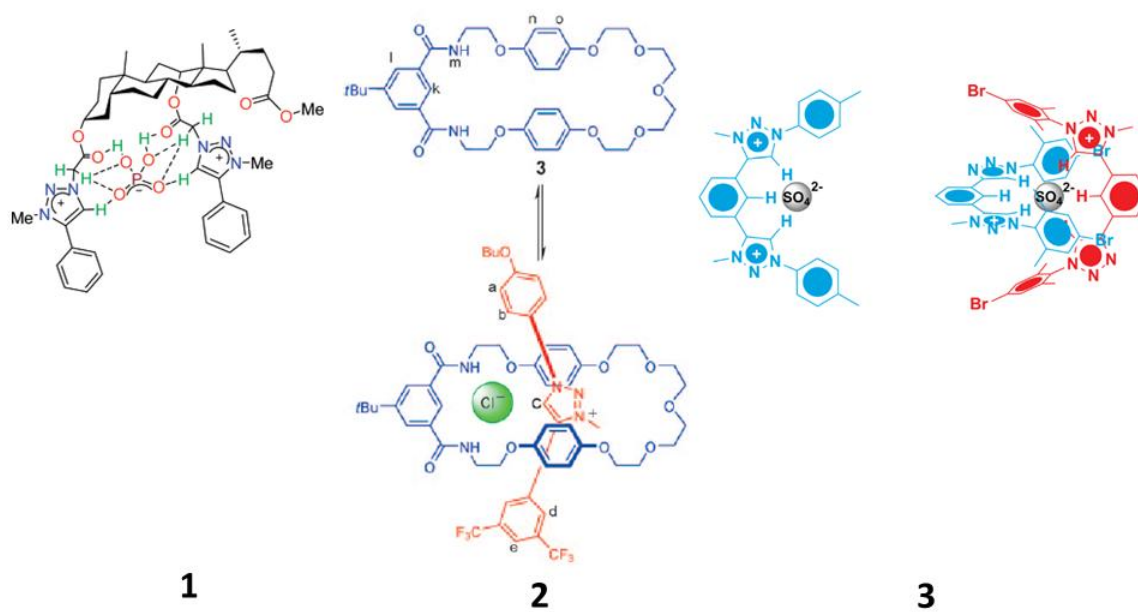


**Figure 1.5:** Structures of various types of receptors containing 1,2,3-triazoliums moieties.<sup>48,49,50</sup>

## 1.6 REFERENCES

- (1) Sessler, J. L.; Gale, P. A.; Cho, W.-S. *Anion Receptor Chemistry*; RSC Publishing: Cambridge, U.K., 2006.
- (2) Fields, S. *Environ. Health Perspect.* **2004**, *112*, A557-A563.
- (3) Lijinsky, W. *J. Environ. Sci. Health* **1986**, *C4*, 1-45.
- (4) Katayev, E. A.; Ustynyuk, Y. A.; Sessler, J. L. *Coord. Chem. Rev.* **2006**, *250*, 3004.
- (5) Xu, S.; He, M.; Yu, H.; Cai, X.; Tan, X.; Lu, B.; Shu, B. *Anal. Biochem.* **2001**, *299*, 188.
- (6) Ronaghi, M.; Karamohamed, S.; Pettersson, B.; Uhlén, M.; Nyrén, P. *Anal. Biochem.* **1996**, *242*, 84.
- (7) Saenger, W. *Principles of Nucleic Acid Structure*; Springer-Verlag: New York, 1988.
- (8) Shannon, R. D. *Acta Cryst.* **1976**, *A32*, 751.
- (9) Marcus, Y. *J. Chem. Soc., Faraday Trans.* **1991**, *87*, 2995.
- (10) Lehn, J.-M. *Supramolecular Chemistry*; Wiley-VCH: Weinheim, 1995.
- (11) Atwood, J. L.; Steed, J. W. *Encyclopedia of Supramolecular Chemistry*. M. Dekker: New York, 2004.
- (12) Desiraju, G. R.; Steiner, T. *The Weak Hydrogen Bond in Structural Chemistry and Biology*. Oxford University Press: Oxford, 1999.
- (13) Beer, P. D.; Gale, P. A. *Angew. Chem., Int. Ed.* **2001**, *40*, 486.
- (14) Bianchi, A.; Bowman-James, K.; García-España, E. *Supramolecular Chemistry of Anions*; Wiley-VCH: Chichester, New York, 1997.
- (15) *Research Needs for High-Level Waste Stored in Tanks and Bins at U.S. Department of Energy Sites*. National Research Council, National Academy Press: Washington, D.C., 2001.
- (16) *Fundamentals and Applications of Anion Separations*. Moyer, B. A.; Singh, R. P. Eds.; Kluwer Academic/Plenum: New York, 2004.
- (17) Schmidtchen, F. P.; Berger, M. *Chem. Rev.* **1997**, *97*, 1609.
- (18) Kumler, W. D. *J. Am. Chem. Soc.* **1935**, *57*, 600.
- (19) Pauling, L. *J. Am. Chem. Soc.* **1935**, *57*, 2680.
- (20) Sutor, D. J. *J. Chem. Soc.* **1963**, 1105.
- (21) Taylor, R.; Kennard, O. *J. Am. Chem. Soc.* **1982**, *104*, 5063.

- (22) Farnham, W. B.; Roe, D. C.; Dixon, D. A.; Calabrese, J. C.; Harlow, R. L. *J. Am. Chem. Soc.* **1990**, *112*, 7707.
- (23) Ilioudis, C. A.; Tocher, D. A.; Steed, J. W. *J. Am. Chem. Soc.* **2004**, *126*, 12395.
- (24) Bryantsev, V. S.; Hay, B. P. *J. Am. Chem. Soc.* **2005**, *127*, 8282.
- (25) Coletti, C.; Re, N. *J. Phys. Chem. A*, **2009**, *113*, 1578.
- (26) Bryantsev, V. S.; Hay, B. P. *Org. Lett.* **2005**, *7*, 5031.
- (27) Zhu, S. S.; Staats, H.; Brandhorst, K.; Grunenberg, J.; Gruppi, F.; Dalcaneale, E.; Luetzen, A.; Rissanen, K.; Schalley, C. A. *Angew. Chem., Int. Ed.* **2008**, *47*, 788.
- (28) Li, Y.; Flood, A. H. *Angew. Chem., Int. Ed.* **2008**, *47*, 2649.
- (29) Juwarker, H.; Lenhardt, J. M.; Pham, D. M.; Craig, S. L. *Angew. Chem., Int. Ed.* **2008**, *47*, 3740.
- (30) Meudtner, R. M.; Hecht, S. *Angew. Chem., Int. Ed.* **2008**, *47*, 4926.
- (31) Yoon, D. W.; Gross, D. E.; Lynch, V. M.; Sessler, J. L.; Hay, B. P.; Lee, C. H. *Angew. Chem., Int. Ed.* **2008**, *47*, 5038.
- (32) Berryman, O. B.; Sather, A. C.; Hay, B. P.; Meisner, J. S.; Johnson, D. W. *J. Am. Chem. Soc.* **2008**, *130*, 10895.
- (33) Li, Y.; Flood, A. H. *J. Am. Chem. Soc.* **2008**, *130*, 12111.
- (34) Maeda, H.; Mihashi, Y.; Haketa, Y. *Org. Lett.* **2008**, *10*, 3179.
- (35) (a) Martínez-Máñez, R.; Sancenón, F. *Chem. Rev.* **2003**, *103*, 4419. (b) Sessler, J. L.; Seidel, D. *Angew. Chem., Int. Ed.* **2003**, *42*, 5134. (c) Gale, P. A. *Coord. Chem. Rev.* **2003**, *240*, 191. (d) Beer, P. D.; Gale, P. A. *Angew. Chem., Int. Ed.* **2001**, *40*, 486. (e) Cho, E. J.; Moon, J. W.; Ko, S. W.; Lee, J. Y.; Kim, S. K.; Yoon, J.; Nam, K. C. *J. Am. Chem. Soc.* **2003**, *125*, 12376. (f) Snowden, T. S.; Anslyn, E. V. *Chem. Biol.* **1999**, *3*, 740. (g) Antonisse, M. M. G.; Reinhoudt, D. N. *Chem. Commun.* **1998**, 143. (h) Schmidtchen, F. P.; Berger, M. *Chem. Rev.* **1997**, *97*, 1609.
- (36) (a) Holbrey, J. D.; Reichert, W. M.; Nieuwenhuyzen, M.; Johnston, S.; Seddon, K. R.; Rogers, R. D. *Chem. Commun.* **2003**, 1636. (b) Holbrey, J. D.; Reichert, W. M.; Rogers, R. D. *Dalton Trans.* **2004**, 2267. (c) Custelcean, R.; Delmau, L. H.; Moyer, B. A.; Sessler, J. L.; Cho, W.-S.; Gross, D.; Bates, G. W.; Brooks, S. J.; Light, M. E.; Gale, P. A. *Angew. Chem., Int. Ed.* **2005**, *44*, 2537.
- (37) Avent, A. G.; Chaloner, P. A.; Day, M. P.; Seddon, K. R.; Welton, T. *J. Chem. Soc., Dalton Trans.* **1994**, 3405.
- (38) Sato, K.; Arai, S.; Yamagishi, T. *Tetrahedron Lett.* **1999**, *40*, 5219.
- (39) Alcalde, E.; Alvarez-Rúa, C.; García-Granda, S.; Gracia-Rodriguez, E.; Mesquida, N.; Pérez-García, L. *Chem. Commun.* **1999**, 295.

- (40) Chellappan, K.; Singh, N. J.; Hwang, I.-C.; Lee, J. W.; Kim, K. S. *Angew. Chem., Int. Ed.* **2005**, *44*, 2899.
- (41) Kwon, J. Y.; Singh, N. J.; Kim, H.; Kim, S. K.; Kim, K. S.; Yoon, J. *J. Am. Chem. Soc.* **2004**, *126*, 8892.
- (42) Dinarès, I.; Garcia de Miguel, C.; Mesquida, N.; Alcalde, E. *J. Org. Chem.* **2009**, *74*, 482.
- (43) Kim, S. K.; Kang, B.-G.; Koh, H. S.; Yoon, Y.-J.; Jung, S. J.; Jeong, B.; Lee, K.-D.; Yoon, J. *Org. Lett.* **2004**, *6*, 4655.
- (44) Ho, H. A.; Leclerc, M. *J. Am. Chem. Soc.* **2003**, *125*, 4412.
- (45) (a) Kolb, H. C.; Finn, M. G.; Sharpless, K. B. *Angew. Chem., Int. Ed.* **2001**, *40*, 2004. (b) Tornøe, C. W.; Meldal, M. *Chem. Rev.* **2008**, *108*, 2952.
- (46) (a) Moses, J. E.; Moorhouse, A. D. *Chem. Soc. Rev.* **2007**, *36*, 1249. (b) Fournier, D.; Hoogenboom, R.; Schubert, U. S. *Chem. Soc. Rev.* **2007**, *36*, 1369. (c) Lutz, J. F. *Angew. Chem., Int. Ed.* **2007**, *46*, 1018. (d) Ladmiral, V.; Mantovani, G.; Clarkson, G. J.; Cauet, S.; Irwin, J. L.; Haddleton, D. M. *J. Am. Chem. Soc.* **2006**, *128*, 4823. (e) Diaz, D. D.; Rajagopal, K.; Strable, E.; Schneider, J.; Finn, M. G. *J. Am. Chem. Soc.* **2006**, *128*, 6056. (f) Whiting, M.; Tripp, J. C.; Lin, Y.-C.; Lindstrom, W.; Olson, A. J.; Elder, J. H.; Sharpless, K. B.; Fokin, V. V. *J. Med. Chem.* **2006**, *49*, 7697. (g) Punna, S.; Kuzelka, J.; Wang, Q.; Finn, M. G. *Angew. Chem., Int. Ed.* **2005**, *44*, 2215. (h) Bodine, K. D.; Gin, D. Y.; Gin, M. S. *J. Am. Chem. Soc.* **2004**, *126*, 1638. (i) Wu, P.; Feldman, A. K.; Nugent, A. K.; Hawker, C. J.; Scheel, A.; Voit, B.; Pyun, J.; Frechet, J. M. J.; Sharpless, K. B.; Fokin, V. V. *Angew. Chem., Int. Ed.* **2004**, *43*, 3928. (j) Wang, Q.; Chan, T. R.; Hilgraf, R.; Fokin, V. V.; Sharpless, K. B.; Finn, M. G. *J. Am. Chem. Soc.* **2003**, *125*, 3192. (k) Link, A. J.; Tirrell, D. A. *J. Am. Chem. Soc.* **2003**, *125*, 11164. (l) Kolb, H. C.; Sharpless, K. B. *Drug Discovery Today* **2003**, *8*, 1128.
- (47) Mathew, P.; Neels, A.; Albrecht, M. *J. Am. Chem. Soc.* **2008**, *130*, 13534.
- (48) Kumar, A.; Pandey, P. S. *Org. Lett.* **2008**, *10*, 165.
- (49) Mullen, K.; Mercurio, J.; Serpell, C.; Beer, P. D. *Angew. Chem., Int. Ed.* **2009**, *48*, 4781.
- (50) Schulze, B.; Friebe, C.; Hager, M. D.; Guenther, W.; Koehn, U.; Jahn, B. O.; Goerls, H.; Schubert, U. S. *Org. Lett.* **2010**, *12*, 2710.
- (51) Hua, Y.; Flood, A. H. *Chem. Soc. Rev.* **2010**, *39*, 1262.
- (52) Yoon, J.; Kim, S. K.; Singh, N. J.; Kim, K. S. *Chem. Soc. Rev.* **2006**, *35*, 355.
- (53) <http://nov.wikipedia.org/wiki/DNA>

## Chapter 2: A Pyrrolyl-Based Triazolophane: A Macrocyclic Receptor with CH and NH Donor Groups That Exhibits a Preference for Pyrophosphate Anions

### 2.1 INTRODUCTION

Pyrophosphate detection has aroused interest in the scientific community not only because pyrophosphate is the product of ATP hydrolysis under cellular conditions<sup>1</sup> but also because it could afford a means of effecting real-time DNA sequencing.<sup>2</sup> Pyrophosphate monitoring may also have a role to play in cancer research since this anion is involved in DNA replication catalyzed by DNA polymerase.<sup>3</sup> Pyrophosphate is also of interest as a larger, more highly charged analogue of inorganic phosphate ( $\text{H}_2\text{PO}_4^-/\text{HPO}_4^{2-}$ ), which has physiological relevance in biological energy storage and signal transduction, in addition to being a structural component in teeth and bones.<sup>4</sup> Not surprisingly, therefore, considerable effort has been devoted recently to the development of synthetic receptors that allow for the recognition, detection, or extraction of pyrophosphate and related species, such as inorganic phosphate.<sup>5</sup> Systems incorporating neutral or cationic NH hydrogen bond donor groups (*e.g.*, pyrrole, indole, ammonium, and guanidinium) or cationic CH hydrogen bond donor motifs (*e.g.*, imidazolium and triazolium) have been particularly effective in this regard. However, to the best of our knowledge, receptors with neutral CH H-bond donors have yet to be exploited for the purpose of pyrophosphate (or phosphate) anion recognition.

CH bonds are present in the overwhelming majority (97%) of chemical compounds.<sup>6</sup> Nevertheless, it is only recently that the importance of CH H-bonds in biological and artificial anion recognition has come to be appreciated.<sup>7</sup> In recent pioneering work, Flood and co-workers reported the synthesis and anion binding

properties of [3<sub>4</sub>]triazolophanes (Figure 2.1). These new macrocycles have a diameter of about 3.8 Å and display a high affinity for the chloride ion.<sup>7c</sup> On the basis of this and previous theoretical and experimental studies,<sup>8</sup> it was suggested that the strength of neutral, triazole-derived C-H ··· X<sup>-</sup> (X<sup>-</sup> = halide) bonds can approach those of more traditional NH donors, such as pyrrole. We thus considered it of interest to combine both these recognition motifs within the same macrocyclic framework. In this chapter, the synthesis and anion binding properties of the first such system, namely the calix[2]1,3-bis(pyrro-2-yl)(1,4)-1,2,3-triazolo-phane (**2.1**) are detailed. As discussed below, this system acts as a highly effective receptor for the pyrophosphate anion, both in the solid state and in organic media.<sup>9</sup> Our findings, supported by theory, provide support for the conclusion that NH-anion bonding interactions are more important than CH-anion interactions, at least in highly symmetric receptor systems incorporating both motifs.

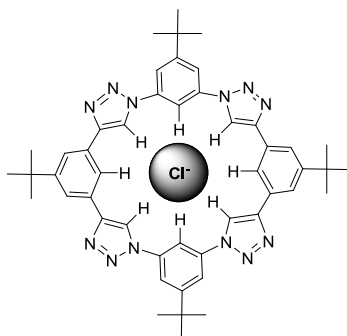


**Figure 2.1:** Chemical structure of the [3<sub>4</sub>]triazolophanes reported by Flood.<sup>7(c)</sup>

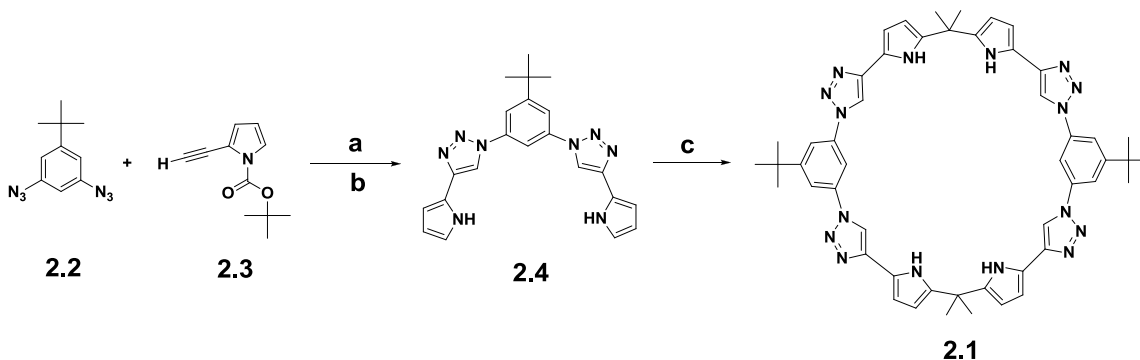
## 2.2 RESULTS AND DISCUSSIONS

The synthesis of **2.1** is shown in Scheme 2.1. Using “click” chemistry conditions, a copper-catalyzed Huisgen 1,3-dipolar cycloaddition<sup>10</sup> was used to couple the bis-azide **2.2**<sup>7(c)</sup> with alkyne **2.3**<sup>27</sup>. This was followed by *t*-BOC deprotection<sup>11</sup> to give 1,3-bis(pyrro-



2-yl)-(1,4)-1,2,3-triazolobenzene (**2.4**) in 24% combined yield for two steps. Condensation of **2.4** with acetone<sup>12</sup> produced **2.1** in 10% yield.

**Scheme 2.1:** Synthesis of Macrocycle **2.1**<sup>a</sup>



Conditions: <sup>a</sup>(a) CuSO<sub>4</sub>, sodium ascorbate, EtOH/H<sub>2</sub>O/toluene (7:3:1); (b) NaOC(CH<sub>3</sub>)<sub>3</sub>, anhydrous THF; (c) acetone, TFA, Ar, RT.

NOESY spectroscopic studies provided support for the notion that **2.1** has a flexible conformation at ambient temperature. This was further verified by variable temperature <sup>1</sup>H NMR spectroscopic studies; specifically, signals that became broader with decreasing temperature were observed (Figure 2.8).

A single crystal X-ray diffraction analysis of **2.1** revealed a nearly flat structure, wherein the pyrrole NH protons on N5 and N5A point out from the center of the core. The distance between the exocyclic C-H or N-H and the nitrogen atoms on the neighboring triazole ring generally proved to be less than 3 Å. This leads us to suggest that intramolecular H-bonding interactions on the exterior of the ring<sup>7r</sup> help stabilize the observed planar conformation in the solid state (Figure 2.2).

The anion properties of **2.1** in solution were first analyzed using UV-vis spectroscopy. Standard titrations, associated curve fittings,<sup>13</sup> and Job plots provided support for pyrophosphate (as the tetrabutylammonium (TBA) salt) being bound to **2.1**

strongly in chloroform at 300 K ( $K_a = (2.30 \pm 0.40) \times 10^6 \text{ M}^{-1}$ ) and with a 1:1 binding stoichiometry. Mass spectrometric analyses also provided support for the conclusion that stable complexes were formed (Table 2.2 and Figure 2.19).

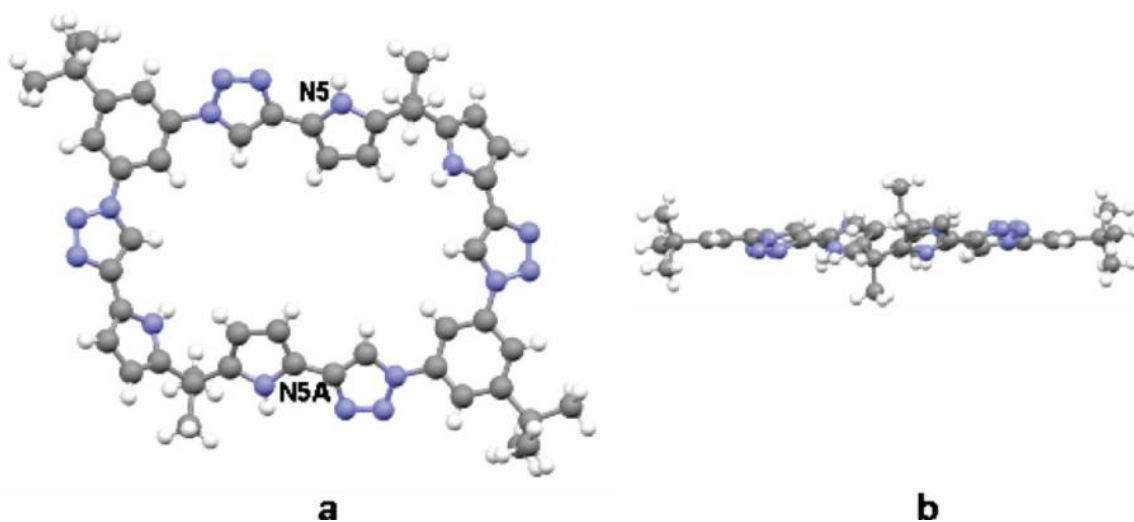


**Figure 2.2:** (a) Top and (b) side views of the single crystal X-ray structure of **2.1**·4CH<sub>3</sub>OH·H<sub>2</sub>O. All solvent molecules have been omitted for clarity. (Crystals used in this study were obtained by the author; The data were collected by the author; The crystal refinement was done by Dr. Xiaoping Yang.)

The association constants ( $K_a$ ) between receptor **2.1** and various other test anions were also determined in chloroform using standard UV-vis absorption titration method. Among the test anions considered, receptor **2.1** displays selectivity for the trianionic pyrophosphate anion, followed by  $\text{HSO}_4^- ((4.98 \pm 0.40) \times 10^5) > \text{H}_2\text{PO}_4^- ((2.38 \pm 0.25) \times 10^5) > \text{Cl}^- ((1.18 \pm 0.07) \times 10^4) > \text{Br}^- ((2.64 \pm 0.09) \times 10^3)$  (all as TBA salts). Macrocyclic **2.1** thus displays a high pyrophosphate/dihydrogenphosphate selectivity ( $K_a(\text{HP}_2\text{O}_7^{3-})/K_a(\text{H}_2\text{PO}_4^-) = 10$ ).

The host-guest interactions between macrocycle **2.1** and the pyrophosphate anion were further analyzed by  $^1\text{H}$  NMR spectroscopy. Specifically, a solution of **2.1** (5 mM,  $\text{CDCl}_3$ ) was titrated with up to 10 equiv. of  $(\text{TBA})_3\text{HP}_2\text{O}_7$  (Figure 2.3). The hydrogen signals for the pyrrole NH, the triazole CH, and the endocyclic hydrogen atom of the N1-linked phenyl unit were seen to shift downfield by 5.09, 1.96, and 1.22 ppm, respectively (Figure 2.3). These changes followed the sequence of expected H acidity, namely pyrrole NH > triazole CH > benzene CH.<sup>14</sup> Thus the trends observed in the NMR spectral studies are consistent with the intrinsic strength of the various H-bond donor groups as inferred from electronic structure calculations carried out with chloride anion. The binding energies (MP2/aug-cc-pVDZ) were computed by our collaborator, Dr. Benjamin Hay. For the complexes of chloride with pyrrole N-H, triazole C-H, and benzene C-H donors, the resulting energies are -22.50, -18.94, and -8.42 kcal mol<sup>-1</sup>, respectively (cf. Section 2.4.7).<sup>15</sup> They are also consistent with the hydrogen bond distances observed in the solid state (see below). Nevertheless, it is important to appreciate that all three hydrogen bond donor motifs play a role in the observed anion recognition. In contrast, only a small downfield shift was seen for the signals ascribed to the exocyclic hydrogen atoms on the phenyl and pyrrole rings ( $\Delta \delta = 0.09$  and 0.10 ppm, respectively); apparently these C-H bonds play little role in anion recognition.

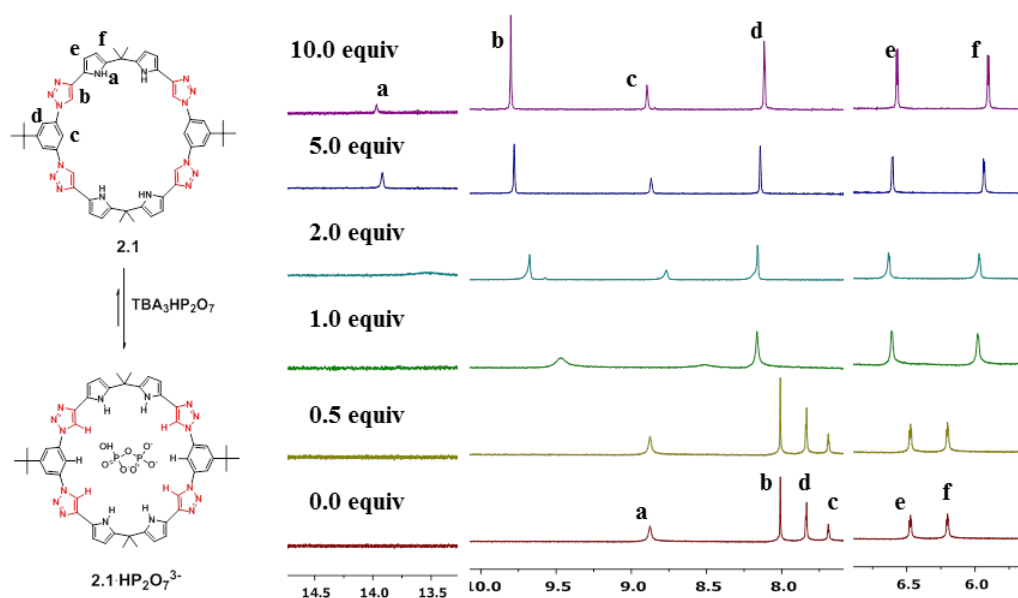


**Figure 2.3:**  $^1\text{H}$  NMR spectra (aromatic region) of **2.1** recorded upon titration with  $(\text{TBA})_3\text{HP}_2\text{O}_7$ ;  $\text{CDCl}_3$ , 300 K.

Additional support for the suggestion that both NH and neutral CH interactions combine to effect pyrophosphate anion recognition in the case of receptor **2.1** came from a single crystal X-ray diffraction analysis of the complex formed between pyrophosphate and **2.1** ( $\mathbf{2.1} \cdot (\text{TBA})_3\text{HP}_2\text{O}_7 \cdot 3\text{H}_2\text{O}$ ) (Figure 2.4). In this complex, the macrocycle displays a folded conformation; this provides a clip-like slot into which the pyrophosphate anion inserts. All the pyrrole NH, triazole CH, and endocyclic benzene CH protons point into the center of the ring and are involved in hydrogen bond interactions with the bound pyrophosphate guest, as inferred from bond distances (pyrrole  $\text{NH} \cdots \text{O}$  *ca.* 1.9 Å, triazole  $\text{CH} \cdots \text{O}$  *ca.* 2.3 Å, benzene  $\text{CH} \cdots \text{O}$  *ca.* 3.7 Å). The resulting conformation thus stands in contrast to what is seen in the case of the free host **2.1**.

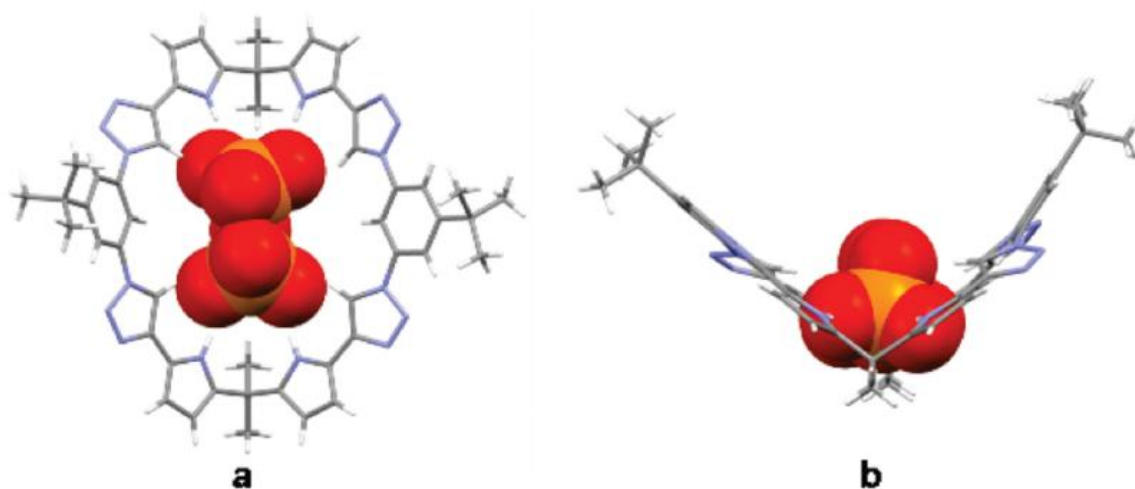


**Figure 2.4:** (a) Top and (b) side views of a single-crystal X-ray diffraction structure of **2.1**·TBA<sub>3</sub>HP<sub>2</sub>O<sub>7</sub>·3H<sub>2</sub>O in which the pyrophosphate anion is in a space filling representation. Solvent molecules and TBA cations have been omitted for clarity.

### 2.3 CONCLUSIONS

In summary, the pyrrolyl-based receptor **2.1** has been prepared in a moderate yield. It binds the pyrophosphate anion in the solid state and displays a high selectivity for this trianion relative to various test monoanions in chloroform solution. The present results thus serve to underscore the utility of new recognition motifs in the design of anion binding agents, particularly those that combine both CH- and NH-anion interactions within a single framework. The present work also helps calibrate directly the relative importance of these interactions. It thus provides a foundation for future receptor design.

## 2.4 EXPERIMENTAL SECTION

### 2.4.1 General Procedures

All reagents and starting materials were obtained from commercial suppliers and used as received unless otherwise noted. Column chromatography was performed on silica gel (40-63  $\mu\text{m}$ , Silicycle, Canada) and Alumina N (50-200  $\mu\text{m}$ , Dynamic Adsorbents Inc., USA). Nuclear magnetic resonance (NMR) spectra were recorded on Varian Mercury 400, Varian Inova 500, and Varian DirectDrive 600 instruments. UV-vis spectra were recorded on a Cary 5000 UV-Vis-NIR Spectrophotometer. Low resolution ESI mass spectra were measured using either a Finnigan LCQ Quadrupole Ion Trap Mass Spectrometer or a Thermo LTQ-XL linear Ion Trap Mass Spectrometer. High resolution ESI mass spectra were obtained on an Ion Spec Fourier Transform mass spectrometer (9.4 T).

### 2.4.2 Synthetic Experimental

**1,3-Bis(pyrro-2-yl)(1,4)-1,2,3-triazolobenzene, 2.4:** A solution of the 3,5-diazido-1-*tert*-butylbenzene **2.2** (432.2 mg, 2.0 mmol), and 2-ethynylpyrrole-1-carboxylic acid *tert*-butyl ester **2.3** (840.8 mg, 4.4 mmol), sodium ascorbate (40.0 mg, 0.2 mmol), and  $\text{CuSO}_4$  (5.0 mg, 0.02 mmol) in a mixture of 14 mL EtOH, 6 mL  $\text{H}_2\text{O}$  and 2 mL toluene was stirred at ambient temperature for 24 hrs. After removal of the solvents in vacuo, a brown solid was obtained. This solid was dissolved in  $\text{CH}_2\text{Cl}_2$  and washed with water ( $3 \times 30$  mL). The aqueous phase was extracted twice with  $\text{CH}_2\text{Cl}_2$  ( $2 \times 50$  mL). The organic extracts were combined and dried over  $\text{MgSO}_4$  and then concentrated under reduced pressure. The brown solid obtained as a result was then dissolved in anhydrous THF and treated with 10 equiv. sodium *tert*-butoxide and left to stir overnight. The

volatiles were removed in vacuo and the brown solid obtained was washed with water (3×30 mL), extracted with ethyl acetate (2×50 mL), dried over MgSO<sub>4</sub> and concentrated under reduced pressure. The crude product was purified by column chromatography (alumina neutral, CH<sub>2</sub>Cl<sub>2</sub>:CH<sub>3</sub>OH, 10:0.1, eluent) and recrystallized from THF and hexane to afford 188 mg (24%, 0.47 mmol) of **2.4** as a pale brown solid. <sup>1</sup>H NMR (DMSO-*d*<sub>6</sub>, 400 MHz) [ppm], δ 11.52 (s, 2 H, NH), 9.11 (s, 2 H, -N-CH=C-), 8.35 (t, *J*=1.8 Hz, 1 H, CH), 8.03 (d, *J*=1.8 Hz, 2 H, CH), 6.87 (dd, *J*<sub>1</sub>=4.0 Hz, *J*<sub>2</sub>=2.4 Hz, 2 H, pyrrole- α -H), 6.51 (m, 2 H, pyrrole- β -H), 6.16 (dd, *J*<sub>1</sub>=5.8 Hz, *J*<sub>2</sub>=2.7 Hz, 2 H, pyrrole- β -H), 1.45 (s, 9 H, CH<sub>3</sub>); <sup>13</sup>C-NMR (*d*-DMSO, 100 MHz) [ppm], δ 31.0, 35.6, 106.7, 109.0, 109.1, 116.8, 117.8, 119.5, 122.0, 137.7, 142.8, 155.4; MS (HR-ESI) Calcd. for C<sub>22</sub>H<sub>23</sub>N<sub>8</sub> (M+H<sup>+</sup>) 399.2046; Found 399.2038 (M+H<sup>+</sup>).

**Calix[2]1,3-bis(pyrro-2-yl)(1,4)-1,2,3-triazolo-phane, 2.1:** Compound **2.4** (500 mg, 1.256 mmol) in acetone (250 mL) was placed in a 1000 mL three-way round bottom flask and degassed for 30 min by bubbling with argon. While flushing the reaction vessel with argon, TFA (20 mL, 0.267 mol) was then added dropwise. The resulting solution was then stirred for 3 hours at ambient temperature before being quenched *via* the addition of solid NaOH (11 g, 0.275 mol). Evaporation of the reaction mixture afforded a brown solid. To this crude product, dichloromethane (100 mL) and water (100 mL) were added. The organic phase was then separated off and washed three times with water (3×100 mL). The organic layer was dried over anhydrous MgSO<sub>4</sub> and evaporated in vacuo to yield a brown solid. This brown solid was purified by column chromatography (silica gel, CH<sub>2</sub>Cl<sub>2</sub>:CH<sub>3</sub>OH, 10:0.1, eluent) and then followed by recrystallization from CHCl<sub>3</sub> and CH<sub>3</sub>OH to give 54 mg (10%, 0.062 mmol) of **2.1** as a white solid. <sup>1</sup>H NMR (CDCl<sub>3</sub>, 400 MHz) [ppm], δ 8.88 (s, 4 H, NH), 8.01 (s, 4 H, -N-CH=C-), 7.83 (d, *J*=2.4

Hz, 4 H, CH), 7.68 (t,  $J=2.0$  Hz, 2 H, CH), 6.47 (m, 4 H, pyrrole- $\beta$ -H), 6.21 (m, 4 H, pyrrole- $\beta$ -H), 1.77 (s, 12 H, CH<sub>3</sub>), 1.43 (s, 18 H, CH<sub>3</sub>); <sup>13</sup>C-NMR (CDCl<sub>3</sub>, 100 MHz) [ppm],  $\delta$  29.3, 31.4, 35.9, 36.0, 105.9, 107.3, 111.9, 116.9, 118.5, 121.4, 138.0, 140.6, 142.9, 156.2; MS (HR-ESI) Calcd. for C<sub>50</sub>H<sub>53</sub>N<sub>16</sub> (M+H<sup>+</sup>) 877.4639; Found 877.4644 (M+H<sup>+</sup>).

### 2.4.3 Conformation analysis for macrocycle **2.1** in CDCl<sub>3</sub>

The <sup>1</sup>H NMR spectrum of **2.1** recorded in CDCl<sub>3</sub> at 300 K showed a set of high resolution signals, which is consistent with the macrocycle either having a fixed conformation with high symmetry or a flexible structure and being involved in a fast reversible equilibrium process (Figure 2.5).<sup>16-19</sup> The 2D NOESY NMR spectrum, Figure 2.6, provides evidence that the triazole CH proton (e) has signals that correspond with the protons on the benzene subunit (g), (f).

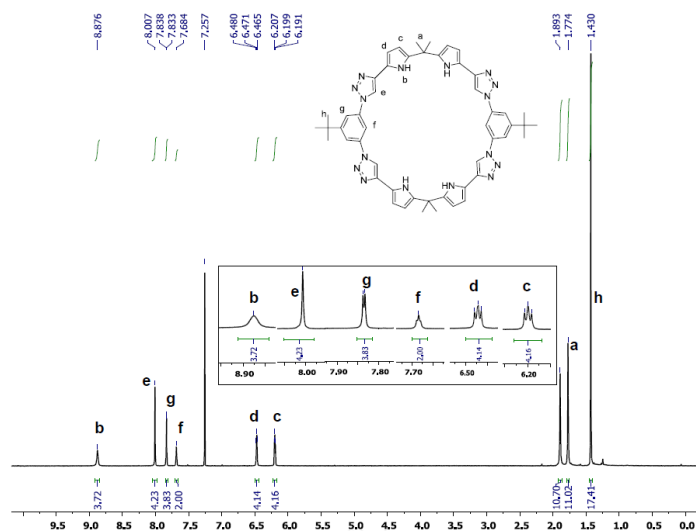


**Figure 2.5:** <sup>1</sup>H NMR spectrum of **2.1** recorded in CDCl<sub>3</sub> at 300 K. Note: The peak 1.89 ppm is ascribed to H<sub>2</sub>O.



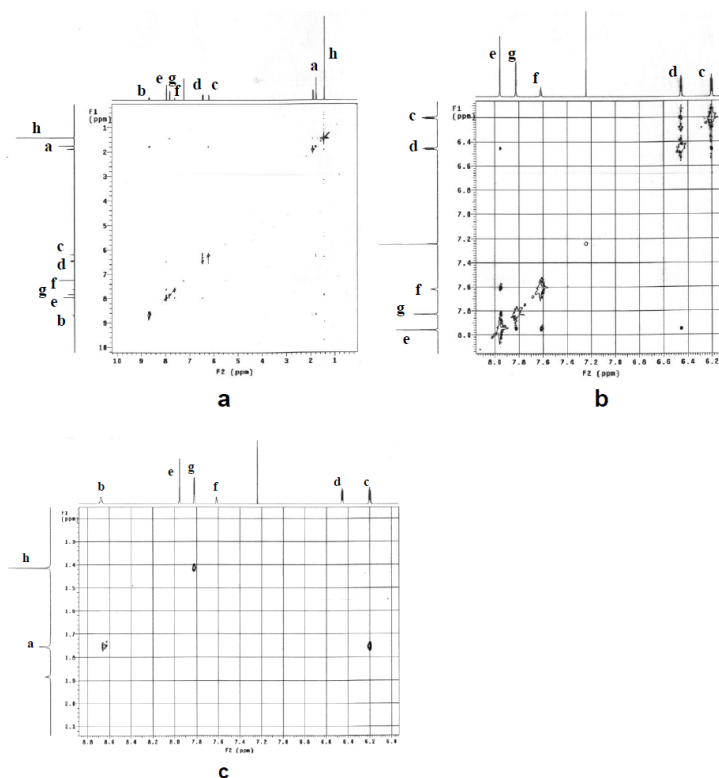


**Figure 2.6:** (a) Full view and (b), (c) expanded views of the 2D NOESY NMR spectrum of **2.1** recorded in  $\text{CDCl}_3$  at 300 K.

Taken in concert, these findings are not consistent with a fixed conformation (Figure 2.7a, b) or with the existence of a single non-equilibrating conformation (Figure 2.7c). Because only one set of signals is seen for hydrogen atoms e, g, f., we propose that the compound has a flexible conformation in solution.

To probe this hypothesis further, variable temperature  $^1\text{H}$  NMR spectral studies were carried out (Figure 2.8). At ambient temperature, the NMR spectra gave defined peaks consistent with bond rotation faster than the NMR time scale. As the temperature was decreased, peak broadening became evident. We attribute this broadening to slowed rotation of the molecule, which allows for the detection of several different conformations.

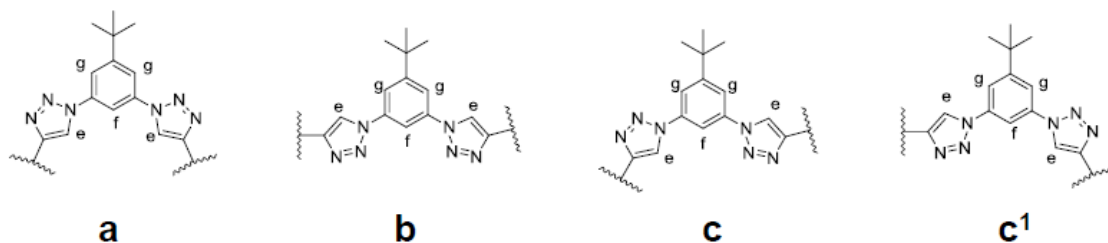


**Figure 2.7:** Limiting conformations for the fragments in **2.1** used to interpret the NOESY NMR spectra. Note that the conformers shown, **c** and **c'** are symmetry related.

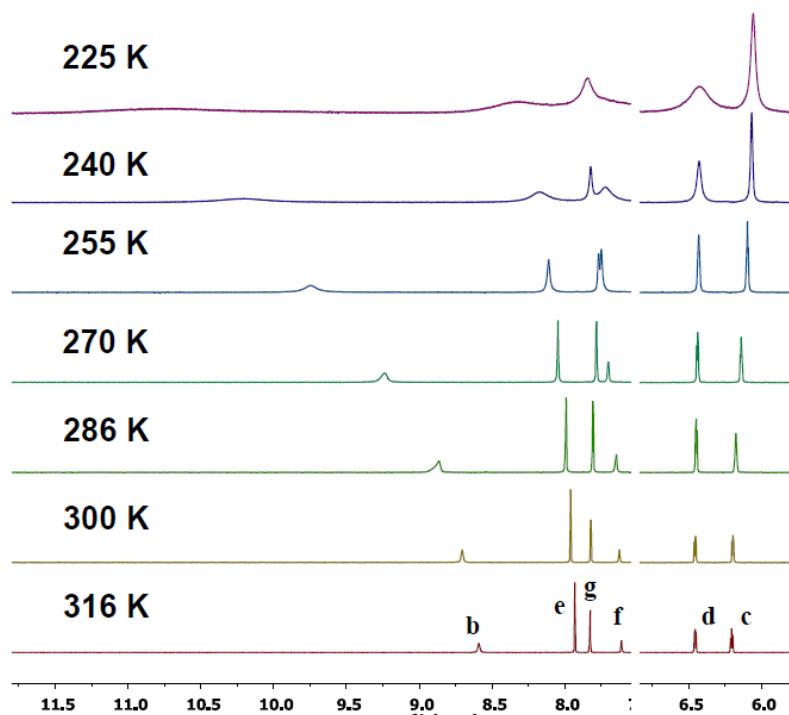


**Figure 2.8:** Variable temperature  $^1\text{H}$  NMR spectrum of macrocycle **2.1** in  $\text{CDCl}_3$ .

#### 2.4.4 UV-Vis Binding Studies

##### UV-Vis Spectroscopic Titrations

Stock solutions of the host molecule being studied were made up in chloroform with the final concentrations being  $1 \times 10^{-5}$  M. Stock solutions of the guest in question were prepared by dissolving 100 - 300 equivalents of the tetrabutylammonium (TBA) salts of the anions under study in 5 mL stock solutions of the host. Making up the anion source solutions in this way allowed the binding studies to be carried out without having to make mathematical corrections to account for changes in host concentration as the result of dilution effects.

The general procedure for the UV-Vis binding studies involved making sequential additions of titrant (anionic guest) using Hamilton pipettes to a 3 mL aliquot of the host stock solution in a spectrometric cell. The data was then collated and combined to produce plots that showed the changes in host spectral features as a function of guest concentration.

#### **Job Plot Construction:**

Stock solutions of the macrocycle ( $1.0 \times 10^{-5}$  M) and TBA<sub>3</sub>HP<sub>2</sub>O<sub>7</sub> ( $1.0 \times 10^{-5}$  M) were prepared separately in CHCl<sub>3</sub>. For the other anions, stock solutions of the macrocycle ( $5.0 \times 10^{-5}$  M) and the tetrabutylammonium anion salts ( $5.0 \times 10^{-5}$  M) were prepared separately in CHCl<sub>3</sub>. The UV-Vis spectrum was taken for each of 11 different solutions containing a total of 3.0 mL of the macrocycle **2.1** and tetrabutylammonium salt in the following ratios: 3.0:0, 2.7:0.3, 2.4:0.6, 2.1:0.9, 1.8:1.2, 1.5:1.5, 1.2:1.8, 0.9:2.1, 0.6:2.4, 0.3:2.7 and 0:3.0. Job's plots were constructed by plotting  $A_{\text{obs}} - A_{\text{M}} - A_{\text{anion}}$  against the  $\gamma$ -coordinate. ( $\gamma = [\text{host}] / ([\text{host}] + [\text{guest}])$ )

### Calculations of Equilibrium Constants, $K_a$

Upon addition of tetrabutylammonium salts, the UV spectra changed gradually. These changes were ascribed to anion binding, with the corresponding association constants ( $K_a$ ) being determined by nonlinear curve fitting of the curves obtained by plotting the absorbance changes at a  $\lambda$  value where the spectral change was maximal ( $\Delta A$ ) against the concentration of the tetrabutylammonium anion salt added,  $[X^-]$ . The data was fitted to the equation,

$$\Delta A = A \cdot \left\{ \left( [2.1] + [X^-] + (1/K_a) \right) - \left\{ \left( [2.1] + [X^-] + (1/K_a) \right)^2 - (4 \cdot [2.1] \cdot [X^-]) \right\}^{1/2} \right\} / (2 \cdot [2.1]) \quad [2.1]$$

where, the one unknown parameter is  $K_a$ , the value of the association constant; this value was obtained by the fit to the data with good fits (*e.g.*,  $R^2 \geq 0.99$ ) being obtained unless noted otherwise.

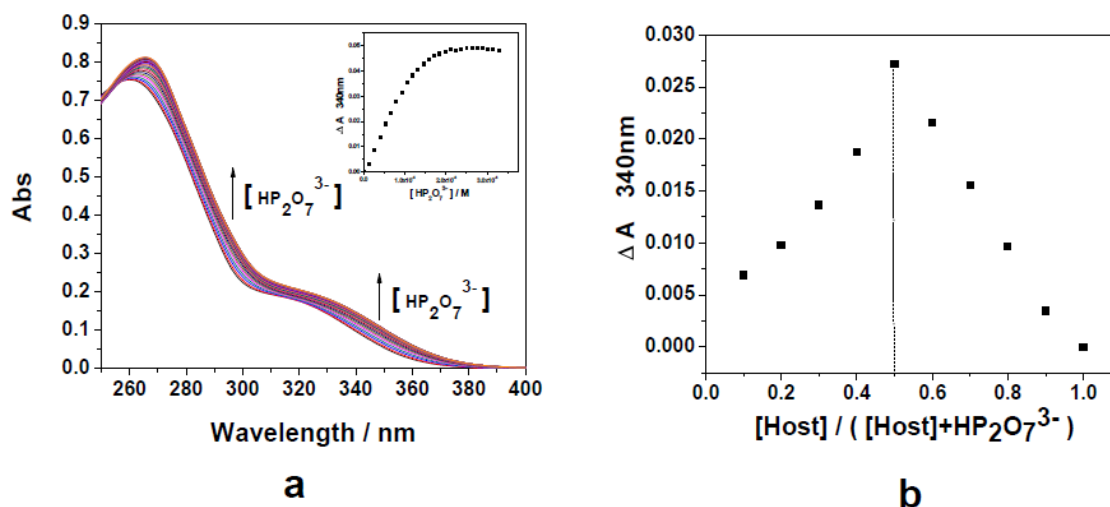


**Figure 2.9:** (a) UV-vis spectra of **2.1** ( $1.00 \times 10^{-5}$  M) in chloroform with increasing ((n-Bu)<sub>4</sub>N)<sub>3</sub>HP<sub>2</sub>O<sub>7</sub> ( $0 \sim 3.0 \times 10^{-5}$  M). (b) Job plot for the interaction between host **2.1** and ((n-Bu)<sub>4</sub>N)<sub>3</sub>HP<sub>2</sub>O<sub>7</sub> in chloroform with  $[\text{host} + \text{guest}] = 1.00 \times 10^{-5}$  M. A maximum value at 0.5 is seen; this is consistent with a 1:1 (host : guest) binding stoichiometry.

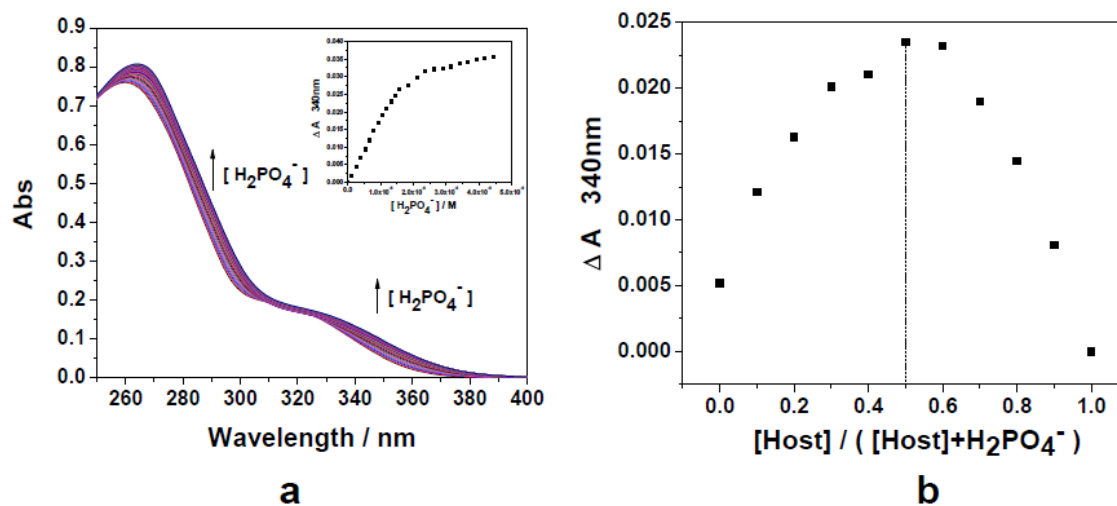


**Figure 2.10:** (a) UV-vis spectra of **2.1** (1.00 × 10<sup>-5</sup> M) in chloroform with increasing (n-Bu)<sub>4</sub>NH<sub>2</sub>PO<sub>4</sub> (0 ~ 5.0 × 10<sup>-5</sup> M). (b) Job plot for the interaction between host **2.1** and (n-Bu)<sub>4</sub>NH<sub>2</sub>PO<sub>4</sub> in chloroform with [host + guest] = 5.00 × 10<sup>-5</sup> M. A maximum value at 0.5 is seen; this is consistent with a 1:1 (host : guest) binding stoichiometry.

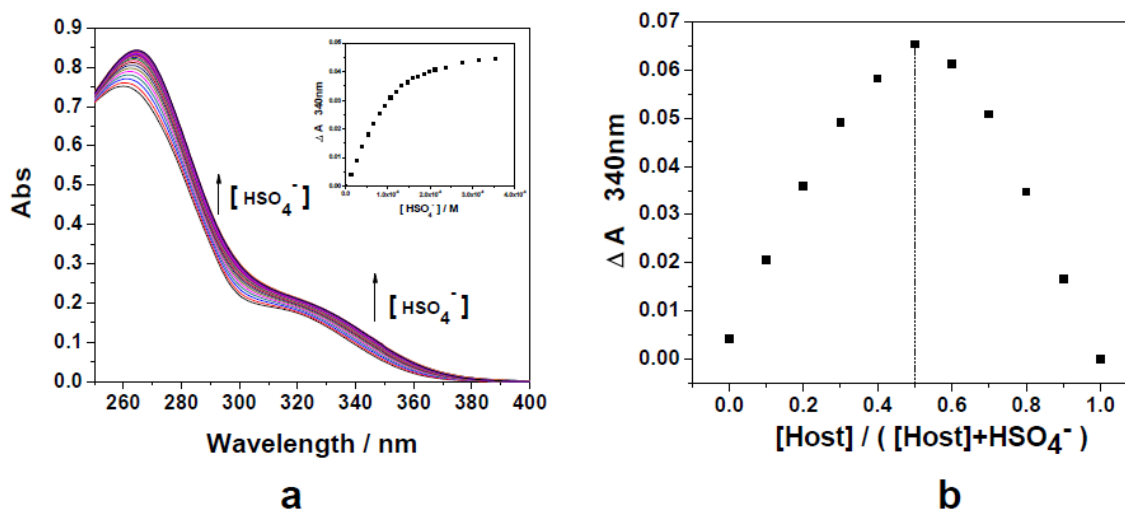


**Figure 2.11:** (a) UV-vis spectra of **2.1** (1.00 × 10<sup>-5</sup> M) in chloroform with increasing (n-Bu)<sub>4</sub>NH<sub>2</sub>SO<sub>4</sub> (0 ~ 3.0 × 10<sup>-5</sup> M). (b) Job plot for the interaction between host **2.1** and (n-Bu)<sub>4</sub>NH<sub>2</sub>SO<sub>4</sub> in chloroform with [host + guest] = 5.00 × 10<sup>-5</sup> M. A maximum value at 0.5 is seen; this is consistent with a 1:1 (host : guest) binding stoichiometry.

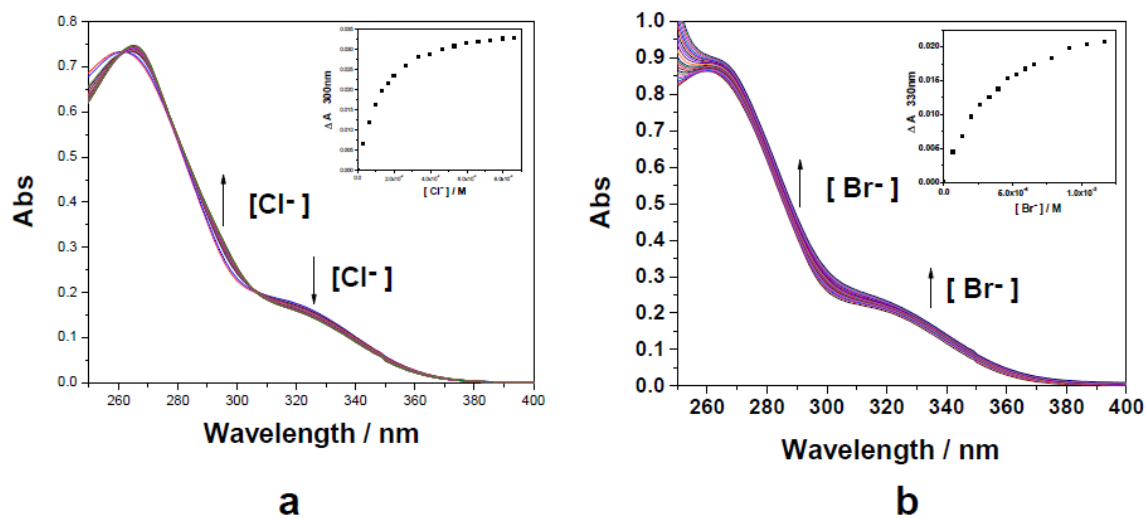


**Figure 2.12:** (a) UV-vis spectra of **2.1** ( $1.00 \times 10^{-5}$  M) in chloroform with increasing (n-Bu)<sub>4</sub>NCl ( $0 \sim 8.0 \times 10^{-4}$  M). (b) UV-vis spectra of **2.1** ( $1.00 \times 10^{-5}$  M) in chloroform with increasing (n-Bu)<sub>4</sub>NBr ( $0 \sim 1.25 \times 10^{-3}$  M).

## Binding Isotherms

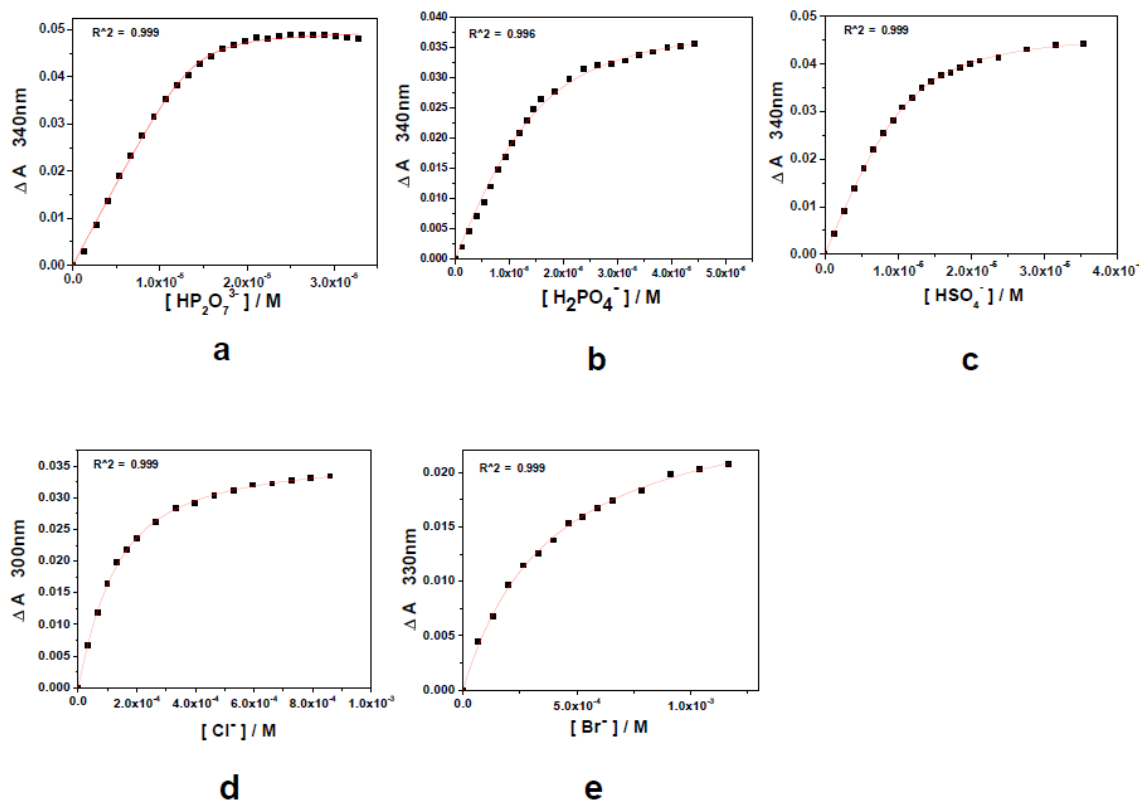


**Figure 2.13:** (a) Variations in the absorbance at 340 nm (▪) of a solution of receptor **2.1** ( $1.00 \times 10^{-5}$  M) in  $\text{CHCl}_3$  as a function of  $(\text{TBA})_3\text{HP}_2\text{O}_7$  concentration ( $0 \sim 3.0 \times 10^{-5}$  M) at 300 K. (b) Variations in absorbance (▪) at 340 nm of a solution of receptor **2.1** ( $1.00 \times 10^{-5}$  M) in  $\text{CHCl}_3$  as a function of  $\text{TBAH}_2\text{PO}_4$  concentration ( $0 \sim 5.0 \times 10^{-5}$  M) at 300 K. (c) Variations in absorbance (▪) at 340 nm of a solution of receptor **2.1** ( $1.00 \times 10^{-5}$  M) in  $\text{CHCl}_3$  as a function of  $\text{TBAHSO}_4$  concentration ( $0 \sim 3.0 \times 10^{-5}$  M) at 300 K. (d) Variations in absorbance (▪) at 300 nm of a solution of receptor **2.1** ( $1.00 \times 10^{-5}$  M) in  $\text{CHCl}_3$  as a function of  $\text{TBACl}$  concentration ( $0 \sim 8.0 \times 10^{-4}$  M) at 300 K. (e) Variations in absorbance (▪) at 300 nm of a solution of receptor **2.1** ( $1.00 \times 10^{-5}$  M) in  $\text{CHCl}_3$  as a function of  $\text{TBABr}$  concentration ( $0 \sim 1.25 \times 10^{-3}$  M) at 300 K.

#### 2.4.5 NMR Anion Recognition Study:

Solutions of receptor **2.1** (5 mM, CDCl<sub>3</sub>, 300 K) were titrated by adding known quantities of a concentrated solution of various tetrabutylammonium anion salts. The anion solutions used to effect the titration contained the receptors at the same concentration as the receptor solutions into which they were being titrated so as to obviate the need to account for dilution effects during the titrations.

**Table 2.1:** Chemical shift changes for selected signals of **2.1** seen in the presence of 10 equiv. TBA<sub>3</sub>HP<sub>2</sub>O<sub>7</sub>, TBAH<sub>2</sub>PO<sub>4</sub>, TBAHSO<sub>4</sub>, TBACl and TBABr. The changes are relative to what is seen for pure **2.1**.

	$\Delta\delta$ / ppm					
<sup>1</sup> H	a	b	c	d	e	f
<b>2.1</b> ·TBA <sub>3</sub> HP <sub>2</sub> O <sub>7</sub>	5.094	1.792	1.211	0.277	0.088	-0.296
<b>2.1</b> ·TBAH <sub>2</sub> PO <sub>4</sub>	2.196	2.114	1.664	0.342	0.189	-0.124
<b>2.1</b> ·TBAHSO <sub>4</sub>	1.265	1.125	0.409	0.299	0.185	-0.111
<b>2.1</b> ·TBACl	3.172	1.072	-0.050	-0.107	0.049	-0.285
<b>2.1</b> ·TBABr	2.102	1.029	-0.068	-0.026	0.075	-0.227

The pyrrole NH hydrogen signal (a), the triazole hydrogen signal (b) and the endocyclic hydrogen atom of the N<sup>1</sup>-linked phenyl unit (c) all undergo significant shifts when anions are added (Table 2.1); this is consistent with the proposition put forward in the text, namely that the various N-H and C-H hydrogen bond donors are involved in anion binding.



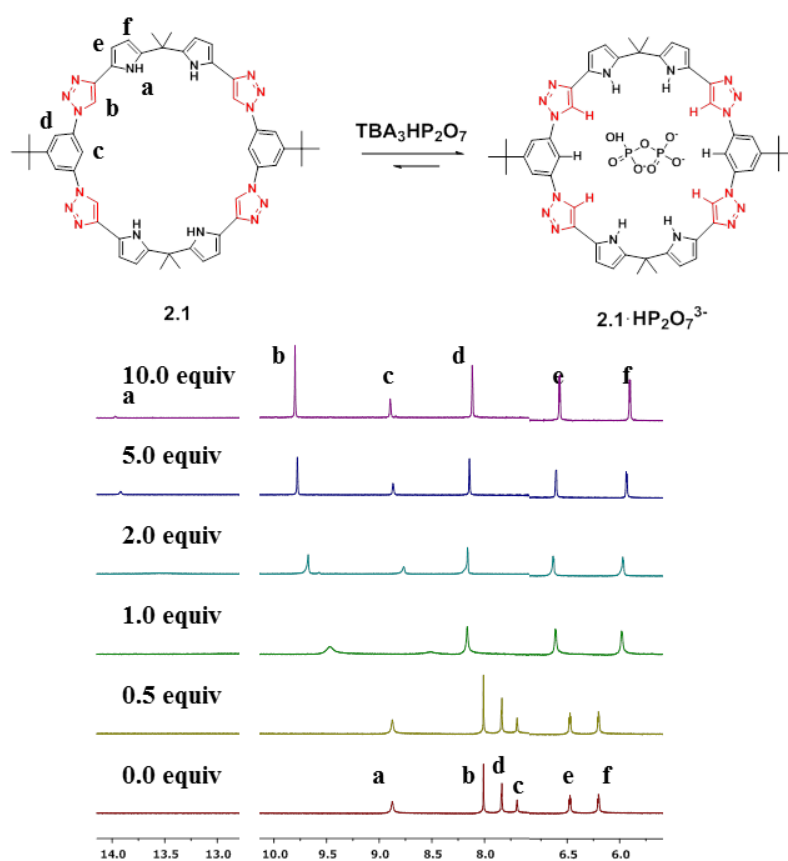


**Figure 2.14:**  $^1\text{H}$  NMR spectrum of macrocycle **2.1** and 0.5, 1.0, 2.0, 5.0, 10.0 equiv.  $(\text{TBA})_3\text{HP}_2\text{O}_7$  recorded in  $\text{CDCl}_3$  at 300 K.

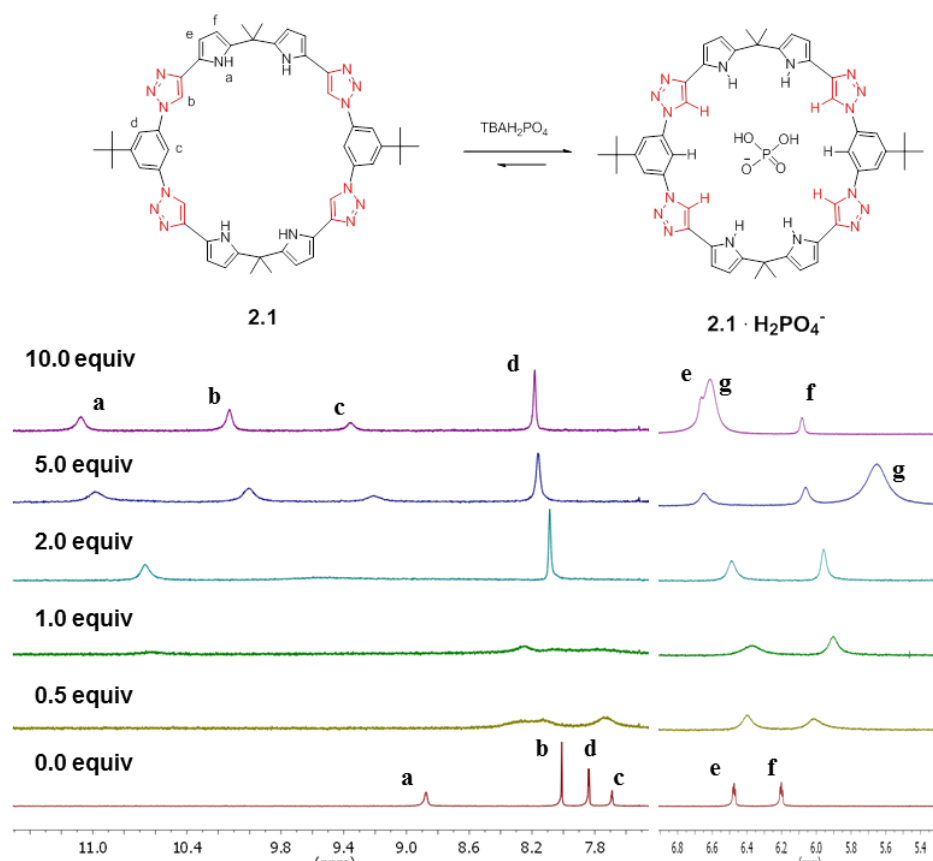


**Figure 2.15:**  $^1\text{H}$  NMR spectrum of macrocycle **2.1** and 0.5, 1.0, 2.0, 5.0, 10.0 equiv. of  $\text{TBAH}_2\text{PO}_4$  recorded in  $\text{CDCl}_3$  at 300 K. (Peak “g” is ascribed to the  $\text{H}_2\text{PO}_4^-$  anion.)

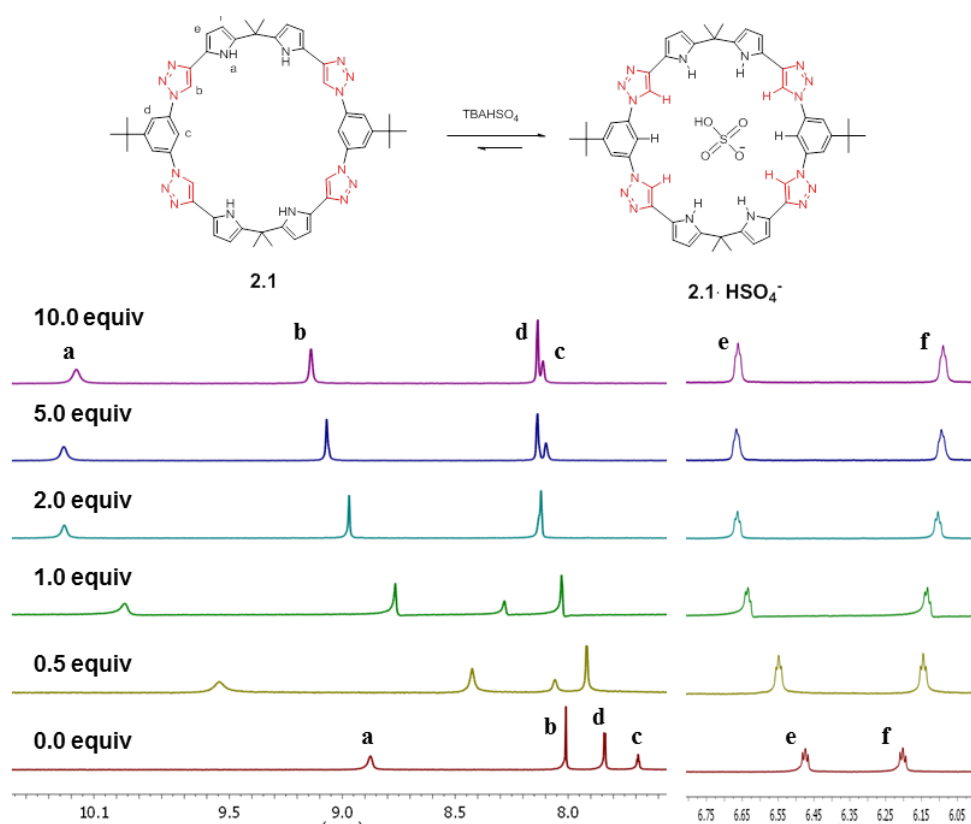


**Figure 2.16:**  $^1\text{H}$  NMR spectrum of macrocycle **2.1** and 0.5, 1.0, 2.0, 5.0, 10.0 equiv. of TBAHSO<sub>4</sub> recorded in CDCl<sub>3</sub> at 300 K.

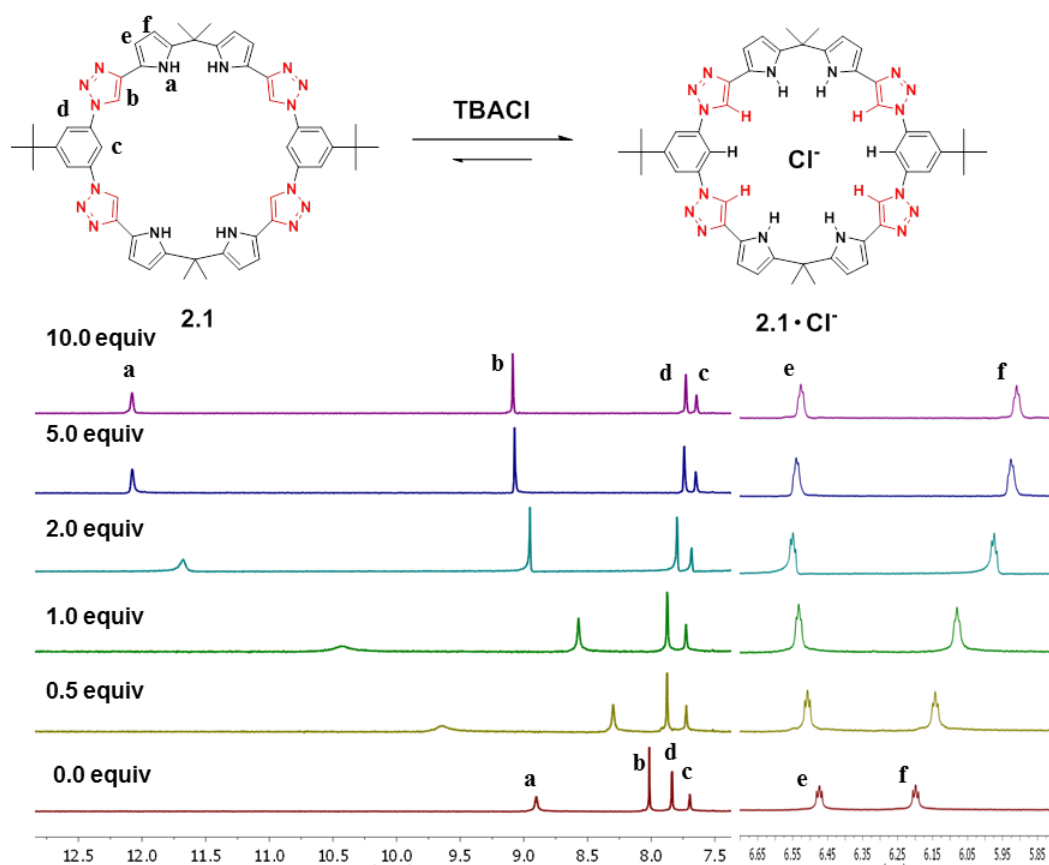


**Figure 2.17:** <sup>1</sup>H NMR spectrum of macrocycle **2.1** and 0.5, 1.0, 2.0, 5.0, 10.0 equiv. of TBACl recorded in CDCl<sub>3</sub> at 300 K.

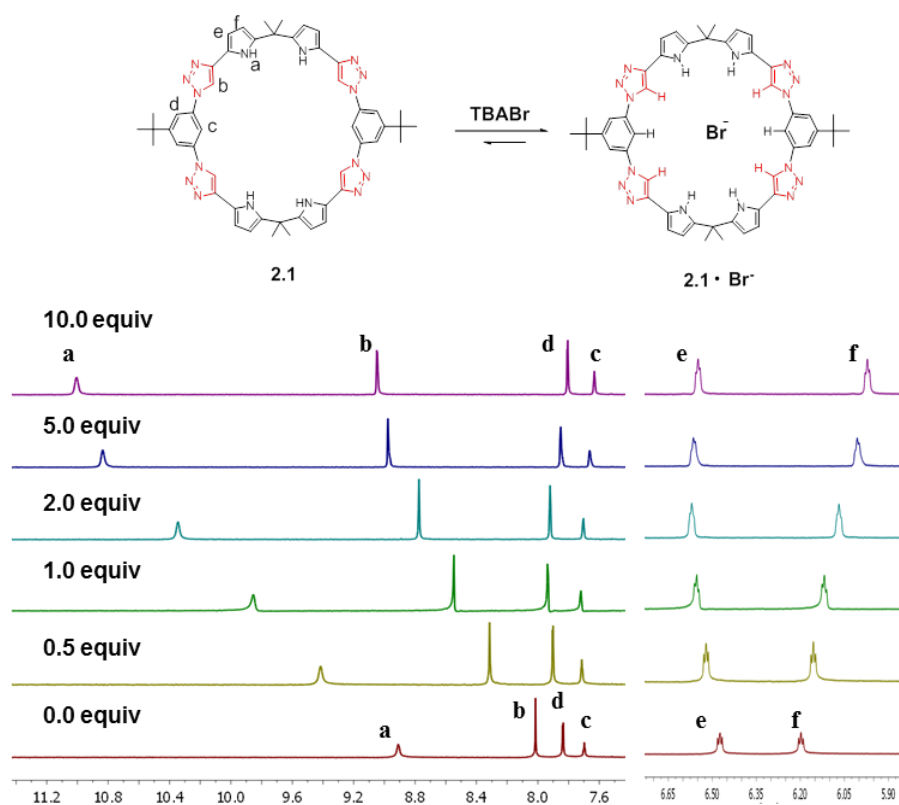


**Figure 2.18:** <sup>1</sup>H NMR spectrum of macrocycle **2.1** and 0.5, 1.0, 2.0, 5.0, 10.0 equiv. of TBABr recorded in CDCl<sub>3</sub> at 300 K.

## 2.4.6 Details of High Resolution ESI Mass Spectrometric Study:

**Table 2.2:** ESI High Resolution Mass Spectra Study for Complexes Stabilized by Receptor **2.1**.

	Host : Guest	Complex	Calculated (m/z)	Found (m/z)
a	1:1	[ (2.1 · TBA <sub>3</sub> HP <sub>2</sub> O <sub>7</sub> ) + TBA ] <sup>+</sup> C <sub>114</sub> H <sub>197</sub> N <sub>20</sub> P <sub>2</sub> O <sub>7</sub>	2020.5143	2020.5171
b	1:1	[ (2.1 · TBAH <sub>2</sub> PO <sub>4</sub> ) + TBA ] <sup>+</sup> C <sub>82</sub> H <sub>126</sub> N <sub>18</sub> PO <sub>4</sub>	1457.9941	1457.9942
c	1:1	[ (2.1 · TBAHSO <sub>4</sub> ) + TBA ] <sup>+</sup> C <sub>82</sub> H <sub>125</sub> N <sub>18</sub> SO <sub>4</sub>	1457.9846	1457.9832
d	1:1	[ (2.1 · TBACl) + TBA ] <sup>+</sup> C <sub>82</sub> H <sub>124</sub> N <sub>18</sub> Cl	1395.9939	1395.9977
e	1:1	[ (2.1 · TBABr) + TBA ] <sup>+</sup> C <sub>82</sub> H <sub>124</sub> N <sub>18</sub> Br	1439.9434	1439.9448

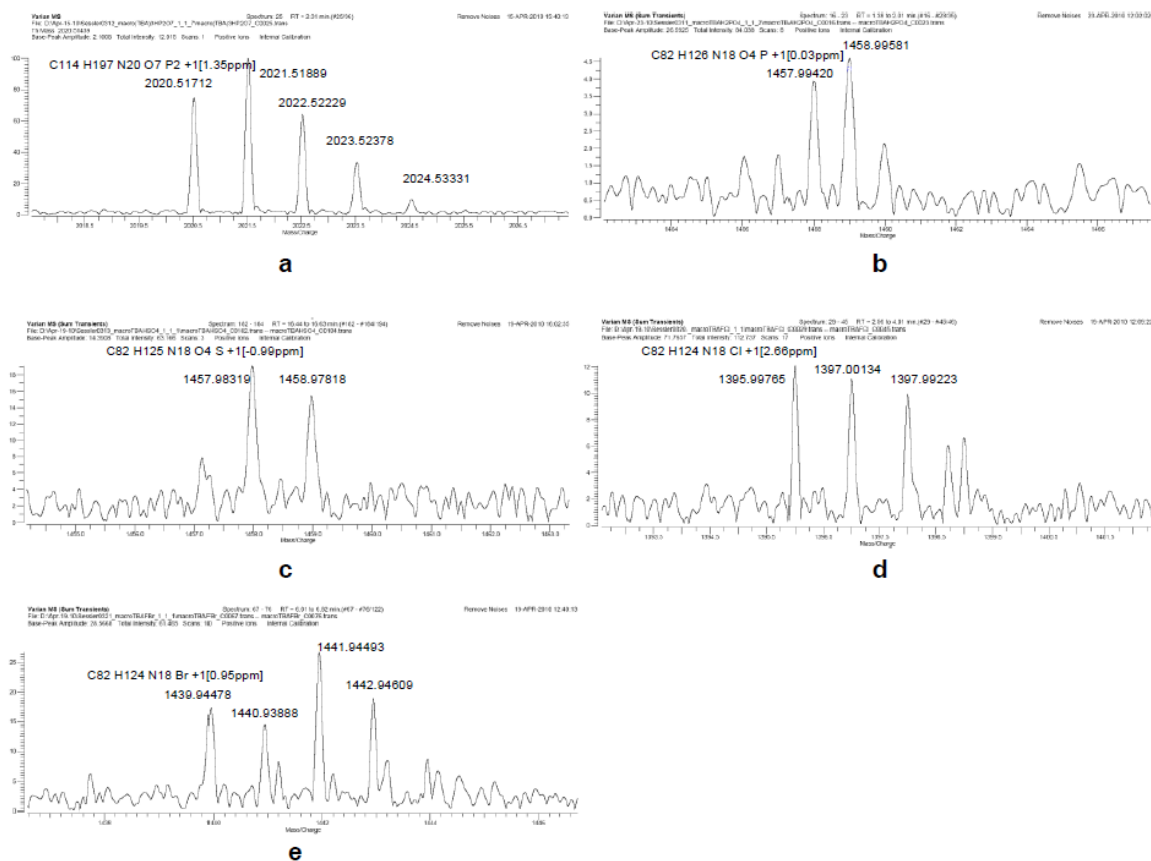


**Figure 2.19:** ESI high resolution mass spectrum of samples containing, respectively, 1 molar equiv. of  $(\text{TBA})_3\text{HP}_2\text{O}_7$  (a),  $\text{TBAH}_2\text{PO}_4$  (b),  $\text{TBAHSO}_4$  (c),  $\text{TBACl}$  (d),  $\text{TBABr}$  (e) and host **2.1**.

#### 2.4.7 Details of Electronic Structure Calculations

These studies were carried out by our collaborator, Dr. Benjamin Hay, and are included here for the benefit of the reader, even though they are not part of the author's dissertation work.

Binding energy,  $\Delta E = E(\text{complex}) - E(\text{chloride}) - E(\text{donor})$  values were calculated at the MP2/aug-cc-pVDZ level of theory with NWChem.<sup>20</sup> Cartesian coordinates and

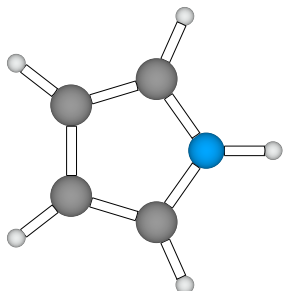
absolute energies for geometries optimized with NWChem at the MP2/aug-cc-pVDZ level of theory using the frozen core approximation are given below.

Cl anion



Energy -459.7227644 hartree

Pyrrole



Energy -209.5630199 hartree

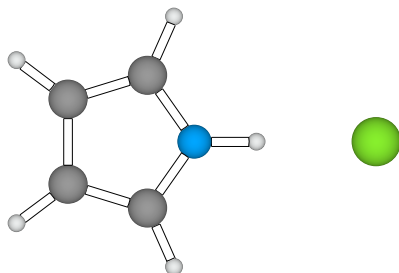
10

C	1.131607	-0.714996	0.029633
C	-0.200928	-1.132996	-0.005264
C	1.131607	0.714996	0.029633
C	-0.200928	1.132996	-0.005264
N	-0.987671	0.000000	-0.025864



H	2.000305	-1.369995	0.052383
H	-0.641785	-2.127000	-0.016815
H	2.000305	1.369995	0.052383
H	-0.641785	2.127000	-0.016815
H	-2.000305	0.000000	-0.052383

Pyrrole chloride complex



N---Cl = 3.073 Å ; N-H---Cl = 2.020 Å

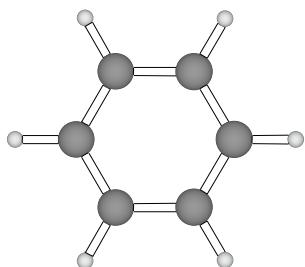
Energy -669.3216376 hartree

11

C	2.157608	-0.714996	-0.226776
C	0.819977	-1.121994	-0.086182
C	2.157608	0.714996	-0.226776
C	0.819977	1.121994	-0.086182
N	0.035309	0.000000	-0.003708
H	3.020859	-1.375000	-0.317505
H	0.374435	-2.112991	-0.039352
H	3.020859	1.375000	-0.317505

H	0.374435	2.112991	-0.039352
H	-1.011917	0.000000	0.106354
Cl	-3.020844	0.000000	0.317505

# Benzene



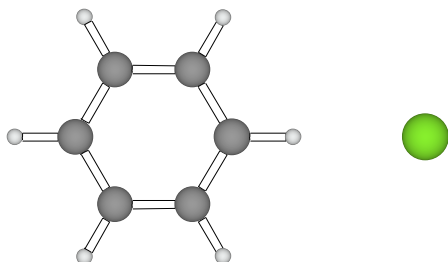
Energy -231.5398383 hartree

12

C	-0.363998	1.359985	0.000000
C	-1.359985	0.363998	0.000000
C	-0.995987	-0.995987	0.000000
C	0.363998	-1.359985	0.000000
C	1.359985	-0.363998	0.000000
C	0.995987	0.995987	0.000000
H	-0.647995	2.416992	0.000000
H	-2.416992	0.647995	0.000000
H	-1.768997	-1.768997	0.000000
H	0.647995	-2.416992	0.000000

H	2.416992	-0.647995	0.000000
H	1.768997	1.768997	0.000000

Benzene chloride complex



C---Cl = 3.491 Å; C-H---Cl = 2.388 Å

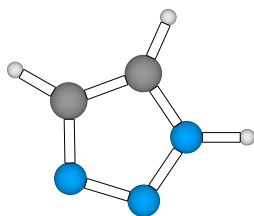
Energy -691.2765323 hartree

13

Cl	3.699539	0.000000	0.291153
C	-1.901123	-1.217987	-0.149612
C	-0.496460	-1.212997	-0.039078
C	0.219315	0.000000	0.017258
C	-0.496460	1.212997	-0.039078
C	-1.901123	1.217987	-0.149612
C	-2.607941	0.000000	-0.205246
H	1.318909	0.000000	0.103790
H	-2.447433	-2.168000	-0.192612
H	0.055832	-2.157990	0.004395
H	0.055832	2.157990	0.004395

H	-2.447433	2.168000	-0.192612
H	-3.699554	0.000000	-0.291153

1,2,3-triazole

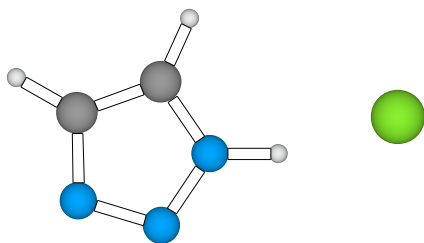


Energy -241.5979766 hartree

8

C	-0.402557	0.546936	0.000000
C	-0.621628	-0.829620	0.000000
N	0.956009	0.644669	0.000000
N	1.561417	-0.566986	0.000000
N	0.583588	-1.478409	0.000000
H	-1.060898	1.410828	0.000000
H	-1.561432	-1.375351	0.000000
H	1.534958	1.478424	0.000000

1,2,3-triazole chloride complex, bound to N-H  
(global minimum geometry)



N---Cl = 2.987 Å; N-H---Cl = 1.950 Å

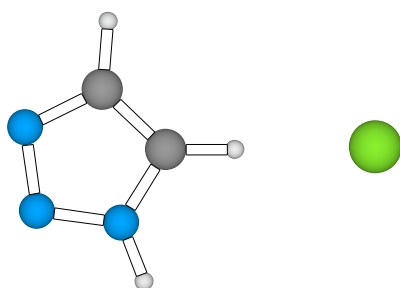
Energy -701.3667612 hartree

9

C	-0.722931	0.623535	0.000000
C	-2.034409	0.142654	0.000000
N	0.041397	-0.496643	0.000000
N	-0.713638	-1.614517	0.000000
N	-2.006256	-1.225784	0.000000
H	-0.277451	1.614517	0.000000
H	-2.974121	0.691391	0.000000
H	1.109436	-0.496643	0.000000
Cl	2.974121	0.072388	0.000000

1,2,3-triazole chloride complex, bound to C-H

(C-H---Cl constrained to 180°)



C---Cl = 3.349 Å; C-H---Cl = 2.244 Å

Energy -701.3509268 hartree

9

C	-0.553238	0.031158	0.000000
C	-1.566360	0.991150	0.000000
N	-1.264648	-1.130493	0.000000
N	-2.606537	-0.947678	0.000000
N	-2.795837	0.382050	0.000000
H	0.551865	0.031174	0.000000
H	-1.473282	2.074097	0.000000
H	-0.891617	-2.074097	0.000000
Cl	2.795853	0.070328	0.000000

#### 2.4.8 Crystallographic Data (CIF)

Crystals used in this study were obtained by the author. They were in the form of multiply intergrown, colorless needles in the case of macrocycle **2.1**·4CH<sub>3</sub>OH·H<sub>2</sub>O, and

yellow prisms in the cases of the complex **2.1**·TBA<sub>3</sub>HP<sub>2</sub>O<sub>7</sub>·3H<sub>2</sub>O. Diffraction grade crystals of macrocycle **2.1**·4CH<sub>3</sub>OH·H<sub>2</sub>O were obtained by slow evaporation from solution using a CHCl<sub>3</sub> / CH<sub>3</sub>OH mixture. Crystals of the complex **2.1**·TBA<sub>3</sub>HP<sub>2</sub>O<sub>7</sub>·3H<sub>2</sub>O were obtained by slow evaporation from solution using CHCl<sub>3</sub>. The data crystals were cut from a cluster of crystals and had the approximate dimensions given in Table 2.3. The data were collected by the author on a Rigaku Saturn CCD diffractometer using a graphite monochromator with MoK  $\alpha$  radiation ( $\lambda = 0.71075 \text{ \AA}$ ). The data were collected using  $\omega$ -scans with a scan range of  $1^\circ$  at low temperature shows using an Oxford Cryostream low temperature device (Table 2.3). Data reduction was performed using DENZO-SMN.<sup>21</sup> The structures were solved by Dr. Xiaoping Yang *via* direct methods using SIR97<sup>22</sup> and refined by full-matrix least-squares on  $F^2$  with anisotropic displacement parameters for the non-H atoms using SHELXL-97.<sup>23</sup> The hydrogen atoms were calculated in ideal positions with isotropic displacement parameters set to  $1.2 \times U_{eq}$  of the attached atom ( $1.5 \times U_{eq}$  for methyl hydrogen atoms).

The function,  $\sum w(|F_o|^2 - |F_c|^2)^2$ , was minimized. Definitions used for calculating  $R(F)$ ,  $R_w(F^2)$  and the goodness of fit,  $S$ , are given below.<sup>24</sup> Neutral atom scattering factors and values used to calculate the linear absorption coefficient are from the International Tables for X-ray Crystallography (1992).<sup>25</sup> All ellipsoid figures were generated using SHELXTL/PC.<sup>26</sup> Tables of positional and thermal parameters, bond lengths and angles, torsion angles, figures and lists of observed and calculated structure factors are located in the cif documents available from the Cambridge Crystallographic Centre *via* quoting ref. numbers 786883 and 786884. These documents also contain details of crystal data, data collection and structure refinement.

**Table 2.3:** X-ray crystallographic data comparison of macrocycle **2.1**·4CH<sub>3</sub>OH·H<sub>2</sub>O and complex **2.1**·TBA<sub>3</sub>HP<sub>2</sub>O<sub>7</sub>·3H<sub>2</sub>O.

	Macrocycle <b>2.1</b> ·4CH <sub>3</sub> OH·H <sub>2</sub> O	Complex <b>2.1</b> ·TBA <sub>3</sub> HP <sub>2</sub> O <sub>7</sub> ·3H <sub>2</sub> O
CCDC No.	786884	786883
empirical formula	C <sub>54</sub> N <sub>16</sub> O <sub>5</sub> H <sub>70</sub>	C <sub>98</sub> N <sub>19</sub> P <sub>2</sub> O <sub>10</sub> H <sub>167</sub>
Fw	1021.24	1826.39
crystal size (mm <sup>3</sup> )	0.31 × 0.13 × 0.02	0.37 × 0.11 × 0.02
Crystal system	Monoclinic	Monoclinic
Space group	P2/c	P2(1)/c
<i>a</i> [Å]	18.799(4)	17.507(4)
<i>b</i> [Å]	7.4924(15)	39.237(8)
<i>c</i> [Å]	23.685(5)	24.684(5)
<i>α</i> [deg]	90.00	90.00
<i>β</i> [deg]	125.38(3)	131.52(3)
<i>γ</i> [deg]	90.00	90.00
<i>V</i> [Å <sup>3</sup> ]	2719.9(9)	12694(4)
<i>d</i> [g/cm <sup>3</sup> ]	1.247	0.956
<i>Z</i>	2	4
<i>T</i> [K]	223(2)	113(1)
R1, wR2 <i>I</i> > 2σ( <i>I</i> )	0.0929, 0.2083	0.0979, 0.2669
R1, wR2 (all data)	0.1945, 0.2700	0.1368, 0.2973
Quality of fit	0.986	0.973



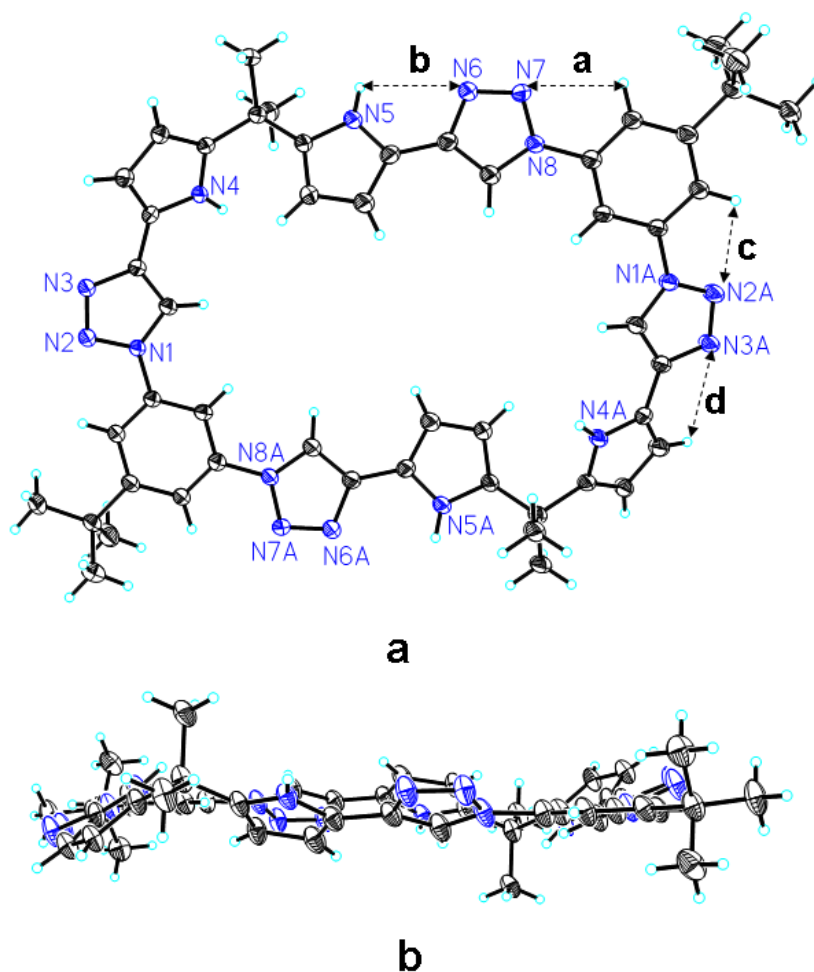


**Figure 2.20:** Views of the single crystal X-ray structure of **2.1**·4CH<sub>3</sub>OH·H<sub>2</sub>O. All solvent molecules have been omitted for clarity and thermal ellipsoids drawn at the 25% probability level. Symmetry operator (-x, 1-y, -z) generates equivalent atoms marked with “A”. **a**, Top view and **b**, side view showing the near planar conformation of **2.1**. Selected distances [Å]: a = 2.558, b = 2.744, c = 2.601, d = 3.056. This leads us to suggest that intramolecular H-bonding interactions on the exterior of the ring help stabilize the observed planar conformation in the solid state; see text proper.

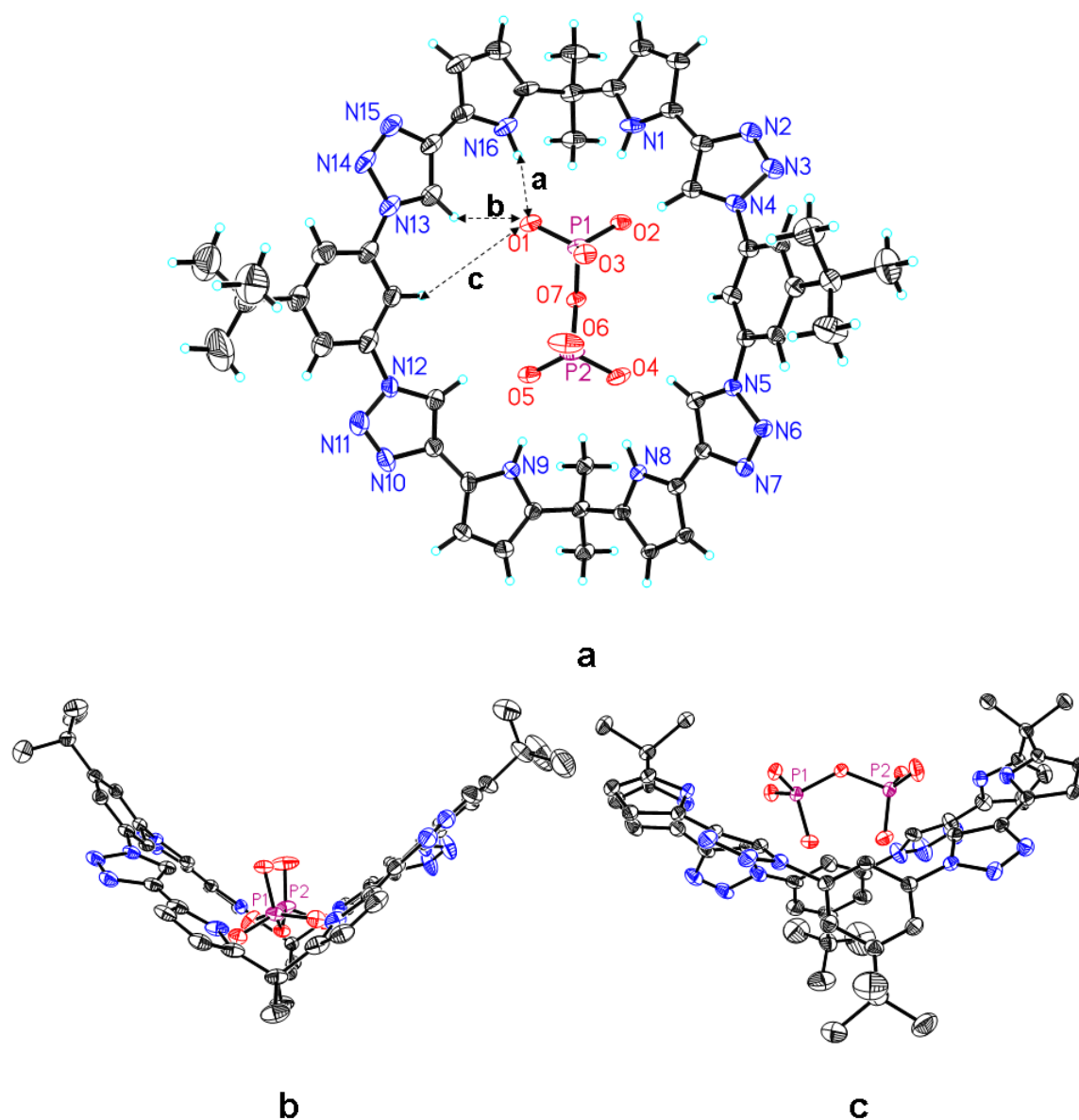


**Figure 2.21:** Views of the single crystal X-ray structure of  $2.1 \cdot \text{TBA}_3\text{HP}_2\text{O}_7 \cdot 3\text{H}_2\text{O}$ . All solvent molecules and TBA cations have been omitted for clarity and thermal ellipsoids drawn at the 25% probability level. **a**, Top view and **b**, **c** side view showing that the pyrophosphate anion is in a space filling representation. Selected distances [Å]:  $a = 1.905$ ,  $b = 2.324$ ,  $c = 3.870$ . This confirms that pyrrole NH and triazole CH protons are involved in hydrogen bond interactions with pyrophosphate guest; see text proper.

## 2.5 REFERENCES

- (1) Mathews, C. P.; van Hold, K. E. *Biochemistry*; The Benjamin/Cummings Publishing Company, Inc.: Redwood City, CA, 1990.
- (2) Ronaghi, M.; Karamohamed, S.; Pettersson, B.; Uhlén, M.; Nyrén, P. *Anal. Biochem.* **1996**, *242*, 84–89.
- (3) Xu, S.; He, M.; Yu, H.; Cai, X.; Tan, X.; Lu, B.; Shu, B. *Anal. Biochem.* **2001**, *299*, 188–193.
- (4) Saenger, W. *Principles of Nucleic Acid Structure*; Springer-Verlag: New York, 1988.
- (5) For review, see: (a) Sessler, J. L.; Gale, P. A.; Cho, W.-S. *Anion Receptor Chemistry*; RSC Publishing: Cambridge, U.K., 2006. (b) Kim, S.-K.; Lee, D.-H.; Hong, J.-I.; Yoon, J.-Y. *Acc. Chem. Res.* **2009**, *42*, 23–31. For recent reports, see: (c) Kumar, A.; Pandey, P. S. *Org. Lett.* **2008**, *10*, 165–168. (d) Chen, K.-H.; Liao, J.-H.; Chan, H.-Y.; Fang, J.-M. *J. Org. Chem.* **2009**, *74*, 895–898. (e) Xu, Z.; Singh, N. J.; Lim, J.; Pan, J.; Kim, H.-N.; Park, S.-S.; Kim, K. S.; Yoon, J.-Y. *J. Am. Chem. Soc.* **2009**, *131*, 15528–15533.
- (6) Of the 18 426 559 molecules in PubChem (March 2008), 17 947 719 (97%) contained one or more CH units. Li, Y.; Flood, A. H. *J. Am. Chem. Soc.* **2008**, *130*, 12111–12122.
- (7) (a) Bryantsev, V. S.; Hay, B. P. *Org. Lett.* **2005**, *7*, 5031–5034. (b) Bryantsev, V. S.; Hay, B. P. *J. Am. Chem. Soc.* **2005**, *127*, 8282–8283. (c) Li, Y.; Flood, A. H. *Angew. Chem., Int. Ed.* **2008**, *47*, 2649–2652. (d) Yoon, D. W.; Gross, D. E.; Lynch, V. M.; Sessler, J. L.; Hay, B. P.; Lee, C.-H. *Angew. Chem., Int. Ed.* **2008**, *47*, 5038–5042. (e) Li, Y.; Pink, M.; Karty, J. A.; Flood, A. H. *J. Am. Chem. Soc.* **2008**, *130*, 17293–17295. (f) Zhu, S. S.; Staats, H.; Brandhorst, K.; Grunenberg, J.; Gruppi, F.; Dalcanale, E.; Lützen, A.; Rissanen, K.; Schalley, C. A. *Angew. Chem., Int. Ed.* **2008**, *47*, 788–792. (g) Juwarker, H.; Lenhardt, J. M.; Pham, D. M.; Craig, S. L. *Angew. Chem., Int. Ed.* **2008**, *47*, 3740–3743. (h) Meudtner, R. M.; Hecht, S. *Angew. Chem., Int. Ed.* **2008**, *47*, 4926–4930. (i) Berryman, O. B.; Sather, A. C.; Hay, B. P.; Meisner, J. S.; Johnson, D. W. *J. Am. Chem. Soc.* **2008**, *130*, 10895–10897. (j) Maeda, H.; Mihashi, Y.; Haketa, Y. *Org. Lett.* **2008**, *10*, 3179–3182. (k) Hay, B. P.; Bryantsev, V. S. *Chem. Commun.* **2008**, 2417–2428. (l) Romero, T.; Caballero, A.; Tárraga, A.; Molina, P. *Org. Lett.* **2009**, *11*, 3466–3469. (m) Mullen, K. M.; Mercurio, J.; Serpell, C. J.; Beer, P. D. *Angew. Chem., Int. Ed.* **2009**, *48*, 4781–4784. (n) Juwarker, H.; Lenhardt, J. M.; Castillo, J. C.; Craig, S. L. *J. Org. Chem.* **2009**, *74*, 8924–8934. (o) Fisher, M. G.; Gale, P. A.; Hiscock, J. R.; Hursthouse, M. B.; Light, M. E.; Schmidtchen, F. P.; Tong, C. C. *Chem. Commun.* **2009**, 3017–3019. (p) Pedzisa, L.; Hay, B. P. *J. Org. Chem.* **2009**, *74*, 2554–2560. (q) Schulze, B.; Friebe, C.; Hager, M. D.; Günther, W.; Köhn, U.; Jahn, B. O.; Görls, H.; Schubert, U. S. *Org. Lett.* **2010**, *12*, 2710–2713.

- (r) Lee, S.; Hua, Y.; Park, H.; Flood, A. H. *Org. Lett.* **2010**, *12*, 2100–2102. (s) Yano, M.; Tong, C. C.; Light, M. E.; Schmidtchen, F. P.; Gale, P. A. *Org. Biomol. Chem.* **2010**, *8*, 4356–4363.
- (8) Hua, Y.; Flood, A. H. *Chem. Soc. Rev.* **2010**, *39*, 1262–1271.
  - (9) Although it does not contain triazole and pyrrole in the same macrocyclic ring, it is to be noted that Gale recently reported a triazole strapped calixpyrrole and showed it to be effective for chloride anion recognition. See: ref 7o and 7s.
  - (10) Rostovtsev, V. V.; Green, L. G.; Fokin, V. V.; Sharpless, K. B. *Angew. Chem., Int. Ed.* **2002**, *41*, 2596–2599.
  - (11) Tom, N. J.; Simon, W. M.; Frost, H. N.; Ewing, M. *Tetrahedron Lett.* **2004**, *45*, 905–906.
  - (12) Kim, S. K.; Sessler, J. L.; Gross, D. E.; Lee, C.-H.; Kim, J. S.; Lynch, V. M.; Delmau, L. H.; Hay, B. P. *J. Am. Chem. Soc.* **2010**, *132*, 5827–5836.
  - (13) Bourson, J.; Pouget, J.; Valeur, B. *J. Phys. Chem.* **1993**, *97*, 4552–4557.
  - (14) Katritzky, A. R. *Handbook of Heterocyclic Chemistry*; Pergamon Press: 2000.
  - (15) The CH binding energies are consistent with a prior description of individual hydrogen-bond contributions within a triazolophane\*Cl<sup>−</sup> complex, which implicated energies of -10 kcal/mol per triazole CH and -3 to -4 kcal/mol per aryl CH: Bandyopadhyay, I.; Raghavachari, K.; Flood, A. H. *ChemPhysChem* **2009**, *10*, 2535–2540.
  - (16) Sandström, J. *Dynamic NMR Spectroscopy*; Academic: London, 1982.
  - (17) Ōki, M. *Applications of Dynamic NMR Spectroscopy to Organic Chemistry*; WILEY-VCH: Weinheim, 1985.
  - (18) Neuhaus, D.; Williamson, M.P. *The Nuclear Overhauser Effect in Structural and Conformational Analysis*; VCH Publishers: Cambridge, U. K., 1989.
  - (19) Friebolin, H. *Basic One- and Two-Dimensional NMR Spectroscopy*; WILEY-VCH: Weinheim, 2005.
  - (20) Bylaska, E. J.; de Jong, W. A.; Kowalski, K.; Straatsma, T. P.; Valiev, M.; Wang, D.; Apra, E.; Windus, T. L.; Hirata, S.; Hackler, M. T.; Zhao, Y.; Fan, P. –D.; Harrison, R. J.; Dupuis, M.; Smith, D. M. A.; Nieplocha, J.; Tipparaju, V.; Krishnan, M.; Auer, A. A.; Nooijen, M.; Brown, E.; Cisneros, G.; Fann, G. I.; Fruchtl, H.; Garza, J.; Hirao, K.; Kendall, R.; Nichols, J. A.; Tsemekhman, K.; Wolinski, K.; Anchell, J.; Bernholdt, D.; Borowski, P.; Clark, T.; Clerc, D.; Dachsel, H.; Deegan, M.; Dyall, K.; Elwood, D.; Glendening, E.; Gutowski, M.; Hess, A.; Jaffe, J.; Johnson, B.; Ju, J.; Kobayashi, R.; Kutteh, R.; Lin, Z.; Littlefield, R.; Long, X.; Meng, B.; Nakajima, T.; Niu, S.; Pollack, L.; Rosing, M.; Sandrone, G.; Stave, M.; Taylor, H.; Thomas, G.; van Lenthe, J.; Wong, A.;

- Zhang, Z. *NWChem, A Computational Chemistry Package for Parallel Computers, Version 5.0*, **2006**, Pacific Northwest National Laboratory, Richland, Washington 99352-0999, USA.
- (21) DENZO-SMN. (**1997**). Otwinowski, Z.; Minor, W. *Methods in Enzymology*, 276: *Macromolecular Crystallography, Part A*, 307 – 326, Carter, C.W.J.; Simon, M.I.; Sweet, R.M. Editors, Academic Press.
  - (22) SIR97. (**1999**). A program for crystal structure solution. Altomare, A.; Burla, M. C.; Camalli, M.; Cascarano, G. L.; Giacovazzo, C.; Guagliardi, A.; Moliterni, A.G. G.; Polidori, G.; Spagna, R. *J. Appl. Cryst.* **1999**, 32, 115-119.
  - (23) Sheldrick, G. M. *SHELXL97. Program for the Refinement of Crystal Structures*; University of Gottingen, Germany, **1994**.
  - (24)  $R_w(F^2) = \{\sum w(|F_o|^2 - |F_c|^2)^2 / \sum w(|F_o|^4)\}^{1/2}$  where w is the weight given each reflection.  $R(F) = \sum(|F_o| - |F_c|) / \sum |F_o|$  for reflections with  $F_o > 4(\sigma(F_o))$ .  $S = [\sum w(|F_o|^2 - |F_c|^2)^2 / (n - p)]^{1/2}$ , where n is the number of reflections and p is the number of refined parameters.
  - (25) *International Tables for X-ray Crystallography*; Wilson, A. J. C., Ed.; Kluwer Academic Press: Boston, **1992**; Vol. C, Tables 4.2.6.8 and 6.1.1.4.
  - (26) Sheldrick, G.M. (**1994**). SHELXTL/PC (Version 5.03). Siemens Analytical X-ray Instruments, Inc., Madison, Wisconsin, USA.
  - (27) Fang, J. –M.; Selvi, S.; Liao, J. –H.; Slanina, Z.; Chen, C. –T.; Chou, P. –T. *J. Am. Chem. Soc.* **2004**, 126, 3559–3566.

## Chapter 3: A Pyrrole-based Triazolium-phane with NH and Cationic CH Donor Groups as a Receptor for Tetrahedral Oxyanions that Functions in Polar Media

### 3.1 INTRODUCTION

One goal of supramolecular chemistry<sup>1</sup> is to create synthetic receptors that have both high affinity and high selectivity for biologically and environmentally important anionic species.<sup>2</sup> Anions are ubiquitous in the natural world and critical to the maintenance of life as we know it.<sup>3</sup> Pyrophosphate, for instance, is a byproduct of ATP hydrolysis under cellular conditions.<sup>4</sup> It is involved in DNA polymerase-catalyzed DNA replication<sup>5</sup> and its detection pyrophosphate could provide for real-time DNA sequencing.<sup>6</sup> Its analogue, inorganic phosphate, has physiological relevance in biological energy storage and signal transduction, in addition to being a structural component in teeth and bones.<sup>7</sup> Sulfate, because of its low solubility (typically *ca.* 1%) in borosilicate glass, has been identified as problematic in the vitrification of radioactive waste.<sup>8</sup> Not surprisingly, therefore, considerable effort has been devoted to the design and synthesis of receptors capable of recognizing and detecting these tetrahedral oxyanions.<sup>2</sup> Systems incorporating neutral or cationic NH hydrogen bond donor groups (*e.g.*, pyrrole, urea, amide, ammonium, and guanidinium)<sup>9</sup> and neutral or cationic CH hydrogen bond donor motifs (*e.g.*, phenyl, triazole, triazolium, and imidazolium)<sup>10,16</sup> have been particularly effective in this regard. It is noteworthy that positively charged imidazolium derivatives can interact with anions through  $(\text{C-H})^+ \cdots \text{X}^-$  type ionic hydrogen bonds, which are generally stronger than the corresponding hydrogen-bonding interactions stabilized by neutral pyrrole and urea moieties.<sup>10(f)</sup> Recently, 1,2,3-triazolium motifs with cationic CH hydrogen bond donor groups have garnered attention for their potential use in transition

metal-based catalysis<sup>11</sup> and organocatalysis.<sup>12</sup> However, they have yet to be exploited extensively in anion recognition chemistry.<sup>10(b),13</sup> In fact, we are aware of only three reports of anion receptors containing 1,2,3-triazolium subunits. None of the systems in question was found to be effective in the presence of water and only one, an open-chain threading element reported by Beer and coworkers,<sup>10(b)</sup> has been structurally characterized in the form of its anion complex (chloride). Here, we report a new synthetic anion receptor, **3.1**<sup>4+</sup>, that combines both pyrrole and triazolium anion recognition motifs within one macrocyclic framework. It exhibits high selectivity and affinity for tetrahedral oxyanions and functions effectively in mixed organic-aqueous media. Based on a combination of theoretical, solution phase, and single crystal X-ray diffraction analyses, we propose that oxyanion recognition is stabilized *via* a combination of C–H $\cdots$  and N–H $\cdots$ anion hydrogen bonding and electrostatic interactions, both in solution and in the solid state. We also conclude that in highly polar media, such as methanol, phenyl CH-anion interactions play a greater stabilizing role in anion binding than do triazolium (CH)<sup>+</sup>–anion interactions.

The paucity of attention devoted to 1,2,3-triazolium-based anion recognition systems stands in marked contrast to what is true for neutral triazoles. These latter motifs, first pioneered for anion recognition by Flood and coworkers, have provided an important new submit for anion recognition.<sup>10(d)</sup> One reason triazole systems are attractive is because they can be accessed via so-called “click” chemistry, specifically the copper(I)–catalyzed azide alkyne 1,3–dipolar cycloaddition (CuAAC) reaction.<sup>14,15</sup> They can also be readily incorporated into a variety of cyclic and acyclic structures. One further appeal of triazoles is that, at least in principle, they can be converted to the corresponding triazolium salts by simple alkylation.<sup>10(b)</sup> With this consideration in mind we sought to prepare the tetracationic macrocycle **3.1**<sup>4+</sup> by subjecting the corresponding triazole system **3.2** to

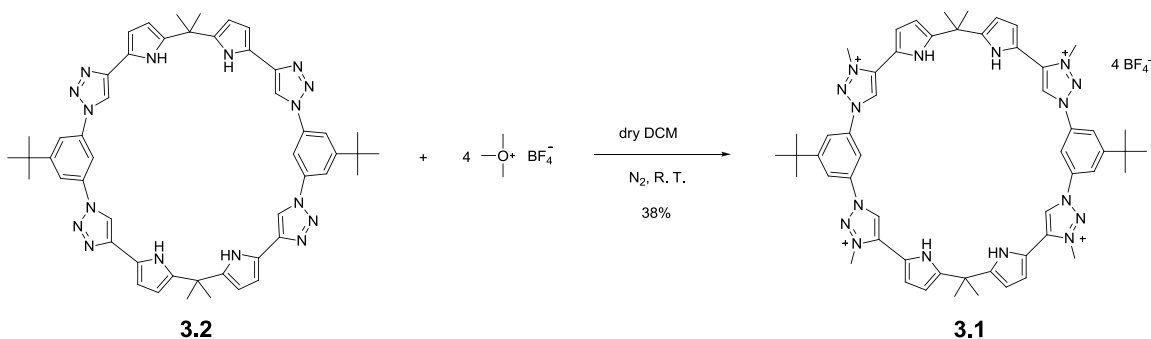
methylation (Scheme 3.1). As detailed below, this strategy proved easy to implement and gave rise to an anion receptor **3.1**<sup>4+</sup> that contains four triazolium subunits. A notable feature of this new system is that it contains three different types of putative hydrogen bond donor groups (benzene CH, triazolium CH, and pyrrole NH). Thus, an ancillary objective associated with the present study was an assessment of the relative importance of the resulting subunit-anion interactions.

### 3.2 RESULTS AND DISCUSSIONS

The synthesis of calix[2]1,3-bis(pyrro-2-yl)(1,4)-1,2,3-triazolo-phane **3.2** (Scheme 3.1) was accomplished in three steps as detailed in chapter 2. Briefly, the key fragment 1,3-bis(pyrro-2-yl)(1,4)-1,2,3-triazolo-benzene was prepared under standard click conditions,<sup>14</sup> followed by removal of the *t*-BOC protecting group;<sup>17</sup> it was then cyclized with acetone to form macrocycle **3.2**.<sup>18</sup> This was followed by a methylation reaction using Meerwein's salt to give the tetracationic triazolium macrocycle tetrafluoroborate salt **3.1**<sup>4+</sup>•4BF<sub>4</sub><sup>-</sup> (**3.1** = calix[2]1,3-bis(pyrro-2-yl)(1,4)-3-methyl-5H-1,2,3-triazolium-phane tetrafluoroborate) in 38% yield.<sup>10(b)</sup> Colorless single crystals of **3.1**<sup>4+</sup>•4BF<sub>4</sub><sup>-</sup> were obtained via vapor diffusion (diethyl ether into a methanol solution of the salt). Salt **3.1**<sup>4+</sup>•4BF<sub>4</sub><sup>-</sup> was characterized on the basis of its spectroscopic properties and *via* single crystal X-ray diffraction analysis.



**Scheme 3.1:** Synthesis of the tetracationic triazolium macrocycle **3.1**<sup>4+</sup>.



A single crystal X-ray diffraction analysis of **3.1**<sup>4+</sup>•4 $\text{BF}_4^-$  revealed a nearly planar macrocyclic structure. Two of the  $\text{BF}_4^-$  counter anions were found to be located within the inner cavity of the tetracationic cyclophane built up from the constituent phenyl, pyrrole, and triazolium subunits. The two other counter anions were found to lie outside the cage and are not involved in any apparent interaction with the macrocycle, at least in the solid state (Figure 3.1). The macrocycle **3.1**<sup>4+</sup>•4 $\text{BF}_4^-$  is centrosymmetric. The pyrrole groups (N4, N4A) and the triazolium motifs (C11, C11A) are twisted out of the plane. The hydrogen atoms on the pyrrole NH (N8, N8A), triazolium CH (C20, C20A) and the endocyclic hydrogen atoms of the N<sup>1</sup>-linked phenyl units (C8, C8A) are pointing into the center of the ring. Based on the geometric parameters (N- and C-F distances of < 3 Å) these endocyclic hydrogen atoms are involved in  $\text{NH}\cdots\text{F}$ ,  $\text{CH}\cdots\text{F}$  hydrogen bond interactions with one of the  $\text{BF}_4^-$  anions bound within the macrocyclic ring.

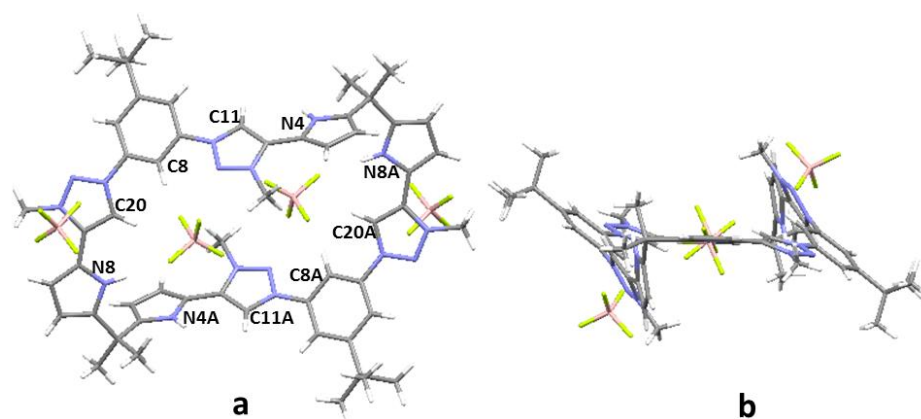


**Figure 3.1:** (a) Top and (b) side views of the single crystal X-ray structure of **3.1**<sup>4+</sup>•4BF<sub>4</sub><sup>-</sup>•CH<sub>3</sub>OH•3H<sub>2</sub>O. All solvent molecules have been omitted for clarity.

The anion binding properties of **3.1**<sup>4+</sup>•4BF<sub>4</sub><sup>-</sup> in solution were analyzed initially using UV–Vis spectroscopy. Standard titrations, associated curve fittings,<sup>19</sup> and Job plots provided support for the proposal that hydrogen pyrophosphate, hydrogen sulfate and dihydrogen phosphate anions (all studied as their corresponding tetrabutylammonium (TBA) salts) are bound to **3.1**<sup>4+</sup>•4BF<sub>4</sub><sup>-</sup> strongly in acetone–H<sub>2</sub>O solution (2:3; pH = 7.2; HEPES buffer) at 300 K (HP<sub>2</sub>O<sub>7</sub><sup>3-</sup>:  $K_a = (2.49 \pm 0.15) \times 10^5 \text{ M}^{-1}$ ; HSO<sub>4</sub><sup>-</sup>:  $K_a = (3.92 \pm 0.36) \times 10^5 \text{ M}^{-1}$ ; H<sub>2</sub>PO<sub>4</sub><sup>-</sup>:  $K_a = (3.53 \pm 0.14) \times 10^4 \text{ M}^{-1}$ ) and with 1:1 binding stoichiometries (Table 3.1). To avoid interference from potential aggregation effects, the effective association constants ( $K_a$ ) were determined at [**3.1**<sup>4+</sup>•4BF<sub>4</sub><sup>-</sup>] ≤ 50 μM and were found to be independent of initial receptor concentration under these conditions. The binding isotherms used to determine the  $K_a$  values were generated by recording the changes in the UV–Vis absorption spectrum as a function of hydrogen sulfate, hydrogen pyrophosphate and dihydrogen phosphate concentration (shown for **3.1**<sup>4+</sup>•4BF<sub>4</sub><sup>-</sup> in Figures 3.2a, b, and c, respectively). Based on Job–plot analyses, which proved consistent with a 1:1 binding stoichiometry in the case of these test anions (Figures 3.2d, e, and f,

respectively), the data were fit to a 1:1 binding isotherm. Analogous studies were carried out in methanol and acetonitrile. The calculated  $K_a$  values and binding stoichiometries (as inferred from Job plots) for all three solvent systems are summarized in Table 3.1.

Strictly speaking the  $K_a$  values in Table 3.1 are displacement constants and reflect any initial interaction between the  $\text{BF}_4^-$  counter anions and receptor **3.1**<sup>4+</sup>. However, in practice the interactions between the  $\text{BF}_4^-$  counter anions and the receptor are expected to be modest. Further, they will be identical for all anions considered in this study. Therefore, we believe that the  $K_a$  values tabulated in Table 3.1, which represent lower bounds, can be used for the purpose of inter-analyte comparisons.

From an inspection of Table 3.1, the effect of solvent on the anion binding behavior of receptor **3.1**<sup>4+</sup>•4 $\text{BF}_4^-$  can be inferred. While in acetonitrile a general lack of anion selectivity is seen (the binding constants for various test anions range between  $10^5$  and  $10^6 \text{ M}^{-1}$ ), in methanol, considerable selectivity for tetrahedral oxyanions is seen relative to other typical anionic analytes (e.g., acetate, nitrate, chloride and bromide; all studied as the corresponding TBA salts). This selectivity is maintained and even enhanced in acetone–H<sub>2</sub>O (2:3; pH = 7.2; HEPES buffer). In fact, under these latter, mixed aqueous solvent conditions, receptor **3.1**<sup>4+</sup> (as its tetrakis  $\text{BF}_4^-$  salt) binds the tetrahedral oxyanions hydrogen sulfate, hydrogen pyrophosphate and dihydrogen phosphate anions with affinities of  $10^4$ – $10^5 \text{ M}^{-1}$ . However, it displays no appreciable affinity for any of the other test anions.

The combination of high affinity and selectivity for tetrahedral oxyanions in mixed aqueous medium is noteworthy. While systems that bind tetrahedral oxyanions in organic media based on hydrogen–bonding interaction are well known, there are few that operate in the presence of large quantities of water. In prior work, Kubik and coworkers demonstrated that synthetic cyclopeptides containing alternating aromatic and L–proline

residues could bind inorganic anions, such as halides and sulfate, efficiently in 80% H<sub>2</sub>O–CH<sub>3</sub>OH, although little appreciable selectivity for the sulfate anion was observed.<sup>20</sup> In separate work, Delgado and coworkers demonstrated that protonated hexaamine–cage receptors could efficiently interact with tetrahedral oxyanions in 50% H<sub>2</sub>O–CH<sub>3</sub>OH at low pH.<sup>21</sup> In earlier work, Lehn and coworkers reported that guanidinium–containing macrocycles could be used for the recognition of phosphate in water.<sup>22</sup> However, these latter receptors formed less stable anion complexes than the corresponding protonated ammonium–based receptors. There thus remains a need for new receptors that are selective for tetrahedral oxyanions and which function in mixed aqueous media at neutral pH.

**Table 3.1:** Binding Affinities of Different Anions to Receptor **3.1**<sup>4+</sup>•4BF<sub>4</sub><sup>-</sup> in Three Different Solvent Systems<sup>a</sup>

Guest	CH <sub>3</sub> CN <sup>b</sup>		CH <sub>3</sub> OH <sup>b</sup>		acetone –H <sub>2</sub> O (2:3) <sup>b</sup> (pH=7.2 in HEPES buffer)	
	Host / Guest	<i>K</i> <sub>a</sub>	Host / Guest	<i>K</i> <sub>a</sub>	Host / Guest	<i>K</i> <sub>a</sub>
HSO <sub>4</sub> <sup>-</sup>	1:1	<i>K</i> <sub>a</sub> = ( 9.88 ± 1.18 ) ×10 <sup>6</sup> M <sup>-1</sup>	1:1	<i>K</i> <sub>a</sub> = ( 1.60 ± 0.22 ) ×10 <sup>7</sup> M <sup>-1</sup>	1:1	<i>K</i> <sub>a</sub> = ( 3.92 ± 0.36 ) ×10 <sup>5</sup> M <sup>-1</sup>
HP <sub>2</sub> O <sub>7</sub> <sup>3-</sup>	1:1	<i>K</i> <sub>a</sub> = ( 9.89 ± 1.06 ) ×10 <sup>5</sup> M <sup>-1</sup>	1:1	<i>K</i> <sub>a</sub> = ( 1.17 ± 0.17 ) ×10 <sup>7</sup> M <sup>-1</sup>	1:1	<i>K</i> <sub>a</sub> = ( 2.49 ± 0.15 ) ×10 <sup>5</sup> M <sup>-1</sup>
H <sub>2</sub> PO <sub>4</sub> <sup>-</sup>	1:2	<i>K</i> <sub>a,1</sub> = ( 6.44 ± 0.16 ) ×10 <sup>3</sup> M <sup>-1</sup> <i>K</i> <sub>a,2</sub> = ( 1.03 ± 0.04 ) ×10 <sup>5</sup> M <sup>-1</sup>	1:1	<i>K</i> <sub>a</sub> = ( 1.73 ± 0.15 ) ×10 <sup>6</sup> M <sup>-1</sup>	1:1	<i>K</i> <sub>a</sub> = ( 3.53 ± 0.14 ) ×10 <sup>4</sup> M <sup>-1</sup>
CH <sub>3</sub> COO <sup>-</sup>	1:1	<i>K</i> <sub>a</sub> = ( 2.25 ± 0.14 ) ×10 <sup>6</sup> M <sup>-1</sup>	1:1	<i>K</i> <sub>a</sub> = ( 1.79 ± 0.01 ) ×10 <sup>3</sup> M <sup>-1</sup>	n.d. <sup>c</sup>	n.d.
NO <sub>3</sub> <sup>-</sup>	1:1	<i>K</i> <sub>a</sub> = ( 5.99 ± 0.61 ) ×10 <sup>5</sup> M <sup>-1</sup>	1:1	<i>K</i> <sub>a</sub> = ( 7.90 ± 0.50 ) ×10 <sup>3</sup> M <sup>-1</sup>	n.d.	n.d.
Cl <sup>-</sup>	1:1	<i>K</i> <sub>a</sub> = ( 4.48 ± 0.53 ) ×10 <sup>6</sup> M <sup>-1</sup>	1:1	<i>K</i> <sub>a</sub> = ( 2.93 ± 0.05 ) ×10 <sup>3</sup> M <sup>-1</sup>	n.d.	n.d.
Br <sup>-</sup>	1:1	<i>K</i> <sub>a</sub> = ( 2.46 ± 0.25 ) ×10 <sup>6</sup> M <sup>-1</sup>	1:1	<i>K</i> <sub>a</sub> = ( 4.90 ± 0.34 ) ×10 <sup>3</sup> M <sup>-1</sup>	n.d.	n.d.

<sup>a</sup>Determined by UV–Vis titrations carried out at 300 K using the tetrabutylammonium (TBA) salts of the indicated anions. <sup>b</sup>For studies in CH<sub>3</sub>CN and CH<sub>3</sub>OH, [3.1<sup>4+</sup>•4BF<sub>4</sub><sup>-</sup>] =

$1.00 \times 10^{-5}$  M; for studies in acetone–H<sub>2</sub>O (2:3; pH = 7.2; HEPES buffer),  $[3.1^{4+} \cdot 4BF_4^-] = 5.00 \times 10^{-5}$  M. <sup>c</sup>n.d. = not determined; affinity too modest to be measured accurately.

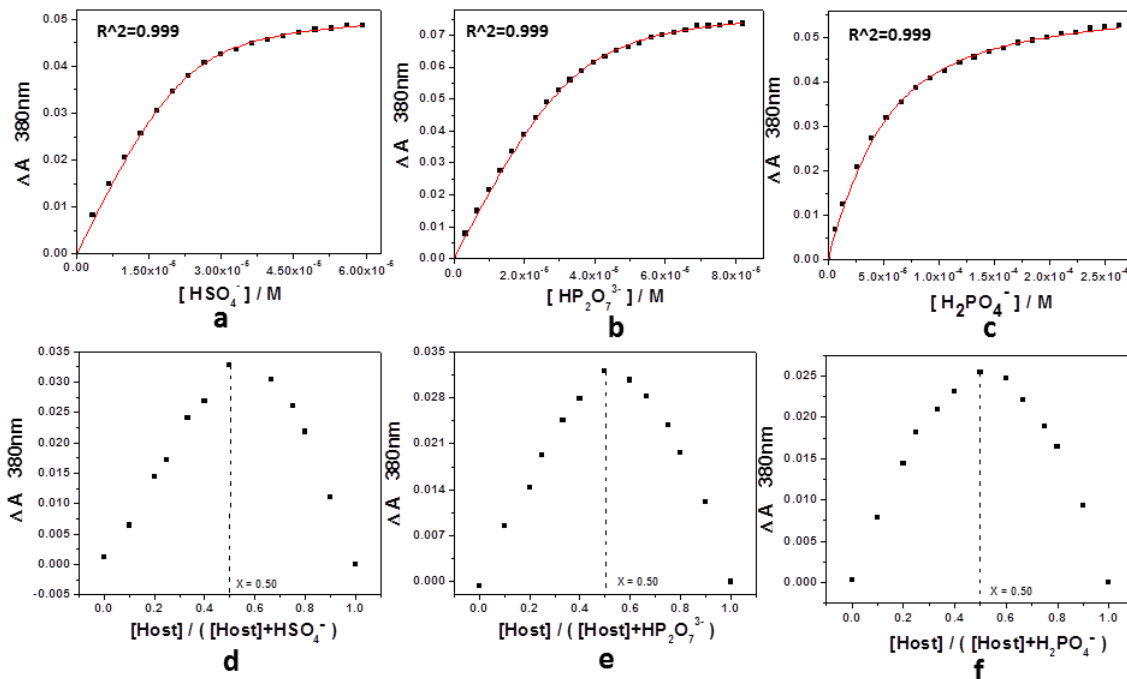


**Figure 3.2:** Variations in absorbance ( $\bullet$ ) at 380nm of a solution of receptor  $3.1^{4+} \cdot 4BF_4^-$  ( $5.00 \times 10^{-5}$  M) in acetone–H<sub>2</sub>O (2:3) (PH = 7.2 in HEPES buffer) as a function of the concentration in TBAHSO<sub>4</sub> ( $0$ – $6.0 \times 10^{-5}$  M) (a), TBA<sub>3</sub>HP<sub>2</sub>O<sub>7</sub> ( $0$ – $8.0 \times 10^{-5}$  M) (b) and TBAH<sub>2</sub>PO<sub>4</sub> ( $0$ – $2.5 \times 10^{-4}$  M) (c) at 300 K. The Job-plot for the complexation between  $3.1^{4+} \cdot 4BF_4^-$  and TBAHSO<sub>4</sub> (d), (TBA)<sub>3</sub>HP<sub>2</sub>O<sub>7</sub> (e) and TBAH<sub>2</sub>PO<sub>4</sub> (f) in acetone–H<sub>2</sub>O (2:3) (PH = 7.2 in HEPES buffer) at 300 K.  $[host] + [guest] = 5.00 \times 10^{-5}$  M. A maximum value at 0.5 is observed; this is consistent with a 1:1 (host : guest) binding stoichiometry.

To understand the solvent dependence noted above and to allow a comparison of the intrinsic hydrogen bonding ability of the donor groups present in receptor  $3.1^{4+}$ ,  $\Delta G$  values for the formation of the representative complexes between the Cl<sup>−</sup> anion and the simple donors shown in Figure 3.3 were computed in the gas phase under vacuum

conditions (cf. Experimental Section for Cartesian coordinates and absolute energies).<sup>23</sup> Similar calculations were carried out in several pure solvents (e.g.,  $\text{CHCl}_3$ , acetone,  $\text{CH}_3\text{CN}$ ,  $\text{CH}_3\text{OH}$ , and  $\text{H}_2\text{O}$ ).<sup>24</sup> In prior studies, comparison of hydrogen bonding interactions between C–H and N–H donor groups with different anion shapes (chloride, nitrate, perchlorate) established that similar binding energy trends are observed for this group of monovalent anions.<sup>10(e),32</sup> Therefore, we have used the chloride as a representative anion, primarily because the system is small and the number of possible minima is limited. The results, summarized in Table 3.2, reveal that although the formation of the triazolium complex is by far the most favorable in vacuum, the binding affinity (as measured by  $\Delta G$ ) decreases dramatically for the corresponding process in  $\text{CHCl}_3$ . This interaction becomes even less favorable in the case of more polar solvents. In the case of higher dielectric constant solvents, i.e.,  $\epsilon > 20$  (acetone,  $\text{CH}_3\text{CN}$ ,  $\text{CH}_3\text{OH}$ , and  $\text{H}_2\text{O}$ ), the calculated  $\Delta G$  values lead to the inference that the driving force for hydrogen bond formation decreases in the following order: pyrrole > triazole > benzene > triazolium cation. The driving force for forming complexes between the  $\text{Cl}^-$  anion and three putative hydrogen bonding donors present in the macrocycle **3.1**<sup>4+</sup>•4 $\text{BF}_4^-$  (pyrrole N–H, benzene C–H and triazolium C–H) all decrease on passing from acetonitrile to methanol (Table 3.2). Such a conclusion is fully consistent with the results of the UV–Vis experimental studies discussed above: In case of both theory and experiment, the binding constants for interactions with monoanions were found to become smaller as the polarity of the medium increased (e.g., on moving from acetonitrile to methanol).<sup>25</sup> However, for tetrahedral oxyanions, the binding constants proved to be both inherently high and rather independent of solvent polarity. This could reflect the greater size and complexity of these latter ions, features that would tend to augment the importance of specific hydrogen bonding interactions relative to competitive anion solvation. Independent of rationale, it

is important to underscore that the theoretical analyses lead to the perhaps counterintuitive conclusion that in methanol the benzene CH-anion hydrogen bond interactions are more important than the corresponding imidazolium CH-anion interactions. Experimental support for this conclusion was obtained from detailed  $^1\text{H}$  NMR analyses as detailed below.

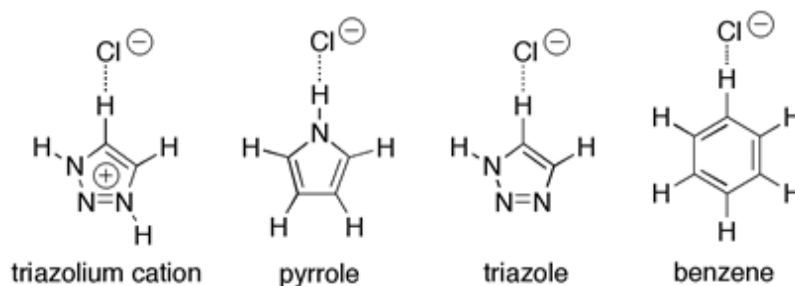


**Figure 3.3:** Representative complexes that provide examples of the hydrogen bonding interactions present in the macrocycles.

**Table 3.2:** Influence of solvent on calculated  $\Delta G$  values (kcal/mol) for the formation of hydrogen-bonded complexes between  $\text{Cl}^-$  and representative simple donors (Figure 3.3)

donor	solvent					
	vacuum	$\text{CHCl}_3$	Acetone	$\text{CH}_3\text{CN}$	$\text{CH}_3\text{OH}$	$\text{H}_2\text{O}$
triazolium C–H	–89.2	–4.0	11.5	14.0	19.5	20.7
pyrrole N–H	–15.6	–3.0	–1.9	–1.3	3.9	4.1
triazole C–H	–12.4	2.5	4.8	5.4	8.7	8.6
benzene C–H	–2.4	5.7	6.1	6.4	8.9	8.6



The host-guest interactions between receptor **3.1**<sup>4+</sup>•4BF<sub>4</sub><sup>-</sup> and representative tetrahedral oxyanions were further analyzed by <sup>1</sup>H NMR spectroscopy. Proton NMR titrations were carried out in deuterated methanol using the respective TBA salts. Unfortunately, solubility considerations precluded analogous titrations being carried out in either CD<sub>3</sub>CN or 60% D<sub>2</sub>O/40% acetone-*d*<sub>6</sub>. The titrations were performed as follows: A solution of receptor **3.1**<sup>4+</sup>•4BF<sub>4</sub><sup>-</sup> (4 mM, CD<sub>3</sub>OD) was titrated with up to 10 equiv. of the TBA anion salt of choice. A representative titration is shown in Figure 3.4 for (TBA)<sub>3</sub>HP<sub>2</sub>O<sub>7</sub>. It is worth noting that the pyrrole NH protons were generally not visible under the conditions of these titrations, presumably as the result of fast exchange with the CD<sub>3</sub>OD solvent. As a general rule, and as can be seen by inspection of Figure 3.4, little shift in the signals for the triazolium CH protons was typically seen. In contrast, the resonances corresponding to the endocyclic hydrogen atoms of the N<sup>1</sup>-linked phenyl unit were observed to shift downfield by 1.01 ppm, 0.48 ppm, and 0.45 ppm upon the addition of 5 equiv. of (TBA)<sub>3</sub>HP<sub>2</sub>O<sub>7</sub>, TBAH<sub>2</sub>PO<sub>4</sub> and TBAHSO<sub>4</sub>, respectively (cf. Experimental Section). Such differing shift behavior is consistent with the differences in the intrinsic strength of the various H-bond donor groups inferred from the electronic structure calculations carried out in methanol using the chloride anion. The calculated ΔG values of the interaction of chloride with benzene C-H and triazolium C-H complexes are 8.9 and 19.5 kcal/mol in methanol (Table 3.2). This combination of theory and experiment provides support for the conclusion that the anion interactions stabilized by a benzene C-H hydrogen bond is stronger than that stabilized by a triazolium C-H hydrogen bond in methanol.

Proton NMR titrations were also carried out in deuterated methanol using receptor **3.1**<sup>4+</sup>•4BF<sub>4</sub><sup>-</sup> and both monoanionic and trigonal planar anionic salts, such as TBAOAc, TBANO<sub>3</sub>, TBACl, and TBABr (cf. Experimental Section). The hydrogen signals for the

endocyclic hydrogen atoms of the N<sup>1</sup>-linked phenyl unit shifted slightly during the associated NMR titrations. On the other hand, little observable shift was seen for the triazolium CH signal. Such findings are consistent with the relative contribution of these two CH donor motifs inferred above. Moreover, they provide support for the conclusions drawn from the UV–Vis titration experiments, namely that in methanol receptor **3.1**<sup>4+</sup>•4BF<sub>4</sub><sup>−</sup> interacts with tetrahedral oxyanions much more strongly than it does with other simple anions.

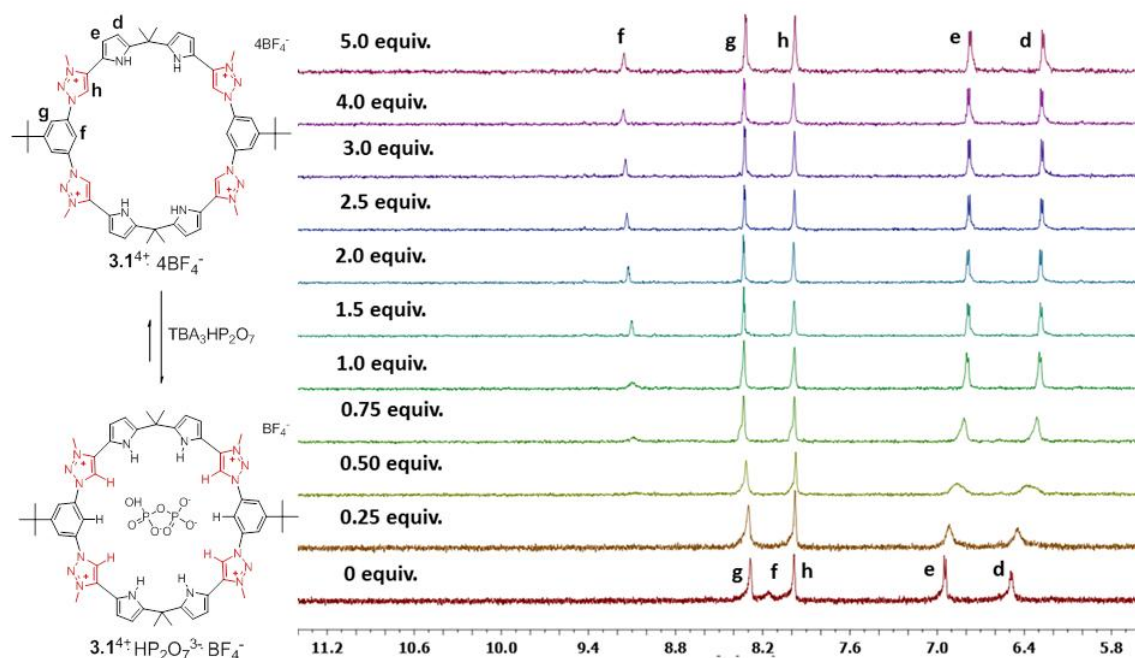


**Figure 3.4:** <sup>1</sup>H NMR spectra (aromatic region) of receptor **3.1**<sup>4+</sup>•4BF<sub>4</sub><sup>−</sup> (4 mM) recorded in the presence of increasing concentrations of (TBA)<sub>3</sub>HP<sub>2</sub>O<sub>7</sub> (CD<sub>3</sub>OD, 300 K).

Further support for the proposal that receptor **3.1**<sup>4+</sup> is able to interact with the pyrophosphate and phosphate anions came from single crystal X-ray diffractions analyses. For instance, crystallization of mixture consisting of the starting salt **3.1**<sup>4+</sup>•4BF<sub>4</sub><sup>-</sup> and (TBA)<sub>3</sub>HP<sub>2</sub>O<sub>7</sub> in methanol via the slow diffusion of diethyl ether afforded crystals of **3.1**<sup>4+</sup>•HP<sub>2</sub>O<sub>7</sub><sup>3-</sup>•BF<sub>4</sub><sup>-</sup>. The resulting structure confirmed that in this mixed salt the receptor/pyrophosphate anion ratio was 1:1 (Figure 3.5). It also revealed that the macrocycle adopts a folded conformation, forming a clip-like slot into which the pyrophosphate anion inserts. The BF<sub>4</sub><sup>-</sup> anion resides outside of the cavity. All the pyrrole NH, triazolium CH and endocyclic benzene CH protons point into the center of the ring and are involved in hydrogen bonding interactions with the bound pyrophosphate guest, as inferred from bond distances (pyrrole NH...O approx. 1.9 Å, triazolium CH...O approx. 2.0 Å, benzene CH...O approx. 3.4 Å). The resulting conformation thus stands in contrast to what is seen in the case of the starting host, **3.1**<sup>4+</sup>•4BF<sub>4</sub><sup>-</sup>.

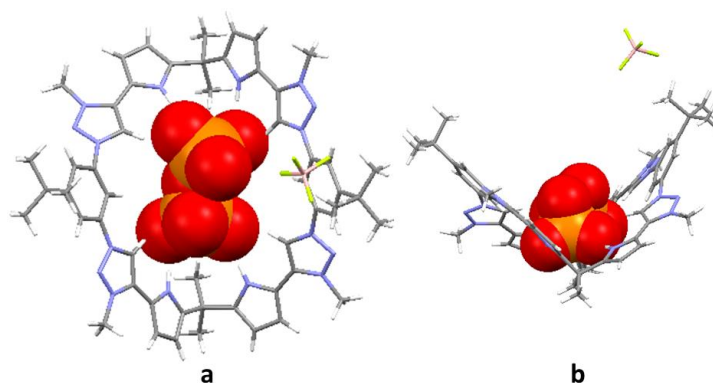


**Figure 3.5:** (a) Top and (b) side views of a single-crystal X-ray diffraction structure of **3.1**<sup>4+</sup>•HP<sub>2</sub>O<sub>7</sub><sup>3-</sup>•BF<sub>4</sub><sup>-</sup> in which the pyrophosphate anion is in a space filling representation and the tetrafluoroborate anion resides outside of the ring.

The addition of tetrabutylammonium dihydrogen phosphate (TBAH<sub>2</sub>PO<sub>4</sub>) to a methanolic solution of **3.1**<sup>4+</sup>•4BF<sub>4</sub><sup>-</sup> and subjecting it to crystallization via diffusion of

diethyl ether resulted in the isolation of single crystals of a complex with a formal stoichiometry  $2(\mathbf{3.1}^{4+}) \cdot 2\text{H}_2\text{PO}_4^- \cdot 6\text{BF}_4^-$ . The resulting structure is shown in Figure 3.6. It includes two complex salts; the first of these consists of  $\mathbf{3.1}^{4+} \cdot 2\text{H}_2\text{PO}_4^- \cdot 2\text{BF}_4^-$ , whereas the latter consists of  $\mathbf{3.1}^{4+} \cdot 4\text{BF}_4^-$  (Figure 3.6a). The structure of  $\mathbf{3.1}^{4+} \cdot 2\text{H}_2\text{PO}_4^- \cdot 2\text{BF}_4^-$  displays the same folded conformation as observed in the case of  $\mathbf{3.1}^{4+} \cdot \text{HP}_2\text{O}_7^{3-} \cdot \text{BF}_4^-$ , with two phosphate anions located in the center of the ring (Figure 3.6b, c). However, in contrast to this latter structure in  $\mathbf{3.1}^{4+} \cdot 2\text{H}_2\text{PO}_4^- \cdot 2\text{BF}_4^-$ , the pyrrole NH (N4, N5) and triazolium CH (C11, C25) protons point away from the center of the ring. N–H $\cdots$ O and C–H $\cdots$ O hydrogen bonds are formed between the macrocycle and phosphate anions (the pyrrole NH $\cdots$ O distance is approx. 2.1 Å; the triazolium CH $\cdots$ O distance is approx. 2.8 Å; the endocyclic benzene CH $\cdots$ O distance is approx. 2.6 Å).

Another  $\mathbf{3.1}^{4+} \cdot 4\text{BF}_4^-$  salt within the mixed complex (Figure 3.6d, e) shows a similar planar conformation as the structure of  $\mathbf{3.1}^{4+} \cdot 4\text{BF}_4^-$  shown in Figure 3.1. However, in the present instance all the pyrrole groups, triazolium motifs and benzene rings are twisted out of the mean macrocyclic plane. As a result, the associated NH, triazolium CH and endocyclic benzene CH protons point away from the center of the ring. Two  $\text{BF}_4^-$  anions are found to be located closely above and below the plane of the ring, presumably as the result of hydrogen bond interactions with the pyrrole NH (N20, N20A) and triazolium CH (C62, C62A) protons. The relevant pyrrole NH $\cdots$ F and triazolium CH $\cdots$ F distances are *ca.* 2.1 Å and 2.7 Å, respectively). Another pair of  $\text{BF}_4^-$  ions is located outside of the ring.

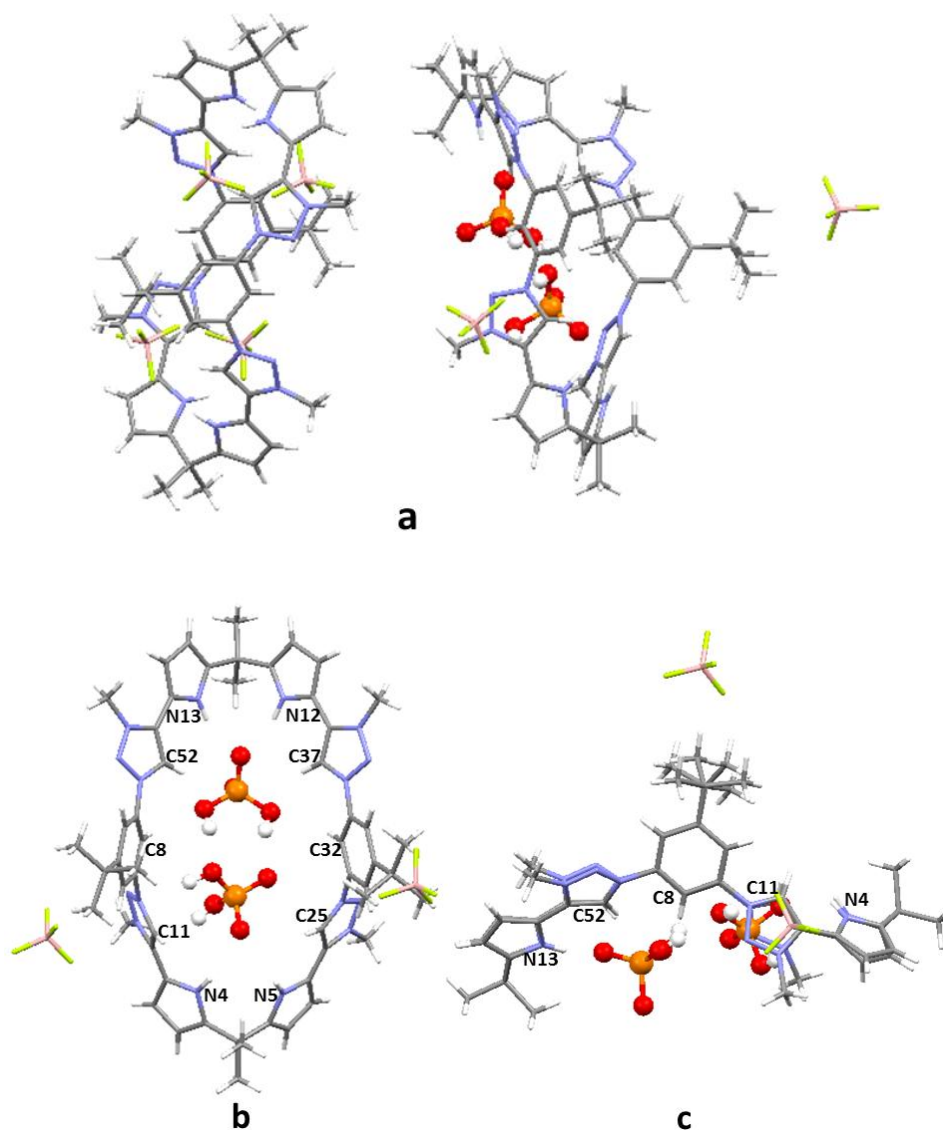
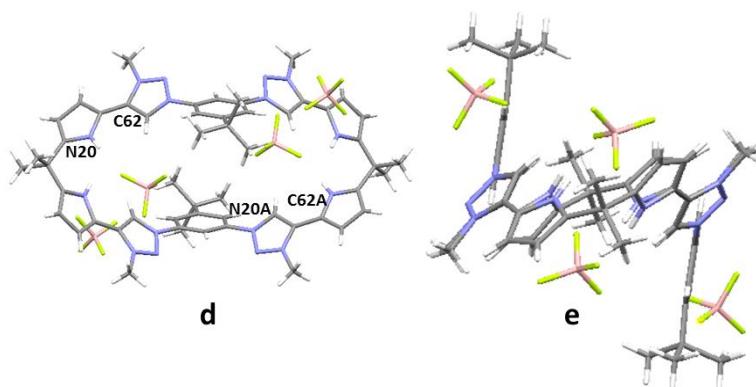


**Figure 3.6:** (a) A single-crystal X-ray diffraction structure of  $2(\mathbf{3.1}^{4+}) \cdot 2\text{H}_2\text{PO}_4^- \cdot 6\text{BF}_4^-$  which contains two parts: one composed of  $\mathbf{3.1}^{4+} \cdot 2\text{H}_2\text{PO}_4^- \cdot 2\text{BF}_4^-$  and the other composed of the free receptor  $\mathbf{3.1}^{4+} \cdot 4\text{BF}_4^-$ . (b) Top and (c) side views of a single-crystal X-ray diffraction structure of  $\mathbf{3.1}^{4+} \cdot 2\text{H}_2\text{PO}_4^- \cdot 2\text{BF}_4^-$  with two phosphate anions located in the center of the ring, which is part of the structure of  $2(\mathbf{3.1}^{4+}) \cdot 2\text{H}_2\text{PO}_4^- \cdot 6\text{BF}_4^-$ . (d) Top and (e) side views of a single-crystal X-ray diffraction structure of  $\mathbf{3.1}^{4+} \cdot 4\text{BF}_4^-$ , which is part of the structure of  $2(\mathbf{3.1}^{4+}) \cdot 2\text{H}_2\text{PO}_4^- \cdot 6\text{BF}_4^-$ .

**Figure 3.6, cont.**



### 3.3 CONCLUSIONS

In summary, the pyrrole-based triazolium-phane **3.1**<sup>4+</sup>•4BF<sub>4</sub><sup>-</sup> has been prepared via the tetraalkylation of a macrocycle originally prepared via click chemistry. It displays a high selectivity for tetrahedral oxyanions relative to various test monoanions and trigonal planar anions in mixed polar organic–aqueous solvent media. This selectivity is solvent dependent and is less pronounced in acetonitrile. Single crystal X-ray diffraction analyses of the mixed salts **3.1**<sup>4+</sup>•HP<sub>2</sub>O<sub>7</sub><sup>3-</sup>•BF<sub>4</sub><sup>-</sup> and 2(**3.1**<sup>4+</sup>)•2H<sub>2</sub>PO<sub>4</sub><sup>-</sup>•6BF<sub>4</sub><sup>-</sup> provided support for the notion that receptor **3.1**<sup>4+</sup> can bind the pyrophosphate and phosphate anions. The present results thus serve to underscore the benefits of combining various hydrogen bond donor motifs within a single receptor to achieve the recognition of particular anionic substrates. The fact that the motifs in question are contained within a relatively rigid macrocyclic framework in the case of **3.1**<sup>4+</sup> allowed for a direct comparison of the relative importance of NH–, CH–, and (CH)<sup>+</sup>–anion interactions. The associated results, both experimental and theoretical, provided support for the perhaps unexpected conclusion that (CH)<sup>+</sup>– anion interactions are less important in an energetic sense than neutral CH–anion interactions in methanol. These findings have important

implications for future receptor design, particularly systems designed to recognize anions in highly polar organic media or aqueous environments.

### 3.4 EXPERIMENTAL SECTION

#### 3.4.1 General Procedures

All reagents and starting materials were obtained from commercial suppliers and used as received unless otherwise noted. Column chromatography was performed on silica gel (40-63  $\mu\text{m}$ , Silicycle, Canada) and Alumina N (50-200  $\mu\text{m}$ , Dynamic Adsorbents Inc., USA). Nuclear magnetic resonance (NMR) spectra were recorded on Varian Mercury 400, Varian Inova 500, and Varian DirectDrive 600 instruments. UV-Vis spectra were recorded on a Cary 5000 UV-Vis-NIR Spectrophotometer. Low resolution ESI mass spectra were measured using either a Finnigan LCQ Quadrupole Ion Trap Mass Spectrometer or a Thermo LTQ-XL linear Ion Trap Mass Spectrometer. High resolution ESI mass spectra were obtained on an Ion Spec Fourier Transform mass spectrometer (9.4 T). PH value was detected by an Orion Model 720A pH meter. Unless otherwise noted, a pH of 7.2 was recorded for the mixed solvent mixture (5 mM HEPES buffer in 60% water/acetone) used to study the macrocycle (**3.1**<sup>4+</sup>·4BF<sub>4</sub><sup>-</sup>;  $5.0 \times 10^{-2}$  mM).

#### 3.4.2 Synthetic Experimental

**Calix[2]1,3-bis(pyrro-2-yl)(1,4)-3-methyl-5*H*-1,2,3-triazolium-phane tetrafluoroborate** [**3.1**<sup>4+</sup>·4BF<sub>4</sub><sup>-</sup>]: Calix[2]1,3-bis(pyrro-2-yl)(1,4)-1,2,3-triazolo-phane (200 mg, 0.228 mmol) and trimethyloxonium tetrafluoroborate (142 mg, 0.960 mmol)

were placed in a 100 mL three-way round bottom flask under nitrogen protection. Then 30 mL dry and degassed dichloromethane was added into the flask by syringe. The resulting solution was stirred for 3 days at room temperature under nitrogen. Methanol (5 mL) was added into the flask and the solution was stirred for 10 mins. Evaporation of the reaction mixture afforded a brown solid. This brown solid was purified by column chromatography (silica gel, CH<sub>2</sub>Cl<sub>2</sub> : CH<sub>3</sub>OH, 10 : 0.8, eluent) and then followed by recrystallization from DMF and ether to give 112 mg (38%, 0.087 mmol) of [**3.1**<sup>4+</sup>·4BF<sub>4</sub><sup>-</sup>] as a white solid. <sup>1</sup>H NMR (DMF-*d*<sub>7</sub>, 400 MHz) [ppm], δ 11.80 (s, 4 H, NH), 9.35 (s, 4 H, -N-CH=C-), 8.45 (d, *J*=2.4 Hz, 4 H, CH), 8.14 (m, 2 H, CH), 7.13 (m, 4 H, pyrrole-β-H), 6.54 (m, 4 H, pyrrole-β-H), 4.68 (s, 12 H, CH<sub>3</sub>), 1.79 (s, 12 H, CH<sub>3</sub>), 1.45 (s, 18 H, CH<sub>3</sub>); <sup>13</sup>C-NMR (CD<sub>3</sub>OD, 100 MHz) [ppm], δ 163.4, 157.3, 144.9, 137.6, 136.1, 122.1, 113.7, 112.4, 107.7, 38.8, 36.1, 35.5, 30.2, 29.7, 28.5; MS (HR-ESI) Calcd. for C<sub>54</sub>H<sub>64</sub>B<sub>3</sub>N<sub>16</sub>F<sub>12</sub> (M-BF<sub>4</sub><sup>-</sup>) 1197.5582; Found 1197.5600 (M-BF<sub>4</sub><sup>-</sup>).

### 3.4.3 Details of Fitting the UV-Vis Binding Curves

#### UV-Vis Anion Recognition Study:

Stock solutions of the host molecule being studied were made up in acetonitrile with the final concentrations being  $1 \times 10^{-5}$  M. Stock solutions of the guest in question were prepared by dissolving 100 - 500 equivalents of the tetrabutylammonium salts of the anions under study in 2 mL stock solutions of the host. Making up the anion source solutions in this way allowed the binding studies to be carried out without having to make mathematical corrections to account for changes in host concentration as the result of dilution effects.



Stock solutions of the host molecule being studied were made up in methanol with the final concentrations being  $1 \times 10^{-5}$  M. Stock solutions of the guest in question were prepared by dissolving 100 - 20000 equivalents of the tetrabutylammonium salts of the anions under study in 2 mL stock solutions of the host. Making up the anion source solutions in this way allowed the binding studies to be carried out without having to make mathematical corrections to account for changes in host concentration as the result of dilution effects.

Stock solutions of the host molecule being studied were made up in 60% water/acetone (pH 7.2 with 5mM HEPES buffer) with the final concentrations being  $5 \times 10^{-5}$  M. Stock solutions of the guest in question were prepared by dissolving 100 - 2000 equivalents of the tetrabutylammonium salts of the anions under study in 2 mL stock solutions of the host. Making up the anion source solutions in this way allowed the binding studies to be carried out without having to make mathematical corrections to account for changes in host concentration as the result of dilution effects.

The general procedure for the UV-Vis binding studies involved making sequential additions of titrant (anionic guest) using Hamilton pipettes to a 3 mL aliquot of the host stock solution in a spectrometric cell. The data was then collated and combined to produce plots that showed the changes in host spectral features as a function of guest concentration.

#### **Job Plot Construction:**

Stock solutions of the macrocycle [**3.1**<sup>4+</sup>·4BF<sub>4</sub><sup>-</sup>] ( $1.0 \times 10^{-5}$  M) and the tetrabutylammonium anion salts ( $1.0 \times 10^{-5}$  M) were prepared separately in acetonitrile. The UV-Vis spectrum was taken for each of 13 different solutions containing a total of 3.0 mL of the macrocycle [**3.1**<sup>4+</sup>·4BF<sub>4</sub><sup>-</sup>] and tetrabutylammonium salt in the following

ratios: 3.0:0, 2.7:0.3, 2.4:0.6, 2.25:0.75, 2.0:1.0, 1.8:1.2, 1.5:1.5, 1.2:1.8, 1.0:2.0, 0.75:2.25, 0.6:2.4, 0.3:2.7 and 0:3.0. Job's plots were constructed by plotting  $A_{\text{obs}} - A_{\text{M}} - A_{\text{anion}}$  against the  $\gamma$ -coordinate. ( $\gamma = [\text{host}] / ([\text{host}] + [\text{guest}])$ )

Stock solutions of the macrocycle [**3.1**<sup>4+</sup>·4BF<sub>4</sub><sup>-</sup>] ( $1.0 \times 10^{-5}$  M) and the tetrabutylammonium anion salts ( $1.0 \times 10^{-5}$  M) were prepared separately in methanol. The UV-Vis spectrum was taken for each of 13 different solutions containing a total of 3.0 mL of the macrocycle [**3.1**<sup>4+</sup>·4BF<sub>4</sub><sup>-</sup>] and tetrabutylammonium salt in the following ratios: 3.0:0, 2.7:0.3, 2.4:0.6, 2.25:0.75, 2.0:1.0, 1.8:1.2, 1.5:1.5, 1.2:1.8, 1.0:2.0, 0.75:2.25, 0.6:2.4, 0.3:2.7 and 0:3.0. Job's plots were constructed by plotting  $A_{\text{obs}} - A_{\text{M}} - A_{\text{anion}}$  against the  $\gamma$ -coordinate. ( $\gamma = [\text{host}] / ([\text{host}] + [\text{guest}])$ )

Stock solutions of the macrocycle [**3.1**<sup>4+</sup>·4BF<sub>4</sub><sup>-</sup>] ( $5.0 \times 10^{-5}$  M) and the tetrabutylammonium anion salts ( $5.0 \times 10^{-5}$  M) were prepared separately in 60% water/acetone (pH 7.2 with 5 mM HEPES buffer). The UV-Vis spectrum was taken for each of 13 different solutions containing a total of 3.0 mL of the macrocycle [**3.1**<sup>4+</sup>·4BF<sub>4</sub><sup>-</sup>] and tetrabutylammonium salt in the following ratios: 3.0:0, 2.7:0.3, 2.4:0.6, 2.25:0.75, 2.0:1.0, 1.8:1.2, 1.5:1.5, 1.2:1.8, 1.0:2.0, 0.75:2.25, 0.6:2.4, 0.3:2.7 and 0:3.0. Job's plots were constructed by plotting  $A_{\text{obs}} - A_{\text{M}} - A_{\text{anion}}$  against the  $\gamma$ -coordinate. ( $\gamma = [\text{host}] / ([\text{host}] + [\text{guest}])$ )

### Calculations of Equilibrium Constants, $K_a$

Upon addition of tetrabutylammonium salts, the UV-Vis spectra changed gradually. These changes were ascribed to anion binding, with the corresponding association constants ( $K_a$ ,  $K_{a1}$ ,  $K_{a2}$ ) being determined by nonlinear curve fitting of the curves obtained by plotting the absorbance changes at a  $\lambda$  value where the spectral

change was maximal ( $\Delta A$ ) against the concentration of the tetrabutylammonium anion salt added,  $[X^-]$ . The data was fitted to the equation,

1:1 binding:

$$\Delta A = A \cdot \{([3.1^{4+} \cdot 4BF_4^-] + [X^-] + (1/K_a)) - \{([3.1^{4+} \cdot 4BF_4^-] + [X^-] + (1/K_a))^2 - (4 \cdot [3.1^{4+} \cdot 4BF_4^-] \cdot [X^-])\}^{1/2}\} / (2 \cdot [3.1^{4+} \cdot 4BF_4^-])$$

1:2 binding:

$$\Delta A = (A1 \cdot [3.1^{4+} \cdot 4BF_4^-] \cdot K_{a1} \cdot [X^-] + A2 \cdot [3.1^{4+} \cdot 4BF_4^-] \cdot K_{a1} \cdot K_{a2} \cdot [X^-]^2) / (1 + K_{a1} \cdot [X^-] + K_{a1} \cdot K_{a2} \cdot [X^-]^2)$$

where, the unknown parameters are  $K_a$ ,  $K_{a1}$ ,  $K_{a2}$ , the value of the association constants; these values were obtained by the fit to the data with good fits (e.g.,  $R^2 \geq 0.99$ ) unless noted otherwise.

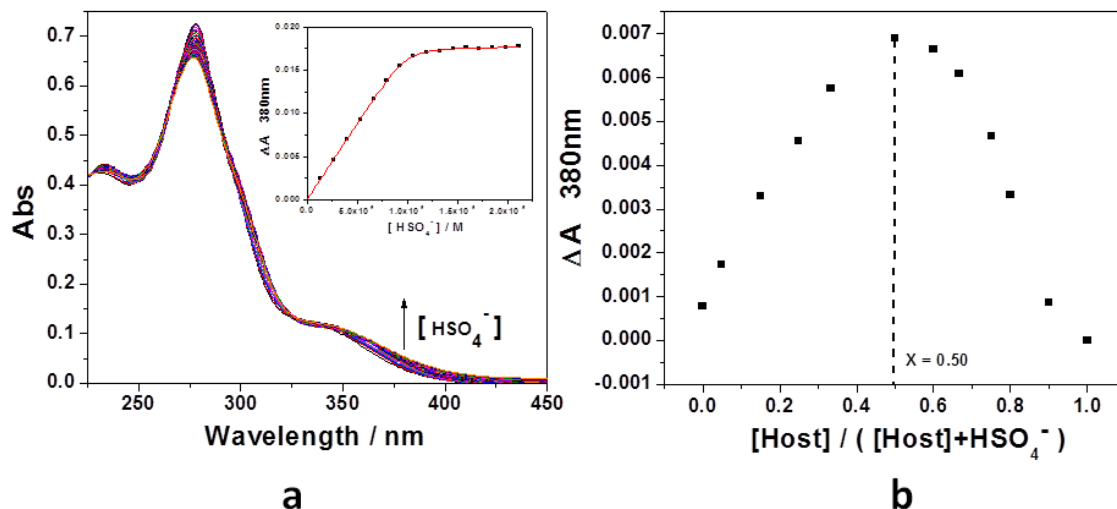


**Figure 3.7:** (a) UV-Vis spectra of  $[3.1^{4+} \cdot 4BF_4^-]$  ( $1.00 \times 10^{-5}$  M) in  $CH_3CN$  with increasing quantities of  $(n-Bu)_4NHSO_4$  ( $0 \sim 2.0 \times 10^{-5}$  M). (b) The job plot corresponding to the complexation between host and  $(n-Bu)_4NHSO_4$  in  $CH_3CN$ .  $[host + guest] = 1.00 \times 10^{-5}$  M. A maximum value at 0.5 is seen; this is consistent with a 1:1(host : guest) binding stoichiometry.

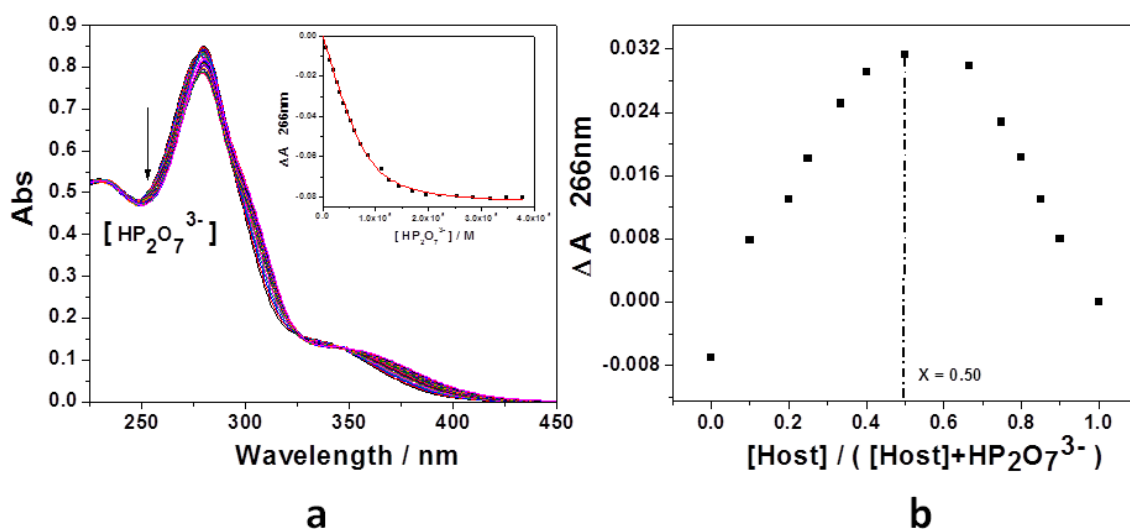


**Figure 3.8:** (a) UV-Vis spectra of  $[3.1^{4+} \cdot 4BF_4^-]$  ( $1.00 \times 10^{-5}$  M) in  $CH_3CN$  with increasing quantities of  $((n-Bu)_4N)_3HP_2O_7$  (0  $\sim$  4.0  $\times 10^{-5}$  M). (b) The job plot corresponding to the complexation between host and  $((n-Bu)_4N)_3HP_2O_7$  in  $CH_3CN$ .  $[host + guest] = 1.00 \times 10^{-5}$  M. A maximum value at 0.5 is seen; this is consistent with a 1:1 (host : guest) binding stoichiometry.

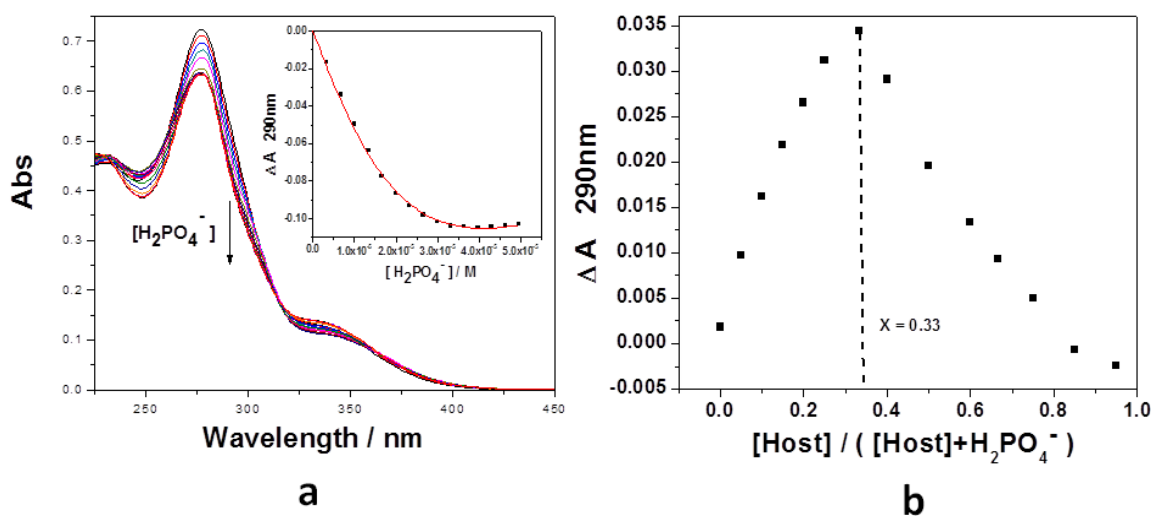


**Figure 3.9:** (a) UV-Vis spectra of  $[3.1^{4+} \cdot 4BF_4^-]$  ( $1.00 \times 10^{-5}$  M) in  $CH_3CN$  with increasing quantities of  $(n-Bu)_4NH_2PO_4$  (0  $\sim$  1.7  $\times 10^{-4}$  M). (b) The job plot corresponding to the complexation between host and  $(n-Bu)_4NH_2PO_4$  in  $CH_3CN$ .  $[host + guest] = 1.00 \times 10^{-5}$  M. A maximum value at 0.33 is seen; this is consistent with a 1:2 (host : guest) binding stoichiometry.

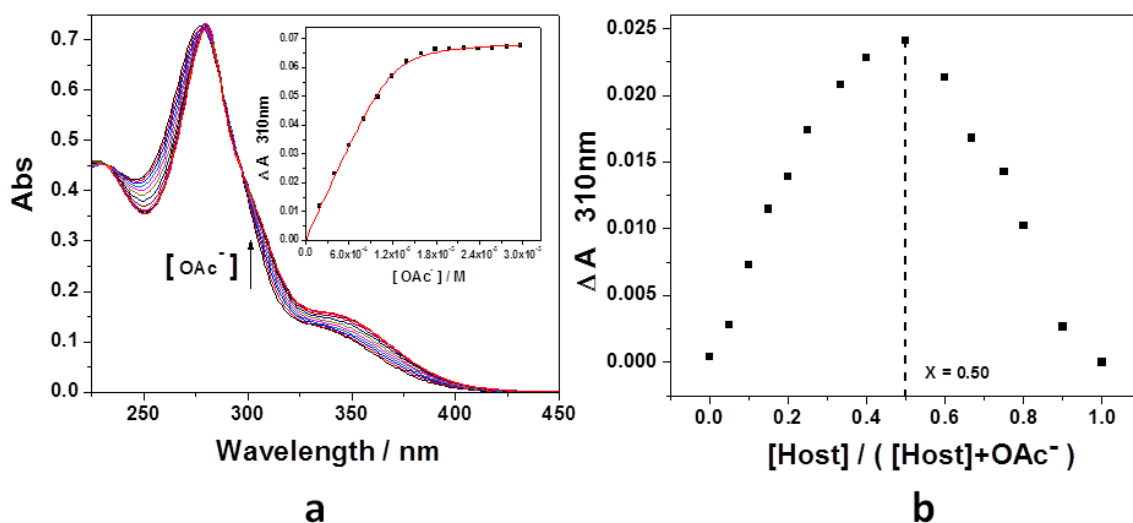


**Figure 3.10:** (a) UV-Vis spectra of  $[3.1^{4+} \cdot 4BF_4^-]$  ( $1.00 \times 10^{-5}$  M) in  $CH_3CN$  with increasing quantities of  $(n-Bu)_4NOAc$  (0  $\sim$   $3.0 \times 10^{-5}$  M). (b) The job plot corresponding to the complexation between host and  $(n-Bu)_4NOAc$  in  $CH_3CN$ .  $[host + guest] = 1.00 \times 10^{-5}$  M. A maximum value at 0.50 is seen; this is consistent with a 1:1 (host: guest) binding stoichiometry.

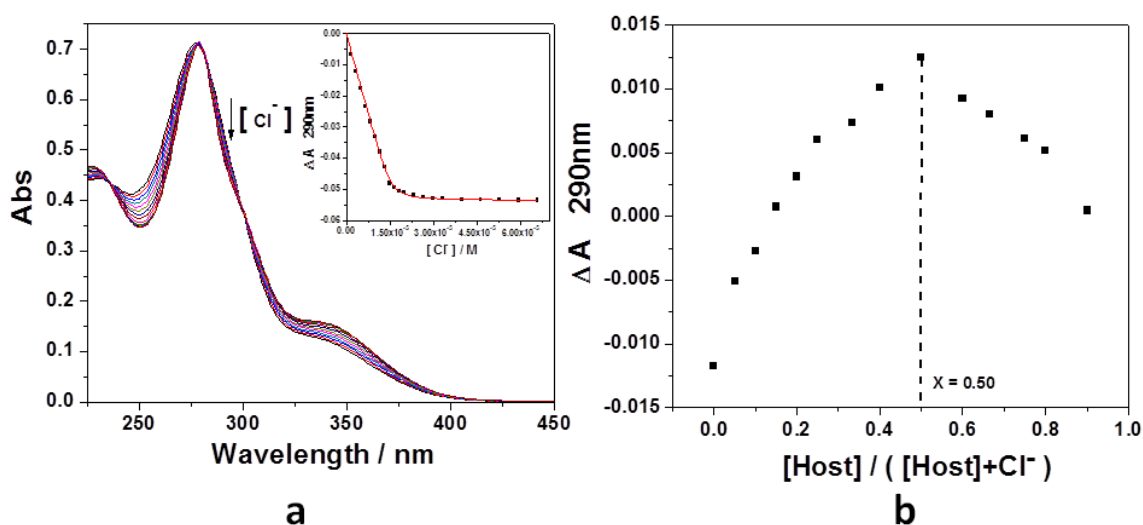


**Figure 3.11:** (a) UV-Vis spectra of  $[3.1^{4+} \cdot 4BF_4^-]$  ( $1.00 \times 10^{-5}$  M) in  $CH_3CN$  with increasing quantities of  $(n-Bu)_4NCl$  (0  $\sim$   $5.0 \times 10^{-5}$  M). (b) The job plot corresponding to the complexation between host and  $(n-Bu)_4NCl$  in  $CH_3CN$ .  $[host + guest] = 1.00 \times 10^{-5}$  M. A maximum value at 0.50 is seen; this is consistent with a 1:1 (host : guest) binding stoichiometry.

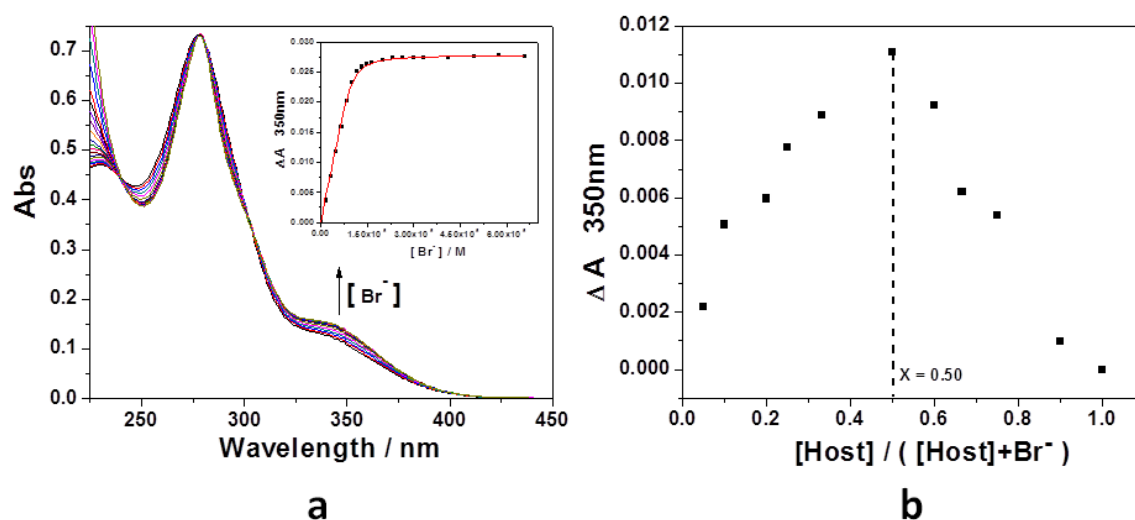


**Figure 3.12:** (a) UV-Vis spectra of  $[3.1]^{4+} \cdot 4BF_4^-$  ( $1.00 \times 10^{-5}$  M) in  $CH_3CN$  with increasing quantities of  $(n-Bu)_4NBr$  ( $0 \sim 1.5 \times 10^{-4}$  M). (b) The job plot corresponding to the complexation between host and  $(n-Bu)_4NBr$  in  $CH_3CN$ .  $[host + guest] = 1.00 \times 10^{-5}$  M. A maximum value at 0.50 is seen; this is consistent with a 1:1 (host : guest) binding stoichiometry.

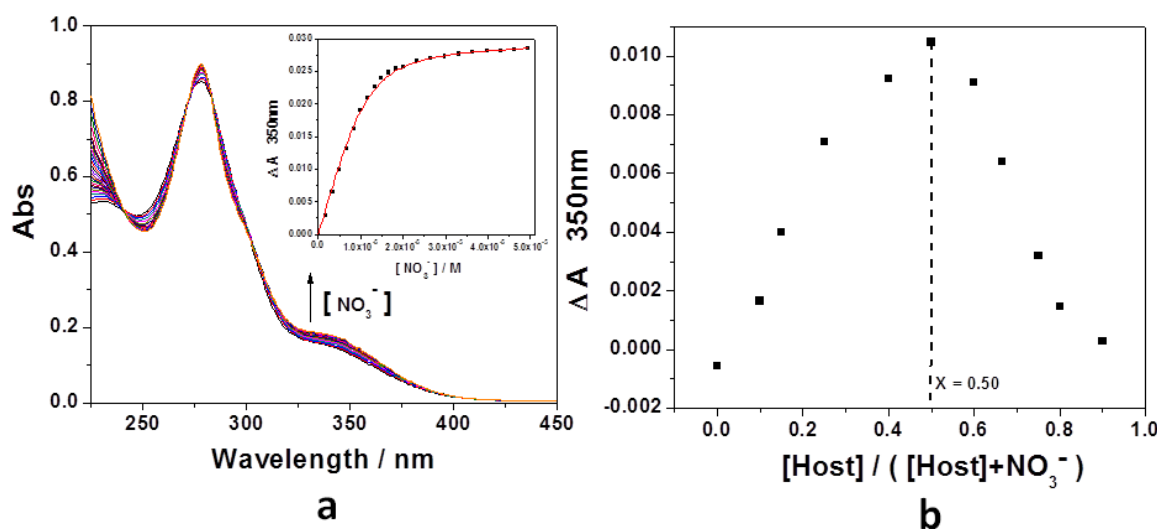


**Figure 3.13:** (a) UV-Vis spectra of  $[3.1]^{4+} \cdot 4BF_4^-$  ( $1.00 \times 10^{-5}$  M) in  $CH_3CN$  with increasing quantities of  $(n-Bu)_4NNO_3$  ( $0 \sim 5.0 \times 10^{-5}$  M). (b) The job plot corresponding to the complexation between host and  $(n-Bu)_4NNO_3$  in  $CH_3CN$ .  $[host + guest] = 1.00 \times 10^{-5}$  M. A maximum value at 0.5 is seen; this is consistent with a 1:1 (host : guest) binding stoichiometry.

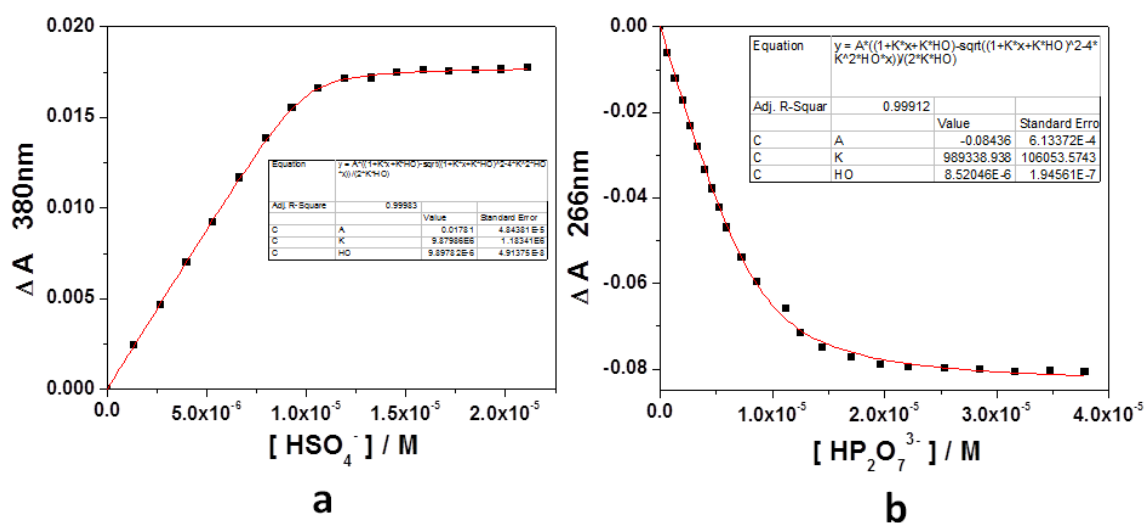
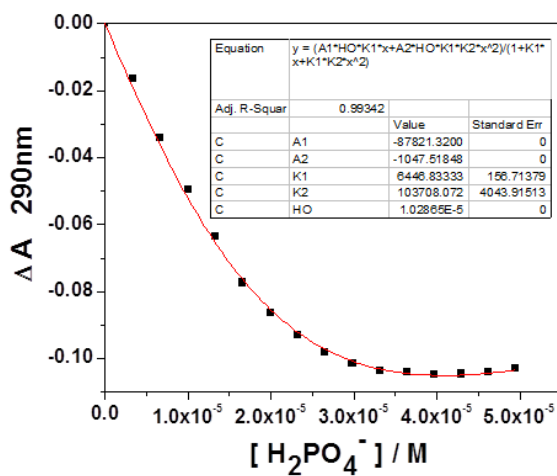
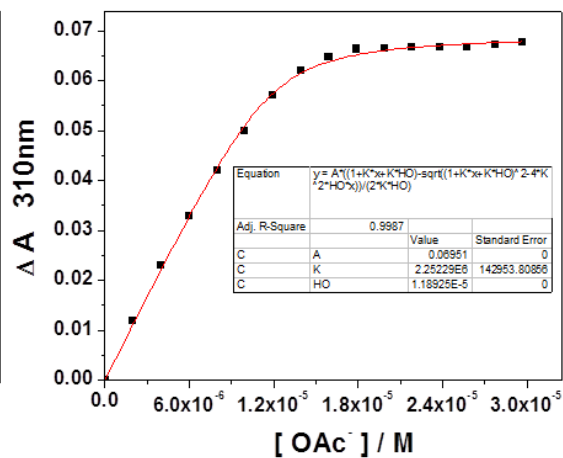


**Figure 3.14:** (a) Variations in the absorbance at 380 nm (▪) of a solution of receptor  $[3.1^{4+} \cdot 4BF_4^-]$  ( $1.00 \times 10^{-5}$  M) in  $CH_3CN$  as a function of TBAHSO<sub>4</sub> concentration ( $0 \sim 2.0 \times 10^{-5}$  M) at 300 K. (b) Variations in the absorbance (▪) at 266 nm of a solution of receptor  $[3.1^{4+} \cdot 4BF_4^-]$  ( $1.00 \times 10^{-5}$  M) in  $CH_3CN$  as a function of TBA<sub>3</sub>HP<sub>2</sub>O<sub>7</sub> concentration ( $0 \sim 4.0 \times 10^{-5}$  M) at 300 K. (c) Variations in the absorbance (▪) at 290 nm of a solution of receptor  $[3.1^{4+} \cdot 4BF_4^-]$  ( $1.00 \times 10^{-5}$  M) in  $CH_3CN$  as a function of TBAH<sub>2</sub>PO<sub>4</sub> concentration ( $0 \sim 5.0 \times 10^{-5}$  M) at 300 K. (d) Variations in the absorbance (▪) at 310 nm of a solution of receptor  $[3.1^{4+} \cdot 4BF_4^-]$  ( $1.00 \times 10^{-5}$  M) in  $CH_3CN$  as a function of TBAOAc concentration ( $0 \sim 3.0 \times 10^{-5}$  M) at 300 K. (e) Variations in the absorbance (▪) at 290 nm of a solution of receptor  $[3.1^{4+} \cdot 4BF_4^-]$  ( $1.00 \times 10^{-5}$  M) in  $CH_3CN$  as a function of TBACl concentration ( $0 \sim 6.0 \times 10^{-5}$  M) at 300 K. (f) Variations in the absorbance (▪) at 350 nm of a solution of receptor  $[3.1^{4+} \cdot 4BF_4^-]$  ( $1.00 \times 10^{-5}$  M) in  $CH_3CN$  as a function of TBABr concentration ( $0 \sim 6.0 \times 10^{-5}$  M) at 300 K. (g) Variations in the absorbance (▪) at 350 nm of a solution of receptor  $[3.1^{4+} \cdot 4BF_4^-]$  ( $1.00 \times 10^{-5}$  M) in  $CH_3CN$  as a function of TBANO<sub>3</sub> concentration ( $0 \sim 5.0 \times 10^{-5}$  M) at 300 K.

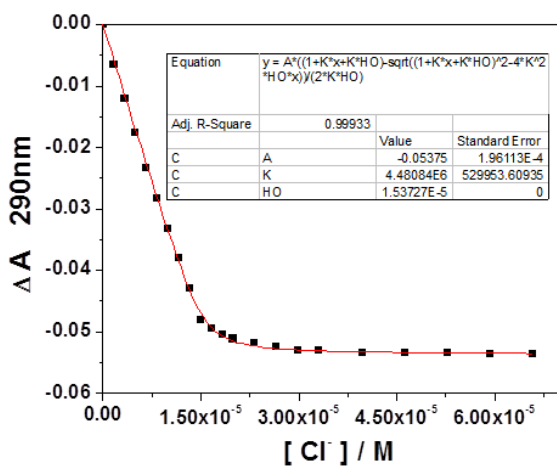
Figure 3.14, cont.



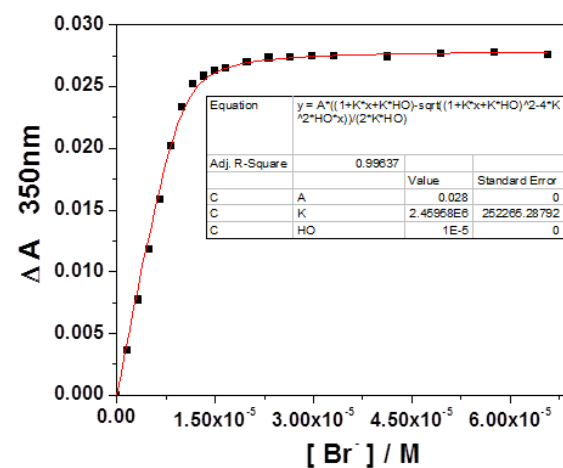
c



d



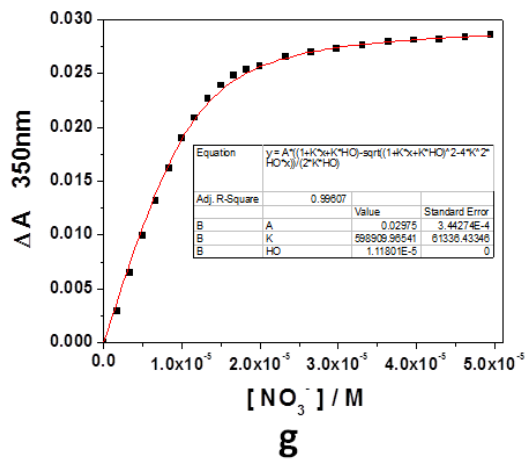
e



f

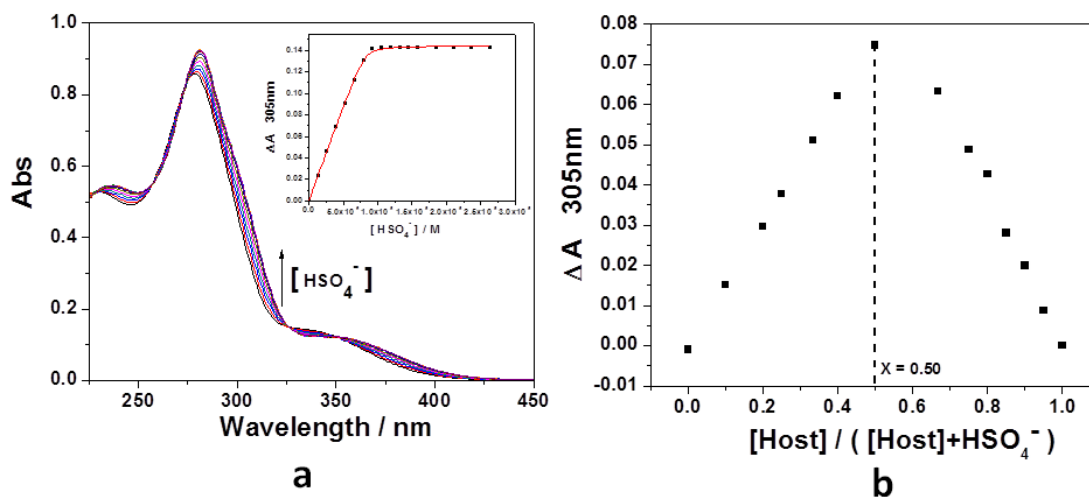


Figure 3.14, cont.



**Table 3.3:** Anion binding constants ( $K_a$ ;  $M^{-1}$ ) for the interaction of anion receptor  $[3.1^{4+} \cdot 4BF_4^-]$  with different anions in  $CH_3CN$  at 300K.

Guest	Stoichiometric ratio Host / Guest	$K_{a,1}$ , $K_{a,2}$
$HSO_4^-$	1:1	$K_a = (9.88 \pm 1.18) \times 10^6 M^{-1}$
$HP_2O_7^{3-}$	1:1	$K_a = (9.89 \pm 1.06) \times 10^5 M^{-1}$
$H_2PO_4^-$	1:2	$K_{a,1} = (6.44 \pm 0.16) \times 10^3 M^{-1}$ $K_{a,2} = (1.03 \pm 0.04) \times 10^5 M^{-1}$
$CH_3COO^-$	1:1	$K_a = (2.25 \pm 0.14) \times 10^6 M^{-1}$
$NO_3^-$	1:1	$K_a = (5.99 \pm 0.61) \times 10^5 M^{-1}$
$Cl^-$	1:1	$K_a = (4.48 \pm 0.53) \times 10^6 M^{-1}$
$Br^-$	1:1	$K_a = (2.46 \pm 0.25) \times 10^6 M^{-1}$



**Figure 3.15:** (a) UV-Vis spectra of  $[3.1^{4+} \cdot 4BF_4^-]$  ( $1.00 \times 10^{-5}$  M) in  $CH_3OH$  with increasing quantities of  $(n-Bu)_4NHSO_4$  ( $0 \sim 3.0 \times 10^{-5}$  M). (b) The job plot corresponding to the complexation between host and  $(n-Bu)_4NHSO_4$  in  $CH_3OH$ .  $[host + guest] = 1.00 \times 10^{-5}$  M. A maximum value at 0.5 is seen; this is consistent with a 1:1 (host : guest) binding stoichiometry.

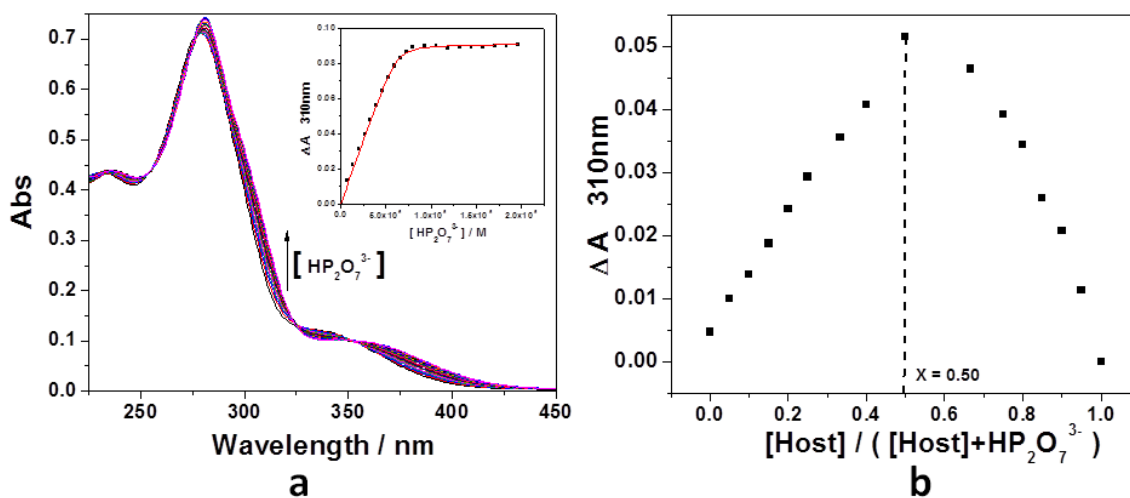


**Figure 3.16:** (a) UV-Vis spectra of  $[3.1^{4+} \cdot 4BF_4^-]$  ( $1.00 \times 10^{-5}$  M) in  $CH_3OH$  with increasing quantities of  $((n-Bu)_4N)_3HP_2O_7$  ( $0 \sim 2.0 \times 10^{-5}$  M). (b) The job plot corresponding to the complexation between host and  $((n-Bu)_4N)_3HP_2O_7$  in  $CH_3OH$ .  $[host + guest] = 1.00 \times 10^{-5}$  M. A maximum value at 0.5 is seen; this is consistent with a 1:1 (host : guest) binding stoichiometry.

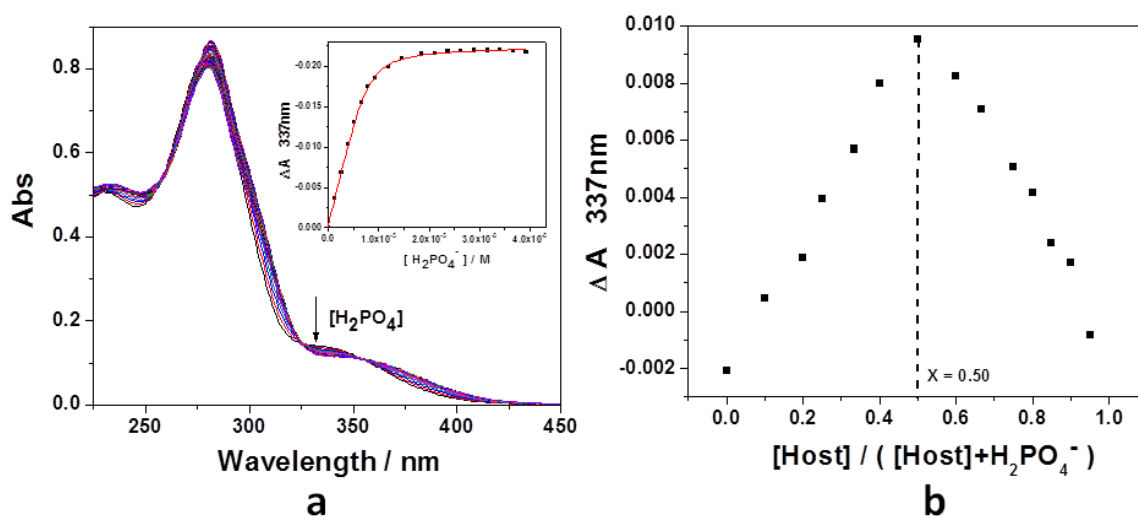


**Figure 3.17:** (a) UV-Vis spectra of  $[3.1^{4+} \cdot 4BF_4^-]$  ( $1.00 \times 10^{-5}$  M) in  $CH_3OH$  with increasing quantities of  $(n-Bu)_4NH_2PO_4$  ( $0 \sim 4.0 \times 10^{-5}$  M). (b) The job plot corresponding to the complexation between host and  $(n-Bu)_4NH_2PO_4$  in  $CH_3OH$ .  $[host + guest] = 1.00 \times 10^{-5}$  M. A maximum value at 0.50 is seen; this is consistent with a 1:1 (host : guest) binding stoichiometry.

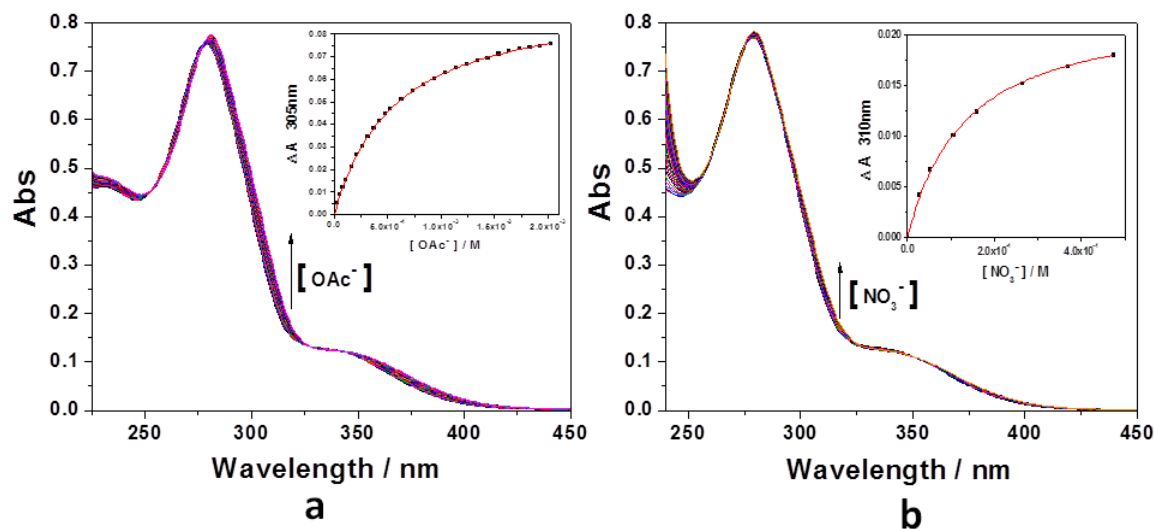


**Figure 3.18:** (a) UV-Vis spectra of  $[3.1^{4+} \cdot 4BF_4^-]$  ( $1.00 \times 10^{-5}$  M) in  $CH_3OH$  with increasing quantities of  $(n-Bu)_4NOAc$  ( $0 \sim 2.0 \times 10^{-3}$  M). (b) UV-Vis spectra of  $[3.1^{4+} \cdot 4BF_4^-]$  ( $1.00 \times 10^{-5}$  M) in  $CH_3OH$  with increasing quantities of  $(n-Bu)_4NNO_3$  ( $0 \sim 9.0 \times 10^{-4}$  M).

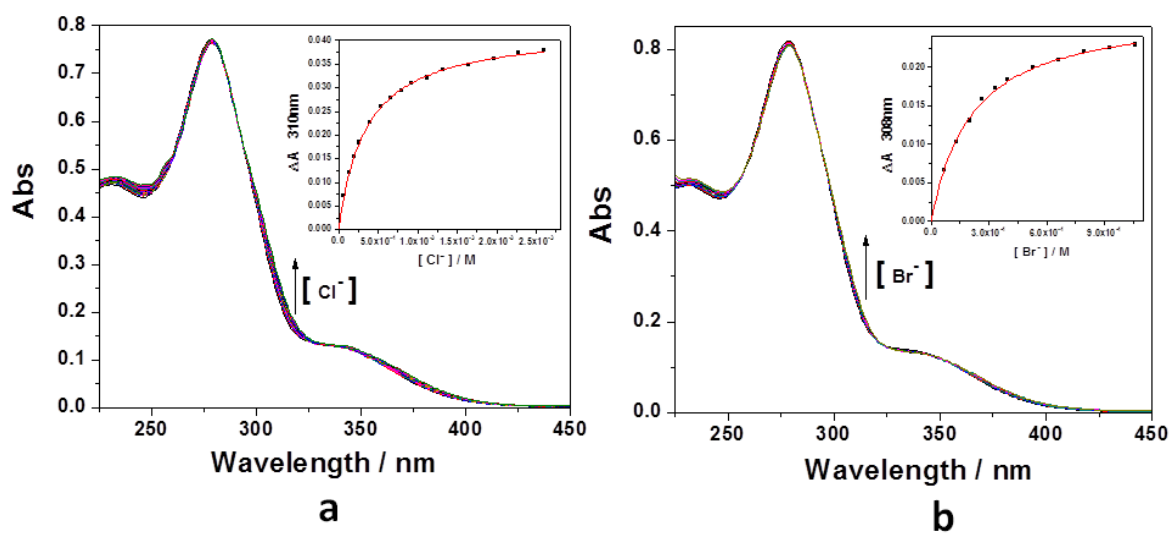


**Figure 3.19:** (a) UV-Vis spectra of  $[3.1^{4+} \cdot 4BF_4^-]$  ( $1.00 \times 10^{-5}$  M) in  $CH_3OH$  with increasing quantities of  $(n-Bu)_4NCl$  ( $0 \sim 2.5 \times 10^{-3}$  M). (b) UV-Vis spectra of  $[3.1^{4+} \cdot 4BF_4^-]$  ( $1.00 \times 10^{-5}$  M) in  $CH_3OH$  with increasing quantities of  $(n-Bu)_4NBr$  ( $0 \sim 1.5 \times 10^{-3}$  M).

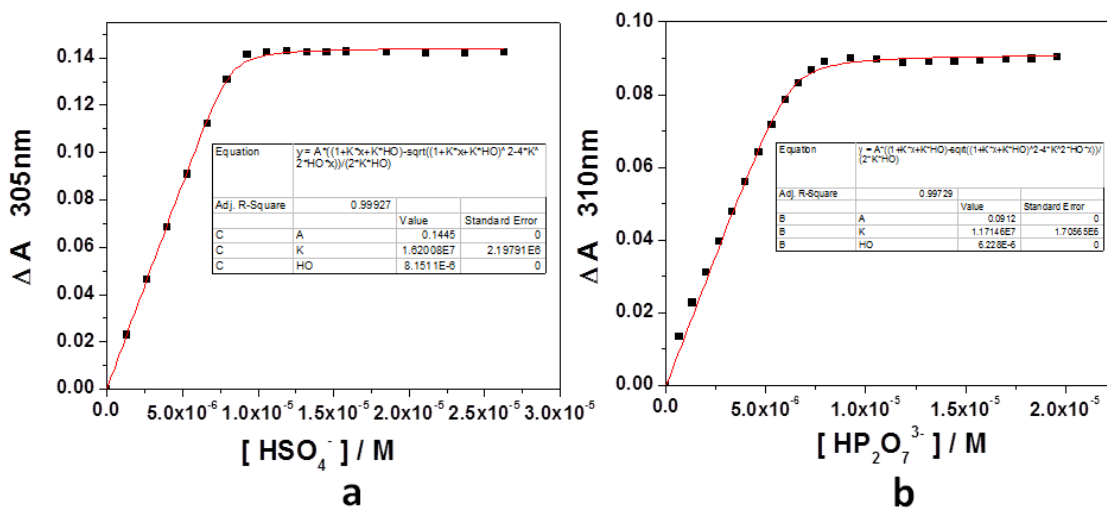
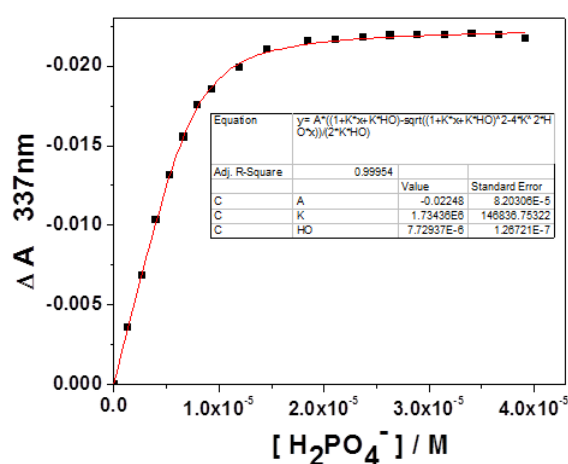
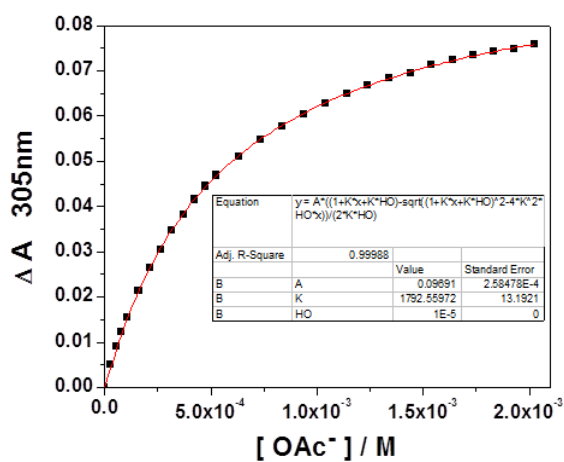


**Figure 3.20:** (a) Variations in the absorbance at 305 nm (▪) of a solution of receptor  $[3.1^{4+} \cdot 4BF_4^-]$  ( $1.00 \times 10^{-5}$  M) in  $CH_3OH$  as a function of TBAHSO<sub>4</sub> concentration ( $0 \sim 3.0 \times 10^{-5}$  M) at 300 K. (b) Variations in the absorbance (▪) at 310 nm of a solution of receptor  $[3.1^{4+} \cdot 4BF_4^-]$  ( $1.00 \times 10^{-5}$  M) in  $CH_3OH$  as a function of TBA<sub>3</sub>HP<sub>2</sub>O<sub>7</sub> concentration ( $0 \sim 2.0 \times 10^{-5}$  M) at 300 K. (c) Variations in the absorbance (▪) at 337 nm of a solution of receptor  $[3.1^{4+} \cdot 4BF_4^-]$  ( $1.00 \times 10^{-5}$  M) in  $CH_3OH$  as a function of TBAH<sub>2</sub>PO<sub>4</sub> concentration ( $0 \sim 4.0 \times 10^{-5}$  M) at 300 K. (d) Variations in the absorbance (▪) at 305 nm of a solution of receptor  $[3.1^{4+} \cdot 4BF_4^-]$  ( $1.00 \times 10^{-5}$  M) in  $CH_3OH$  as a function of TBAOAc concentration ( $0 \sim 2.0 \times 10^{-3}$  M) at 300 K. (e) Variations in the absorbance (▪) at 310 nm of a solution of receptor  $[3.1^{4+} \cdot 4BF_4^-]$  ( $1.00 \times 10^{-5}$  M) in  $CH_3OH$  as a function of TBACl concentration ( $0 \sim 2.5 \times 10^{-3}$  M) at 300 K. (f) Variations in the absorbance (▪) at 308 nm of a solution of receptor  $[3.1^{4+} \cdot 4BF_4^-]$  ( $1.00 \times 10^{-5}$  M) in  $CH_3OH$  as a function of TBABr concentration ( $0 \sim 1.2 \times 10^{-3}$  M) at 300 K. (g) Variations in the absorbance (▪) at 310 nm of a solution of receptor  $[3.1^{4+} \cdot 4BF_4^-]$  ( $1.00 \times 10^{-5}$  M) in  $CH_3OH$  as a function of TBANO<sub>3</sub> concentration ( $0 \sim 5.0 \times 10^{-4}$  M) at 300 K.

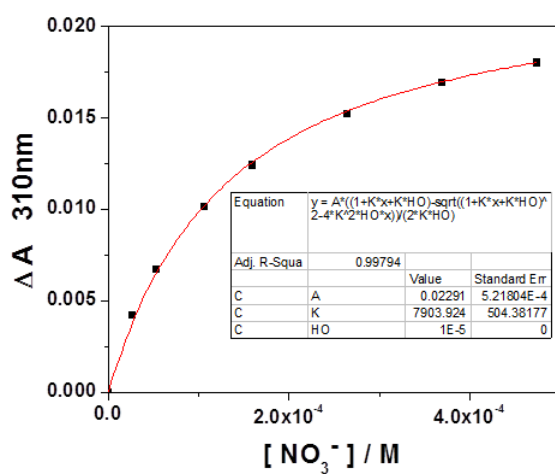
Figure 3.20, cont.



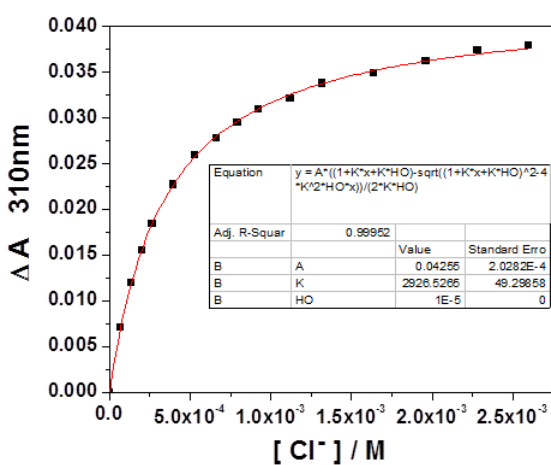
c



d

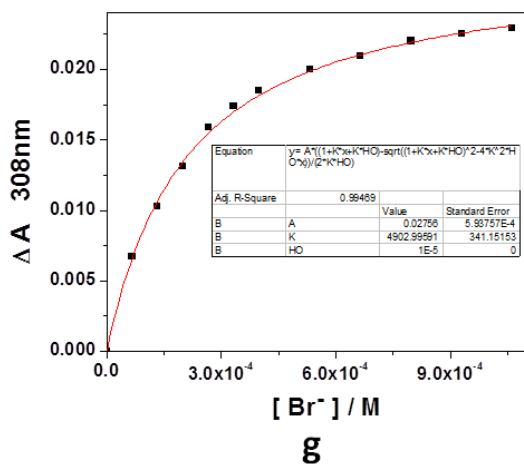


e



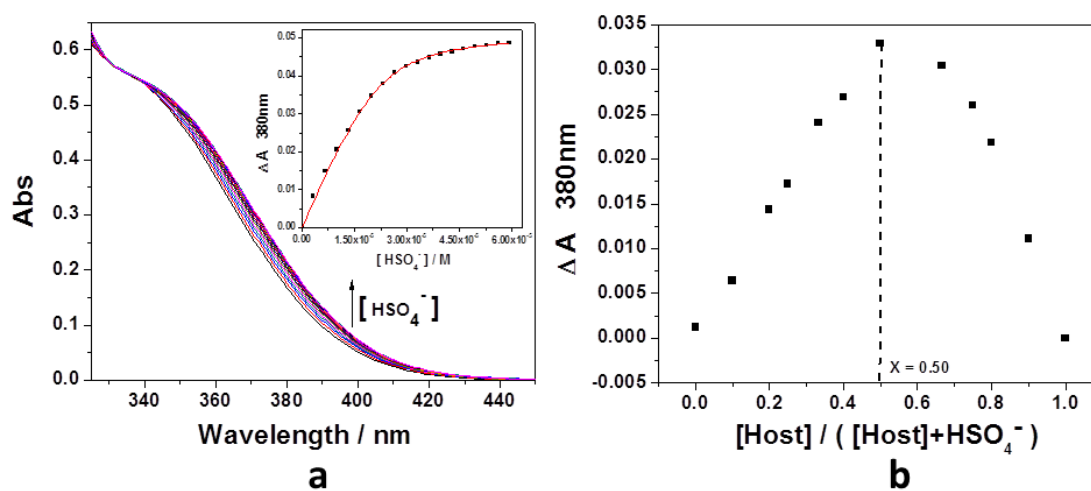
f

Figure 3.20, cont.



**Table 3.4:** Anion binding constants ( $K_a$ ;  $M^{-1}$ ) for the interaction of anion receptor  $[3.1^{4+} \cdot 4BF_4^-]$  with different anions in  $CH_3OH$  at 300K.

Guest	Stoichiometric ratio Host / Guest	$K_a$
$HSO_4^-$	1:1	$K_a = (1.60 \pm 0.22) \times 10^7 M^{-1}$
$HP_2O_7^{3-}$	1:1	$K_a = (1.17 \pm 0.17) \times 10^7 M^{-1}$
$H_2PO_4^-$	1:1	$K_a = (1.73 \pm 0.15) \times 10^6 M^{-1}$
$CH_3COO^-$	1:1	$K_a = (1.79 \pm 0.01) \times 10^3 M^{-1}$
$NO_3^-$	1:1	$K_a = (7.90 \pm 0.50) \times 10^3 M^{-1}$
$Cl^-$	1:1	$K_a = (2.93 \pm 0.05) \times 10^3 M^{-1}$
$Br^-$	1:1	$K_a = (4.90 \pm 0.34) \times 10^3 M^{-1}$



**Figure 3.21:** (a) UV-Vis spectra of  $[3.1]^{4+} \cdot 4\text{BF}_4^-$  ( $5.00 \times 10^{-5}$  M) in acetone-H<sub>2</sub>O (2 : 3) with increasing quantities of (n-Bu)<sub>4</sub>NHSO<sub>4</sub> ( $0 \sim 6.0 \times 10^{-5}$  M). The solution was buffered at pH 7.2 with HEPES buffer ( $5.00 \times 10^{-3}$  M). (b) The job plot corresponding to the complexation between host and (n-Bu)<sub>4</sub>NHSO<sub>4</sub> in acetone-H<sub>2</sub>O (2 : 3). The solution was buffered at pH 7.2 with HEPES buffer ( $5.00 \times 10^{-3}$  M).  $[\text{host} + \text{guest}] = 5.00 \times 10^{-5}$  M. A maximum value at 0.5 is seen; this is consistent with a 1:1 (host : guest) binding stoichiometry.



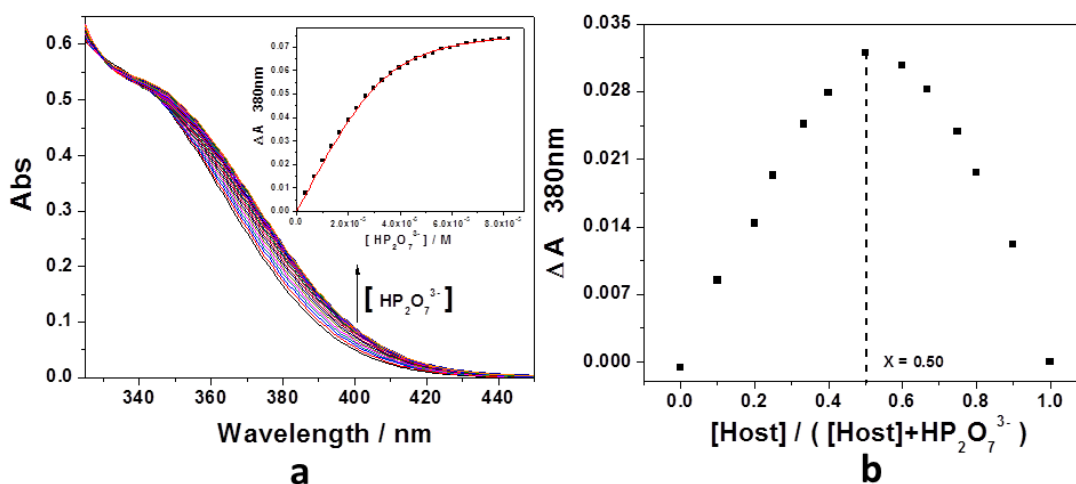


**Figure 3.22:** (a) UV-Vis spectra of  $[3.1]^{4+} \cdot 4BF_4^-$  ( $5.00 \times 10^{-5}$  M) in acetone-H<sub>2</sub>O (2 : 3) with increasing quantities of  $((n-Bu)_4N)_3HP_2O_7$  ( $0 \sim 8.0 \times 10^{-5}$  M). The solution was buffered at pH 7.2 with HEPES buffer ( $5.00 \times 10^{-3}$  M). (b) The job plot corresponding to the complexation between host and  $((n-Bu)_4N)_3HP_2O_7$  in acetone-H<sub>2</sub>O (2 : 3). The solution was buffered at pH 7.2 with HEPES buffer ( $5.00 \times 10^{-3}$  M).  $[host + guest] = 5.00 \times 10^{-5}$  M. A maximum value at 0.5 is seen; this is consistent with a 1:1 (host : guest) binding stoichiometry.

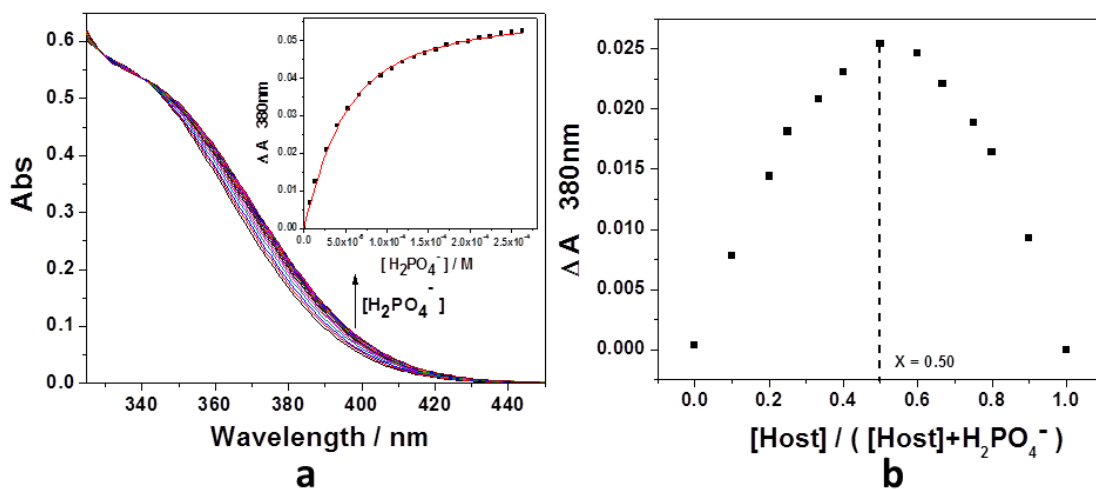


**Figure 3.23:** (a) UV-Vis spectra of  $[3.1]^{4+} \cdot 4BF_4^-$  ( $5.00 \times 10^{-5}$  M) in acetone-H<sub>2</sub>O (2 : 3) with increasing quantities of (n-Bu)<sub>4</sub>NH<sub>2</sub>PO<sub>4</sub> ( $0 \sim 2.5 \times 10^{-4}$  M). The solution was buffered at pH 7.2 with HEPES buffer ( $5.00 \times 10^{-3}$  M). (b) The job plot corresponding to the complexation between host and (n-Bu)<sub>4</sub>NH<sub>2</sub>PO<sub>4</sub> in acetone-H<sub>2</sub>O (2 : 3). The solution was buffered at pH 7.2 with HEPES buffer ( $5.00 \times 10^{-3}$  M). [host + guest] =  $5.00 \times 10^{-5}$  M. A maximum value at 0.50 is seen; this is consistent with a 1:1 (host : guest) binding stoichiometry.

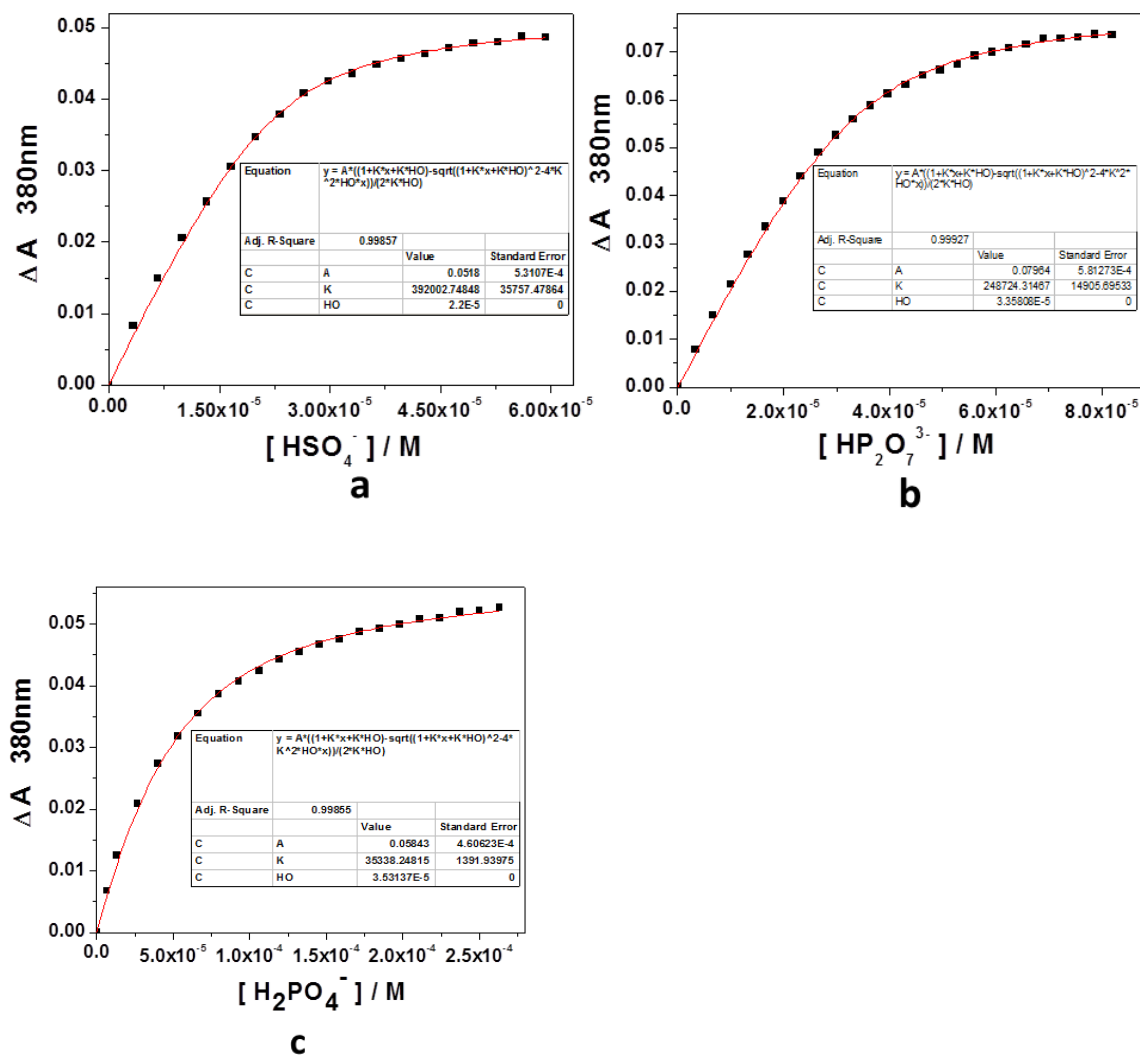


**Figure 3.24:** (a) Variations in the absorbance at 380 nm (▪) of a solution of receptor  $[3.1^{4+} \cdot 4BF_4^-]$  ( $5.00 \times 10^{-5}$  M) in acetone–H<sub>2</sub>O (2 : 3) as a function of TBAHSO<sub>4</sub> concentration ( $0 \sim 6.0 \times 10^{-5}$  M) at 300 K. The solution was buffered at pH 7.2 with HEPES buffer ( $5.00 \times 10^{-3}$  M). (b) Variations in the absorbance (▪) at 380 nm of a solution of receptor  $[3.1^{4+} \cdot 4BF_4^-]$  ( $5.00 \times 10^{-5}$  M) in acetone–H<sub>2</sub>O (2 : 3) as a function of (TBA)<sub>3</sub>HP<sub>2</sub>O<sub>7</sub> concentration ( $0 \sim 8.0 \times 10^{-5}$  M) at 300 K. The solution was buffered at pH 7.2 with HEPES buffer ( $5.00 \times 10^{-3}$  M). (c) Variations in the absorbance (▪) at 380 nm of a solution of receptor  $[3.1^{4+} \cdot 4BF_4^-]$  ( $5.00 \times 10^{-5}$  M) in acetone–H<sub>2</sub>O (2 : 3) as a function of TBAH<sub>2</sub>PO<sub>4</sub> concentration ( $0 \sim 2.5 \times 10^{-4}$  M) at 300 K. The solution was buffered at pH 7.2 with HEPES buffer ( $5.00 \times 10^{-3}$  M).

**Table 3.5:** Anion binding constants ( $K_a$ ;  $M^{-1}$ ) for the interaction of anion receptor  $[3.1^{4+} \cdot 4BF_4^-]$  with different anions in acetone–H<sub>2</sub>O (2 : 3) at 300K. The solution was buffered at pH 7.2 with HEPES buffer ( $5.00 \times 10^{-3}$  M). <sup>a</sup>n.d. = not able to determine.

Guest	Stoichiometric ratio Host / Guest	$K_a$
HSO <sub>4</sub> <sup>-</sup>	1:1	$K_a = (3.92 \pm 0.36) \times 10^5 M^{-1}$
HP <sub>2</sub> O <sub>7</sub> <sup>3-</sup>	1:1	$K_a = (2.49 \pm 0.15) \times 10^5 M^{-1}$
H <sub>2</sub> PO <sub>4</sub> <sup>-</sup>	1:1	$K_a = (3.53 \pm 0.14) \times 10^4 M^{-1}$
CH <sub>3</sub> COO <sup>-</sup>	n.d. <sup>a</sup>	n.d.
NO <sub>3</sub> <sup>-</sup>	n.d.	n.d.
Cl <sup>-</sup>	n.d.	n.d.
Br <sup>-</sup>	n.d.	n.d.

#### 3.4.4 NMR Anion Recognition Study:

Solutions of receptor  $[3.1^{4+} \cdot 4BF_4^-]$  (4 mM, CD<sub>3</sub>OD, 300 K) were titrated by adding known quantities of a concentrated solution of various tetrabutylammonium anion salts.

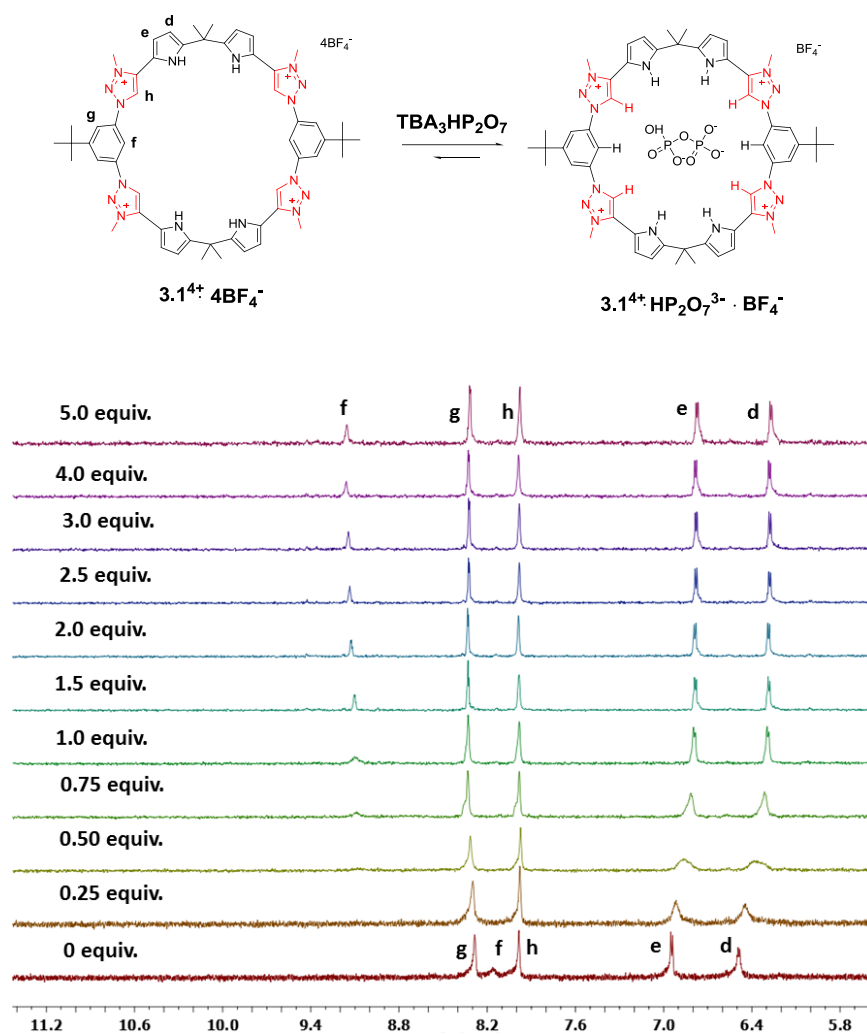


**Figure 3.25:**  $^1\text{H}$  NMR spectrum of anion receptor  $[3.1^{14+} \cdot 4\text{BF}_4^-]$  and 0.25, 0.50, 0.75, 1.0, 1.5, 2.0, 2.5, 3.0, 4.0, 5.0 equiv.  $(\text{TBA})_3\text{HP}_2\text{O}_7$  recorded in  $\text{CD}_3\text{OD}$  at 300 K.

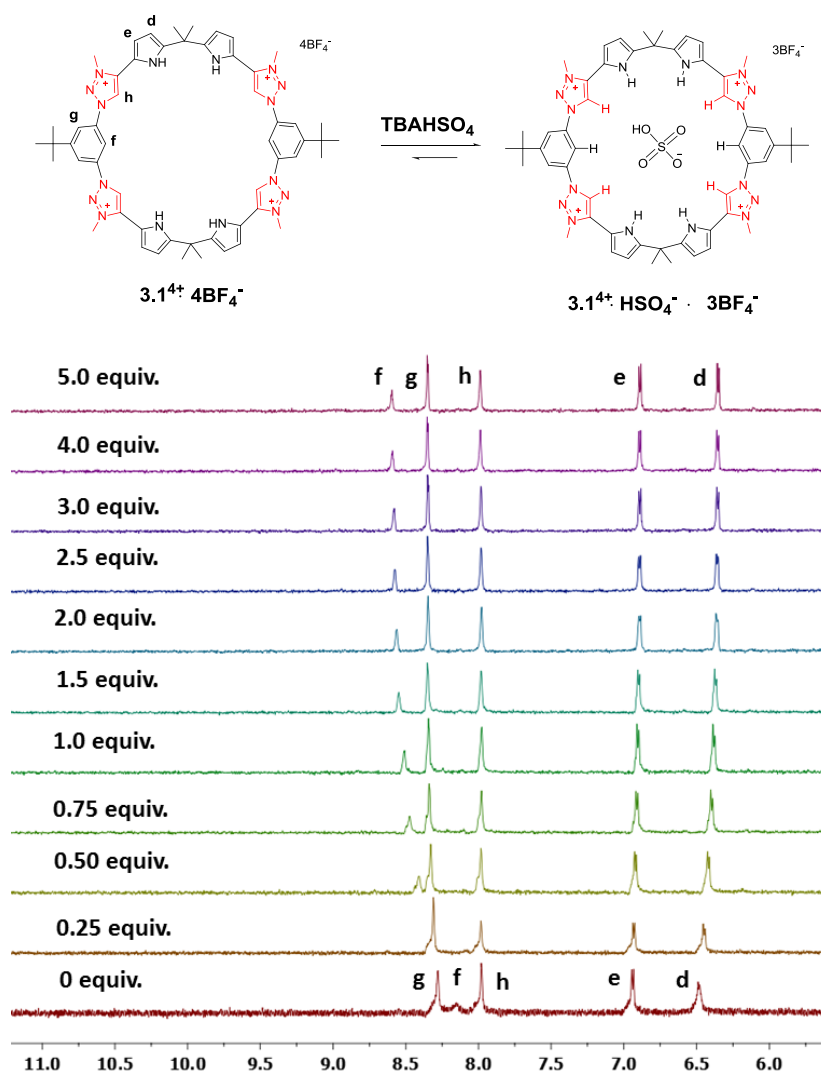


**Figure 3.26:**  $^1\text{H}$  NMR spectrum of anion receptor  $[3.1]^{4+} \cdot 4\text{BF}_4^-$  and 0.25, 0.50, 0.75, 1.0, 1.5, 2.0, 2.5, 3.0, 4.0, 5.0 equiv.  $\text{TBAHSO}_4$  recorded in  $\text{CD}_3\text{OD}$  at 300 K.

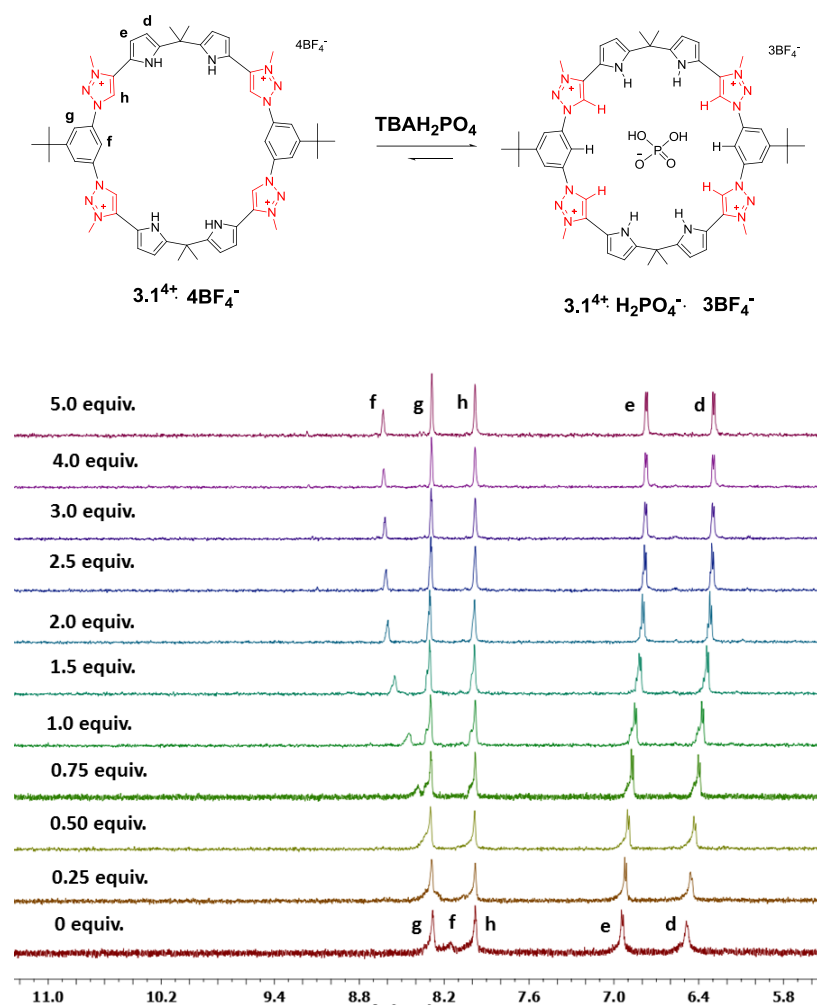


**Figure 3.27:** <sup>1</sup>H NMR spectrum of anion receptor [**3.14<sup>4+</sup>**·4BF<sub>4</sub><sup>-</sup>] and 0.25, 0.50, 0.75, 1.0, 1.5, 2.0, 2.5, 3.0, 4.0, 5.0 equiv. TBAH<sub>2</sub>PO<sub>4</sub> recorded in CD<sub>3</sub>OD at 300 K.

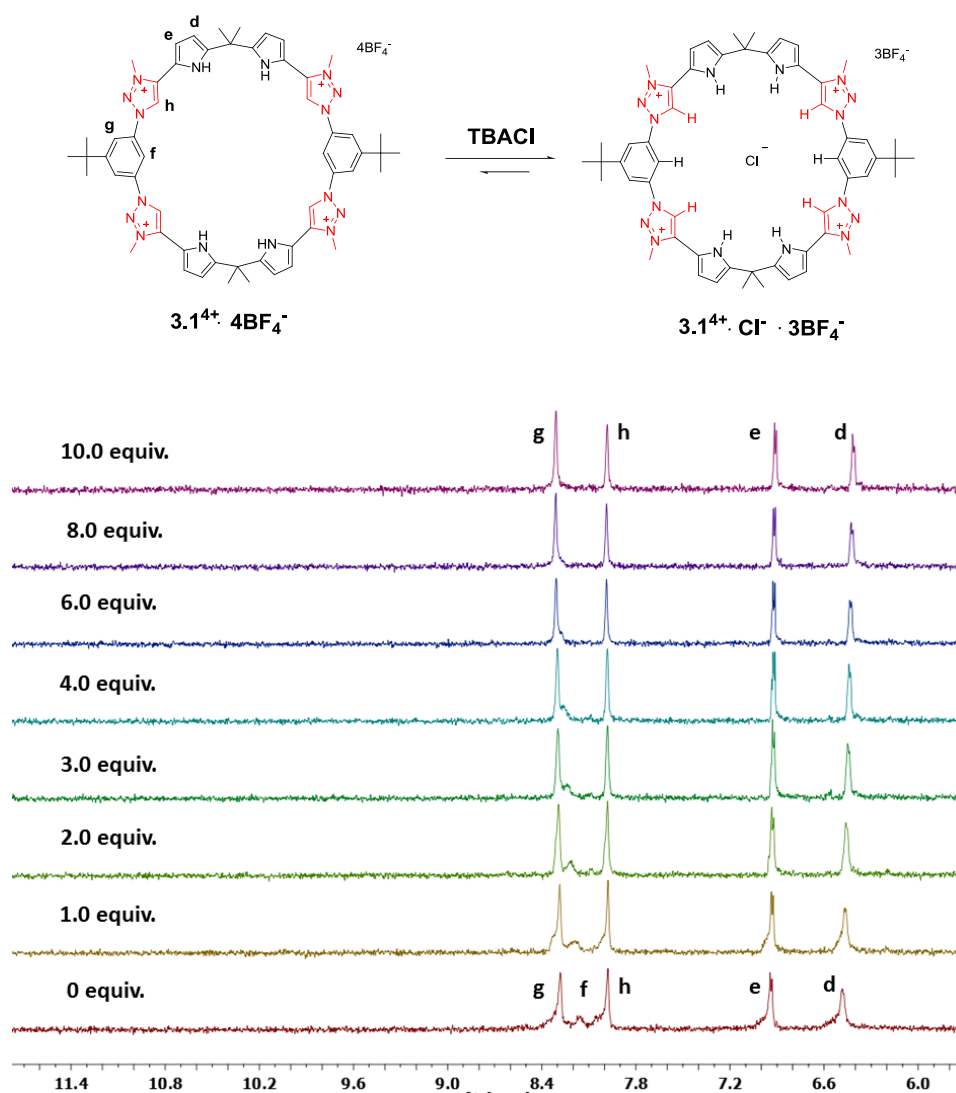


**Figure 3.28:**  $^1\text{H}$  NMR spectrum of anion receptor  $[3.1^{4+} \cdot 4\text{BF}_4^-]$  and 1.0, 2.0, 3.0, 4.0, 6.0, 8.0, 10.0 equiv. TBACl recorded in  $\text{CD}_3\text{OD}$  at 300 K.



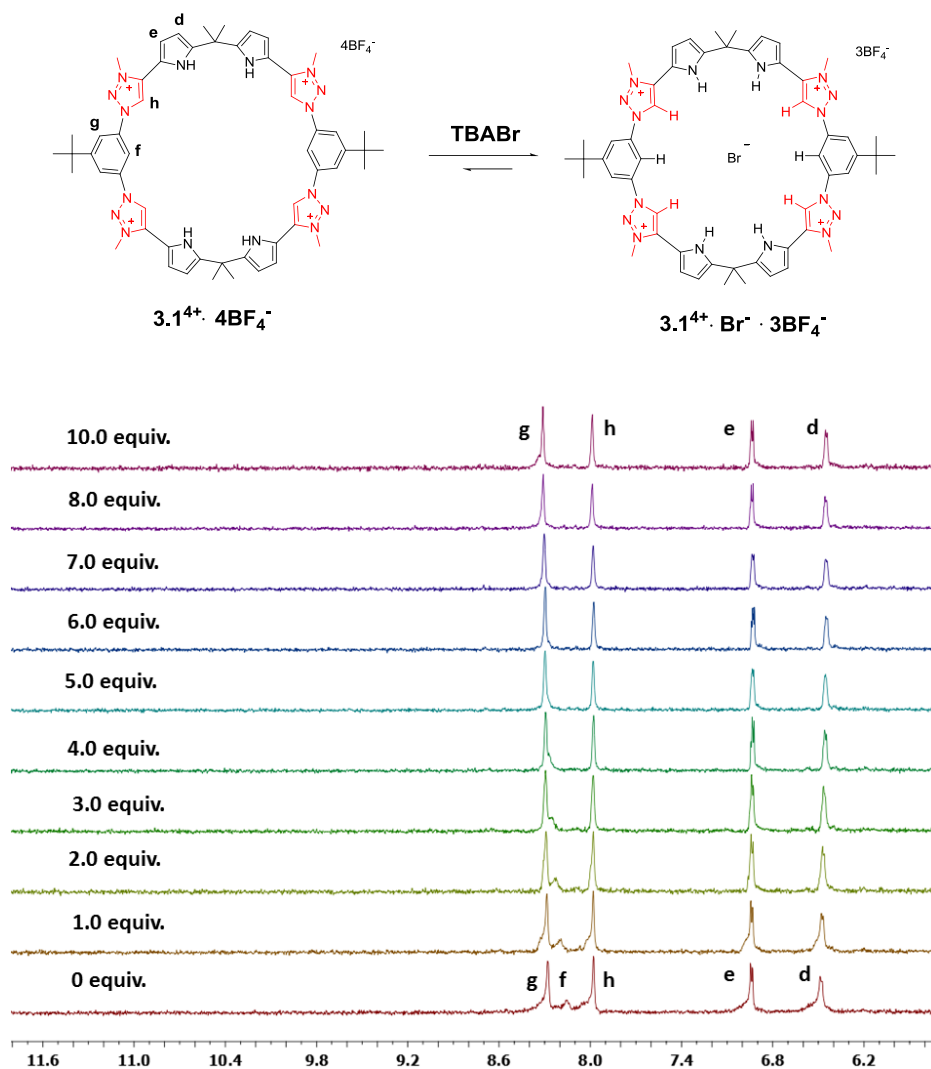


**Figure 3.29:**  $^1\text{H}$  NMR spectrum of anion receptor  $[3.1^{4+} \cdot 4\text{BF}_4^-]$  and 1.0, 2.0, 3.0, 4.0, 5.0, 6.0, 7.0, 8.0, 10.0 equiv. TBABr recorded in  $\text{CD}_3\text{OD}$  at 300 K.

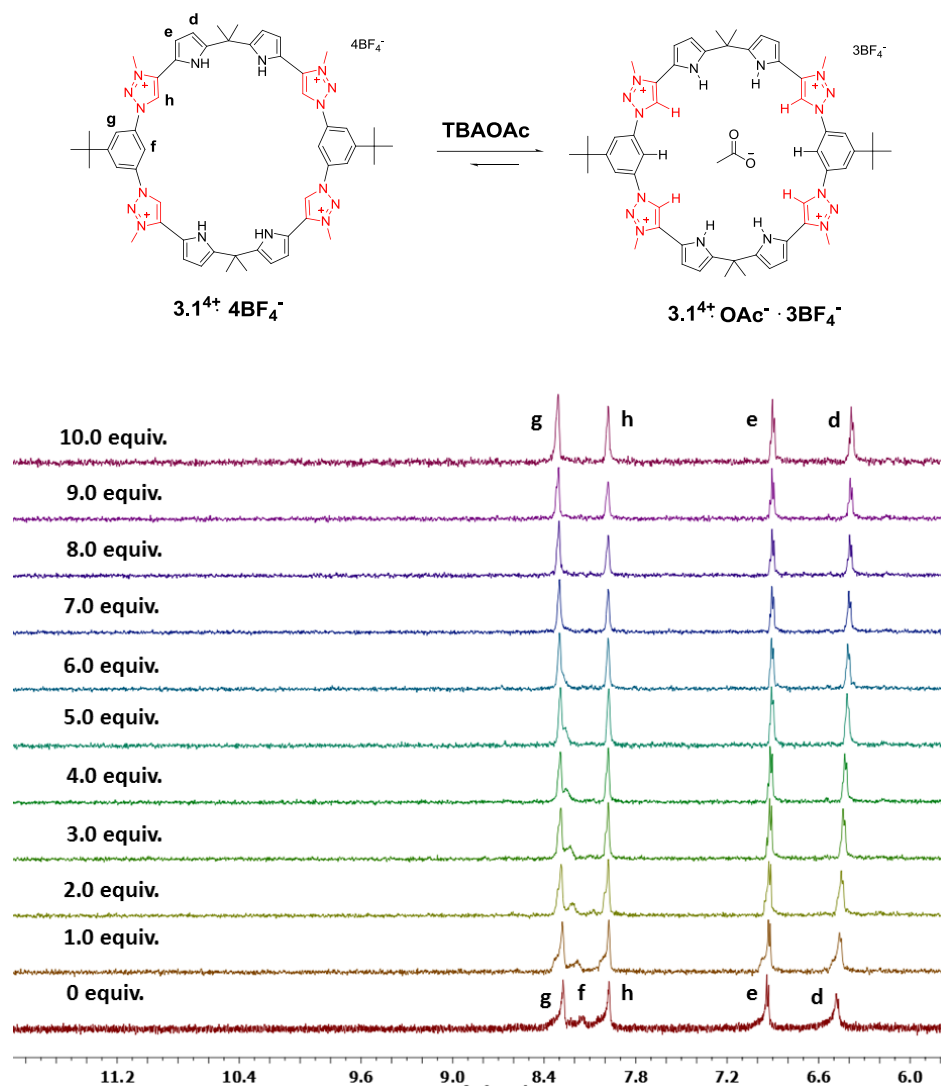


**Figure 3.30:** <sup>1</sup>H NMR spectrum of anion receptor [**3.1<sup>4+</sup>·4BF<sub>4</sub><sup>-</sup>**] and 1.0, 2.0, 3.0, 4.0, 5.0, 6.0, 7.0, 8.0, 9.0, 10.0 equiv. TBAOAc recorded in CD<sub>3</sub>OD at 300 K.

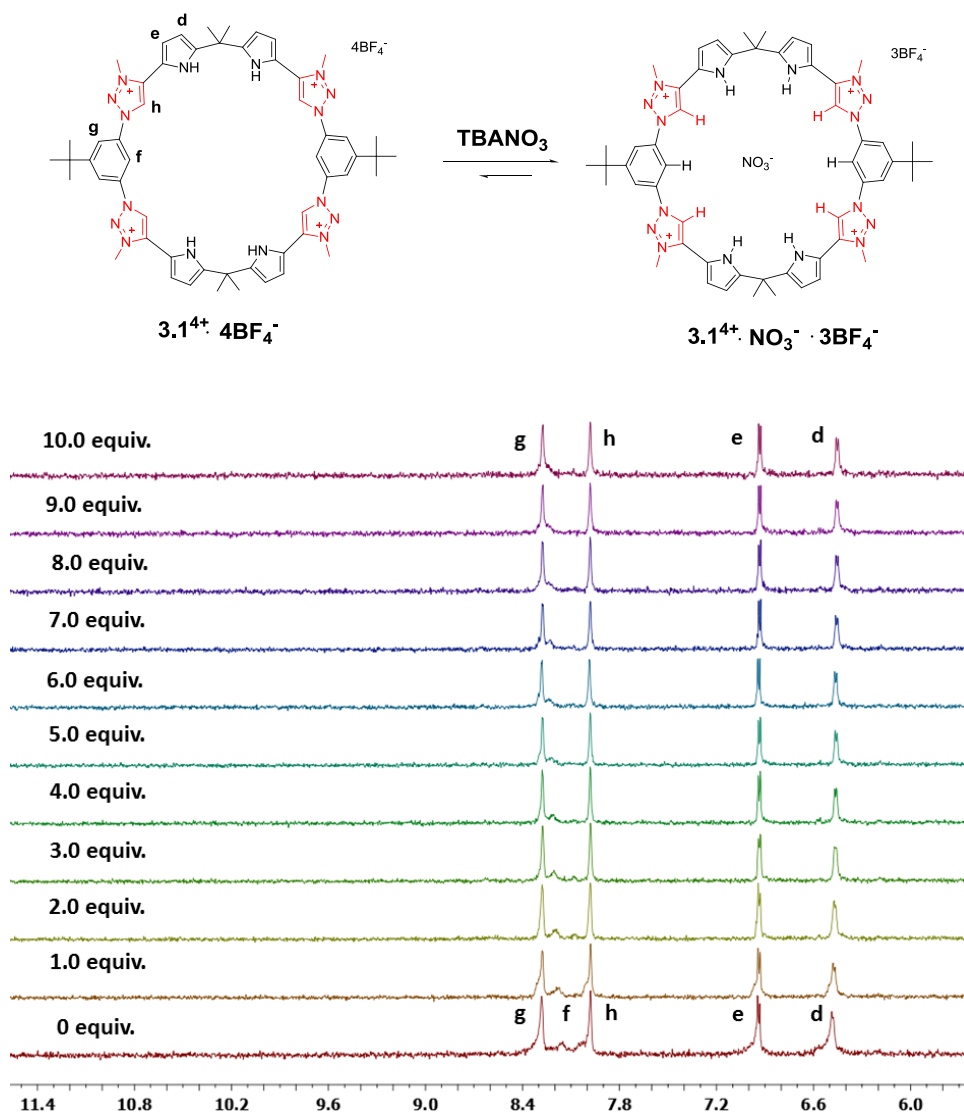


**Figure 3.31:**  $^1\text{H}$  NMR spectrum of anion receptor  $[3.1]^{4+} \cdot 4\text{BF}_4^-$  and 1.0, 2.0, 3.0, 4.0, 5.0, 6.0, 7.0, 8.0, 9.0, 10.0 equiv.  $\text{TBANO}_3$  recorded in  $\text{CD}_3\text{OD}$  at 300 K.

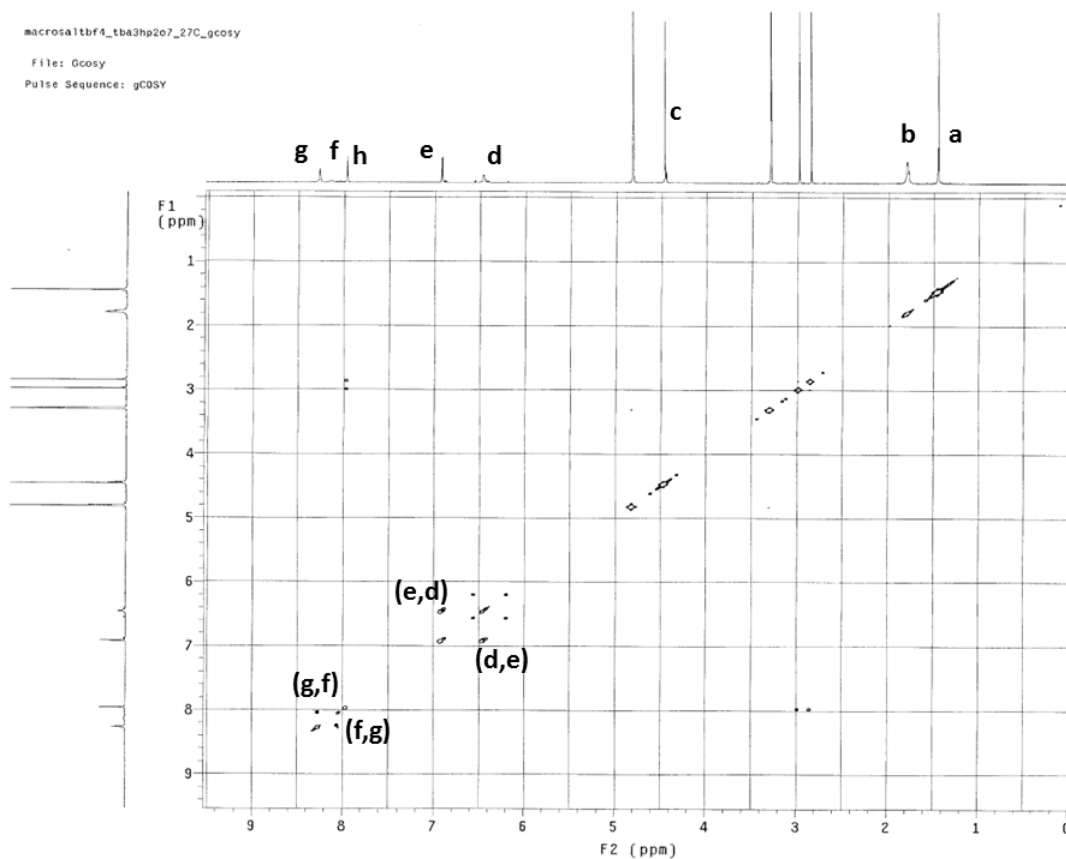


**Figure 3.32:** Full view of the 2D COSY NMR spectrum of  $3.1^{4+} \cdot 4\text{BF}_4^-$  recorded in  $\text{CD}_3\text{OD}$  at 300 K. (The peaks at 2.74 ppm and 2.91 ppm belong to the DMF solvent. Macrocycle  $3.1^{4+} \cdot 4\text{BF}_4^-$  was recrystallized from DMF and ether solvents. The DMF solvent was wrapped inside the compound and was hard to get rid of.)

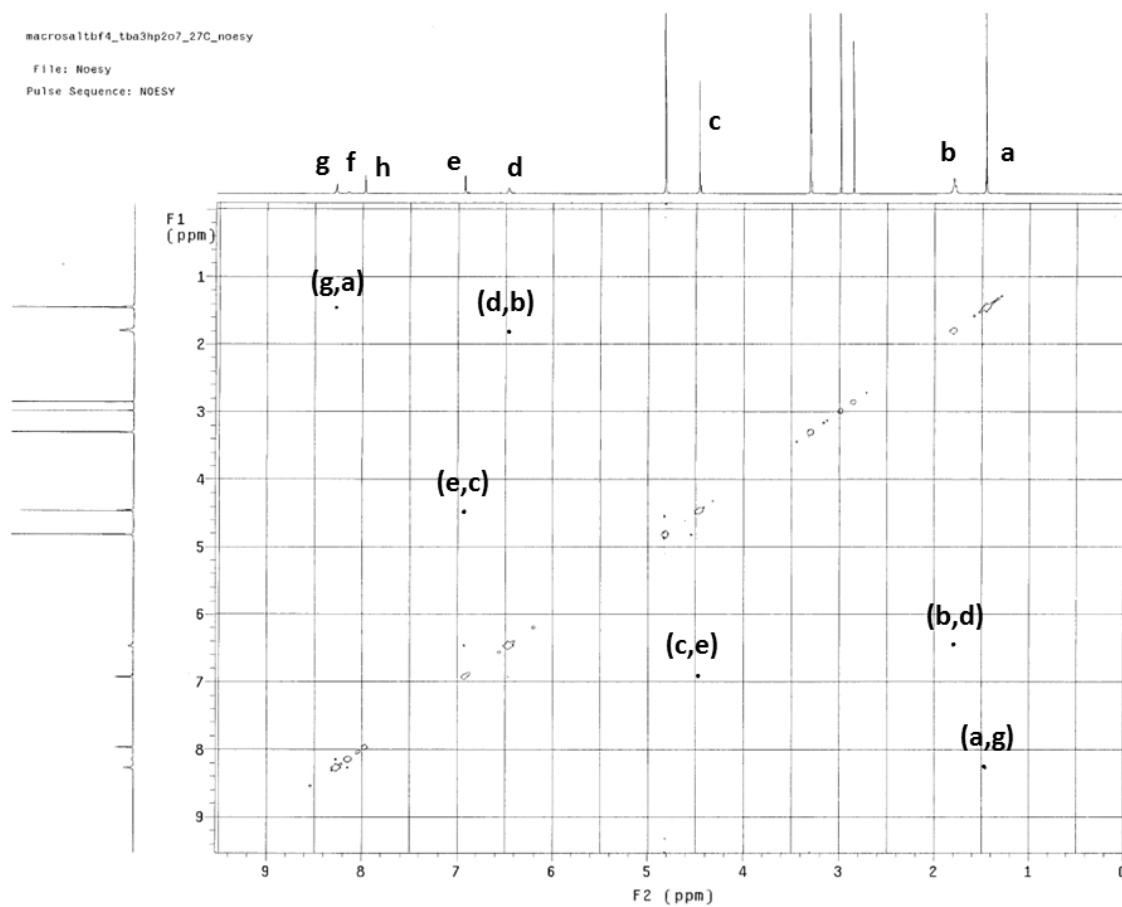


**Figure 3.33:** Full view of the 2D NOESY NMR spectrum of  $3.1^{4+} \cdot 4\text{BF}_4^-$  recorded in  $\text{CD}_3\text{OD}$  at 300 K. (The peaks at 2.74 ppm and 2.91 ppm belong to the DMF solvent. Macrocycle  $3.1^{4+} \cdot 4\text{BF}_4^-$  was recrystallized from DMF and ether solvents. The DMF solvent was wrapped inside the compound and was hard to get rid of.)

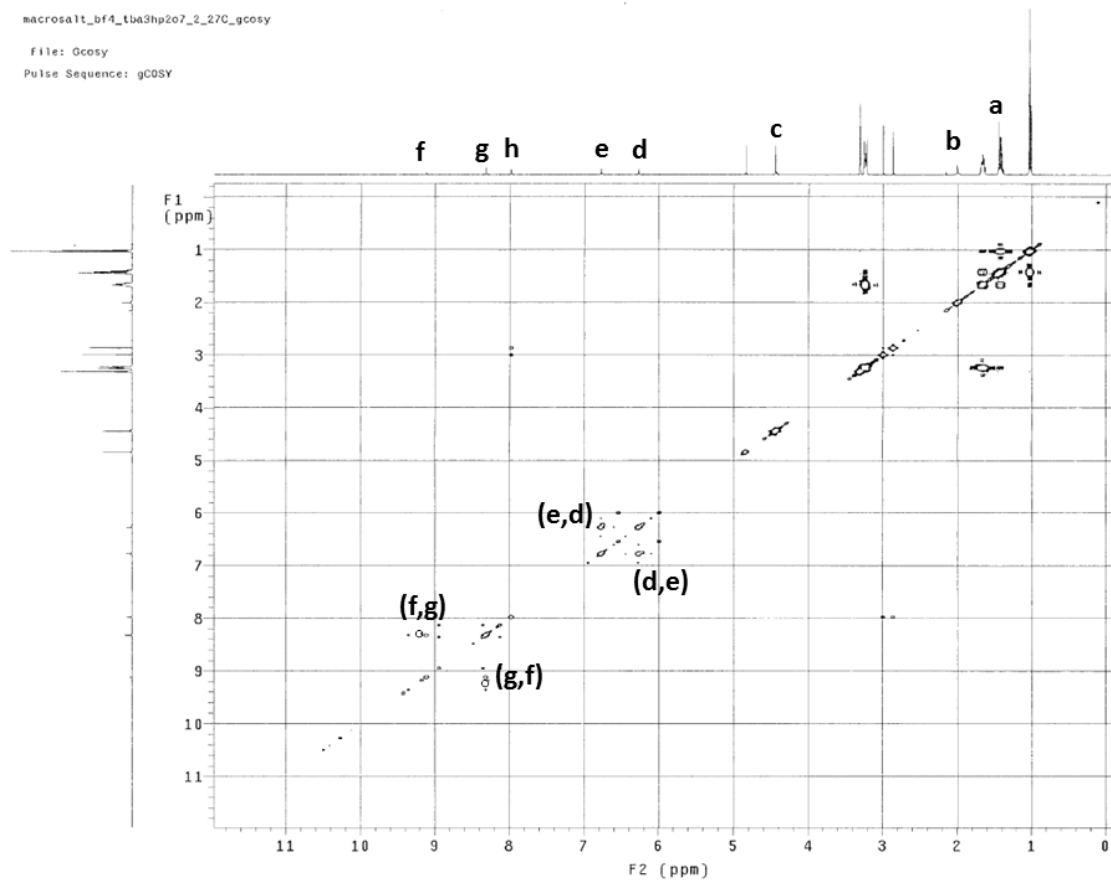


**Figure 3.34:** Full view of the 2D COSY NMR spectrum of  $3.1^{4+} \cdot 4\text{BF}_4^-$  containing two equivalent  $\text{TBA}_3\text{HP}_2\text{O}_7$  recorded in  $\text{CD}_3\text{OD}$  at 300 K. (The peak at 2.74 ppm and 2.91 ppm belong to the DMF solvent. Macrocycle  $3.1^{4+} \cdot 4\text{BF}_4^-$  was recrystallized from DMF and ether solvents. The DMF solvent was wrapped inside the compound and was hard to get rid of.)

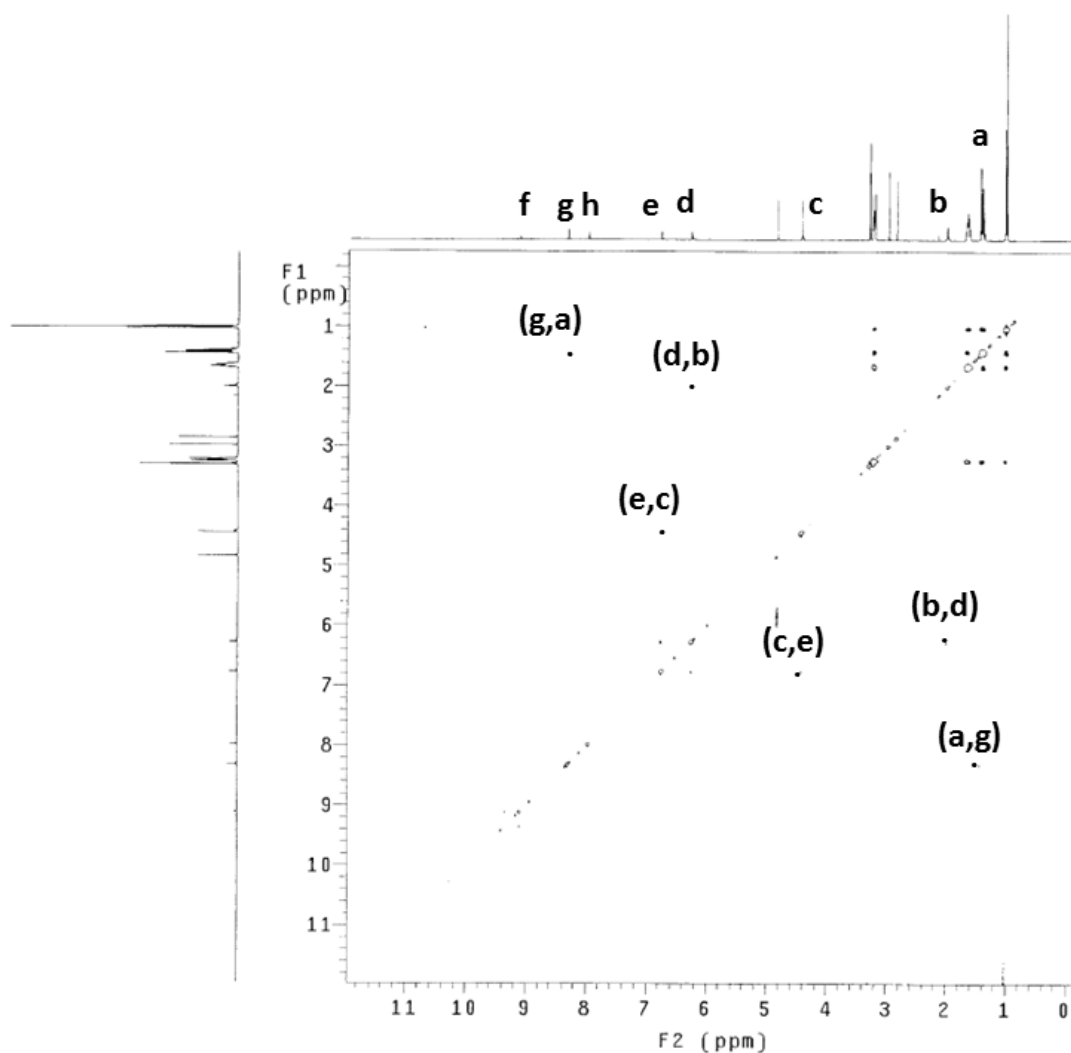


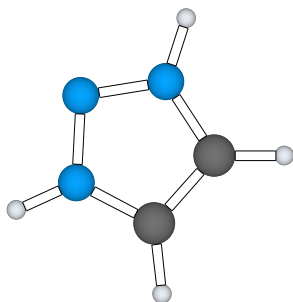
**Figure 3.35:** Full view of the 2D NOESY NMR spectrum of  $3.1^{4+} \cdot 4BF_4^{-}$  containing two equivalent  $TBA_3HP_2O_7$  recorded in  $CD_3OD$  at 300 K. (The peaks at 2.74 ppm and 2.91 ppm belong to the DMF solvent. Macrocycle  $3.1^{4+} \cdot 4BF_4^{-}$  was recrystallized from DMF and ether solvents. The DMF solvent was wrapped inside the compound and was hard to get rid of.)

### 3.4.5 Details of Electronic Structure Calculations

These studies were carried out by our collaborator, Dr. Benjamin Hay, and are included here for the benefit of the reader, even though they are not part of the author's dissertation work.

Cartesian coordinates and absolute energies for geometries optimized with NWChem at the MP2/aug-cc-pVDZ level of theory using the frozen core approximation are reported below.<sup>24</sup>

triazolium cation



Energy -241.9461853 hartree

9

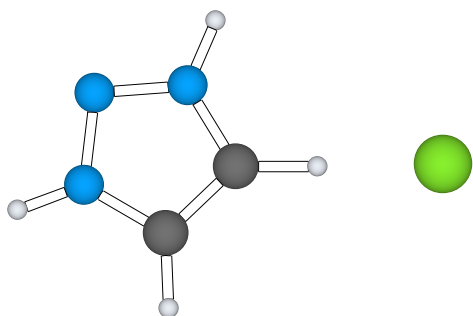
N	0.239243	1.138535	0.001495
N	-1.078491	0.926712	0.001495
N	-1.146255	-0.406097	0.001495
C	0.061417	-1.030823	0.001495
C	0.991974	0.007126	0.002487
H	0.555115	2.111511	-0.000504
H	2.078964	0.006821	-0.000504



H	0.178375	-2.111496	-0.002502
H	-2.078964	-0.825241	0.002487

triazolium chloride complex, bound to C-H

(C-H---Cl constrained to 180°)



Energy -701.8212085 hartree

10

N	-2.119019	-0.277893	-0.019836
N	-1.965775	1.051239	-0.098282
N	-0.628586	1.156158	-0.081802
C	0.068222	-0.009811	0.001282
C	-0.945557	-0.970505	0.042526
H	-3.071793	-0.634415	-0.014389
H	-0.903168	-2.053558	0.109329
H	1.241745	-0.008270	0.021286
H	-0.223953	2.091415	-0.130920
Cl	3.050644	0.024841	0.050232

### 3.4.6 Crystallographic Data (CIF)

Crystals used in this study were obtained by the author. They are in the form of multiply intergrown, colorless needles in the case of macrocycle  $\mathbf{3.1^{4+} \cdot 4BF_4^- \cdot CH_3OH \cdot 3H_2O}$ , yellow prisms in the cases of the complex  $\mathbf{3.1^{4+} \cdot HP_2O_7^{3-} \cdot BF_4^-}$ , and yellow prisms in the cases of the complex  $\mathbf{2(3.1^{4+}) \cdot 2H_2PO_4^- \cdot 6BF_4^-}$ . Diffraction grade crystals of macrocycle  $\mathbf{3.1^{4+} \cdot 4BF_4^- \cdot CH_3OH \cdot 3H_2O}$  were obtained by vapor diffusion from diethyl ether to methanol. Crystals of the complex  $\mathbf{3.1^{4+} \cdot HP_2O_7^{3-} \cdot BF_4^-}$  were obtained by vapor diffusion from diethyl ether to methanol. Crystals of the complex  $\mathbf{2(3.1^{4+}) \cdot 2H_2PO_4^- \cdot 6BF_4^-}$  were obtained by vapor diffusion from diethyl ether to methanol. The data crystals were cut from a cluster of crystals and had the approximate dimensions given in Table 3.6. The data were collected by the author on a Rigaku Saturn CCD diffractometer using a graphite monochromator with MoK $\alpha$  radiation ( $\lambda = 0.71075 \text{ \AA}$ ). The data were collected using  $\omega$ -scans with a scan range of  $1^\circ$  at low temperature shows using an Oxford Cryostream low temperature device (*cf.* Table 3.6). Data reduction was performed using DENZO-SMN.<sup>26</sup> The structures were solved by Dr. Xiaoping Yang *via* direct methods using SIR97<sup>27</sup> and refined by full-matrix least-squares on  $F^2$  with anisotropic displacement parameters for the non-H atoms using SHELXL-97.<sup>28</sup> The hydrogen atoms were calculated in ideal positions with isotropic displacement parameters set to  $1.2 \times U_{eq}$  of the attached atom ( $1.5 \times U_{eq}$  for methyl hydrogen atoms).

The function,  $\Sigma w(|F_o|^2 - |F_c|^2)^2$ , was minimized. Definitions used for calculating  $R(F)$ ,  $R_w(F^2)$  and the goodness of fit,  $S$ , are given below.<sup>29</sup> Neutral atom scattering factors and values used to calculate the linear absorption coefficient are from the International Tables for X-ray Crystallography (1992).<sup>30</sup> All ellipsoid figures were generated using SHELXTL/PC.<sup>31</sup> Tables of positional and thermal parameters, bond lengths and angles, torsion angles, figures and lists of observed and calculated structure

factors are located in the cif documents available from the Cambridge Crystallographic Centre *via* quoting ref. numbers 849576, 849577 and 849578. These documents also contain details of crystal data, data collection and structure refinement.

**Table 3.6:** X-ray crystallographic data comparison of macrocycle  $\mathbf{3.1^{4+} \cdot 4BF_4^- \cdot CH_3OH \cdot 3H_2O}$ , complex  $\mathbf{3.1^{4+} \cdot HP_2O_7^{3-} \cdot BF_4^-}$ , and complex  $\mathbf{2(3.1^{4+}) \cdot 2H_2PO_4^- \cdot 6BF_4^-}$

	Macrocycle $\mathbf{3.1^{4+} \cdot 4BF_4^- \cdot CH_3OH \cdot 3H_2O}$	Complex $\mathbf{3.1^{4+} \cdot HP_2O_7^{3-} \cdot BF_4^-}$	Complex $\mathbf{2(3.1^{4+}) \cdot 2H_2PO_4^- \cdot 6BF_4^-}$
CCDC No.	849576	849577	849578
empirical formula	$C_{55}H_{68}B_4F_{16}N_{16}O_4$	$C_{54}H_{64}BF_4N_{16}O_7P_2$	$C_{162}H_{200}B_8F_{32}N_{48}O_{16}P_4$
Fw	1364.49	1197.96	3894.06
crystal size (mm <sup>3</sup> )	0.20 × 0.18 × 0.15	0.22 × 0.17 × 0.10	0.21 × 0.18 × 0.16
Crystal system	Monoclinic	Monoclinic	Monoclinic
Space group	P2(1)/n	P2(1)/n	P2(1)/n
<i>a</i> [Å]	15.7015(5)	19.726(9)	20.554(6)
<i>b</i> [Å]	12.8679(3)	15.697(6)	16.552(5)
<i>c</i> [Å]	18.0196(6)	22.564(9)	31.568(10)

**Table 3.6**, cont.

$\alpha$ [deg]	90.00	90.00	90.00
$\beta$ [deg]	105.0640(10)	101.404(6)	93.445(7)
$\gamma$ [deg]	90.00	90.00	90.00
$V$ / [Å <sup>3</sup> ]	3515.66(18)	6849(5)	10720(6)
$d$ / [g/cm <sup>3</sup> ]	1.099	1.278	1.328
$Z$	2	4	2
$T$ [K]	153(1)	153(1)	153(1)
F(000)	1224	2760	4480
$\mu$ , mm <sup>-1</sup>	0.084	0.142	0.138
$\theta$ rang, deg	3.07-25.00	3.01-25.00	3.01-25.00
reflns meads	31167	48859	91128
reflns used	6166	12025	18667
params	388	1037	1586
R1, wR2 $I > 2\sigma(I)$	0.1050, 0.2782	0.0924, 0.2326	0.0981, 0.2262
R1, wR2 (all data)	0.1138, 0.2881	0.1617, 0.2684	0.1924, 0.2681
Quality of fit	1.091	0.946	0.939

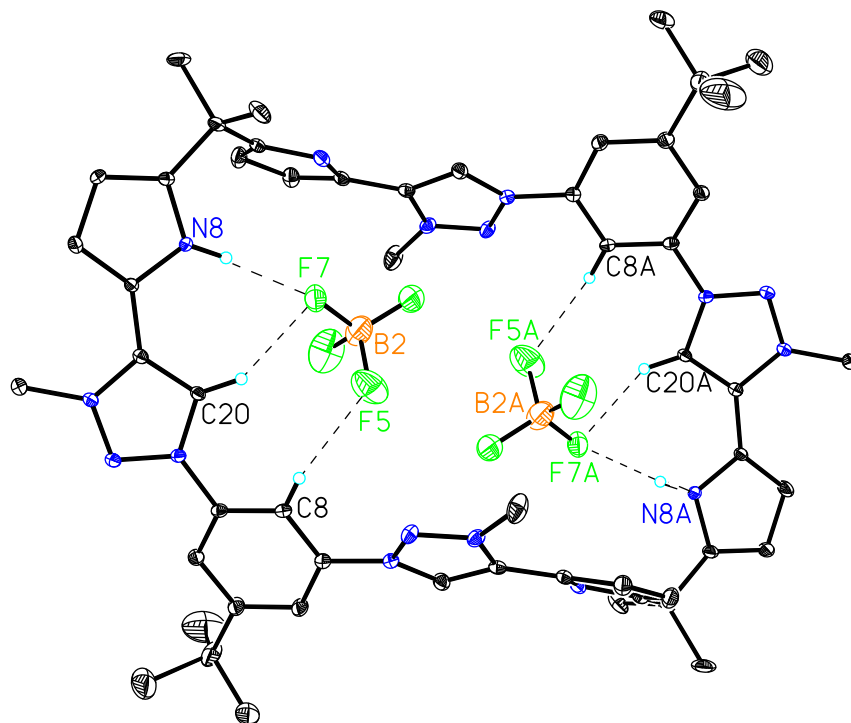


**Figure 3.36.** N-H $\cdots$ F and C-H $\cdots$ F hydrogen bonded interactions in the single crystal structure of **3.1**<sup>4+</sup>·4BF<sub>4</sub><sup>-</sup>·CH<sub>3</sub>OH·3H<sub>2</sub>O: C(8)-H $\cdots$ F(5): 2.399 Å, C-H-F 128.9°; C(20)-H $\cdots$ F(7): 2.230 Å, C-H-F 148.1°; N(8)-H $\cdots$ F(7): 1.983 Å, N-H-F 165.1°.

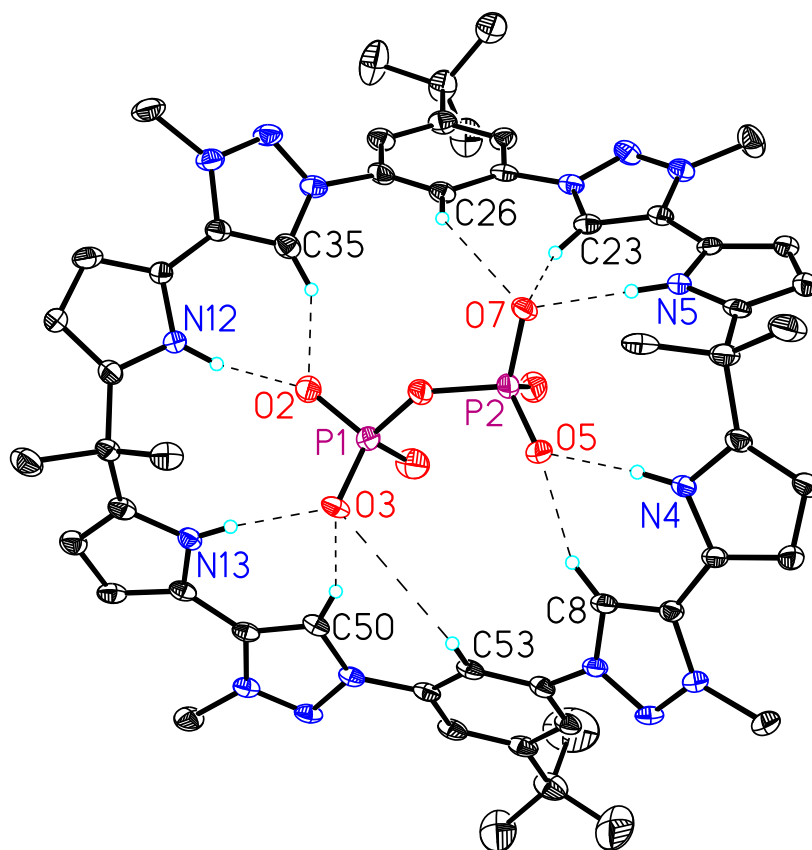


**Figure 3.37.** N-H $\cdots$ O and C-H $\cdots$ O hydrogen bonded interactions in the single crystal structure of **3.1**<sup>4+</sup>•HP<sub>2</sub>O<sub>7</sub><sup>3-</sup>•BF<sub>4</sub><sup>-</sup>: N(4)-H $\cdots$ O(5): 1.896 Å, N-H-O 170.5°; N(5)-H $\cdots$ O(7): 1.924 Å, N-H-O 168.5°; N(12)-H $\cdots$ O(2): 1.802 Å, N-H-O 163.9°; N(13)-H $\cdots$ O(3): 1.981 Å, N-H-O 166.6°; C(50)-H $\cdots$ O(3): 1.969 Å, C-H-O 156.6°; C(53)-H $\cdots$ O(3): 3.337 Å, C-H-O 143.5°; C(8)-H $\cdots$ O(5): 2.245 Å, C-H-O 147.5°; C(23)-H $\cdots$ O(7): 2.123 Å, C-H-O 150.6°; C(26)-H $\cdots$ O(7): 3.388 Å, C-H-O 154.4°; C(35)-H $\cdots$ O(2): 2.013 Å, C-H-O 145.3°.

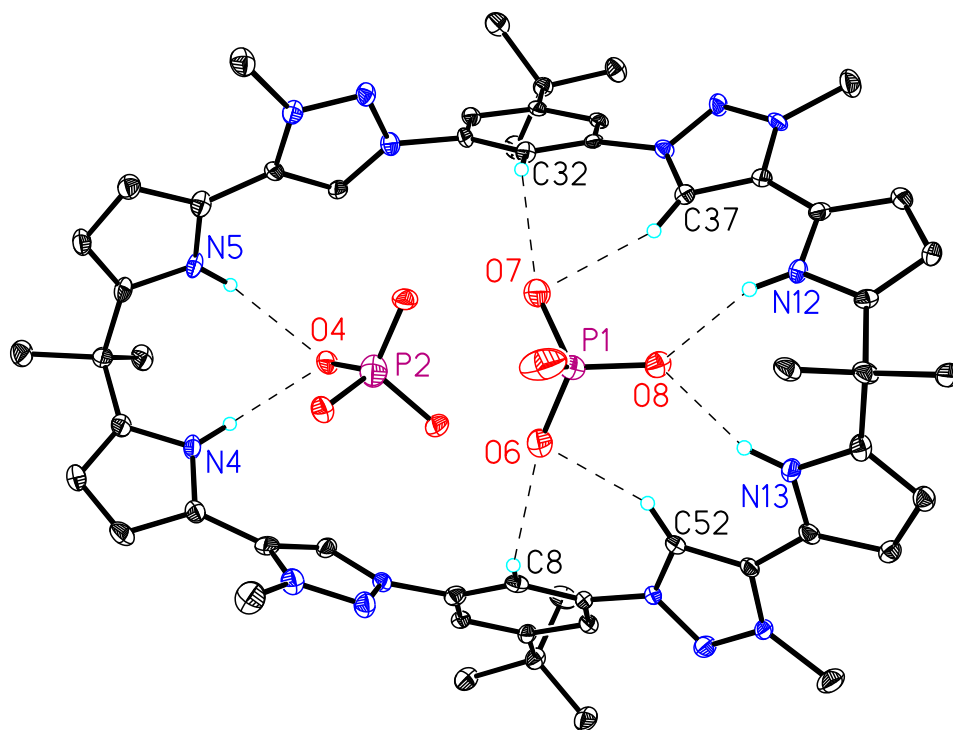


**Figure 3.38.** N-H $\cdots$ O and C-H $\cdots$ O hydrogen bonded interactions in the single crystal structure of 2(**3.1**<sup>4+</sup>) $\cdot$ 2H<sub>2</sub>PO<sub>4</sub><sup>-</sup> $\cdot$ 6BF<sub>4</sub><sup>-</sup>: N(4)-H $\cdots$ O(4): 2.246 Å, N-H-O 136.7°; N(5)-H $\cdots$ O(4): 2.485 Å, N-H-O 123.1°; N(12)-H $\cdots$ O(8): 1.982 Å, N-H-O 157.9°; N(13)-H $\cdots$ O(8): 2.004 Å, N-H-O 159.6°; C(8)-H $\cdots$ O(6): 2.661 Å, C-H-O 145.9°; C(52)-H $\cdots$ O(6): 2.341 Å, C-H-O 154.7°; C(37)-H $\cdots$ O(7): 2.411 Å, C-H-O 159.2°; C(32)-H $\cdots$ O(7): 2.598 Å, C-H-O 143.6°.

### 3.5 REFERENCES

- (1) Lehn, J.-M. *Science* **2002**, 295, 2400.
- (2) (a) de Hoog, P.; Gamez, P.; Mutikainen, I.; Turpeinen, U.; Reedijk, J. *Angew. Chem., Int. Ed.* **2004**, 43, 5815. (b) Sessler, J. L.; Seidel, D. *Angew. Chem., Int. Ed.* **2003**, 42, 5134. (c) Gale, P. A. *Coord. Chem. Rev.*, **2003**, 240, 191. (d) Beer, P. D.; Gale, P. A. *Angew. Chem., Int. Ed.* **2001**, 40, 486. (e) Schmidtchen, P.; Berger, M. *Chem. Rev.* **1997**, 97, 1609. (f) Bianchi, A.; Bowman-James, K.; García-España, E. *Supramolecular Chemistry of Anions*; Wiley-VCH: Chichester, New York, 1997.
- (3) Sessler, J. L.; Gale, P. A.; Cho, W.-S. *Anion Receptor Chemistry*; RSC Publishing: Cambridge, U.K., 2006.
- (4) Mathews, C. P.; van Hold, K. E. *Biochemistry*; The Benjamin/Cummings Publishing Company, Inc.: Redwood City, CA, 1990.
- (5) Xu, S.; He, M.; Yu, H.; Cai, X.; Tan, X.; Lu, B.; Shu, B. *Anal. Biochem.* **2001**, 299, 188.
- (6) Ronaghi, M.; Karamohamed, S.; Pettersson, B.; Uhlén, M.; Nyrén, P. *Anal. Biochem.* **1996**, 242, 84.
- (7) Saenger, W. *Principles of Nucleic Acid Structure*; Springer-Verlag: New York, 1988.
- (8) Lumetta, G. J. In *Fundamentals and Applications of Anion Separations*; Moyer, B. A.; Singh, R. P. Eds.; Kluwer Academic/Plenum: New York, 2004, 107.
- (9) (a) Sessler, J. L.; Kim, S.-K.; Gross, D. E.; Lee, C.-H.; Kim, J.-S.; Lynch, V. M. *J. Am. Chem. Soc.* **2008**, 130, 13162. (b) Kang, S.-O.; Powell, D.; Day, V. W.; Bowman-James, K. *Angew. Chem., Int. Ed.* **2006**, 45, 1921. (c) Bondy, C. R.; Gale, P. A.; Loeb, S. J. *J. Am. Chem. Soc.* **2004**, 126, 5030. (d) Tobey, S. L.; Anslyn, E. V. *J. Am. Chem. Soc.* **2003**, 125, 14807.
- (10) (a) Sessler, J. L.; Cai, J.; Gong, H.-Y.; Yang, X.; Arambula, J. F.; Hay, B. P. *J. Am. Chem. Soc.* **2010**, 132, 14058. (b) Mullen, K.; Mercurio, J.; Serpell, C.; Beer, P. D. *Angew. Chem., Int. Ed.* **2009**, 48, 4781. (c) Yoon, D. W.; Gross, D. E.; Lynch, V. M.; Sessler, J. L.; Hay, B. P.; Lee, C.-H. *Angew. Chem., Int. Ed.* **2008**, 47, 5038. (d) Li, Y.; Flood, A. H. *Angew. Chem., Int. Ed.* **2008**, 47, 2649. (e) Bryantsev, V. S.; Hay, B. P. *J. Am. Chem. Soc.* **2005**, 127, 8282. (f) Chellappan, K.; Singh, N. J.; Hwang, I.-C.; Lee, J. W.; Kim, K. S. *Angew. Chem., Int. Ed.* **2005**, 44, 2899.
- (11) (a) Keitz, B. K.; Bouffard, J.; Bertrand, G.; Grubbs, R. H. *J. Am. Chem. Soc.* **2011**, 133, 8498. (b) Bouffard, J.; Keitz, B. K.; Tonner, R.; Guisado-Barrios, G.; Frenking, G.; Grubbs, R. H.; Bertrand, G. *Organometallics* **2011**, 30, 2617. (c) Cai, J.; Yang, X.; Arumugam, K.; Bielawski, C. W.; Sessler, J. L.



- Organometallics* **2011**, *30*, 5033. (d) Saravanakumar, R.; Ramkumar, V.; Sankararaman, S. *Organometallics* **2011**, *30*, 1689. (e) Prades, A.; Peris, E.; Albrecht, M. *Organometallics* **2011**, *30*, 1162.
- (12) Ohmatsu, K.; Kiyokawa, M.; Ooi, T. *J. Am. Chem. Soc.* **2011**, *133*, 1307.
- (13) (a) Kilah, N. L.; Wise, M. D.; Serpell, C. J.; Thompson, A. L.; White, N. G.; Christensen, K. E.; Beer, P. D. *J. Am. Chem. Soc.* **2010**, *132*, 11893. (b) Schulze, B.; Friebe, C.; Hager, M. D.; Guenther, W.; Koehn, U.; Jahn, B. O.; Goerls, H.; Schubert, U. S. *Org. Lett.* **2010**, *12*, 2710. (c) Kumar, A.; Pandey, P. S. *Org. Lett.* **2008**, *10*, 165.
- (14) (a) Kolb, H. C.; Finn, M. G.; Sharpless, K. B. *Angew. Chem., Int. Ed.* **2001**, *40*, 2004. (b) Tornøe, C. W.; Meldal, M. *Chem. Rev.* **2008**, *108*, 2952.
- (15) (a) Moses, J. E.; Moorhouse, A. D. *Chem. Soc. Rev.* **2007**, *36*, 1249. (b) Fournier, D.; Hoogenboom, R.; Schubert, U. S. *Chem. Soc. Rev.* **2007**, *36*, 1369. (c) Lutz, J. F. *Angew. Chem., Int. Ed.* **2007**, *46*, 1018. (d) Ladmiral, V.; Mantovani, G.; Clarkson, G. J.; Cauet, S.; Irwin, J. L.; Haddleton, D. M. *J. Am. Chem. Soc.* **2006**, *128*, 4823. (e) Diaz, D. D.; Rajagopal, K.; Strable, E.; Schneider, J.; Finn, M. G. *J. Am. Chem. Soc.* **2006**, *128*, 6056. (f) Whiting, M.; Tripp, J. C.; Lin, Y.-C.; Lindstrom, W.; Olson, A. J.; Elder, J. H.; Sharpless, K. B.; Fokin, V. V. *J. Med. Chem.* **2006**, *49*, 7697. (g) Punna, S.; Kuzelka, J.; Wang, Q.; Finn, M. G. *Angew. Chem., Int. Ed.* **2005**, *44*, 2215. (h) Bodine, K. D.; Gin, D. Y.; Gin, M. S. *J. Am. Chem. Soc.* **2004**, *126*, 1638. (i) Wu, P.; Feldman, A. K.; Nugent, A. K.; Hawker, C. J.; Scheel, A.; Voit, B.; Pyun, J.; Frechet, J. M. J.; Sharpless, K. B.; Fokin, V. V. *Angew. Chem., Int. Ed.* **2004**, *43*, 3928. (j) Wang, Q.; Chan, T. R.; Hilgraf, R.; Fokin, V. V.; Sharpless, K. B.; Finn, M. G. *J. Am. Chem. Soc.* **2003**, *125*, 3192. (k) Link, A. J.; Tirrell, D. A. *J. Am. Chem. Soc.* **2003**, *125*, 11164. (l) Kolb, H. C.; Sharpless, K. B. *Drug Discovery Today* **2003**, *8*, 1128.
- (16) (a) Lee, S.; Hua, Y.; Park, H.; Flood, A. H. *Org. Lett.* **2010**, *12*, 2100. (b) Yano, M.; Tong, C. C.; Light, M. E.; Schmidtchen, F. P.; Gale, P. A. *Org. Biomol. Chem.* **2010**, *8*, 4356. (c) Hua, Y.; Flood, A. H. *J. Am. Chem. Soc.* **2010**, *132*, 12838. (d) Hua, Y.; Flood, A. H. *Chem. Soc. Rev.* **2010**, *39*, 1262. (e) Romero, T.; Caballero, A.; Tárraga, A.; Molina, P. *Org. Lett.* **2009**, *11*, 3466. (f) Juwarker, H.; Lenhardt, J. M.; Castillo, J. C.; Craig, S. L. *J. Org. Chem.* **2009**, *74*, 8924. (g) Fisher, M. G.; Gale, P. A.; Hiscock, J. R.; Hursthouse, M. B.; Light, M. E.; Schmidtchen, F. P.; Tong, C. C. *Chem. Commun.* **2009**, 3017. (h) Li, Y.; Pink, M.; Karty, J. A.; Flood, A. H. *J. Am. Chem. Soc.* **2008**, *130*, 17293. (i) Juwarker, H.; Lenhardt, J. M.; Pham, D. M.; Craig, S. L. *Angew. Chem., Int. Ed.* **2008**, *47*, 3740. (j) Meudtner, R. M.; Hecht, S. *Angew. Chem., Int. Ed.* **2008**, *47*, 4926.
- (17) Tom, N. J.; Simon, W. M.; Frost, H. N.; Ewing, M. *Tetrahedron Lett.* **2004**, *45*, 905.

- (18) Kim, S. K.; Sessler, J. L.; Gross, D. E.; Lee, C.-H.; Kim, J. S.; Lynch, V. M.; Delmau, L. H.; Hay, B. P. *J. Am. Chem. Soc.* **2010**, *132*, 5827.
- (19) Bourson, J.; Pouget, J.; Valeur, B. *J. Phys. Chem.* **1993**, *97*, 4552.
- (20) (a) Kubik, S.; Goddard, R.; Kirchner, R.; Nolting, D.; Seidel, J. *Angew. Chem., Int. Ed.* **2001**, *40*, 2648. (b) Kubik, S.; Goddard, R. *Proc. Natl. Acad. Sci. U. S. A.* **2002**, *99*, 5127. (c) Kubik, S.; Kirchner, R.; Nolting, D.; Seidel, J. *J. Am. Chem. Soc.* **2002**, *124*, 12752. (d) Otto, S.; Kubik, S. *J. Am. Chem. Soc.* **2003**, *125*, 7804.
- (21) (a) Mateus, P.; Delgado, R.; Brandão, P.; Félix, V. *J. Org. Chem.* **2009**, *74*, 8638. (b) Mateus, P.; Delgado, R.; Brandão, P.; Carvalho, S.; Félix, V. *Org. Biomol. Chem.* **2009**, *7*, 4661.
- (22) Dietrich, B.; Fyles, D. L.; Fyles, T. M.; Lehn, J. -M. *Helv. Chim. Acta.* **1979**, *62*, 2763.
- (23)  $\Delta G = G(\text{complex}) - G(\text{chloride}) - G(\text{donor})$  values in vacuum were calculated at the MP2/aug-cc-pVDZ level of theory with *NWChem*: (a) Kendall, R. A.; Apra, E.; Bernholdt, D. E.; Bylaska, E. J.; Dupuis, M.; Fann, G. I.; Harrison, R. J.; Ju, J. L.; Nichols, J. A.; Nieplocha, J.; Straatsma, T. P.; Windus, T. L.; Wong, A. T. *Comput. Phys. Commun.* **2000**, *128*, 260. (b) Valiev, M.; Bylaska, E. J.; Govind, N.; Kowalski, K.; Straatsma, T. P.; Van Dam, H. J. J.; Wang, D.; Nieplocha, J.; Apra, E.; Windus, T. L.; de Jong, W. *Comput. Phys. Commun.* **2010**, *181*, 1477.
- (24) (a)  $\Delta G$  values in different solvents were computed with the SM8 solvation model<sup>22(b)</sup> as implemented in *Spartan*<sup>22(c)</sup> after performing RHF/6-31+G\* single-point energy calculations on MP2/aug-cc-pVDZ vacuum geometries. (b) Marenich, A. V.; Olson, R. M.; Kelly, C. P.; Cramer, C. J.; Truhlar, D. G. *J. Chem. Theory Comput.* **2007**, *3*, 2011. (c) *Spartan 10*, Wavefunction, Inc., Irvine, California 92612.
- (25) Macrocycle **1**<sup>4+</sup>•4BF<sub>4</sub><sup>-</sup> is insoluble in CHCl<sub>3</sub> or pure H<sub>2</sub>O. It can be dissolved in acetone, but precipitates when treated with tetrabutylammonium salts.
- (26) DENZO-SMN. (1997). Otwinowski, Z.; Minor, W. *Methods in Enzymology*, 276: *Macromolecular Crystallography, Part A*, 307 – 326, Carter, C.W.J.; Simon, M.I.; Sweet, R.M. Editors, Academic Press.
- (27) SIR97. (1999). A program for crystal structure solution. Altomare, A.; Burla, M. C.; Camalli, M.; Cascarano, G. L.; Giacovazzo, C.; Guagliardi, A.; Moliterni, A.G. G.; Polidori, G.; Spagna, R. *J. Appl. Cryst.* **1999**, *32*, 115-119.
- (28) Sheldrick, G. M. *SHELXL97. Program for the Refinement of Crystal Structures*; University of Gottingen, Germany, **1994**.
- (29)  $R_w(F^2) = \{\sum w(|F_o|^2 - |F_c|^2)^2 / \sum w|F_o|^4\}^{1/2}$  where  $w$  is the weight given each reflection.  $R(F) = \sum(|F_o| - |F_c|) / \sum|F_o|$  for reflections with  $F_o > 4(\sigma(F_o))$ .  $S =$

$[\Sigma w(|F_o|^2 - |F_c|^2)^2/(n - p)]^{1/2}$ , where n is the number of reflections and p is the number of refined parameters.

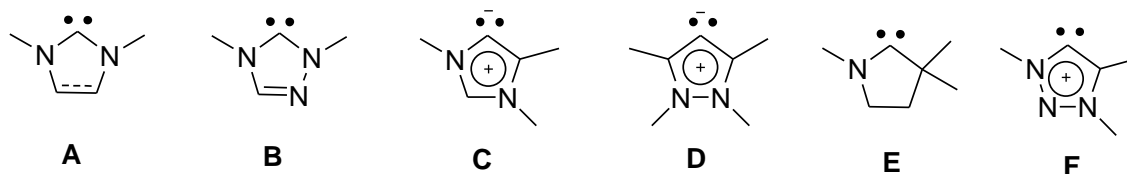
- (30) *International Tables for X-ray Crystallography*; Wilson, A. J. C., Ed.; Kluwer Academic Press: Boston, **1992**; Vol. C, Tables 4.2.6.8 and 6.1.1.4.
- (31) Sheldrick, G.M. (**1994**). SHELXTL/PC (Version 5.03). Siemens Analytical X-ray Instruments, Inc., Madison, Wisconsin, USA.
- (32) (a) Hay, B. P.; Firman, T. K.; Moyer, B. A. *J. Am. Chem. Soc.* **2005**, *109*, 832. (b) Bryantsev, V. S.; Hay, B. P. *Org. Lett.* **2005**, *7*, 5031.

## Chapter 4: Structurally Characterized Cationic Silver(I) and Ruthenium(II) Carbene Complexes of 1,2,3-Triazol-5-ylidenes

### 4.1 INTRODUCTION

N-heterocyclic carbenes (NHCs) have attracted considerable attention recently as ligands for use in transition metal-based catalysis,<sup>1</sup> as promoters of organocatalysis,<sup>2</sup> and in many other applications, as detailed by the Bielawski group at the University of Texas at Austin<sup>3a-f</sup> and by others.<sup>1b,3g-3i</sup> In general, NHC complexes exhibit higher thermal stabilities than their phosphine analogues, an effect ascribed in part to the fact that NHC ligands are strong donors.<sup>4</sup> To date, the majority of work with NHCs has focused on the 1,3-disubstituted imidazolyliidenes **A** and 1,4-disubstituted 1,2,4-triazolyliidenes **B** (Chart 1).<sup>5</sup> Both of these species display remarkable stability, in addition to utility in catalytically active complexes. This enhancement has prompted efforts to explore and to develop NHCs with other structural features. An early example was reported by Crabtree and co-workers in 2001, who described an abnormal NHC complex that featured an imidazole ring bound at the C5 position rather than at the C2 position (**C**, Chart 1).<sup>6</sup> Since that time, several other abnormal NHC complexes derived from other nonclassic NHC ligands have been reported; these include the pyrazolin-4-ylidene **D**<sup>7</sup> and the cyclic (alkyl)-(amino)carbene **E**.<sup>8</sup> It has also been shown recently that mesoionic carbenes (MICs) **C**, **D**, and **F** can be isolated in their free states.<sup>9</sup> Compared to more classical NHCs, these MICs are relatively strong  $\sigma$ -donors,<sup>10</sup> a feature that has made them of interest in terms of exploring their utility in catalysis.<sup>11</sup>

**Chart 4.1:** N-Heterocyclic Carbenes, Including “Classical” NHC Systems (A, B) As Well As Representatives of Various Subclasses (C-F)



To date, relatively few reports have described the synthesis of 1,2,3-triazolylidene-supported transition metal complexes and their application to catalyst studies.<sup>12,20,21</sup> In 2008, Albrecht and co-workers first reported the synthesis of 1,2,3-triazolylidenes (structure **F**; Chart 1) as highly modular precursors for a new class of carbenes and their coordination chemistry with a variety of transition metals (Pd, Ru, Rh, and Ir).<sup>12a</sup> Since then, silver complexes of these carbenes have been extensively studied. While we are aware of 11 reports of 1,2,3-triazolylidene silver complexes,<sup>12a-j,20</sup> to the best of our knowledge none of the complexes in question have been structurally characterized *via* single-crystal X-ray diffraction analysis. In collaboration with the Bielawski group, we envisioned overcoming this deficiency through the use of modified 1,2,3-triazolylidene ligands containing ancillary coordinating groups. With this consideration in mind, we have prepared and report here the first structurally characterized 1,2,3-triazolylidene silver complex **4.3**, a species synthesized from the pyrrole-containing triazole and triazolium precursors, **4.1** and **4.2**. We also report the first structurally characterized bis-ruthenium complex supported by a 1,2,3-triazolylidene-containing framework. Both complexes are identified by an overall 1:2 ligand-to-metal stoichiometry. The Ag(I) complex was found to exist as an eight silver atom cluster, whereas its Ru congener proved to be a discrete bimetallic complex. The Ru(II) complex was explored as a ring-opening metathesis polymerization (ROMP) catalyst and, as

detailed below, proved active for the polymerization of norbornene when activated with (trimethylsilyl)-diazomethane (TMSD).

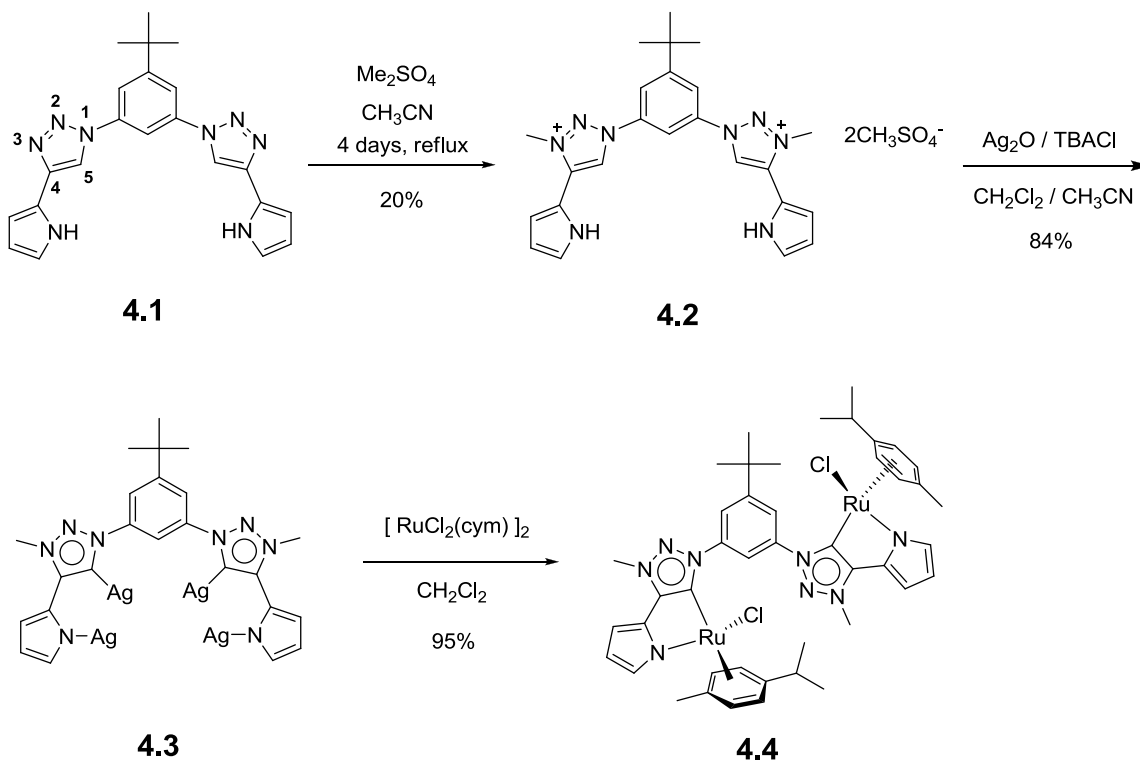
## 4.2 RESULTS AND DISCUSSIONS

The design of complex **4.4** was predicated on the combined use of 1,2,3-triazolylidene donor subunits and pyrrole chelating groups. Pyrrole is known to be a useful ligand in catalytic systems when chelated to various transition metals.<sup>13</sup> Its use in the present instance was expected to allow for the ditopic coordination of a ruthenium(II) center. Likewise, the incorporation of two pyrrole subunits, along with two 1,2,3-triazole moieties, into a single molecular framework was expected to allow for the complexation of two Ru(II) cations, while simplifying the synthesis of the starting metal-free form, **4.1**.

The synthesis of **4.1** has been reported earlier.<sup>14</sup> It utilizes the “click”-type copper-catalyzed [3+2] cycloaddition of an aryl diazide and with an alkyne-functionalized pyrrole to create the key triazole functionality.<sup>15</sup> A variety of 1,2,3-triazoles bearing a wide range of functional groups at the 1- and 4- positions can be synthesized *via* the click reaction.<sup>16</sup> In the present instance, dimethylsulfate was used to alkylate the 3-position of the simple triazole **4.1** to afford the triazolium salt **4.2** in 20% yield (Scheme 1).

The triazolium salt **4.2** was tested as a possible carbene precursor by subjecting it to metalation with silver oxide in the presence of tetrabutylammonium chloride. This afforded the bis(triazolylidene) silver complex **4.3** in 84% yield,<sup>17</sup> wherein the silver atom is attached to carbon C(5) (Scheme 1). Complex **4.3**, in turn, was tested as a carbene transfer agent. For example, the new bisruthenium(II) complex **4.4**, containing two triazolylidene donor groups, was prepared in 95% yield via a transmetalation procedure that consisted of adding [Ru(*p*-cymene)Cl<sub>2</sub>]<sub>2</sub> to the silver complex **4.3** in CH<sub>2</sub>Cl<sub>2</sub>.

**Scheme 4.1:** Synthesis of Compounds 4.1-4.4



The structures of **4.2-4.4** were elucidated by X-ray diffraction analysis (Table 4.1). In salt **4.2**, the bis-1,2,3-triazolium ligand displayed a twisted conformation with the two triazolium rings rotated in opposite directions relative to the central benzene ring (Figure 4.1). The dihedral angle between the two triazolium rings was measured to be  $53.4^\circ$ . In each arm of the ligand, the triazolium and pyrrole rings were found to be nearly planar, with dihedral angles between the pair of triazolium and pyrrole rings being  $9.1^\circ$  and  $5.4^\circ$ , respectively. In complex **4.3**, eight  $\text{Ag}^+$  ions are surrounded by four abnormal bis-1,2,3-triazolyldiene ligands to form a twisted macrocycle (Figure 4.2). All eight  $\text{Ag}^+$  ions have similar coordination environments, and each is coordinated to one abnormal NHC carbon atom and one pyrrole nitrogen atom. The C–Ag–N bond angles were nearly linear and range from  $170.2(2)^\circ$  to  $176.2(3)^\circ$ . The average Ag–C and Ag–N distances

were measured to be 2.074 and 2.088 Å, respectively, which are close to literature values.<sup>18</sup> The average Ag–Ag distance between two adjacent Ag<sup>+</sup> ions was measured to be 2.843 Å, which is shorter than the sum of the van der Waals radii for silver(0), 3.440 Å, a finding consistent with a strong metal–metal interaction.<sup>19</sup> It is also noteworthy that the triazolylidene and pyrrole rings appear to rotate in different directions relative to one another, with the dihedral angles between these two subunits varying from 26.9° to 44.4°. These variations are much larger than those present in the metal-free triazolium precursor **4.2**. Intramolecular  $\pi$ – $\pi$  and C–H $\cdots$  $\pi$  interactions are also inferred from the X-ray structure of **4.3** (Figure 4.2). For instance, the distances between the adjacent aryl units range from 3.387 to 3.576 Å. These values are consistent with interaryl interactions, which may add to the overall stability of the twisted macrocyclic structure. On the basis of the results of a microanalytic study (cf. section 4.4.2), it is believed that the key tetrameric structure of **4.3** is also present in the bulk material.

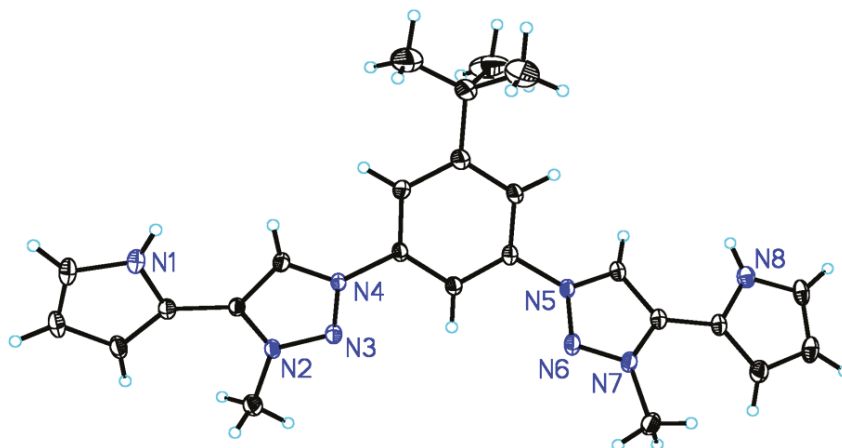


**Figure 4.1:** Single-crystal X-ray structure of **4.2**. All solvent molecules have been omitted for clarity. The dihedral angle between the two triazolium rings is 53.4°. The dihedral angles between the triazolium and pyrrole rings are 9.1° (Plane<sub>N5</sub>/Plane<sub>N8</sub>) and 5.4° (Plane<sub>N2</sub>/Plane<sub>N1</sub>).



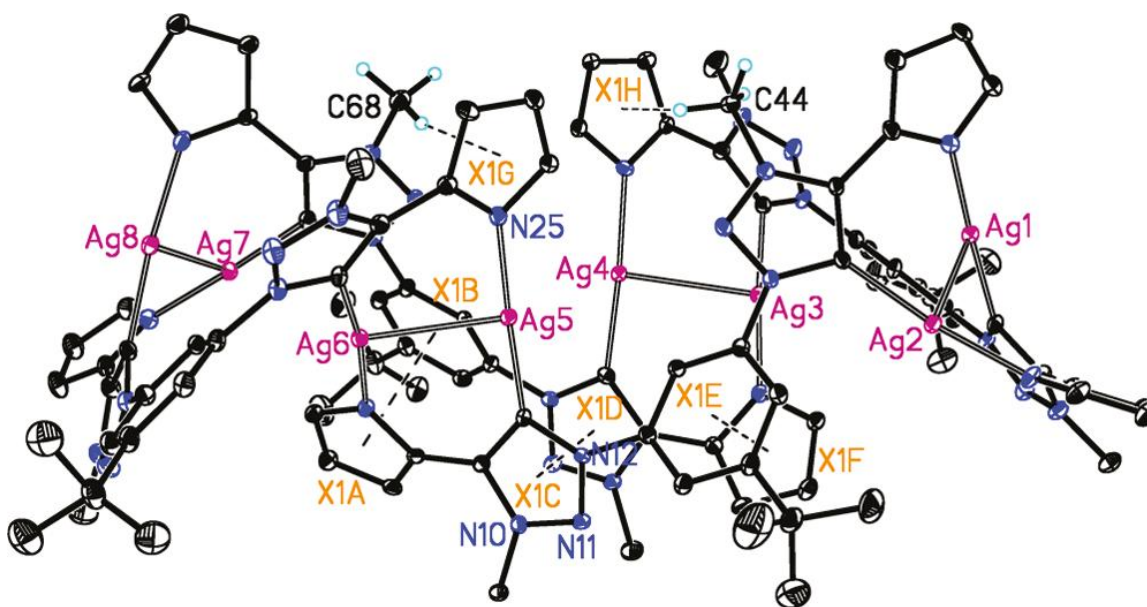


**Figure 4.2:** Single-crystal X-ray structure of **4.3**. All solvent molecules have been omitted for clarity. Short intermolecular  $\pi$ - $\pi$  distances (X1A...X1B: 3.543 Å, X1C...X1D: 3.387 Å, and X1E...X1F: 3.576 Å) and C-H... $\pi$  interactions (C(68)-H... $\pi$ : 2.484 Å, C-H- $\pi$ : 164.6° and C(44)-H... $\pi$ : 2.894 Å and C-H- $\pi$ : 111.2°) are seen in this octa-Ag(I) complex.

In complex **4.4**, two  $\text{Ru}^{2+}$  ions are present on either face of what is formally a ditopic ligand; they are separated from one another by 8.149 Å (Figure 4.3). Both  $\text{Ru}^{2+}$  ions have three-legged piano stool geometries, and each is coordinated to one carbene nucleus, one pyrrole nitrogen atom, one  $\text{Cl}^-$  anion, and one cymene group. The average Ru-C distance is 2.035 Å, a value that is similar to that reported for other complexes in the literature.<sup>20</sup> Interestingly, the bis-1,2,3-triazolylidene ligand present in complex **4.4** shows the same twisted conformation as that found in precursor **4.2**.

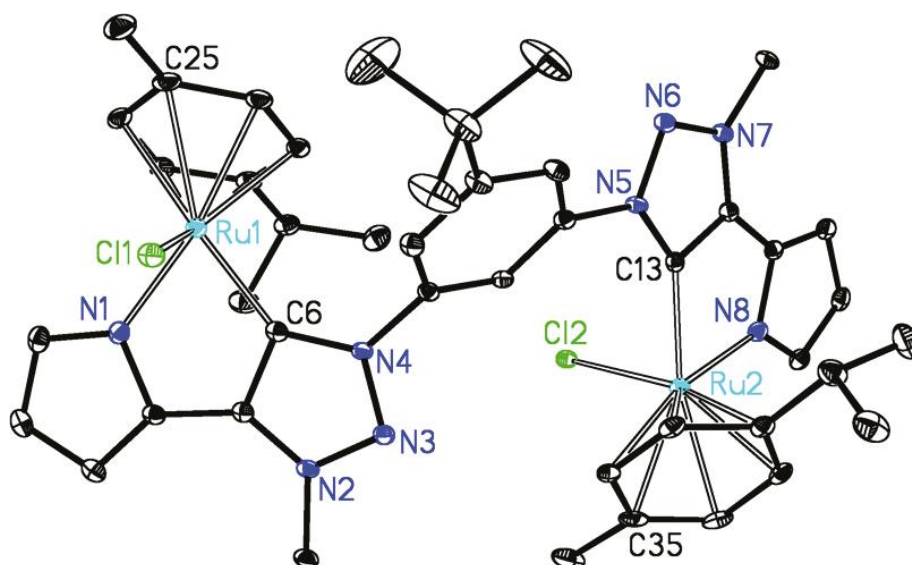


**Figure 4.3:** Single-crystal X-ray structure of **4.4**. All solvent molecules have been omitted for clarity. The dihedral angle between two triazolyldiene rings is 50.9°. The dihedral angles between the triazolyldiene and pyrrole rings are 3.0° (Plane<sub>N5</sub>/Plane<sub>N8</sub>) and 4.1° (Plane<sub>N2</sub>/Plane<sub>N1</sub>). Selected bond lengths and angles: Ru(1)–C(6) = 2.025(6) Å, Ru(1)–N(1) = 2.096(6) Å, Ru(1)–Cl(1) = 2.432(2) Å, Ru(1)–C(centroid) = 1.708 Å; C(6)–Ru(1)–N(1) = 76.3(2)°, C(6)–Ru(1)–Cl(1) = 85.21(18)°, N(1)–Ru(1)–Cl(1) = 87.74(16)°.

Proton nuclear magnetic resonance spectroscopic studies show that both complexes **4.3** and **4.4** are stable in DMSO-*d*<sub>6</sub> solutions at 300 K. As can be seen from an inspection of Figure 4.4, the <sup>1</sup>H NMR spectrum contains 14 signals corresponding to the ruthenium ditopic complex, which is in good agreement with the solid-state structure described above. A 2D-COSY NMR analysis allowed for assignment of the signals (Figure 4.7). Complex **4.4** displays three signals corresponding to the pyrrole ligand. These resonances appear at δ 7.31, 6.45, and 6.09 ppm, respectively, and are shifted to higher field than those of the free ligand, **4.2**. The silver complex **4.3** was also analyzed by <sup>1</sup>H NMR spectroscopy in DMSO-*d*<sub>6</sub>; this revealed a spectrum consistent with the structure deduced from the solid-state structural analysis (Figure 4.6).

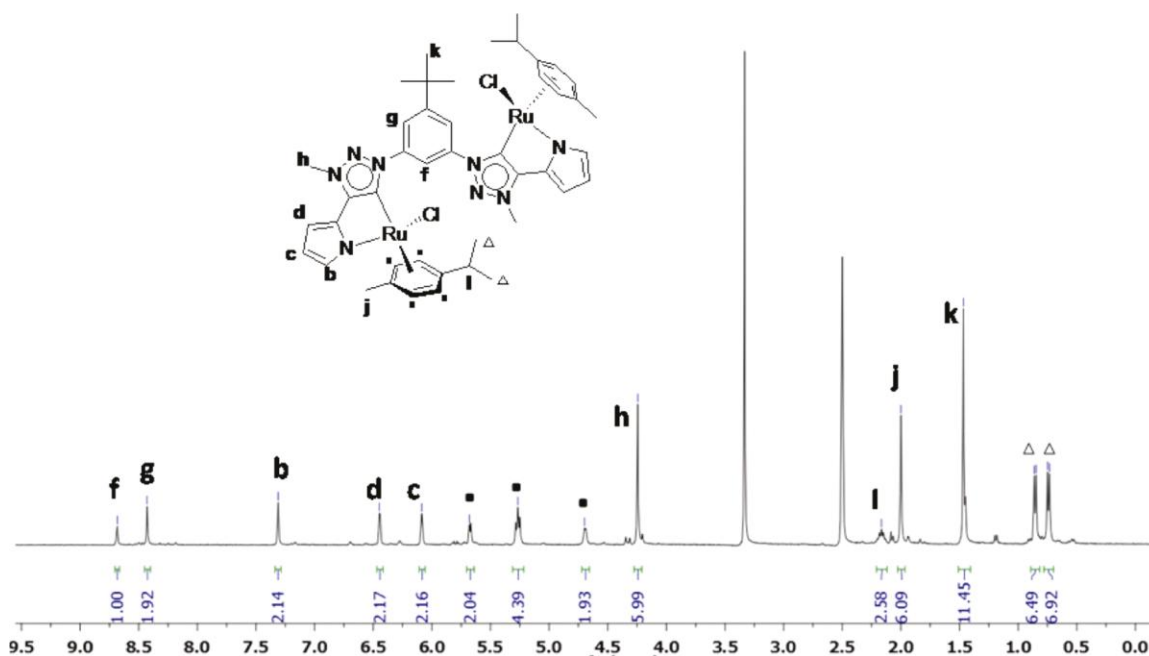


**Figure 4.4:** <sup>1</sup>H NMR spectrum of **4.4** in DMSO-*d*<sub>6</sub> at 300 K.

Upon completing the synthesis and characterization of the ruthenium complex **4.4**, it was tested as a ROMP catalyst.<sup>21</sup> When (trimethylsilyl)diazomethane was added as an initiator,<sup>22</sup> the complex initiated the ROMP of norbornene. The norbornene polymerization reaction was carried out in chlorobenzene under an atmosphere of nitrogen at 60 °C for 15 h with 0.5 mol % of **4.4** and 3.0 mol % of TMSD. Under these conditions, a 95% yield of polynorbornene was obtained (Scheme 4.2). The polymer was determined by gel permeation chromatography to exhibit a number average molecular weight of 46.3 kDa and a polydispersity index of 1.52 relative to polystyrene standards. The importance of the TMSD can be seen in the polymerization kinetics profiles shown in Figure 4.5. Although effective for norbornene, it is to be noted that the combination of **4.4** and TMSD did not prove active for the ROMP of low-strain cyclic olefins, such as cyclooctene, *cis,cis*-1,5-cyclooctadiene, and cyclopentene.

**Scheme 4.2:** Polymerization of Norbornene by the Bis-ruthenium Complex **4.4**

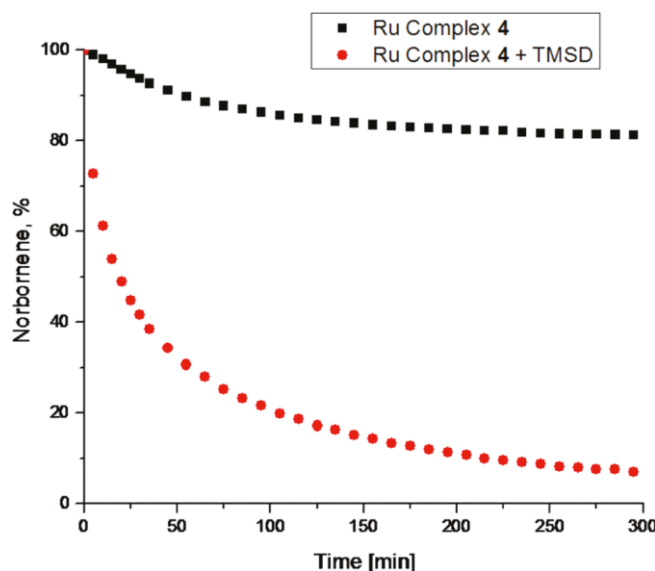
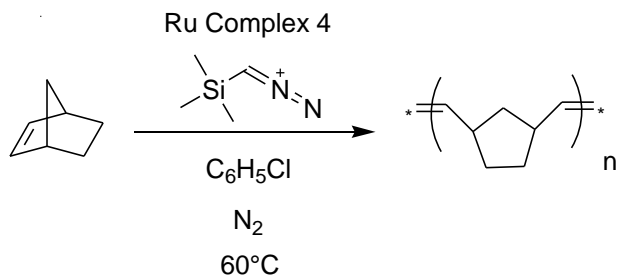


**Figure 4.5:** Norbornene conversion as a function of time with two different catalyst systems.

### 4.3 CONCLUSIONS

In summary, we have successfully synthesized a novel 1,3,4-substituted 1,2,3-triazolium salt that functioned as an effective precursor for the synthesis of new carbene complexes with silver(I) and ruthenium(II) cations. The presence of pyrrole subunits within the ligand framework contributes to the complexation of the Ru(II) centers in a ditopic fashion and gave rise to a novel bis-ruthenium complex that is capable of

polymerizing norbornene when activated with (trimethylsilyl)diazomethane. On the basis of these results, triazolylidene ligands such as those described here are expected to find utility both in the stabilization of new transition metal complexes and in the development of new catalytic systems.

## **4.4 EXPERIMENTAL SECTION**

### **4.4.1 General Procedures**

All reagents and starting materials were obtained from commercial suppliers and used as received unless otherwise noted. Column chromatography was performed on silica gel (40-63  $\mu\text{m}$ , Silicycle, Canada) and Alumina N (50-200  $\mu\text{m}$ , Dynamic Adsorbents Inc., USA). Nuclear magnetic resonance (NMR) spectra were recorded on Varian Mercury 400, Varian Inova 500, or Varian DirectDrive 600 instruments. Low resolution ESI mass spectra were measured using either a Finnigan LCQ Quadrupole Ion Trap mass spectrometer or a Thermo LTQ-XL Linear Ion Trap mass spectrometer. High resolution ESI mass spectra were obtained on an Ion Spec Fourier Transform mass spectrometer (9.4 T). Gel permeation chromatography (GPC) was performed on a Viscotek system equipped with a VE 1122 pump, a VE 7510 degasser, two fluorinated polystyrene columns (IMBHW-3078 and I-MBLMW-3078) thermostated to 30  $^{\circ}\text{C}$  (using a ELDEX CH 150 column heater) and arranged in series or on a homebuilt system equipped with a Waters Model 510 HPLC pump, two fluorinated polystyrene columns (IMBHW-3078 and I-MBLMW-3078) arranged in series, and a Waters 486 Tunable Absorbance Detector. Molecular weight and polydispersity data are reported relative to polystyrene standards in tetrahydrofuran (THF). Microanalyses were performed by Atlantic Microlab, Inc.

#### 4.4.2 Synthetic Experimental

##### Synthesis of 4.2:

A 250 mL round bottom flask was charged with 100 mL acetonitrile, 2.00 g (5.02 mmol) of **4.1** and 3.81 g (30.15 mmol) dimethylsulfate and the resulting mixture was heated at reflux for 4 days. After removal of the solvent *in vacuo*, a brown oil was obtained. This crude product was purified by column chromatography (silica gel, CH<sub>2</sub>Cl<sub>2</sub>:CH<sub>3</sub>OH, 10:0.5, eluent) to yield 651 mg (20%, 1.00 mmol) of a white powder corresponding to **4.2**. X-ray diffraction quality crystals were obtained by vapor diffusion of diethyl ether into a concentrated dimethylformamide solution. <sup>1</sup>H NMR (DMF-*d*<sub>7</sub>, 400 MHz) [ppm], δ 12.23 (s, 2H, NH), 9.97 (s, 2H, -N-CH=C-), 8.77 (t, *J* = 2.0 Hz, 1H, CH), 8.55 (d, *J* = 2.0 Hz, 2H, CH), 7.41 (m, 2H, pyrrole-α-H), 7.13 (dd, *J*<sub>1</sub> = 4.8 Hz, *J*<sub>2</sub> = 1.2 Hz, 2H, pyrrole-β-H), 6.49 (m, 2H, pyrrole-β-H), 4.73 (s, 6H, Trz-CH<sub>3</sub>), 3.53 (s, 6H, CH<sub>3</sub>), 1.53 (s, 9H, CH<sub>3</sub>); <sup>13</sup>C NMR (DMF-*d*<sub>7</sub>, 100 MHz) [ppm], δ 157.7, 138.6, 136.9, 125.5, 125.2, 122.5, 114.3, 114.1, 113.5, 111.3, 53.6, 40.4, 36.7, 30.9; MS (HR-ESI) Calcd. for C<sub>25</sub>H<sub>31</sub>N<sub>8</sub>SO<sub>4</sub> ([M-CH<sub>3</sub>SO<sub>4</sub>]<sup>+</sup>) 539.2184; Found 539.2186 ([M-CH<sub>3</sub>SO<sub>4</sub>]<sup>+</sup>).

##### Synthesis of 4.3:

A 100 mL round bottom flask was charged with compound **4.2** (100 mg, 0.154 mmol), silver oxide (71 mg, 0.308 mmol) and tetrabutylammonium chloride (86 mg, 0.308 mmol) and a mixture of 20 mL dichloromethane and 20 mL acetonitrile. The resulting reaction mixture was stirred for 24 hrs at room temperature under aluminum foil to provide protection from ambient light. After 24 hours, the mixture was filtered through Celite and the solvent was removed using a rotary evaporator. A yellow solid, corresponding to compound **4.3**, was then obtained after recrystallizing the crude residue from a mixture of dichloromethane and acetonitrile to yield 82 mg (84%, 0.032 mmol).

X-ray diffraction quality crystals were obtained by dissolving in a mixture of dichloromethane and acetonitrile and allowing the resulting solution to undergo slow evaporation.  $^1\text{H}$  NMR ( $\text{CDCl}_3$ , 400 MHz) [ppm],  $\delta$  9.68 (m, 2 H,  $\text{H}_{\text{ar}}$ ), 8.65 (m, 2 H,  $\text{H}_{\text{ar}}$ ), 8.47 (m, 2 H,  $\text{H}_{\text{ar}}$ ), 8.01 (m, 4 H,  $\text{H}_{\text{ar}}$ ), 7.79 (m, 2 H,  $\text{H}_{\text{ar}}$ ), 7.14 (m, 2 H, pyrrole-H), 6.83 (m, 2 H, pyrrole-H), 6.67 (m, 2 H, pyrrole-H), 6.57 (m, 6 H, pyrrole-H), 6.46 (m, 6 H, pyrrole-H), 6.34 (m, 4 H, pyrrole-H), 5.91 (m, 2 H, pyrrole-H), 4.27 (s, 12 H, Trz- $\text{CH}_3$ ), 4.11 (s, 6 H, Trz- $\text{CH}_3$ ), 3.52 (s, 6 H, Trz- $\text{CH}_3$ ), 1.35 (s, 18 H,  $\text{CH}_3$ ), 1.29 (s, 18 H,  $\text{CH}_3$ );  $^{13}\text{C}$  NMR ( $\text{CD}_2\text{Cl}_2$ , 100 MHz) [ppm],  $\delta$  159.6, 158.7, 158.2, 157.4, 156.4, 155.9, 155.1, 152.3, 150.0, 149.1, 148.1, 141.0, 140.8, 139.8, 135.5, 132.8, 132.2, 131.2, 125.5, 124.8, 123.2, 120.6, 116.5, 115.8, 114.6, 112.1, 111.5, 110.29, 109.2, 77.6, 59.2, 38.5, 37.4, 35.1, 30.8, 29.7, 24.0, 19.8, 13.2, 1.6; MS (HR-ESI) Calcd. for  $\text{C}_{48}\text{H}_{52}\text{N}_{16}\text{Ag}_2$  ( $[\text{M}/2+4\text{H}-2\text{Ag}]^{2+}$ ) 533.13292; Found 533.13259 ( $[\text{M}/2+4\text{H}-2\text{Ag}]^{2+}$ ); Anal. Calcd for  $\text{C}_{96}\text{H}_{96}\text{Ag}_8\text{N}_{32}$ : C, 45.02; H, 3.78; N, 17.50. Found: C, 44.66; H, 3.81; N, 17.15.

#### Synthesis of 4.4:

A 100 mL round bottom flask was charged with compound **4.3** (78 mg, 0.031 mmol) and dichloro(*p*-cymene) ruthenium(II) dimer (84 mg, 0.138 mmol) in 50 mL dichloromethane. The resulting reaction mixture was stirred for 24 hrs at room temperature under aluminum foil to provide protection from ambient light. The reaction mixture was then filtered through Celite and the solvent removed using a rotary evaporator. After recrystallizing from a mixture of chloroform and hexane, a yellow solid, corresponding to **4.4**, was obtained in 95% yield (112 mg, 0.116 mmol). X-ray diffraction quality crystals were obtained by dissolving in a mixture of chloroform and hexane and allowing the resulting solution to undergo slow evaporation.  $^1\text{H}$  NMR ( $\text{CDCl}_3$ , 400 MHz) [ppm],  $\delta$  8.80 (t,  $J = 2.0$  Hz, 1 H, CH), 8.37 (m, 2 H, CH), 7.38 (m, 2

H, pyrrole- $\alpha$ -H), 6.47 (dd,  $J_1 = 2.8$  Hz,  $J_2 = 0.8$  Hz, 2H, pyrrole- $\beta$ -H), 6.34 (m, 2H, pyrrole- $\beta$ -H), 5.40 (d,  $J = 6$  Hz, 2 H, CH), 5.22 (d,  $J = 6$  Hz, 2 H, CH), 5.17 (d,  $J = 5.6$  Hz, 2 H, CH), 4.77 (d,  $J = 5.6$  Hz, 2 H, CH), 4.18 (s, 6 H, Trz-CH<sub>3</sub>), 2.31 (m, 2 H, CH), 2.05 (s, 6 H, CH<sub>3</sub>), 1.52 (s, 9 H, CH<sub>3</sub>), 0.98 (d,  $J = 6.8$  Hz, 6 H, CH<sub>3</sub>), 0.86 (d,  $J = 7.2$  Hz, 6 H, CH<sub>3</sub>); <sup>13</sup>C NMR (CD<sub>2</sub>Cl<sub>2</sub>, 100 MHz) [ppm],  $\delta$  168.7, 155.5, 147.6, 140.3, 135.3, 128.5, 124.6, 119.5, 111.2, 105.4, 104.6, 101.40, 86.2, 86.0, 84.8, 80.3, 36.9, 36.2, 31.7, 31.5, 22.6, 22.2, 19.3; MS (HR-ESI) Calcd. for C<sub>44</sub>H<sub>52</sub>N<sub>8</sub>Ru<sub>2</sub> ([M-2Cl]<sup>2+</sup>) 448.11955; Found 448.12002 ([M-2Cl]<sup>2+</sup>).

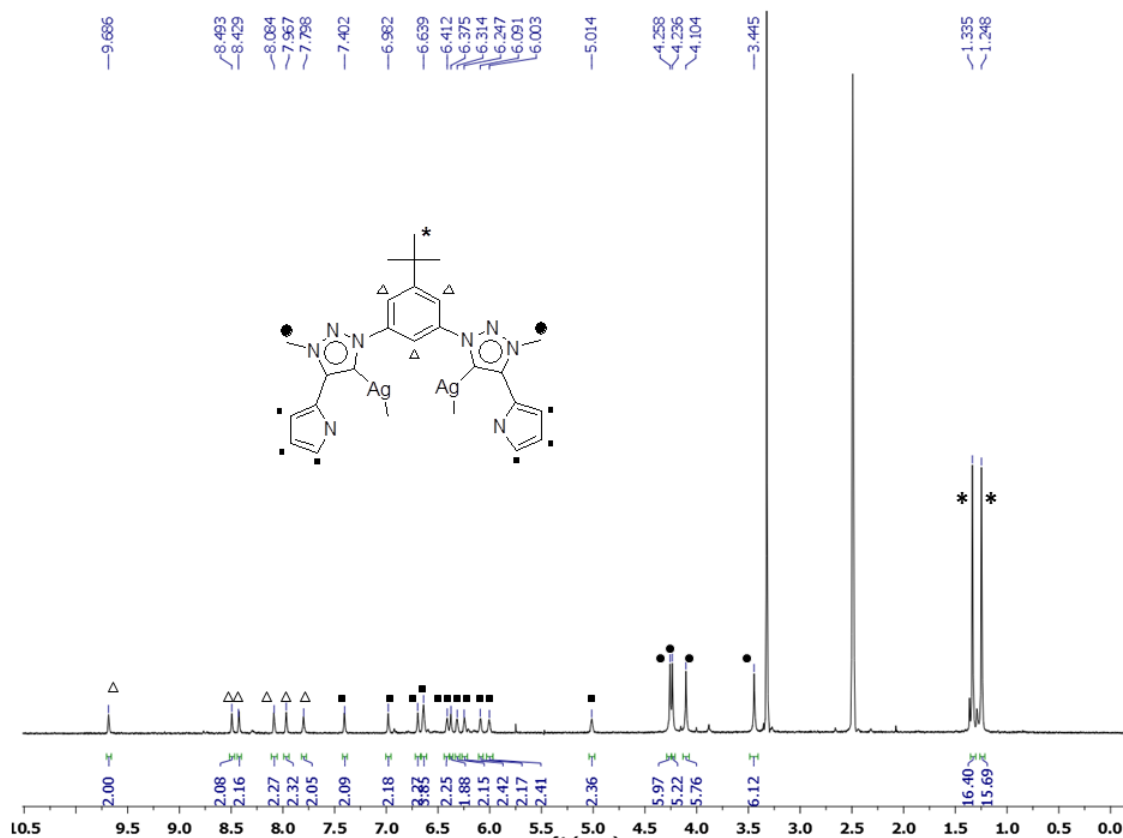


**Figure 4.6:** <sup>1</sup>H NMR spectrum of **4.3** recorded in DMSO-*d*<sub>6</sub> at 300 K.



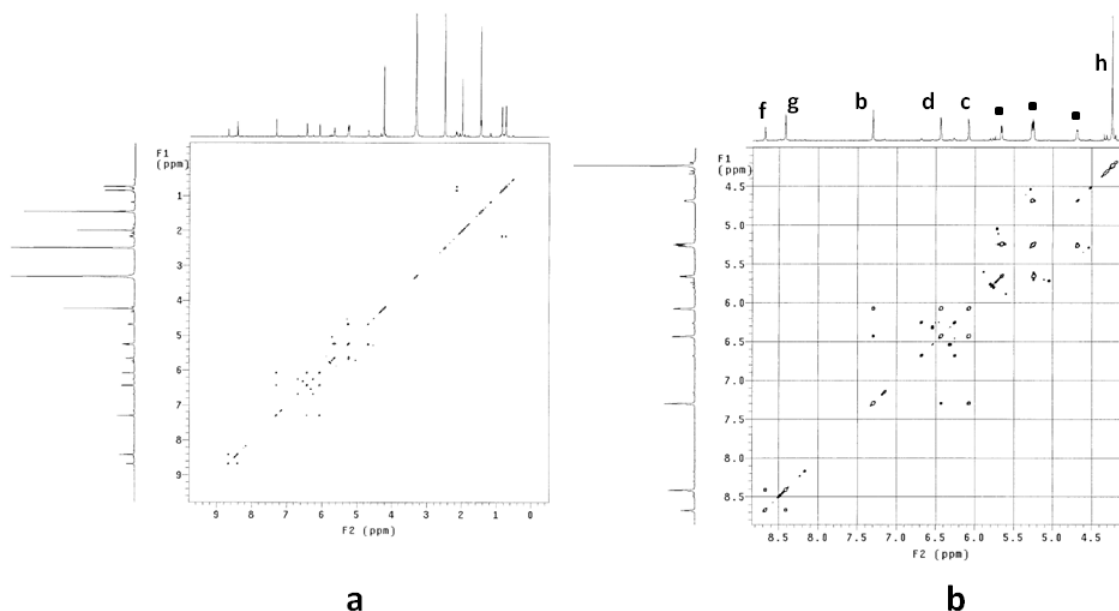


**Figure 4.7:** (a) Full view and (b) expanded view of the 2D COSY NMR spectrum of **4.4** recorded in DMSO-*d*<sub>6</sub> at 300 K

#### 4.4.3 Ring Opening Metathesis Polymer

##### Typical procedure for the ROMP of norbornene

Inside an N<sub>2</sub>-filled dry box, a small vial was charged with 100 mg (1.062 mmol) of norbornene, 4.5 mL of chlorobenzene and a stir bar. The vial was sealed. A separate vial was charged with 5.13 mg (5.310 μmol) of catalyst **4.4** and 0.5 mL of chlorobenzene. The catalyst solution was then transferred to the vial containing norbornene *via* syringe. At this point 15.93 μL (31.86 μmol) (trimethylsilyl)diazomethane (TMSD, 2.0 M in hexanes) was added *via* syringe. After 15 hrs at 60 °C, 344 μL (2.655 mmol, 500 equiv relative to catalyst) of butyl vinyl ether was added to quench the polymerization. The reaction mixture was then poured into excess methanol (30 mL) with stirring; this caused precipitation of a white solid. After collecting the solid by filtration, it was washed with

fresh methanol (10 mL) three times giving the polymer **4.5** in yields up to 95%. The resulting polymer was analyzed by GPC and NMR spectroscopy.

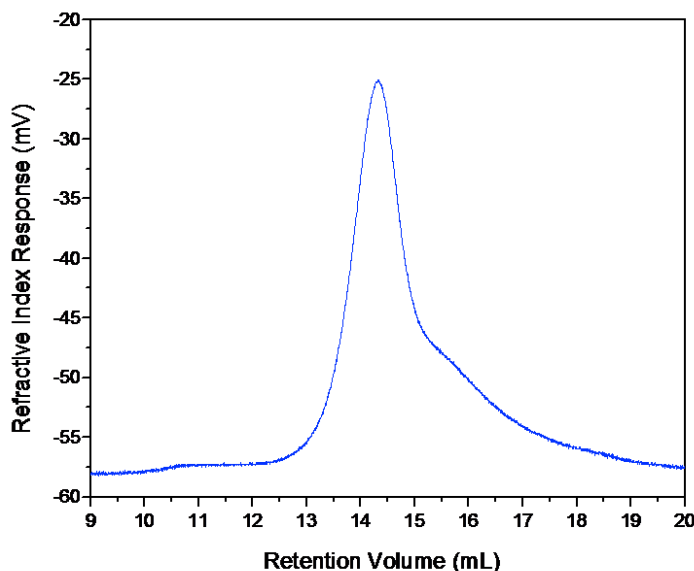


**Figure 4.8:** Gel permeation chromatography of polynorbornene **4.5**. Its number average molar mass ( $M_n$ ) is 46364 Daltons. Its weight average molar mass ( $M_w$ ) is 70240 Daltons.

Inside an  $N_2$ -filled dry box, a small vial was charged with 100 mg (1.062 mmol) of norbornene, 4.5 mL of chlorobenzene and a stir bar. The vial was sealed. A separate vial was charged with 5.13 mg (5.310  $\mu$ mol) of catalyst **4.4** and 0.5 mL of chlorobenzene. The catalyst solution was then transferred to the vial containing norbornene *via* syringe. After 15 hrs at 60  $^{\circ}C$ , 344  $\mu$ L (2.655 mmol, 500 equiv. relative to catalyst) of butyl vinyl ether was added to quench the polymerization. The reaction mixture was then poured into excess stirring methanol (30 mL), causing precipitation of a white solid. After filtering, the resulting solid was washed with fresh methanol (10 mL) three times to give the

expected polymer **4.6** in less than 1% yield. In spite of the low yield, the polymer obtained this way was analyzed by GPC.

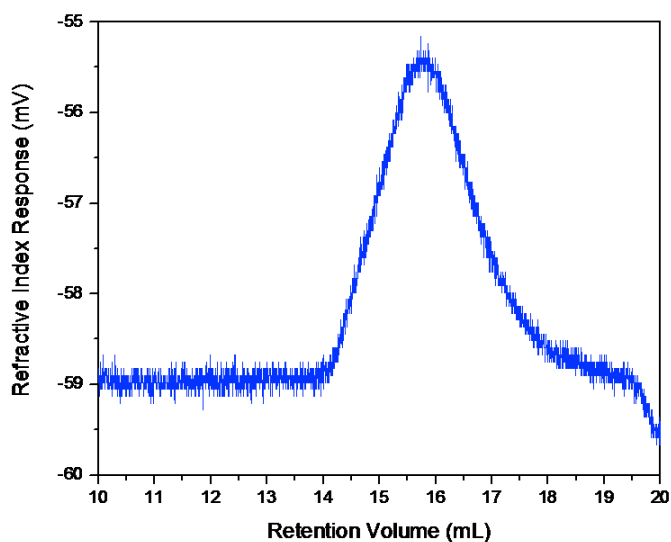


**Figure 4.9:** Gel permeation chromatography of polynorbornene **4.6**. Its number average molar mass ( $M_n$ ) is 29279 Daltons. Its weight average molar mass ( $M_w$ ) is 31496 Daltons.

#### 4.4.4 NMR Spectroscopic-based Kinetic Studies

An NMR tube with a screw-cap septum top was charged inside a glovebox with 20 mg (0.213 mmol) of norbornene and 0.7 mL of deuterated chlorobenzene. A 1 mL glass syringe was charged inside a glovebox with 1.03 mg (1.065  $\mu$ mol) of catalyst **4.4** and 0.3 mL of deuterated chlorobenzene. The norbornene solution was equilibrated at 60 °C in the NMR instrument. The spectrum of the starting material was collected. Then the NMR tube was taken out of the NMR instrument. The catalyst **4.4** solution prepared before and 3.2  $\mu$ L (6.390  $\mu$ mol) (trimethylsilyl)diazomethane (TMSD, 2.0 M in hexanes)

were added into the NMR tube *via* syringe. Data points were collected every five minutes at 60 °C for five hours. Norbornene conversion was monitored by NMR spectroscopy.

An NMR tube with a screw-cap septum top was charged inside a glovebox with 20 mg (0.213 mmol) of norbornene and 0.7 mL of deuterated chlorobenzene. A 1 mL glass syringe was charged inside a glovebox with 1.03 mg (1.065  $\mu$ mol) of catalyst **4.4** and 0.3 mL of deuterated chlorobenzene. The norbornene solution was equilibrated at 60 °C in the NMR instrument. The spectrum of the starting material was collected. Then the NMR tube was taken out of the NMR instrument. The catalyst **4.4** solution prepared before was added into the NMR tube *via* syringe. Data points were collected every five minutes at 60 °C for five hours. Norbornene conversion was monitored by NMR spectroscopy.

#### 4.4.5 Crystallographic Data (CIF)

Crystals used in this study were obtained by the author. They were in the form of multiply intergrown, colorless prisms in the case of compound **4.2**·DMF, yellow prisms in the case of the complex **4.3**, and red prisms in the case of complex **4.4** · 3CHCl<sub>3</sub>. Diffraction grade crystals of compound **4.2** · DMF were obtained by vapor diffusion of diethyl ether into a concentrated dimethyl formide solution. Crystals of the complex **4.3** were obtained by slow evaporation from solution using a mixture of CH<sub>2</sub>Cl<sub>2</sub> / CH<sub>3</sub>CN as the solvent. Crystals of the complex **4.4** · 3CHCl<sub>3</sub> were obtained by slow evaporation from solution using a mixture of CHCl<sub>3</sub> / hexane. The data crystals were cut from a

cluster of crystals and had the approximate dimensions given in Table 4.1. The data were collected by the author on a Rigaku Saturn CCD diffractometer using a graphite monochromator with MoK $\alpha$  radiation ( $\lambda = 0.71075 \text{ \AA}$ ). The data were collected using  $\omega$ -scans with a scan range of  $1^\circ$  at low temperature shows using an Oxford Cryostream low temperature device (Table 4.1). Data reduction was performed using DENZO-SMN.<sup>23</sup> The structures were solved by Dr. Xiaoping Yang *via* direct methods using SIR97<sup>24</sup> and refined by full-matrix least-squares on  $F^2$  with anisotropic displacement parameters for the non-H atoms using SHELXL-97.<sup>25</sup> The hydrogen atoms were calculated in ideal positions with isotropic displacement parameters set to  $1.2 \times U_{eq}$  of the attached atom ( $1.5 \times U_{eq}$  for methyl hydrogen atoms).

The function,  $\Sigma w(|F_o|^2 - |F_c|^2)^2$ , was minimized. Definitions used for calculating  $R(F)$ ,  $R_w(F^2)$  and the goodness of fit,  $S$ , are given below.<sup>26</sup> Neutral atom scattering factors and values used to calculate the linear absorption coefficient are from the International Tables for X-ray Crystallography (1992).<sup>27</sup> All ellipsoid figures were generated using SHELXTL/PC.<sup>28</sup> Tables of positional and thermal parameters, bond lengths and angles, torsion angles, figures and lists of observed and calculated structure factors are located in the cif documents available from the Cambridge Crystallographic Centre *via* quoting ref. numbers 815272, 815273 and 815274. These documents also contain details of crystal data, data collection and structure refinement.

**Table 4.1:** X-ray crystallographic data comparison of compound 4.2·DMF, complex 4.3 and complex 4.4·3CHCl<sub>3</sub>.

	compound 4.2·DMF	complex 4.3	complex 4.4·3CHCl <sub>3</sub>
CCDC No.	815272	815273	815274
empirical formula	C <sub>29</sub> H <sub>41</sub> N <sub>9</sub> O <sub>9</sub> S <sub>2</sub>	C <sub>96</sub> H <sub>96</sub> Ag <sub>8</sub> N <sub>32</sub>	C <sub>47</sub> H <sub>55</sub> Cl <sub>11</sub> N <sub>8</sub> Ru <sub>2</sub>
Fw	723.83	2561.01	1324.08
crystal size (mm <sup>3</sup> )	0.20 × 0.20 × 0.20	0.20 × 0.20 × 0.20	0.20 × 0.15 × 0.15
Crystal system	Monoclinic	Monoclinic	Triclinic
Space group	P2(1)/c	P2(1)/c	P-1
<i>a</i> [Å]	7.8083(10)	28.467(9)	12.278(11)
<i>b</i> [Å]	24.654(3)	20.046(5)	15.409(13)
<i>c</i> [Å]	18.254(3)	24.278(7)	15.539(14)
<i>α</i> [deg]	90.00	90.00	86.89(4)
<i>β</i> [deg]	91.028(4)	107.549(4)	79.58(4)
<i>γ</i> [deg]	90.00	90.00	73.46(4)
<i>V</i> [Å <sup>3</sup> ]	3513.5(8)	13209(7)	2772(4)
<i>d</i> [g/cm <sup>3</sup> ]	1.368	1.288	1.587
<i>Z</i>	4	4	2
<i>T</i> [K]	113(1)	113(1)	113(1)
R1, wR2 <i>I</i> > 2σ( <i>I</i> )	0.0875, 0.2304	0.0552, 0.1582	0.0700, 0.1865
R1, wR2 (all data)	0.1101, 0.2500	0.0778, 0.1767	0.0789, 0.1949
Quality of fit	1.131	1.040	1.055

## 4.5 REFERENCES

- (1) (a) Herrmann, W. *Angew. Chem., Int. Ed.* **2002**, *41*, 1290. (b) Nolan, S. P., Ed. *N-Heterocyclic Carbene in Synthesis*; Wiley-VCH: New York, 2006.
- (2) (a) Enders, D.; Balensiefer, T. *Acc. Chem. Res.* **2004**, *37*, 534. (b) Enders, D.; Niemeier, O.; Henseler, A. *Chem. Rev.* **2007**, *107*, 5606. (c) Biju, A. T.; Kuhl, N.; Glorius, F. *Acc. Chem. Res.* **2011**, in press, doi: 10.1021/ar2000716.
- (3) (a) Coady, D. J.; Bielawski, C. W. *Macromolecules* **2006**, *39*, 8895. (b) Coady, D. J.; Norris, B. C.; Lynch, V. M.; Bielawski, C. W. *Macromolecules* **2008**, *41*, 3775. (c) Rosen, E. L.; Varnado, C. D., Jr.; Tennyson, A. G.; Khramov, D. M.; Kamplain, J. W.; Sung, D. H.; Cresswell, P. T.; Lynch, V. M.; Bielawski, C. W. *Organometallics* **2009**, *28*, 6695. (d) Varnado C. D., Jr.; Lynch, V. M.; Bielawski, C. W. *Dalton Trans.* **2009**, 7253. (e) Coady, D. J.; Khramov, D. M.; Norris, B. C.; Tennyson, A. G.; Bielawski, C. W. *Angew. Chem. Int. Ed.* **2009**, *48*, 5187. (f) Norris, B. C.; Bielawski, C. W. *Macromolecules* **2010**, *43*, 3591. (g) Crabtree, R. H., Ed. *Coord. Chem. Rev.* **2007**, *251*, 595. (h) Glorius, F., Ed. *Top. Organomet. Chem.* **2007**, *21*. (i) Hahn, F. E.; Jahnke, M. C. *Angew. Chem., Int. Ed.* **2008**, *47*, 3122.
- (4) Bourissou, D.; Guerret, O.; Gabbai, F. P.; Bertrand, G. *Chem. Rev.* **2000**, *100*, 39.
- (5) (a) Enders, D.; Breuer, K.; Kallfass, U.; Balensiefer, T. *Synthesis* **2003**, *8*, 1292. (b) Frey, G. D.; Schütz, J.; Herdtweck, E.; Herrmann, W. A. *Organometallics* **2005**, *24*, 4416. (c) Poyatos, M.; McNamara, W.; Incarvito, C.; Peris, E.; Crabtree, R. H. *Chem. Commun.* **2007**, 2267. (d) Gnanamgari, D.; Moores, A.; Rajaseelan, E.; Crabtree, R. H. *Organometallics* **2007**, *26*, 1226. (e) Diez-Gonzalez, S.; Marion, N.; Nolan, S. P. *Chem. Rev.* **2009**, *109*, 3612.
- (6) (a) Gründemann S.; Kovacevic, A.; Albrecht, M.; Faller, J. W.; Crabtree, R. H. *Chem. Commun.* **2001**, 2274; (b) Gründemann, S.; Kovacevic, A.; Albrecht, M.; Faller, J. W.; Crabtree, R. H. *J. Am. Chem. Soc.* **2002**, *124*, 10473.
- (7) Han, Y.; Huynh, H. V. *Chem. Commun.* **2007**, 1089.
- (8) Lavallo, V.; Canac, Y.; Präsang, C.; Donnadiou, B.; Bertrand, G. *Angew. Chem., Int. Ed.* **2005**, *44*, 5705.
- (9) (a) Lavallo, V.; Dyker, C. A.; Donnadiou, B.; Bertrand, G. *Angew. Chem. Int. Ed.* **2008**, *47*, 5411. (b) Aldeco-Perez, E.; Rosenthal, A. J.; Donnadiou, B.; Parameswaran, P.; Frenking, G.; Bertrand, G. *Science* **2009**, *326*, 556. (c) Guisado-Barrios, G.; Bouffard, J.; Donnadiou, B.; Bertrand, G. *Angew. Chem. Int. Ed.* **2010**, *49*, 4759.
- (10) (a) Albrecht, M. *Chem. Commun.* **2008**, 3601. (b) Song, G.; Zhang, Y.; Li, X. *Organometallics* **2008**, *27*, 1936. (c) Schuster, O.; Yang, L.; Raubenheimer, H. G.; Albrecht, M. *Chem. Rev.* **2009**, *109*, 3445. (d) Melaimi, M.; Soleilhavoup, M.; Bertrand, G. *Angew. Chem. Int. Ed.* **2010**, *49*, 8810.

- (11) (a) Lebel, H.; Janes, M. K.; Charette, A. B.; Nolan, S. P. *J. Am. Chem. Soc.* **2004**, *126*, 5046. (b) Heckenroth, M.; Kluser, E.; Neels, A.; Albrecht, M. *Angew. Chem., Int. Ed.* **2007**, *46*, 6293. (c) Yang, L.; Krüger, A.; Neels, A.; Albrecht, M. *Organometallics* **2008**, *27*, 3161.
- (12) (a) Mathew, P.; Neels, A.; Albrecht, M. *J. Am. Chem. Soc.* **2008**, *130*, 13534. (b) Karthikeyan, T.; Sankararaman, S. *Tetrahedron Lett.* **2009**, *50*, 5834. (c) Nakamura, T.; Ogata, K.; Fukuzawa, S. *Chem. Lett.* **2010**, *39*, 920. (d) Lalrempuia, R.; McDaniel, N. D.; Müller-Bunz, H.; Bernhard, S.; Albrecht, M. *Angew. Chem. Int. Ed.* **2010**, *49*, 9765. (e) Saravanakumar, R.; Ramkumar, V.; Sankararaman, S. *Organometallics* **2011**, *30*, 1689. (f) Poulain, A.; Canseco-Gonzalez, D.; Hynes-Roche, R.; Albrecht, M. *Organometallics* **2011**, *30*, 1021. (g) Nakamura, T.; Terashima, T.; Ogata, K.; Fukuzawa, S. *Org. Lett.* **2011**, *13*, 620. (h) Kilpin, K. J.; Paul, U. S. D.; Lee, A.; Crowley, J. D. *Chem. Commun.* **2011**, *47*, 328. (i) Schulze, B.; Escudero, D.; Friebe, C.; Siebert, R.; Görls, H.; Köhn, U.; Altuntas, E.; Baumgaertel, A.; Hager, M. D.; Winter, A.; Dietzek, B.; Popp, J.; González, L.; Schubert, U. S. *Chem. Eur. J.* **2011**, *17*, 5494. (j) Bernet, L.; Lalrempuia, R.; Ghattas, W.; Mueller-Bunz, H.; Vigara, L.; Llobet, A.; Albrecht, M. *Chem. Commun.* **2011**, *47*, 8058. (k) Hohloch, S.; Su, C-Y.; Sarkar, B. *Eur. J. Inorg. Chem.* **2011**, 3067. (l) Schuster, E. M.; Botoshansky, M.; Gandelman, M. *Dalton Trans.* **2011**, in press, doi: 10.1039/C1DT10264H.
- (13) (a) Altman, R. A.; Anderson, K. W.; Buchwald, S. L. *J. Org. Chem.* **2008**, *73*, 5167. (b) Zi, G-F; Xiang, L.; Song, H-B. *Organometallics* **2008**, *27*, 1242.
- (14) Sessler, J. L.; Cai, J.; Gong, H-Y.; Yang, X.; Arambula, J. F.; Hay, B. P. *J. Am. Chem. Soc.* **2010**, *132*, 14058.
- (15) Rostovtsev, V. V.; Green, L. G.; Fokin, V. V.; Sharpless, K. B. *Angew. Chem., Int. Ed.* **2002**, *41*, 2596.
- (16) (a) Tornøe, C. W.; Christensen, C.; Meldal, M. *J. Org. Chem.* **2002**, *67*, 3057. (b) Hawker, C. J.; Wooley, K. L. *Science* **2005**, *309*, 1200. (c) Devaraj, N. K.; Dnolfo, P. H.; Chidsey, C. E. D.; Collman, J. P. *J. Am. Chem. Soc.* **2006**, *128*, 1794. (d) Burley, G. A.; Gierlich, J.; Mofid, M. R.; Nir, H.; Tal, S.; Eichen, Y.; Carell, T. *J. Am. Chem. Soc.* **2006**, *128*, 1398. (e) Meldal, M.; Tornøe, C. W. *Chem. Rev.* **2008**, *108*, 2952.
- (17) Lee, K. M.; Wang, H. M. J.; Lin, I. J. B. *J. Chem. Soc., Dalton Trans.* **2002**, 2852.
- (18) Arduengo, A. J., III; Dias, H. V. R.; Calabrese, J. C.; Davidson, F. *Organometallics* **1993**, *12*, 3405.
- (19) (a) Garrison, J. C.; Youngs, W. J. *Chem. Rev.* **2005**, *105*, 3978. (b) Hahn, F. E.; Radloff, C.; Pape, T.; Hepp, A. *Chem. Eur. J.* **2008**, *14*, 10900.
- (20) Prades, A.; Peris, E.; Albrecht, M. *Organometallics* **2011**, *30*, 1162.



- (21) (a) Keitz, B. K.; Bouffard, J.; Bertrand, G.; Grubbs, R. H. *J. Am. Chem. Soc.* **2011**, *133*, 8498. (b) Bouffard, J.; Keitz, B. K.; Tonner, R.; Guisado-Barrios, G.; Frenking, G.; Grubbs, R. H.; Bertrand, G. *Organometallics* **2011**, *30*, 2617. (c) Bielawski, C. W.; Grubbs, R. H. *Prog. Polym. Sci.* **2007**, *32*, 1.
- (22) Demonceau, A.; Stumpf, A. W.; Saive, E.; Noels, A. F. *Macromolecules* **1997**, *30*, 3127.
- (23) DENZO-SMN. (1997). Otwinowski, Z.; Minor, W. *Methods in Enzymology*, 276: *Macromolecular Crystallography, Part A*, 307 – 326, Carter, C.W.J.; Simon, M.I.; Sweet, R. M. Editors, Academic Press.
- (24) SIR97. (1999). A program for crystal structure solution. Altomare, A.; Burla, M. C.; Camalli, M.; Cascarano, G. L.; Giacovazzo, C.; Guagliardi, A.; Moliterni, A.G. G.; Polidori, G.; Spagna, R. *J. Appl. Cryst.* **1999**, *32*, 115-119.
- (25) Sheldrick, G. M. *SHELXL97. Program for the Refinement of Crystal Structures*; University of Gottingen, Germany, **1994**.
- (26)  $R_w(F^2) = \{\sum w(|F_o|^2 - |F_c|^2)^2 / \sum w(|F_o|^4)\}^{1/2}$  where  $w$  is the weight given each reflection.  $R(F) = \sum(|F_o| - |F_c|) / \sum |F_o|$  for reflections with  $F_o > 4(\sigma(F_o))$ .  $S = [\sum w(|F_o|^2 - |F_c|^2)^2 / (n - p)]^{1/2}$ , where  $n$  is the number of reflections and  $p$  is the number of refined parameters.
- (27) *International Tables for X-ray Crystallography*; Wilson, A. J. C., Ed.; Kluwer Academic Press: Boston, **1992**; Vol. C, Tables 4.2.6.8 and 6.1.1.4.
- (28) Sheldrick, G.M. (1994). SHELXTL/PC (Version 5.03). Siemens Analytical X-ray Instruments, Inc., Madison, Wisconsin, USA.

## References

- (1) Sessler, J. L.; Gale, P. A.; Cho, W.-S. *Anion Receptor Chemistry*; RSC Publishing: Cambridge, U.K., 2006.
- (2) Fields, S. *Environ. Health Perspect.* **2004**, *112*, A557-A563.
- (3) Lijinsky, W. *J. Environ. Sci. Health* **1986**, *C4*, 1-45.
- (4) Katayev, E. A.; Ustynyuk, Y. A.; Sessler, J. L. *Coord. Chem. Rev.* **2006**, *250*, 3004.
- (5) Xu, S.; He, M.; Yu, H.; Cai, X.; Tan, X.; Lu, B.; Shu, B. *Anal. Biochem.* **2001**, *299*, 188.
- (6) Ronaghi, M.; Karamohamed, S.; Pettersson, B.; Uhlén, M.; Nyren, P. *Anal. Biochem.* **1996**, *242*, 84.
- (7) Saenger, W. *Principles of Nucleic Acid Structure*; Springer-Verlag: New York, 1988.
- (8) Shannon, R. D. *Acta Cryst.* **1976**, *A32*, 751.
- (9) Marcus, Y. *J. Chem. Soc., Faraday Trans.* **1991**, *87*, 2995.
- (10) Lehn, J.-M. *Supramolecular Chemistry*; Wiley-VCH: Weinheim, 1995.
- (11) Atwood, J. L.; Steed, J. W. *Encyclopedia of Supramolecular Chemistry*. M. Dekker: New York, 2004.
- (12) Desiraju, G. R.; Steiner, T. *The Weak Hydrogen Bond in Structural Chemistry and Biology*. Oxford University Press: Oxford, 1999.
- (13) Beer, P. D.; Gale, P. A. *Angew. Chem., Int. Ed.* **2001**, *40*, 486.
- (14) Bianchi, A.; Bowman-James, K.; García-España, E. *Supramolecular Chemistry of Anions*; Wiley-VCH: Chichester, New York, 1997.
- (15) *Research Needs for High-Level Waste Stored in Tanks and Bins at U.S. Department of Energy Sites*. National Research Council, National Academy Press: Washington, D.C., 2001.
- (16) *Fundamentals and Applications of Anion Separations*. Moyer, B. A.; Singh, R. P. Eds.; Kluwer Academic/Plenum: New York, 2004.
- (17) Schmidtchen, F. P.; Berger, M. *Chem. Rev.* **1997**, *97*, 1609.
- (18) Kumler, W. D. *J. Am. Chem. Soc.* **1935**, *57*, 600.
- (19) Pauling, L. *J. Am. Chem. Soc.* **1935**, *57*, 2680.

- (20) Sutor, D. J. *J. Chem. Soc.* **1963**, 1105.
- (21) Taylor, R.; Kennard, O. *J. Am. Chem. Soc.* **1982**, *104*, 5063.
- (22) Farnham, W. B.; Roe, D. C.; Dixon, D. A.; Calabrese, J. C.; Harlow, R. L. *J. Am. Chem. Soc.* **1990**, *112*, 7707.
- (23) Ilioudis, C. A.; Tocher, D. A.; Steed, J. W. *J. Am. Chem. Soc.* **2004**, *126*, 12395.
- (24) Bryantsev, V. S.; Hay, B. P. *J. Am. Chem. Soc.* **2005**, *127*, 8282.
- (25) Coletti, C.; Re, N. *J. Phys. Chem. A*, **2009**, *113*, 1578.
- (26) Bryantsev, V. S.; Hay, B. P. *Org. Lett.* **2005**, *7*, 5031.
- (27) Zhu, S. S.; Staats, H.; Brandhorst, K.; Grunenberg, J.; Gruppi, F.; Dalcanele, E.; Luetzen, A.; Rissanen, K.; Schalley, C. A. *Angew. Chem., Int. Ed.* **2008**, *47*, 788.
- (28) Li, Y.; Flood, A. H. *Angew. Chem., Int. Ed.* **2008**, *47*, 2649.
- (29) Juwarker, H.; Lenhardt, J. M.; Pham, D. M.; Craig, S. L. *Angew. Chem., Int. Ed.* **2008**, *47*, 3740.
- (30) Meudtner, R. M.; Hecht, S. *Angew. Chem., Int. Ed.* **2008**, *47*, 4926.
- (31) Yoon, D. W.; Gross, D. E.; Lynch, V. M.; Sessler, J. L.; Hay, B. P.; Lee, C. H. *Angew. Chem., Int. Ed.* **2008**, *47*, 5038.
- (32) Berryman, O. B.; Sather, A. C.; Hay, B. P.; Meisner, J. S.; Johnson, D. W. *J. Am. Chem. Soc.* **2008**, *130*, 10895.
- (33) Li, Y.; Flood, A. H. *J. Am. Chem. Soc.* **2008**, *130*, 12111.
- (34) Maeda, H.; Mihashi, Y.; Haketa, Y. *Org. Lett.* **2008**, *10*, 3179.
- (35) (a) Martínez-Máñez, R.; Sancenón, F. *Chem. Rev.* **2003**, *103*, 4419. (b) Sessler, J. L.; Seidel, D. *Angew. Chem., Int. Ed.* **2003**, *42*, 5134. (c) Gale, P. A. *Coord. Chem. Rev.* **2003**, *240*, 191. (d) Beer, P. D.; Gale, P. A. *Angew. Chem., Int. Ed.* **2001**, *40*, 486. (e) Cho, E. J.; Moon, J. W.; Ko, S. W.; Lee, J. Y.; Kim, S. K.; Yoon, J.; Nam, K. C. *J. Am. Chem. Soc.* **2003**, *125*, 12376. (f) Snowden, T. S.; Anslyn, E. V. *Chem. Biol.* **1999**, *3*, 740. (g) Antonisse, M. M. G.; Reinhoudt, D. N. *Chem. Commun.* **1998**, 143. (h) Schmidtchen, F. P.; Berger, M. *Chem. Rev.* **1997**, *97*, 1609.
- (36) (a) Holbrey, J. D.; Reichert, W. M.; Nieuwenhuyzen, M.; Johnston, S.; Seddon, K. R.; Rogers, R. D. *Chem. Commun.* **2003**, 1636. (b) Holbrey, J. D.; Reichert, W. M.; Rogers, R. D. *Dalton Trans.* **2004**, 2267. (c) Custelcean, R.; Delmau, L. H.; Moyer, B. A.; Sessler, J. L.; Cho, W.-S.; Gross, D.; Bates, G. W.; Brooks, S. J.; Light, M. E.; Gale, P. A. *Angew. Chem., Int. Ed.* **2005**, *44*, 2537.
- (37) Avent, A. G.; Chaloner, P. A.; Day, M. P.; Seddon, K. R.; Welton, T. *J. Chem. Soc., Dalton Trans.* **1994**, 3405.

- (38) Sato, K.; Arai, S.; Yamagishi, T. *Tetrahedron Lett.* **1999**, *40*, 5219.
- (39) Alcalde, E.; Alvarez-Rúa, C.; García-Granda, S.; Gracia-Rodriguez, E.; Mesquida, N.; Pérez-García, L. *Chem. Commun.* **1999**, 295.
- (40) Chellappan, K.; Singh, N. J.; Hwang, I.-C.; Lee, J. W.; Kim, K. S. *Angew. Chem., Int. Ed.* **2005**, *44*, 2899.
- (41) Kwon, J. Y.; Singh, N. J.; Kim, H.; Kim, S. K.; Kim, K. S.; Yoon, J. *J. Am. Chem. Soc.* **2004**, *126*, 8892.
- (42) Dinarès, I.; Garcia de Miguel, C.; Mesquida, N.; Alcalde, E. *J. Org. Chem.* **2009**, *74*, 482.
- (43) Kim, S. K.; Kang, B.-G.; Koh, H. S.; Yoon, Y.-J.; Jung, S. J.; Jeong, B.; Lee, K.-D.; Yoon, J. *Org. Lett.* **2004**, *6*, 4655.
- (44) Ho, H. A.; Leclerc, M. *J. Am. Chem. Soc.* **2003**, *125*, 4412.
- (45) (a) Kolb, H. C.; Finn, M. G.; Sharpless, K. B. *Angew. Chem., Int. Ed.* **2001**, *40*, 2004. (b) Tornøe, C. W.; Meldal, M. *Chem. Rev.* **2008**, *108*, 2952.
- (46) (a) Moses, J. E.; Moorhouse, A. D. *Chem. Soc. Rev.* **2007**, *36*, 1249. (b) Fournier, D.; Hoogenboom, R.; Schubert, U. S. *Chem. Soc. Rev.* **2007**, *36*, 1369. (c) Lutz, J. F. *Angew. Chem., Int. Ed.* **2007**, *46*, 1018. (d) Ladmiral, V.; Mantovani, G.; Clarkson, G. J.; Cauet, S.; Irwin, J. L.; Haddleton, D. M. *J. Am. Chem. Soc.* **2006**, *128*, 4823. (e) Diaz, D. D.; Rajagopal, K.; Strable, E.; Schneider, J.; Finn, M. G. *J. Am. Chem. Soc.* **2006**, *128*, 6056. (f) Whiting, M.; Tripp, J. C.; Lin, Y.-C.; Lindstrom, W.; Olson, A. J.; Elder, J. H.; Sharpless, K. B.; Fokin, V. V. *J. Med. Chem.* **2006**, *49*, 7697. (g) Punna, S.; Kuzelka, J.; Wang, Q.; Finn, M. G. *Angew. Chem., Int. Ed.* **2005**, *44*, 2215. (h) Bodine, K. D.; Gin, D. Y.; Gin, M. S. *J. Am. Chem. Soc.* **2004**, *126*, 1638. (i) Wu, P.; Feldman, A. K.; Nugent, A. K.; Hawker, C. J.; Scheel, A.; Voit, B.; Pyun, J.; Frechet, J. M. J.; Sharpless, K. B.; Fokin, V. V. *Angew. Chem., Int. Ed.* **2004**, *43*, 3928. (j) Wang, Q.; Chan, T. R.; Hilgraf, R.; Fokin, V. V.; Sharpless, K. B.; Finn, M. G. *J. Am. Chem. Soc.* **2003**, *125*, 3192. (k) Link, A. J.; Tirrell, D. A. *J. Am. Chem. Soc.* **2003**, *125*, 11164. (l) Kolb, H. C.; Sharpless, K. B. *Drug Discovery Today* **2003**, *8*, 1128.
- (47) Mathew, P.; Neels, A.; Albrecht, M. *J. Am. Chem. Soc.* **2008**, *130*, 13534.
- (48) Kumar, A.; Pandey, P. S. *Org. Lett.* **2008**, *10*, 165.
- (49) Mullen, K.; Mercurio, J.; Serpell, C.; Beer, P. D. *Angew. Chem., Int. Ed.* **2009**, *48*, 4781.
- (50) Schulze, B.; Friebe, C.; Hager, M. D.; Guenther, W.; Koehn, U.; Jahn, B. O.; Goerls, H.; Schubert, U. S. *Org. Lett.* **2010**, *12*, 2710.
- (51) Hua, Y.; Flood, A. H. *Chem. Soc. Rev.* **2010**, *39*, 1262.
- (52) Yoon, J.; Kim, S. K.; Singh, N. J.; Kim, K. S. *Chem. Soc. Rev.* **2006**, *35*, 355.

- (53) <http://nov.wikipedia.org/wiki/DNA>
- (54) Mathews, C. P.; van Hold, K. E. *Biochemistry*; The Benjamin/Cummings Publishing Company, Inc.: Redwood City, CA, 1990.
- (55) Ronaghi, M.; Karamohamed, S.; Pettersson, B.; Uhlén, M.; Nyrén, P. *Anal. Biochem.* **1996**, *242*, 84–89.
- (56) Xu, S.; He, M.; Yu, H.; Cai, X.; Tan, X.; Lu, B.; Shu, B. *Anal. Biochem.* **2001**, *299*, 188–193.
- (57) Saenger, W. *Principles of Nucleic Acid Structure*; Springer-Verlag: New York, 1988.
- (58) For review, see: (a) Sessler, J. L.; Gale, P. A.; Cho, W.-S. *Anion Receptor Chemistry*; RSC Publishing: Cambridge, U.K., 2006. (b) Kim, S.-K.; Lee, D.-H.; Hong, J.-I.; Yoon, J.-Y. *Acc. Chem. Res.* **2009**, *42*, 23–31. For recent reports, see: (c) Kumar, A.; Pandey, P. S. *Org. Lett.* **2008**, *10*, 165–168. (d) Chen, K.-H.; Liao, J.-H.; Chan, H.-Y.; Fang, J.-M. *J. Org. Chem.* **2009**, *74*, 895–898. (e) Xu, Z.; Singh, N. J.; Lim, J.; Pan, J.; Kim, H.-N.; Park, S.-S.; Kim, K. S.; Yoon, J.-Y. *J. Am. Chem. Soc.* **2009**, *131*, 15528–15533.
- (59) Of the 18 426 559 molecules in PubChem (March 2008), 17 947 719 (97%) contained one or more CH units. Li, Y.; Flood, A. H. *J. Am. Chem. Soc.* **2008**, *130*, 12111–12122.
- (60) (a) Bryantsev, V. S.; Hay, B. P. *Org. Lett.* **2005**, *7*, 5031–5034. (b) Bryantsev, V. S.; Hay, B. P. *J. Am. Chem. Soc.* **2005**, *127*, 8282–8283. (c) Li, Y.; Flood, A. H. *Angew. Chem., Int. Ed.* **2008**, *47*, 2649–2652. (d) Yoon, D. W.; Gross, D. E.; Lynch, V. M.; Sessler, J. L.; Hay, B. P.; Lee, C.-H. *Angew. Chem., Int. Ed.* **2008**, *47*, 5038–5042. (e) Li, Y.; Pink, M.; Karty, J. A.; Flood, A. H. *J. Am. Chem. Soc.* **2008**, *130*, 17293–17295. (f) Zhu, S. S.; Staats, H.; Brandhorst, K.; Grunenberg, J.; Gruppi, F.; Dalcanale, E.; Lützen, A.; Rissanen, K.; Schalley, C. A. *Angew. Chem., Int. Ed.* **2008**, *47*, 788–792. (g) Juwarker, H.; Lenhardt, J. M.; Pham, D. M.; Craig, S. L. *Angew. Chem., Int. Ed.* **2008**, *47*, 3740–3743. (h) Meudtner, R. M.; Hecht, S. *Angew. Chem., Int. Ed.* **2008**, *47*, 4926–4930. (i) Berryman, O. B.; Sather, A. C.; Hay, B. P.; Meisner, J. S.; Johnson, D. W. *J. Am. Chem. Soc.* **2008**, *130*, 10895–10897. (j) Maeda, H.; Mihashi, Y.; Haketa, Y. *Org. Lett.* **2008**, *10*, 3179–3182. (k) Hay, B. P.; Bryantsev, V. S. *Chem. Commun.* **2008**, 2417–2428. (l) Romero, T.; Caballero, A.; Tárraga, A.; Molina, P. *Org. Lett.* **2009**, *11*, 3466–3469. (m) Mullen, K. M.; Mercurio, J.; Serpell, C. J.; Beer, P. D. *Angew. Chem., Int. Ed.* **2009**, *48*, 4781–4784. (n) Juwarker, H.; Lenhardt, J. M.; Castillo, J. C.; Craig, S. L. *J. Org. Chem.* **2009**, *74*, 8924–8934. (o) Fisher, M. G.; Gale, P. A.; Hiscock, J. R.; Hursthouse, M. B.; Light, M. E.; Schmidtchen, F. P.; Tong, C. C. *Chem. Commun.* **2009**, 3017–3019. (p) Pedzisa, L.; Hay, B. P. *J. Org. Chem.* **2009**, *74*, 2554–2560. (q) Schulze, B.; Friebe, C.; Hager, M. D.; Günther, W.; Köhn, U.; Jahn, B. O.; Görls, H.; Schubert, U. S. *Org. Lett.* **2010**, *12*, 2710–2713.

- (r) Lee, S.; Hua, Y.; Park, H.; Flood, A. H. *Org. Lett.* **2010**, *12*, 2100–2102. (s) Yano, M.; Tong, C. C.; Light, M. E.; Schmidtchen, F. P.; Gale, P. A. *Org. Biomol. Chem.* **2010**, *8*, 4356–4363.
- (61) Hua, Y.; Flood, A. H. *Chem. Soc. Rev.* **2010**, *39*, 1262–1271.
- (62) Although it does not contain triazole and pyrrole in the same macrocyclic ring, it is to be noted that Gale recently reported a triazole strapped calixpyrrole and showed it to be effective for chloride anion recognition. See: ref 7o and 7s.
- (63) Rostovtsev, V. V.; Green, L. G.; Fokin, V. V.; Sharpless, K. B. *Angew. Chem., Int. Ed.* **2002**, *41*, 2596–2599.
- (64) Tom, N. J.; Simon, W. M.; Frost, H. N.; Ewing, M. *Tetrahedron Lett.* **2004**, *45*, 905–906.
- (65) Kim, S. K.; Sessler, J. L.; Gross, D. E.; Lee, C.-H.; Kim, J. S.; Lynch, V. M.; Delmau, L. H.; Hay, B. P. *J. Am. Chem. Soc.* **2010**, *132*, 5827–5836.
- (66) Bourson, J.; Pouget, J.; Valeur, B. *J. Phys. Chem.* **1993**, *97*, 4552–4557.
- (67) Katritzky, A. R. *Handbook of Heterocyclic Chemistry*; Pergamon Press: 2000.
- (68) The CH binding energies are consistent with a prior description of individual hydrogen-bond contributions within a triazolophane\*Cl<sup>-</sup> complex, which implicated energies of -10 kcal/mol per triazole CH and -3 to -4 kcal/mol per aryl CH: Bandyopadhyay, I.; Raghavachari, K.; Flood, A. H. *ChemPhysChem* **2009**, *10*, 2535–2540.
- (69) Sandström, J. *Dynamic NMR Spectroscopy*; Academic: London, 1982.
- (70) Ōki, M. *Applications of Dynamic NMR Spectroscopy to Organic Chemistry*; WILEY-VCH: Weinheim, 1985.
- (71) Neuhaus, D.; Williamson, M.P. *The Nuclear Overhauser Effect in Structural and Conformational Analysis*; VCH Publishers: Cambridge, U. K., 1989.
- (72) Friebolin, H. *Basic One- and Two-Dimensional NMR Spectroscopy*; WILEY-VCH: Weinheim, 2005.
- (73) Bylaska, E. J.; de Jong, W. A.; Kowalski, K.; Straatsma, T. P.; Valiev, M.; Wang, D.; Apra, E.; Windus, T. L.; Hirata, S.; Hackler, M. T.; Zhao, Y.; Fan, P. –D.; Harrison, R. J.; Dupuis, M.; Smith, D. M. A.; Nieplocha, J.; Tipparaju, V.; Krishnan, M.; Auer, A. A.; Nooijen, M.; Brown, E.; Cisneros, G.; Fann, G. I.; Fruchtl, H.; Garza, J.; Hirao, K.; Kendall, R.; Nichols, J. A.; Tsemekhman, K.; Wolinski, K.; Anchell, J.; Bernholdt, D.; Borowski, P.; Clark, T.; Clerc, D.; Dachsel, H.; Deegan, M.; Dyall, K.; Elwood, D.; Glendening, E.; Gutowski, M.; Hess, A.; Jaffe, J.; Johnson, B.; Ju, J.; Kobayashi, R.; Kutteh, R.; Lin, Z.; Littlefield, R.; Long, X.; Meng, B.; Nakajima, T.; Niu, S.; Pollack, L.; Rosing, M.; Sandrone, G.; Stave, M.; Taylor, H.; Thomas, G.; van Lenthe, J.; Wong, A.;

- Zhang, Z. *NWChem, A Computational Chemistry Package for Parallel Computers, Version 5.0*, **2006**, Pacific Northwest National Laboratory, Richland, Washington 99352-0999, USA.
- (74) DENZO-SMN. (1997). Otwinowski, Z.; Minor, W. *Methods in Enzymology*, 276: *Macromolecular Crystallography, Part A*, 307 – 326, Carter, C.W.J.; Simon, M.I.; Sweet, R.M. Editors, Academic Press.
- (75) SIR97. (1999). A program for crystal structure solution. Altomare, A.; Burla, M. C.; Camalli, M.; Cascarano, G. L.; Giacovazzo, C.; Guagliardi, A.; Moliterni, A.G. G.; Polidori, G.; Spagna, R. *J. Appl. Cryst.* **1999**, 32, 115-119.
- (76) Sheldrick, G. M. *SHELXL97. Program for the Refinement of Crystal Structures*; University of Gottingen, Germany, **1994**.
- (77)  $R_w(F^2) = \{\Sigma w(|F_o|^2 - |F_c|^2)^2 / \Sigma w(|F_o|^4)\}^{1/2}$  where  $w$  is the weight given each reflection.  $R(F) = \Sigma(|F_o| - |F_c|) / \Sigma |F_o|$  for reflections with  $F_o > 4(\sigma(F_o))$ .  $S = [\Sigma w(|F_o|^2 - |F_c|^2)^2 / (n - p)]^{1/2}$ , where  $n$  is the number of reflections and  $p$  is the number of refined parameters.
- (78) *International Tables for X-ray Crystallography*; Wilson, A. J. C., Ed.; Kluwer Academic Press: Boston, **1992**; Vol. C, Tables 4.2.6.8 and 6.1.1.4.
- (79) Sheldrick, G.M. (1994). SHELXTL/PC (Version 5.03). Siemens Analytical X-ray Instruments, Inc., Madison, Wisconsin, USA.
- (80) Fang, J. –M.; Selvi, S.; Liao, J. –H.; Slanina, Z.; Chen, C. –T.; Chou, P. –T. *J. Am. Chem. Soc.* **2004**, 126, 3559–3566.
- (81) Lehn, J.–M. *Science* **2002**, 295, 2400.
- (82) (a) de Hoog, P.; Gamez, P.; Mutikainen, I.; Turpeinen, U.; Reedijk, J. *Angew. Chem., Int. Ed.* **2004**, 43, 5815. (b) Sessler, J. L.; Seidel, D. *Angew. Chem., Int. Ed.* **2003**, 42, 5134. (c) Gale, P. A. *Coord. Chem. Rev.*, **2003**, 240, 191. (d) Beer, P. D.; Gale, P. A. *Angew. Chem., Int. Ed.* **2001**, 40, 486. (e) Schmidtchen, P.; Berger, M. *Chem. Rev.* **1997**, 97, 1609. (f) Bianchi, A.; Bowman-James, K.; García-España, E. *Supramolecular Chemistry of Anions*; Wiley–VCH: Chichester, New York, 1997.
- (83) Sessler, J. L.; Gale, P. A.; Cho, W.–S. *Anion Receptor Chemistry*; RSC Publishing: Cambridge, U.K., 2006.
- (84) Mathews, C. P.; van Hold, K. E. *Biochemistry*; The Benjamin/Cummings Publishing Company, Inc.: Redwood City, CA, 1990.
- (85) Xu, S.; He, M.; Yu, H.; Cai, X.; Tan, X.; Lu, B.; Shu, B. *Anal. Biochem.* **2001**, 299, 188.
- (86) Ronaghi, M.; Karamohamed, S.; Pettersson, B.; Uhlén, M.; Nyrén, P. *Anal. Biochem.* **1996**, 242, 84.

- (87) Saenger, W. *Principles of Nucleic Acid Structure*; Springer-Verlag: New York, 1988.
- (88) Lumetta, G. J. In *Fundamentals and Applications of Anion Separations*; Moyer, B. A.; Singh, R. P. Eds.; Kluwer Academic/Plenum: New York, 2004, 107.
- (89) (a) Sessler, J. L.; Kim, S.-K.; Gross, D. E.; Lee, C.-H.; Kim, J.-S.; Lynch, V. M. *J. Am. Chem. Soc.* **2008**, *130*, 13162. (b) Kang, S.-O.; Powell, D.; Day, V. W.; Bowman-James, K. *Angew. Chem., Int. Ed.* **2006**, *45*, 1921. (c) Bondy, C. R.; Gale, P. A.; Loeb, S. J. *J. Am. Chem. Soc.* **2004**, *126*, 5030. (d) Tobey, S. L.; Anslyn, E. V. *J. Am. Chem. Soc.* **2003**, *125*, 14807.
- (90) (a) Sessler, J. L.; Cai, J.; Gong, H.-Y.; Yang, X.; Arambula, J. F.; Hay, B. P. *J. Am. Chem. Soc.* **2010**, *132*, 14058. (b) Mullen, K.; Mercurio, J.; Serpell, C.; Beer, P. D. *Angew. Chem., Int. Ed.* **2009**, *48*, 4781. (c) Yoon, D. W.; Gross, D. E.; Lynch, V. M.; Sessler, J. L.; Hay, B. P.; Lee, C.-H. *Angew. Chem., Int. Ed.* **2008**, *47*, 5038. (d) Li, Y.; Flood, A. H. *Angew. Chem., Int. Ed.* **2008**, *47*, 2649. (e) Bryantsev, V. S.; Hay, B. P. *J. Am. Chem. Soc.* **2005**, *127*, 8282. (f) Chellappan, K.; Singh, N. J.; Hwang, I.-C.; Lee, J. W.; Kim, K. S. *Angew. Chem., Int. Ed.* **2005**, *44*, 2899.
- (91) (a) Keitz, B. K.; Bouffard, J.; Bertrand, G.; Grubbs, R. H. *J. Am. Chem. Soc.* **2011**, *133*, 8498. (b) Bouffard, J.; Keitz, B. K.; Tonner, R.; Guisado-Barrios, G.; Frenking, G.; Grubbs, R. H.; Bertrand, G. *Organometallics* **2011**, *30*, 2617. (c) Cai, J.; Yang, X.; Arumugam, K.; Bielawski, C. W.; Sessler, J. L. *Organometallics* **2011**, *30*, 5033. (d) Saravanakumar, R.; Ramkumar, V.; Sankararaman, S. *Organometallics* **2011**, *30*, 1689. (e) Prades, A.; Peris, E.; Albrecht, M. *Organometallics* **2011**, *30*, 1162.
- (92) Ohmatsu, K.; Kiyokawa, M.; Ooi, T. *J. Am. Chem. Soc.* **2011**, *133*, 1307.
- (93) (a) Kilah, N. L.; Wise, M. D.; Serpell, C. J.; Thompson, A. L.; White, N. G.; Christensen, K. E.; Beer, P. D. *J. Am. Chem. Soc.* **2010**, *132*, 11893. (b) Schulze, B.; Friebe, C.; Hager, M. D.; Guenther, W.; Koehn, U.; Jahn, B. O.; Goerls, H.; Schubert, U. S. *Org. Lett.* **2010**, *12*, 2710. (c) Kumar, A.; Pandey, P. S. *Org. Lett.* **2008**, *10*, 165.
- (94) (a) Kolb, H. C.; Finn, M. G.; Sharpless, K. B. *Angew. Chem., Int. Ed.* **2001**, *40*, 2004. (b) Tornøe, C. W.; Meldal, M. *Chem. Rev.* **2008**, *108*, 2952.
- (95) (a) Moses, J. E.; Moorhouse, A. D. *Chem. Soc. Rev.* **2007**, *36*, 1249. (b) Fournier, D.; Hoogenboom, R.; Schubert, U. S. *Chem. Soc. Rev.* **2007**, *36*, 1369. (c) Lutz, J. F. *Angew. Chem., Int. Ed.* **2007**, *46*, 1018. (d) Ladmiral, V.; Mantovani, G.; Clarkson, G. J.; Cauet, S.; Irwin, J. L.; Haddleton, D. M. *J. Am. Chem. Soc.* **2006**, *128*, 4823. (e) Diaz, D. D.; Rajagopal, K.; Strable, E.; Schneider, J.; Finn, M. G. *J. Am. Chem. Soc.* **2006**, *128*, 6056. (f) Whiting, M.; Tripp, J. C.; Lin, Y.-C.; Lindstrom, W.; Olson, A. J.; Elder, J. H.; Sharpless, K. B.; Fokin, V. V. *J. Med.*



- Chem.* **2006**, *49*, 7697. (g) Punna, S.; Kuzelka, J.; Wang, Q.; Finn, M. G. *Angew. Chem., Int. Ed.* **2005**, *44*, 2215. (h) Bodine, K. D.; Gin, D. Y.; Gin, M. S. *J. Am. Chem. Soc.* **2004**, *126*, 1638. (i) Wu, P.; Feldman, A. K.; Nugent, A. K.; Hawker, C. J.; Scheel, A.; Voit, B.; Pyun, J.; Frechet, J. M. J.; Sharpless, K. B.; Fokin, V. V. *Angew. Chem., Int. Ed.* **2004**, *43*, 3928. (j) Wang, Q.; Chan, T. R.; Hilgraf, R.; Fokin, V. V.; Sharpless, K. B.; Finn, M. G. *J. Am. Chem. Soc.* **2003**, *125*, 3192. (k) Link, A. J.; Tirrell, D. A. *J. Am. Chem. Soc.* **2003**, *125*, 11164. (l) Kolb, H. C.; Sharpless, K. B. *Drug Discovery Today* **2003**, *8*, 1128.
- (96) (a) Lee, S.; Hua, Y.; Park, H.; Flood, A. H. *Org. Lett.* **2010**, *12*, 2100. (b) Yano, M.; Tong, C. C.; Light, M. E.; Schmidtchen, F. P.; Gale, P. A. *Org. Biomol. Chem.* **2010**, *8*, 4356. (c) Hua, Y.; Flood, A. H. *J. Am. Chem. Soc.* **2010**, *132*, 12838. (d) Hua, Y.; Flood, A. H. *Chem. Soc. Rev.* **2010**, *39*, 1262. (e) Romero, T.; Caballero, A.; Tárraga, A.; Molina, P. *Org. Lett.* **2009**, *11*, 3466. (f) Juwarker, H.; Lenhardt, J. M.; Castillo, J. C.; Craig, S. L. *J. Org. Chem.* **2009**, *74*, 8924. (g) Fisher, M. G.; Gale, P. A.; Hiscock, J. R.; Hursthouse, M. B.; Light, M. E.; Schmidtchen, F. P.; Tong, C. C. *Chem. Commun.* **2009**, 3017. (h) Li, Y.; Pink, M.; Karty, J. A.; Flood, A. H. *J. Am. Chem. Soc.* **2008**, *130*, 17293. (i) Juwarker, H.; Lenhardt, J. M.; Pham, D. M.; Craig, S. L. *Angew. Chem., Int. Ed.* **2008**, *47*, 3740. (j) Meudtner, R. M.; Hecht, S. *Angew. Chem., Int. Ed.* **2008**, *47*, 4926.
- (97) Tom, N. J.; Simon, W. M.; Frost, H. N.; Ewing, M. *Tetrahedron Lett.* **2004**, *45*, 905.
- (98) Kim, S. K.; Sessler, J. L.; Gross, D. E.; Lee, C.-H.; Kim, J. S.; Lynch, V. M.; Delmau, L. H.; Hay, B. P. *J. Am. Chem. Soc.* **2010**, *132*, 5827.
- (99) Bourson, J.; Pouget, J.; Valeur, B. *J. Phys. Chem.* **1993**, *97*, 4552.
- (100) (a) Kubik, S.; Goddard, R.; Kirchner, R.; Nolting, D.; Seidel, J. *Angew. Chem., Int. Ed.* **2001**, *40*, 2648. (b) Kubik, S.; Goddard, R. *Proc. Natl. Acad. Sci. U. S. A.* **2002**, *99*, 5127. (c) Kubik, S.; Kirchner, R.; Nolting, D.; Seidel, J. *J. Am. Chem. Soc.* **2002**, *124*, 12752. (d) Otto, S.; Kubik, S. *J. Am. Chem. Soc.* **2003**, *125*, 7804.
- (101) (a) Mateus, P.; Delgado, R.; Brandão, P.; Félix, V. *J. Org. Chem.* **2009**, *74*, 8638. (b) Mateus, P.; Delgado, R.; Brandão, P.; Carvalho, S.; Félix, V. *Org. Biomol. Chem.* **2009**, *7*, 4661.
- (102) Dietrich, B.; Fyles, D. L.; Fyles, T. M.; Lehn, J. -M. *Helv. Chim. Acta.* **1979**, *62*, 2763.
- (103)  $\Delta G = G(\text{complex}) - G(\text{chloride}) - G(\text{donor})$  values in vacuum were calculated at the MP2/aug-cc-pVDZ level of theory with *NWChem*: (a) Kendall, R. A.; Apra, E.; Bernholdt, D. E.; Bylaska, E. J.; Dupuis, M.; Fann, G. I.; Harrison, R. J.; Ju, J. L.; Nichols, J. A.; Nieplocha, J.; Straatsma, T. P.; Windus, T. L.; Wong, A. T. *Comput. Phys. Commun.* **2000**, *128*, 260. (b) Valiev, M.; Bylaska, E. J.; Govind,

- N.; Kowalski, K.; Straatsma, T. P.; Van Dam, H. J. J.; Wang, D.; Nieplocha, J.; Apra, E.; Windus, T. L.; de Jong, W. *Comput. Phys. Commun.* **2010**, *181*, 1477.
- (104) (a)  $\Delta G$  values in different solvents were computed with the SM8 solvation model<sup>22(b)</sup> as implemented in *Spartan*<sup>22(c)</sup> after performing RHF/6-31+G\* single-point energy calculations on MP2/aug-cc-pVDZ vacuum geometries. (b) Marenich, A. V.; Olson, R. M.; Kelly, C. P.; Cramer, C. J.; Truhlar, D. G. *J. Chem. Theory Comput.* **2007**, *3*, 2011. (c) *Spartan 10*, Wavefunction, Inc., Irvine, California 92612.
- (105) Macrocycle **1**<sup>4+</sup>•4BF<sub>4</sub><sup>-</sup> is insoluble in CHCl<sub>3</sub> or pure H<sub>2</sub>O. It can be dissolved in acetone, but precipitates when treated with tetrabutylammonium salts.
- (106) DENZO-SMN. (1997). Otwinowski, Z.; Minor, W. *Methods in Enzymology*, 276: *Macromolecular Crystallography, Part A*, 307 – 326, Carter, C.W.J.; Simon, M.I.; Sweet, R.M. Editors, Academic Press.
- (107) SIR97. (1999). A program for crystal structure solution. Altomare, A.; Burla, M. C.; Camalli, M.; Cascarano, G. L.; Giacovazzo, C.; Guagliardi, A.; Moliterni, A.G. G.; Polidori, G.; Spagna, R. *J. Appl. Cryst.* **1999**, *32*, 115-119.
- (108) Sheldrick, G. M. *SHELXL97. Program for the Refinement of Crystal Structures*; University of Gottingen, Germany, **1994**.
- (109)  $R_w(F^2) = \{\sum w(|F_o|^2 - |F_c|^2)^2 / \sum w(|F_o|^4)\}^{1/2}$  where w is the weight given each reflection.  $R(F) = \sum(|F_o| - |F_c|) / \sum |F_o|$  for reflections with  $F_o > 4(\sigma(F_o))$ .  $S = [\sum w(|F_o|^2 - |F_c|^2)^2 / (n - p)]^{1/2}$ , where n is the number of reflections and p is the number of refined parameters.
- (110) *International Tables for X-ray Crystallography*; Wilson, A. J. C., Ed.; Kluwer Academic Press: Boston, **1992**; Vol. C, Tables 4.2.6.8 and 6.1.1.4.
- (111) Sheldrick, G.M. (1994). SHELXTL/PC (Version 5.03). Siemens Analytical X-ray Instruments, Inc., Madison, Wisconsin, USA.
- (112) (a) Hay, B. P.; Firman, T. K.; Moyer, B. A. *J. Am. Chem. Soc.* **2005**, *109*, 832. (b) Bryantsev, V. S.; Hay, B. P. *Org. Lett.* **2005**, *7*, 5031.
- (113) (a) Herrmann, W. *Angew. Chem., Int. Ed.* **2002**, *41*, 1290. (b) Nolan, S. P., Ed. *N-Heterocyclic Carbene in Synthesis*; Wiley-VCH: New York, 2006.
- (114) (a) Enders, D.; Balensiefer, T. *Acc. Chem. Res.* **2004**, *37*, 534. (b) Enders, D.; Niemeier, O.; Henseler, A. *Chem. Rev.* **2007**, *107*, 5606. (c) Biju, A. T.; Kuhl, N.; Glorius, F. *Acc. Chem. Res.* **2011**, in press, doi: 10.1021/ar2000716.
- (115) (a) Coady, D. J.; Bielawski, C. W. *Macromolecules* **2006**, *39*, 8895. (b) Coady, D. J.; Norris, B. C.; Lynch, V. M.; Bielawski, C. W. *Macromolecules* **2008**, *41*, 3775. (c) Rosen, E. L.; Varnado, C. D., Jr.; Tennyson, A. G.; Khramov, D. M.; Kamplain, J. W.; Sung, D. H.; Cresswell, P. T.; Lynch, V. M.; Bielawski, C. W. *Organometallics* **2009**, *28*, 6695. (d) Varnado C. D., Jr.; Lynch, V. M.; Bielawski,

- C. W. *Dalton Trans.* **2009**, 7253. (e) Coady, D. J.; Khramov, D. M.; Norris, B. C.; Tennyson, A. G.; Bielawski, C. W. *Angew. Chem. Int. Ed.* **2009**, *48*, 5187. (f) Norris, B. C.; Bielawski, C. W. *Macromolecules* **2010**, *43*, 3591. (g) Crabtree, R. H., Ed. *Coord. Chem. Rev.* **2007**, *251*, 595. (h) Glorius, F., Ed. *Top. Organomet. Chem.* **2007**, *21*. (i) Hahn, F. E.; Jahnke, M. C. *Angew. Chem., Int. Ed.* **2008**, *47*, 3122.
- (116) Bourissou, D.; Guerret, O.; Gabbai, F. P.; Bertrand, G. *Chem. Rev.* **2000**, *100*, 39.
- (117) (a) Enders, D.; Breuer, K.; Kallfass, U.; Balensiefer, T. *Synthesis* **2003**, *8*, 1292. (b) Frey, G. D.; Schütz, J.; Herdtweck, E.; Herrmann, W. A. *Organometallics* **2005**, *24*, 4416. (c) Poyatos, M.; McNamara, W.; Incarvito, C.; Peris, E.; Crabtree, R. H. *Chem. Commun.* **2007**, 2267. (d) Gnanamgari, D.; Moores, A.; Rajaseelan, E.; Crabtree, R. H. *Organometallics* **2007**, *26*, 1226. (e) Diez-Gonzalez, S.; Marion, N.; Nolan, S. P. *Chem. Rev.* **2009**, *109*, 3612.
- (118) (a) Gründemann S.; Kovacevic, A.; Albrecht, M.; Faller, J. W.; Crabtree, R. H. *Chem. Commun.* **2001**, 2274; (b) Gründemann, S.; Kovacevic, A.; Albrecht, M.; Faller, J. W.; Crabtree, R. H. *J. Am. Chem. Soc.* **2002**, *124*, 10473.
- (119) Han, Y.; Huynh, H. V. *Chem. Commun.* **2007**, 1089.
- (120) Lavallo, V.; Canac, Y.; Präsang, C.; Donnadiou, B.; Bertrand, G. *Angew. Chem., Int. Ed.* **2005**, *44*, 5705.
- (121) (a) Lavallo, V.; Dyker, C. A.; Donnadiou, B.; Bertrand, G. *Angew. Chem. Int. Ed.* **2008**, *47*, 5411. (b) Aldeco-Perez, E.; Rosenthal, A. J.; Donnadiou, B.; Parameswaran, P.; Frenking, G.; Bertrand, G. *Science* **2009**, *326*, 556. (c) Guisado-Barrios, G.; Bouffard, J.; Donnadiou, B.; Bertrand, G. *Angew. Chem. Int. Ed.* **2010**, *49*, 4759.
- (122) (a) Albrecht, M. *Chem. Commun.* **2008**, 3601. (b) Song, G.; Zhang, Y.; Li, X. *Organometallics* **2008**, *27*, 1936. (c) Schuster, O.; Yang, L.; Raubenheimer, H. G.; Albrecht, M. *Chem. Rev.* **2009**, *109*, 3445. (d) Melaimi, M.; Soleilhavoup, M.; Bertrand, G. *Angew. Chem. Int. Ed.* **2010**, *49*, 8810.
- (123) (a) Lebel, H.; Janes, M. K.; Charette, A. B.; Nolan, S. P. *J. Am. Chem. Soc.* **2004**, *126*, 5046. (b) Heckenroth, M.; Kluser, E.; Neels, A.; Albrecht, M. *Angew. Chem., Int. Ed.* **2007**, *46*, 6293. (c) Yang, L.; Krüger, A.; Neels, A.; Albrecht, M. *Organometallics* **2008**, *27*, 3161.
- (124) (a) Mathew, P.; Neels, A.; Albrecht, M. *J. Am. Chem. Soc.* **2008**, *130*, 13534. (b) Karthikeyan, T.; Sankararaman, S. *Tetrahedron Lett.* **2009**, *50*, 5834. (c) Nakamura, T.; Ogata, K.; Fukuzawa, S. *Chem. Lett.* **2010**, *39*, 920. (d) Lalrempuia, R.; McDaniel, N. D.; Müller-Bunz, H.; Bernhard, S.; Albrecht, M. *Angew. Chem. Int. Ed.* **2010**, *49*, 9765. (e) Saravanakumar, R.; Ramkumar, V.; Sankararaman, S. *Organometallics* **2011**, *30*, 1689. (f) Poulain, A.; Canseco-Gonzalez, D.; Hynes-Roche, R.; Albrecht, M. *Organometallics* **2011**, *30*, 1021.

- (g) Nakamura, T.; Terashima, T.; Ogata, K.; Fukuzawa, S. *Org. Lett.* **2011**, *13*, 620. (h) Kilpin, K. J.; Paul, U. S. D.; Lee, A.; Crowley, J. D. *Chem. Commun.* **2011**, *47*, 328. (i) Schulze, B.; Escudero, D.; Friebe, C.; Siebert, R.; Görls, H.; Köhn, U.; Altuntas, E.; Baumgaertel, A.; Hager, M. D.; Winter, A.; Dietzek, B.; Popp, J.; González, L.; Schubert, U. S. *Chem. Eur. J.* **2011**, *17*, 5494. (j) Bernet, L.; Lalrempuia, R.; Ghattas, W.; Mueller-Bunz, H.; Vigara, L.; Llobet, A.; Albrecht, M. *Chem. Commun.* **2011**, *47*, 8058. (k) Hohloch, S.; Su, C-Y.; Sarkar, B. *Eur. J. Inorg. Chem.* **2011**, 3067. (l) Schuster, E. M.; Botoshansky, M.; Gandelman, M. *Dalton Trans.* **2011**, in press, doi: 10.1039/C1DT10264H.
- (125) (a) Altman, R. A.; Anderson, K. W.; Buchwald, S. L. *J. Org. Chem.* **2008**, *73*, 5167. (b) Zi, G-F; Xiang, L.; Song, H-B. *Organometallics* **2008**, *27*, 1242.
- (126) Sessler, J. L.; Cai, J.; Gong, H-Y.; Yang, X.; Arambula, J. F.; Hay, B. P. *J. Am. Chem. Soc.* **2010**, *132*, 14058.
- (127) Rostovtsev, V. V.; Green, L. G.; Fokin, V. V.; Sharpless, K. B. *Angew. Chem., Int. Ed.* **2002**, *41*, 2596.
- (128) (a) Tornøe, C. W.; Christensen, C.; Meldal, M. *J. Org. Chem.* **2002**, *67*, 3057. (b) Hawker, C. J.; Wooley, K. L. *Science* **2005**, *309*, 1200. (c) Devaraj, N. K.; Dnolfo, P. H.; Chidsey, C. E. D.; Collman, J. P. *J. Am. Chem. Soc.* **2006**, *128*, 1794. (d) Burley, G. A.; Gierlich, J.; Mofid, M. R.; Nir, H.; Tal, S.; Eichen, Y.; Carell, T. *J. Am. Chem. Soc.* **2006**, *128*, 1398. (e) Meldal, M.; Tornøe, C. W. *Chem. Rev.* **2008**, *108*, 2952.
- (129) Lee, K. M.; Wang, H. M. J.; Lin, I. J. B. *J. Chem. Soc., Dalton Trans.* **2002**, 2852.
- (130) Arduengo, A. J., III; Dias, H. V. R.; Calabrese, J. C.; Davidson, F. *Organometallics* **1993**, *12*, 3405.
- (131) (a) Garrison, J. C.; Youngs, W. J. *Chem. Rev.* **2005**, *105*, 3978. (b) Hahn, F. E.; Radloff, C.; Pape, T.; Hepp, A. *Chem. Eur. J.* **2008**, *14*, 10900.
- (132) Prades, A.; Peris, E.; Albrecht, M. *Organometallics* **2011**, *30*, 1162.
- (133) (a) Keitz, B. K.; Bouffard, J.; Bertrand, G.; Grubbs, R. H. *J. Am. Chem. Soc.* **2011**, *133*, 8498. (b) Bouffard, J.; Keitz, B. K.; Tonner, R.; Guisado-Barrios, G.; Frenking, G.; Grubbs, R. H.; Bertrand, G. *Organometallics* **2011**, *30*, 2617. (c) Bielawski, C. W.; Grubbs, R. H. *Prog. Polym. Sci.* **2007**, *32*, 1.
- (134) Demonceau, A.; Stumpf, A. W.; Saive, E.; Noels, A. F. *Macromolecules* **1997**, *30*, 3127.
- (135) DENZO-SMN. (1997). Otwinowski, Z.; Minor, W. *Methods in Enzymology*, 276: *Macromolecular Crystallography, Part A*, 307 – 326, Carter, C.W.J.; Simon, M.I.; Sweet, R. M. Editors, Academic Press.

- (136) SIR97. (1999). A program for crystal structure solution. Altomare, A.; Burla, M. C.; Camalli, M.; Cascarano, G. L.; Giacovazzo, C.; Guagliardi, A.; Moliterni, A.G. G.; Polidori, G.; Spagna, R. *J. Appl. Cryst.* **1999**, 32, 115-119.
- (137) Sheldrick, G. M. *SHELXL97. Program for the Refinement of Crystal Structures*; University of Gottingen, Germany, **1994**.
- (138)  $R_w(F^2) = \{\Sigma w(|F_o|^2 - |F_c|^2)^2 / \Sigma w(|F_o|^4)\}^{1/2}$  where w is the weight given each reflection.  $R(F) = \Sigma(|F_o| - |F_c|) / \Sigma |F_o|$  for reflections with  $F_o > 4(\sigma(F_o))$ .  $S = [\Sigma w(|F_o|^2 - |F_c|^2)^2 / (n - p)]^{1/2}$ , where n is the number of reflections and p is the number of refined parameters.
- (139) *International Tables for X-ray Crystallography*; Wilson, A. J. C., Ed.; Kluwer Academic Press: Boston, **1992**; Vol. C, Tables 4.2.6.8 and 6.1.1.4.
- (140) Sheldrick, G.M. (1994). SHELXTL/PC (Version 5.03). Siemens Analytical X-ray Instruments, Inc., Madison, Wisconsin, USA.